International Conference on Light Pollution Theory, Modelling and Measurements

April 15 – 18, 2013, Smolenice, Slovak Republic

Proceedings



Organised by: Astronomical Institute, Slovak Academy of Sciences – Cégep de Sherbrook – Institute of Construction and Architecture, Slovak Academy of Sciences

Editors: M. Kocifaj and M. Aubé

ISBN 978-80-970059-5-5
EAN 9788097005955

Astronomical Institute, Slovak Academy of Sciences
Dúbravská cesta 9, 845 04 Bratislava, Slovak Republic

Organized by

Astronomical Institute, Slovak Academy of Sciences
Dúbravská cesta 9, 845 04 Bratislava, Slovak Republic

Cégep de Sherbrooke
475 Rue du Cégep Sherbrooke, QC J1E 4K1, Canada

and

Institute of Construction and Architecture, Slovak Academy of Sciences
Dúbravská cesta 9, 845 03 Bratislava, Slovak Republic

Astronomical Institute SAS, Bratislava 2013

Sponsored by



Association for Aerosol Research
http://www.gaef.de/



Cégep de Sherbrooke
http://cegepsherbrooke.qc.ca/



Ledtech International
http://www.ledtechcanada.com/



Siemens Slovakia
http://www.siemens.com/entry/cee/sk/



Slovak Astronomical Society
http://sas.astro.sk/

Scientific Organizing Committee

Christian Luginbuhl, US Naval Observatory
Chadwick Moore, US National Park Service
Chris Baddiley, retired scientist from UK
Martin Aubé, Cégep de Sherbrooke,Canada
Miroslav Kocifaj, Slovak Academy of Sciences

Local Organizing Committee

Miroslav Kocifaj, Slovak Academy of Sciences
Martin Aubé, Cégep de Sherbrooke, Canada
Ladislav Kómar, Slovak Academy of Sciences
Hector Lamphar, Slovak Academy of Sciences
Igor Kohút, Slovak Academy of Sciences
Martin Bednárik, Slovak Academy of Sciences

The meeting will focus on recent advances in scientific investigations on light pollution and its impact on astronomical observations.

The study of light pollution is undergoing a renaissance due to development of high performance computers that can significantly reduce the time needed for more accurate numerical simulations. Theoretical solutions, numerical modeling, and field campaigns represent diverse approaches to the analysis, prediction, and characterization of light pollution levels and behaviour.

The meeting aim is to bring together the experts in that field to discuss the current state of the art and to formulate new research directions. The conference aims to facilitate a more intensive development in this field of research.

Topics:

1. Theoretical concepts of modelling light pollution
2. Numerical tools and simulation experiments
3. Effects of atmospheric aerosols and obstacles on light pollution
4. Impact of spectral characteristics of light sources and reflecting surfaces
5. Observational techniques, data, and products
6. Design and evaluation of dark sky friendly lighting technologies

The meeting takes place at
Congress Centre Smolenice of the SAS, Slovak Republic

For further information see the conference home page **http://lptmm.org/**

PROCEEDINGS

Sky brightness measurement and light pollution mapping Case study: Eskisehir city center and surroundings

Metin Altan[1,2], Bulent Aslan[1], Samet Ozdemir[3] and Zeki Aslan[4]

[1] *Anadolu University, Physics Department, Yunusemre Campus, 26470 Eskisehir, Turkey*
[2] *Anadolu University, Earth and Space Sciences Institute, Ikieylul Campus, 26555 Eskisehir, Turkey*
[3] *Anadolu University, Graduate School of Sciences, Advanced Technologies Research Unit: Nanotechnology, Yunusemre Campus, 26470 Eskisehir, Turkey*
[4] *Istanbul Kultur University, Physics Department, Bakirkoy, 34156 Istanbul, Turkey,*
tel: +90 222 335 0580 ext 3656, fax: +90 222 335 4910, e-mail: bulentaslan@anadolu.edu.tr

Abstract

Night sky brightness (i.e. light pollution) mapping and modeling of Eskisehir city center, Turkey, and its surroundings are realized within this pilot project for rendering the Turkey's night sky brightness map. The city center was divided into 112 homogenous 1x1 km^2 regions for data collection. In the surroundings, data were collected from 132 different points within an area of 30x36 km^2. Measured values were positioned in the database with scaled, coordinated and projection defined interactive digital map capability. Using the statistical algorithms, the distribution of the values over the field of study has then been modeled with equi-brightness surfaces. A new model was then developed to estimate luminous flux from night sky brightness data and the total energy loss due to light pollution was estimated by a numerical method.

1 Introduction

Measuring night sky brightness aims at evaluating different aspects of the light pollution such as economical, biological, environmental, and cultural impacts in general, and negative effects on professional and amateur astronomy in particular. Light pollution studies are also important to raise public awareness and to promote legal action against light pollution. In this work, we present the results of a detailed study conducted in and around the city of Eskisehir, Turkey. This study is a part of a larger project for measuring the night sky brightness on a national scale in Turkey [1] and it consists of systematic data collection, digital mapping with interactive database and modeling.

2 Field of study and methodology

In the scope of this project, the field of study, Eskisehir (a city in the northwest of central Turkey), was divided into "*city center*" and "*near surroundings*" (see Fig. 1). The city center covers 14x8 km^2 area and consists of two municipalities and 64 districts. As for the near surroundings, area of 30x36 km^2 were selected. It is important for the sake of proper data analysis that the field of study should be rectangular in shape.

In this study, planning and positional association were done on the image from the IKONOS earth observation satellite and on the digital map with interactive database capability by using Remote Sensing (RS) and Geographical Information System (GIS) techniques. GIS techniques elicit the positional relations between the features such as topological properties on the map in the digital media. Each feature's characteristic information is recorded in the space allotted for the class where that feature is affiliated to. This characteristic information associated with the graphical data on the map lays the groundwork for inquiry, analysis, and modeling. As GIS software, *GeoMedia Professional 6.1* is used.

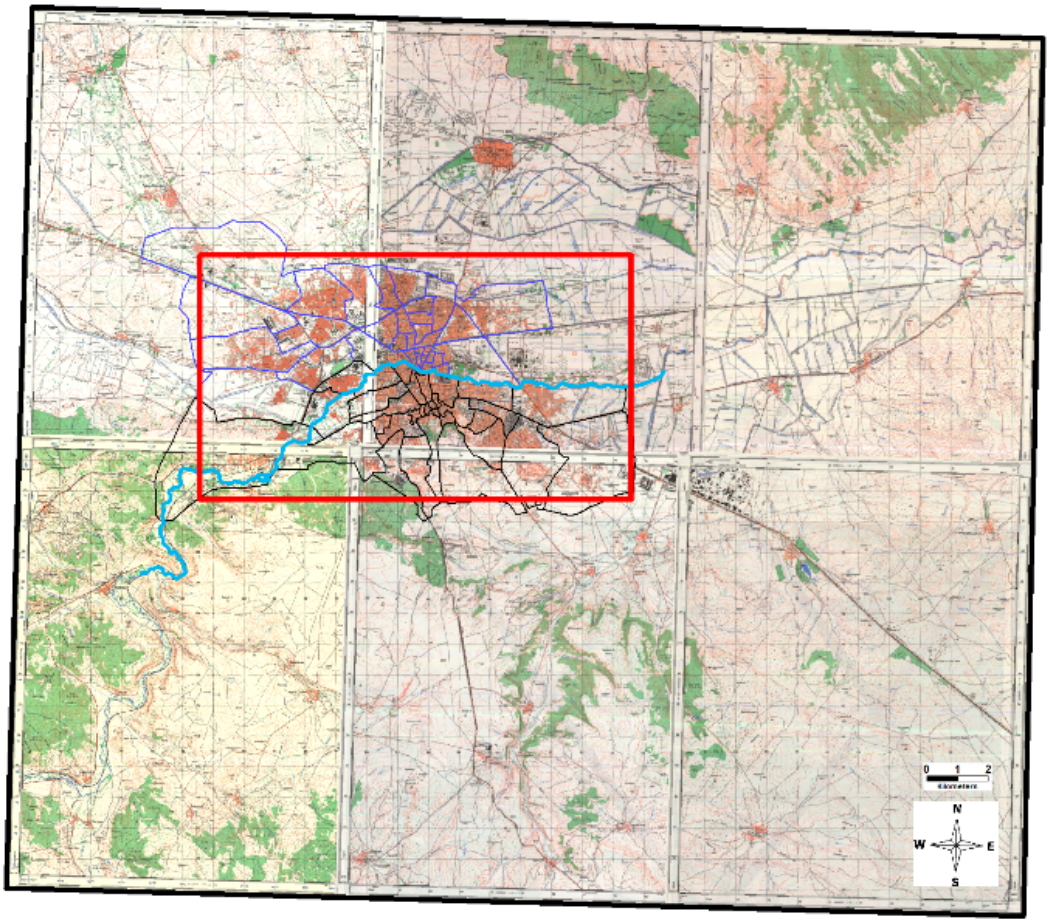


Figure 1. Field of study: Eskisehir, Turkey. The *city center* (red, small frame) and *near surroundings* (black, larger frame) are shown in a map with a scale of 1/25,000. The ragged blue line across the city center is the river Porsuk and used as a reference for each figure.

The measured values were located at their real coordinates on a digital map which is scaled, projection defined and database interactively. The IKONOS satellite image for the field of study was coordinated as a different raster map layer under the square grids drawn as a different vector map layer. In order to prevent confusion in the presentation, each class of the map features was structured as different layers. Another layer was assigned only for measured points where each point has different coordinates obtained on the field from a global positioning system device (GPS). Thus, they could be evaluated independently of other features on the map in analysis and modeling procedures. The distribution of the values over the field of study has then been modeled and their positional correlations have been extracted by using statistical algorithms [2, 3] during the analysis.

2.1 Data Collection

Night sky brightness at each point outlined below was measured using calibrated Sky Quality Meter (SQM) [4]. The SQM has 20° full width half maximum (FWHM) angular sensitivity and measures the brightness of the night sky in magnitudes per square arcsecond. All the measurements were obtained on moonless clear nights within astronomically dark hours. As a rule, the measurements were taken with the instrument pointed at the zenith, except that at one selected point in the city centre, data were collected at varying zenith angle in cardinal directions (see section 3.1). At each point in the field, five or more measurements with intervals of a few seconds were taken. Their average value, or the median, depending on the situation, was finally assigned to that particular point with coordinates recorded by a GPS.

2.1.1 City Center

For the purpose of systematic and controlled data collection, the field of study was divided into 112 regions of size 1x1 km^2 (grids) on the digital map as seen in Fig. 2. The city center was branched into two sections and the measurements were conducted simultaneously by two teams with two persons each. Data presented in this work were collected during April 16 – 23, 2012 before 24 hours local time. They were taken at, or close to, the center of each square kilometer as far as possible by avoiding temporary or irregular lights such as car lights or flashing lights.

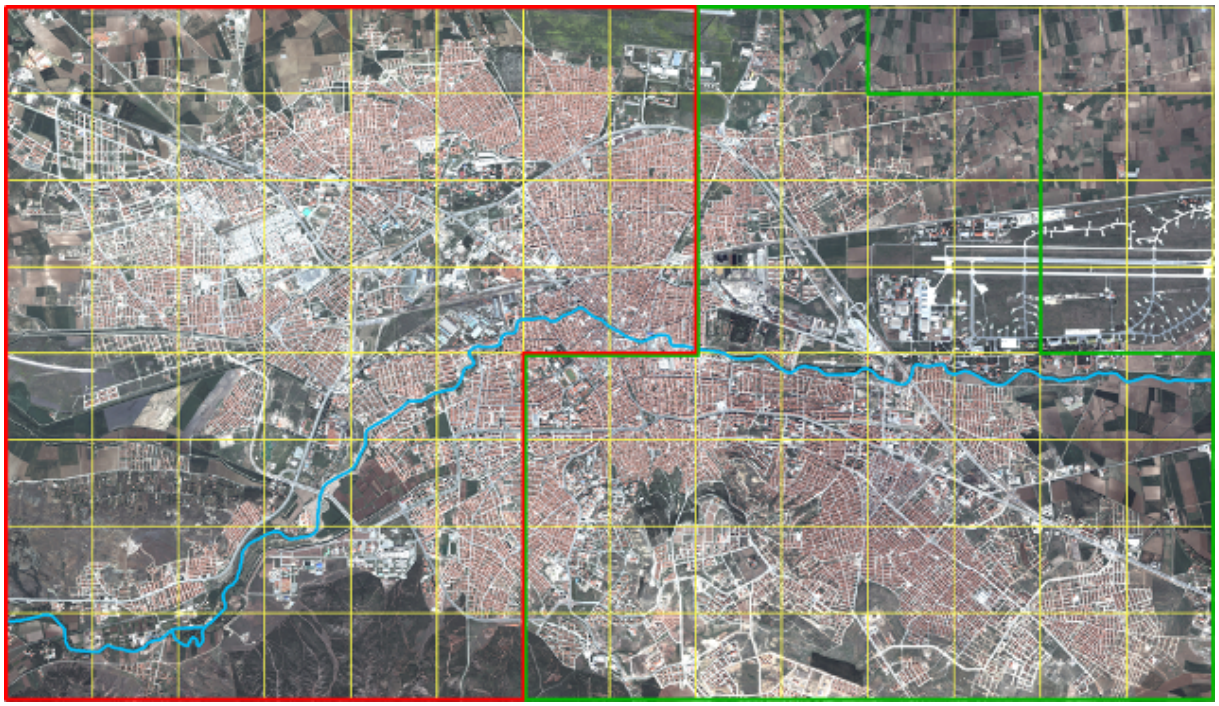


Figure 2. Field of study: city center. 1x1 km^2 grids (yellow) are positioned on the image (IKONOS) and divided into two sections (red and green) for simultaneous measurements by two teams. The ragged blue line across the map is the river Porsuk.

2.1.2 Near Surroundings

30x36 km^2 area was chosen as the field of study for *near surroundings* and the data presented here were collected during July 18 – 25, 2012 along the roads through suburbs, villages, and regions without settlements. The distribution of the points of measurement is displayed in Fig. 5. Measurements were taken just at the borders of the settlements when it was not possible to get a reliable reading inside due to high post lamps shining directly on the SQM instrument. Note that the data collection hours were not limited to 24 hours local time as in the case of city center since the effect of time dependence of the lighting is negligible for the near surroundings.

3 Results and Discussions

Night sky brightness values stored in the interactive database were compared according to their positions on the digital map. Fig. 3 shows the data points for the city center on their exact coordinates positioned on the IKONOS satellite image. There are no data in some of the pixels at the south and the north east of the city since we did not have access to those regions: they were in protection area and in military base, respectively. The minimum and maximum SQM readings are recorded as 16.15 mag/arcsec^2 (the brightest) and 20.04 mag/arcsec^2 (the darkest) respectively. This range was then divided into ten equal steps and color coded as seen in Fig. 3. When each datum is considered to

represent the sky brightness for its grid, the distribution map obtained is a low resolution one. Therefore, to evaluate the differences in more detail throughout the field of study, high resolution distribution map is obtained with the help of statistical algorithms as shown in Fig. 4 with color coded equi-brightness surfaces. Note that the color coding in Fig. 4 is different from the one in Fig. 3. As seen in Fig. 4, the data analysis technique has revealed two major *hot spots* in the south and southeast of the city, which are due to bad lighting in the newly developing areas.

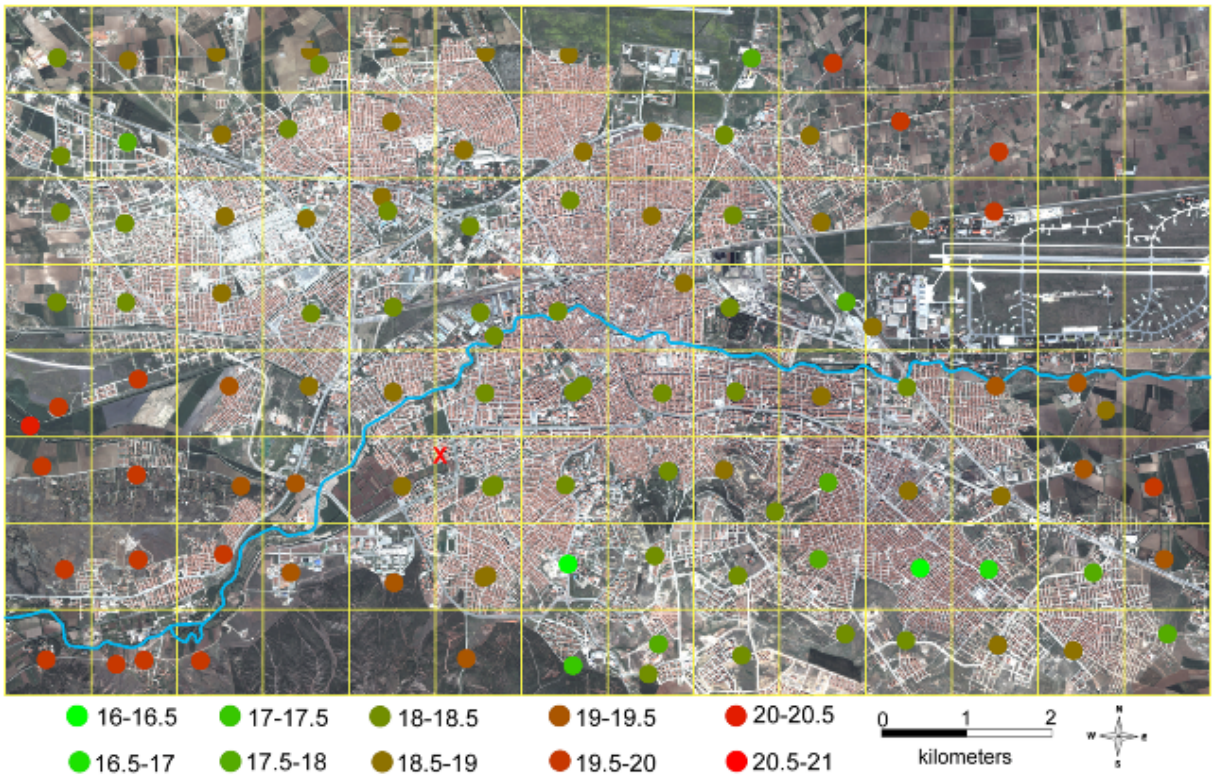


Figure 3. Distribution of the measured night sky brightness values in the *city center*. Data points are shown with color coded spots marked on their exact coordinates. SQM reading range (16 to 21 mag/arcsec^2) is divided into 10 equal steps.

In Fig. 5 and Fig. 6, the distribution of color-coded individual data points on a map with scale of 1/25,000 and the corresponding equi-brightness surfaces for the *near surroundings* are shown respectively. The minimum and maximum SQM readings are 18.52 mag/arcsec^2 (the brightest) and 21.47 mag/arcsec^2 (the darkest). This range was then divided into ten equal steps and color coded. Note that the city center and the near surroundings were separately evaluated in this study and therefore the city center values presented above have not been shown in Fig. 5 and Fig. 6. The number of data points towards the top left (north east) is intentionally increased to reveal the decreasing night sky brightness with distance from the city center in more detail. Few data points have been left outside the region presented in figures, because the method we use (Kriging based approach) in the analysis requires rectangular sections for proper data analysis. In fact, the highest SQM reading for near surroundings was recorded on the south of the lower right corner.

3.1 Estimating total luminous flux: Model

Having obtained the distribution of night sky brightness throughout the city center, we proceed to estimate the total luminous flux from the night sky, which will then be used to estimate the corresponding energy loss due to light pollution. The luminous flux Φ in *lumens* (lm) is given by

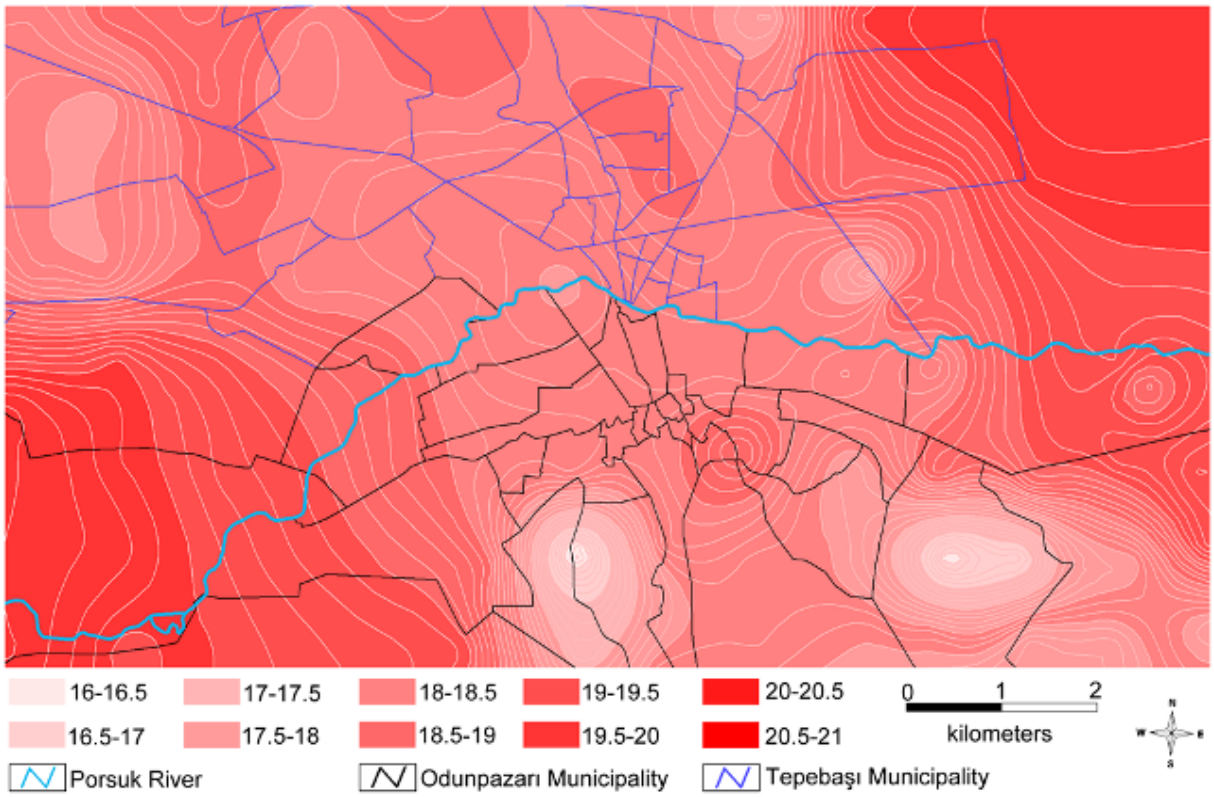


Figure 4. Equi-brightness surfaces generated from the data shown in Fig. 3. Data range was divided into 10 equal color coded steps. Blue and black lines show the borders of districts for two municipalities.

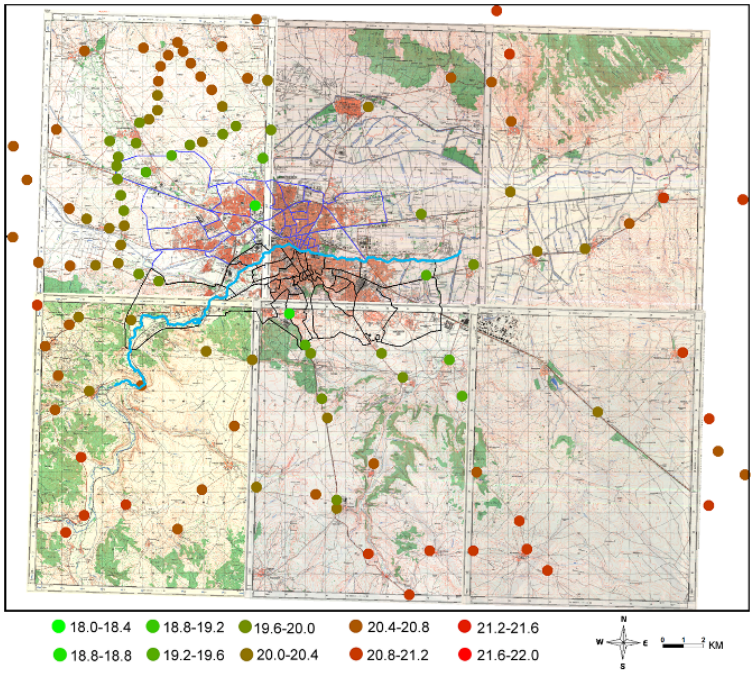


Figure 5. Distribution of color-coded individual data points for the *near surroundings*. Data range was divided into 10 equal color coded steps. The density of data points towards the top left (north east) is intentionally made higher to reveal the decreasing night sky brightness with distance from the city center in detail.

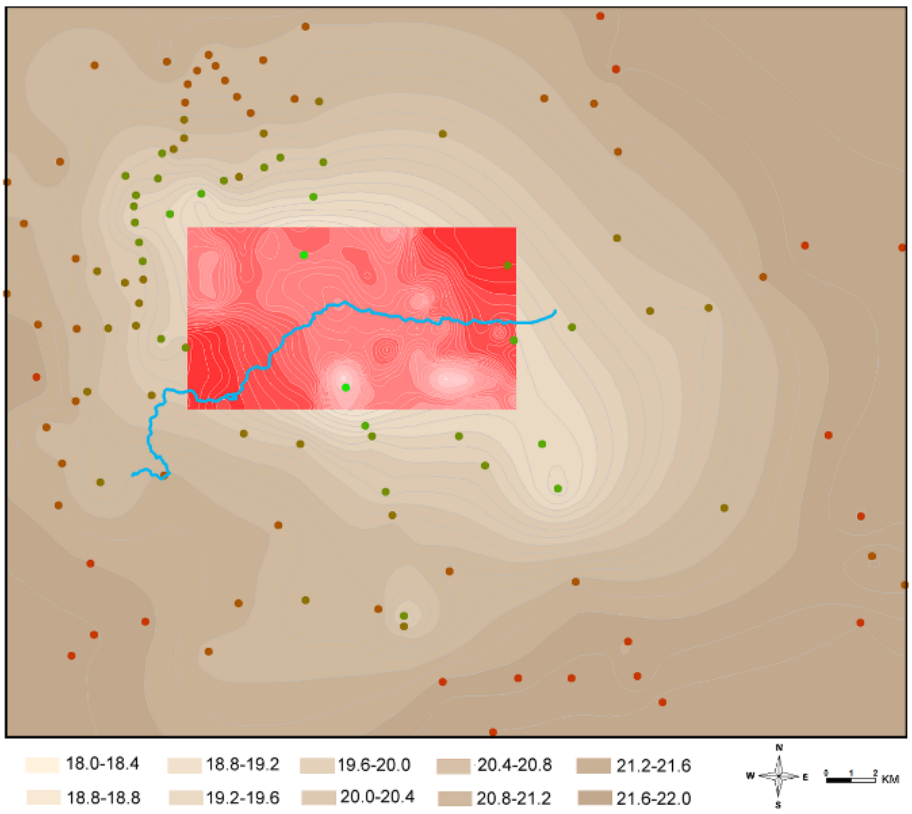


Figure 6. Equi-brightness surfaces generated from the data shown in Fig. 5. Data range was divided into 10 equal color coded steps. Red region represents the city center; it is the replica of Fig. 4.

$$\Phi = I\,\Omega = I\,2\pi\,(1 - \cos(A/2)) \tag{1}$$

where I is the luminous intensity in *candelas* (cd), A is the apex angle of the cone of acceptance of the measuring instrument and Ω is the corresponding solid angle. The luminous intensity is normally a function of wavelength; therefore, it must be integrated over the wavelengths of interest to get the total luminous intensity. Since the sky brightness recorded by the SQM instrument corresponds approximately to Johnson V filter [4], the wavelength dependence is already incorporated in the readings. Luminous intensity per unit area (i.e. cd/m^2) is then given by

$$I' = 10.8 \times 10^4 \times 10^{-0.4m} \tag{2}$$

where m is the sky brightness in *magnitudes/arcsecond*^{2} [5].

SQM instrument measures the sky brightness through a cone of full vertex angle of 20° at the instrument as mentioned before. If the sky brightness is about the same in all directions, the luminous flux per unit area from the entire hemisphere will be

$$\Phi'_0 = I'\,\Omega = 2\,\pi \times 10.8 \times 10^4 \times 10^{-0.4m} \tag{3}$$

where m is normally measured at the zenith.

In polluted cities, however, m usually varies with the zenith distance. The variation in the SQM readings versus angle from the zenith to different cardinal directions for Eskisehir is given in Fig. 7. Note that all the SQM readings plotted in Fig. 7 were taken at the same point in the city, marked by a red cross in Fig. 3. In estimating the total luminous flux from the entire hemisphere, such a variation should therefore be taken into account. Even though the dependence on zenith angle is slightly different for each cardinal direction, we may ignore any dependence on azimuth for the present purpose.

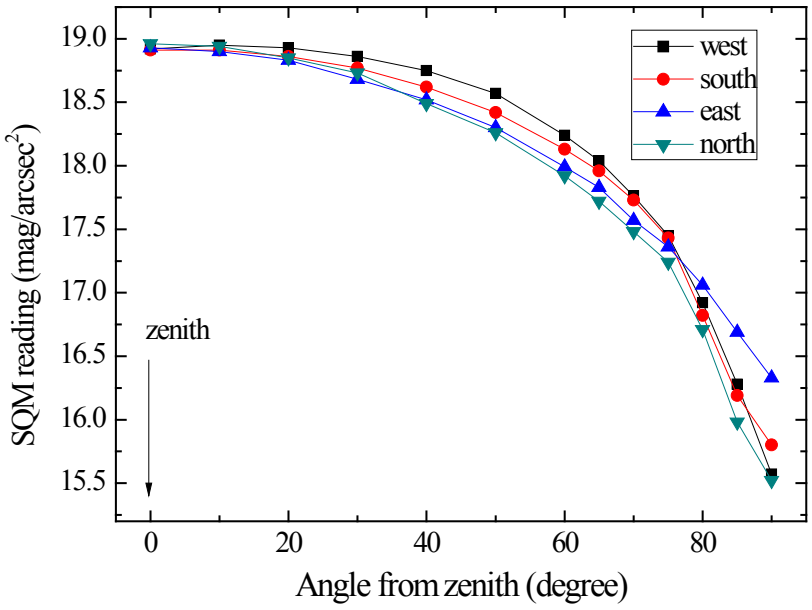


Figure 7. Dependence of sky brightness on zenith distance at cardinal azimuth angles for Eskisehir.

In the analysis, we assume that the sky brightness over the solid angle of the SQM instrument is uniform and equal to the measured value, and that dependence on azimuth is negligible. In such a case, the total luminous flux on a unit area from all directions may be estimated by summing the solid angles over azimuth at a given zenith angle and then by zenith distance. When the axis of the cone of apex angle 2θ is rotated around the vertical axis, it will trace a circular cross section 2θ wide (see Fig. 8). The corresponding solid angle will then be equal to the difference between the solid angles of apex angles 2z+2θ and 2z-2θ. When the expression for the solid angle introduced in Eq. (1) is used, the following equations are obtained;

$$\delta\Omega_z = \Omega_0 = 2\pi\,(1 - \cos\theta) \qquad \text{for } z = 0 \tag{4a}$$

$$\delta\Omega_z = \Omega_{z+\theta} - \Omega_{z-\theta} = 4\pi \sin\theta \sin z \qquad \text{for } z > \theta \tag{4b}$$

Note that for the SQM instrument $\theta = 10°$, as mentioned above. With the introduction of the zenith angle dependence, Eq. (3) is modified, thus the luminous flux from the solid angle $\delta\Omega_z$ will be

$$d\Phi'(z) = I'(z)\,\delta\Omega_z = 10.8 \times 10^4 \times 10^{-0.4m(z)}\,\delta\Omega_z \tag{5}$$

where $\delta\Omega_z$ is given by Eq.4. The total luminous flux per unit area over the entire hemisphere (Fig. 7) will therefore be

$$\Phi' = I'(0)\,\Omega_0 + I'(20)\,\delta\Omega_{20} + I'(40)\,\delta\Omega_{40} + I'(60)\,\delta\Omega_{60} + I'(80)\,\delta\Omega_{80} \tag{6}$$

For more precise analysis, one can interpolate SQM values in Fig. 7 corresponding to a smaller apex angle θ. For even more precise analysis, it is possible to represent the variation in Fig. 7 with a continuous curve and use a differential approach, where the differential solid angle corresponding to the zenith angle of dz (corresponding to an apex angle of 2dz) can be written as

$$d\Omega_z = 2\pi \sin z\, dz \tag{7}$$

by differentiating the solid angle $\Omega_z = 2\pi\,(1 - \cos z)$. We may take a step size of $dz \sim \delta z$, and write Eq. 5 as

$$\Phi'(z) = I'(z)\,\delta\Omega_z = I'(z)\,2\pi \sin z\,\delta z \tag{8}$$

This can then be numerically integrated over the continuous curve to estimate the total luminous flux.

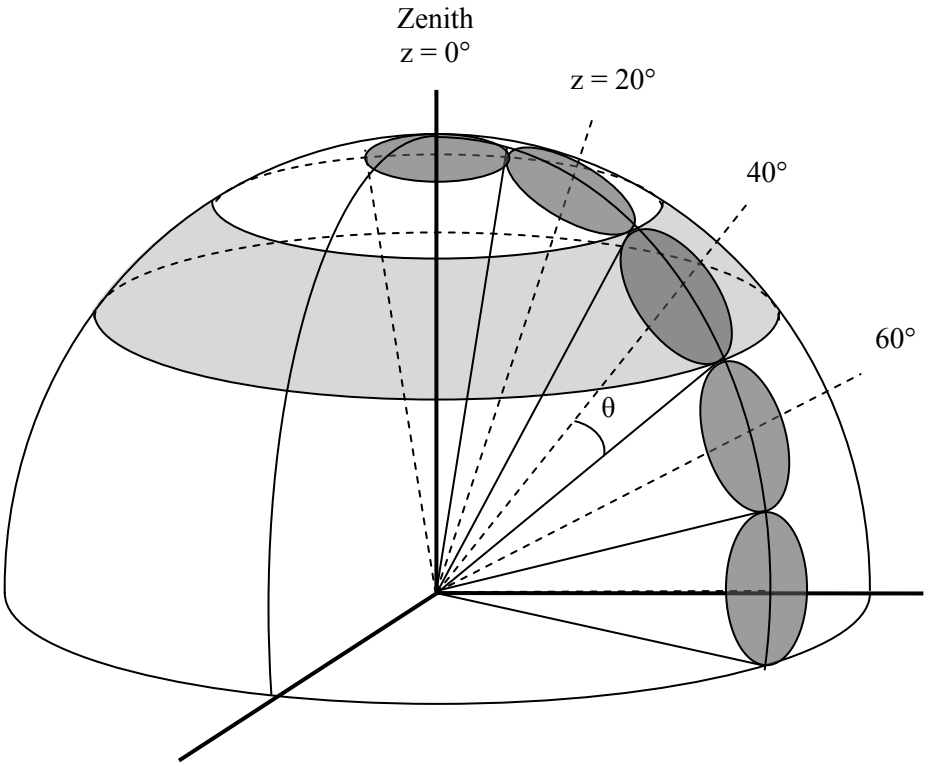


Figure 8. Schematic representation of the solid angles for light polluted cities used in our model.

3.2 Numerical calculations

Using the scheme outlined above, we estimated the total luminous flux per unit area for the point where the data in Fig. 6 were collected. (i) First, Eq. (6) was used for each cardinal direction with the observed values to estimate the total flux for the whole hemisphere. (ii) Next, the experimental data points were interpolated in such a way that the step size in zenith angle was 2° (it was 20° in the first case), expected to be more accurate. (iii) Finally, for the sake of completeness, a nonlinear continuous function was introduced as the best fit for each direction in Fig. 6; the luminous flux values were then calculated by numerical integration using Eq. (8). All the calculated luminous flux values per unit area at the point of interest are summarized in Table 1 for easy comparison. It is seen that the total flux is underestimated when the step size in the zenith angle is bigger and that the results with the smaller steps approach to the values obtained by numerical integration, which is assumed to be the most precise. To reveal the effect of the zenith angle dependence in the analysis, we define by

$$\Phi' = c\,\Phi'_0 \tag{9}$$

the ratio, c, of the total hemisphere flux obtained from Eq. 6, or by numerical integration of Eq. 8 over the zenith distance, to the hemisphere flux calculated using Eq. (3) from the night sky brightness observed at the zenith only. The calculated values of this ratio for each cardinal direction at the point marked by a red cross in Fig. 3 are also tabulated in Table 1. We suggest that one can estimate the total luminous flux per unit area from the SQM reading at the zenith only using this ratio as a correction factor in order to take the zenith angle dependence into account. It is seen in Table 1 that the average correction factor corresponding to smaller step size is ~ 4 for the Eskisehir city center. Consequently, total luminous flux over the city center can be estimated by using the data used in Fig. 3 and Fig. 4.

Table 1. Total luminous fluxes calculated from data presented in Fig. 7.

Cardinal direction	**Measured points (z = 20° steps)**		**Interpolated points (z = 2° steps)**		**Numeric integral**	
	Φ' lumens/m²	***c***	**Φ' lumens/m²**	***c***	**Φ' lumens/m²**	***c***
West	0.0571	3.11	0.0705	3.84	0.0704	4.00
South	0.0628	3.39	0.0722	3.90	0.0708	3.77
East	0.0564	3.10	0.0610	3.36	0.0610	3.41
North	0.0706	3.99	0.0864	4.88	0.0841	4.69
Average	0.0617	3.40	0.0725	3.99	0.0716	3.97

3.3 Estimating energy loss

It is now possible to estimate the energy loss due to light pollution from the results of night sky brightness measurements described above. The entire range of the SQM readings over the city center was divided into equal steps of 0.1 mag/arcsec^2 and obtained a very high resolution distribution map similar to the one in Fig. 4. This distribution map provided 124 discrete equi-brightness surfaces with different surface areas. The luminous flux in lumens for each section can be found by using the equation

$$\Phi_i = \Phi'_i \, A_i = c_i \, \Phi'_{0i} \, A_i \tag{10}$$

where A_i is the surface area of the i-th section and Φ'_i is the corresponding luminous flux value derived from SQM readings as described above. Assuming that the correction factor is the same for each point over the city center, total luminous flux from all directions was calculated from

$$\Phi_{\text{total}} = \sum_{i=1}^{124} \Phi'_i A_i = c \sum_{i=1}^{124} \Phi'_{0i} A_i \tag{11}$$

The total luminous flux for the Eskisehir city center comes out to be $\Phi_{\text{total}} \sim 1.03 \times 10^7$ lm when the correction factor is taken as 4 (see Table 1). Note that the value obtained for total luminous flux corresponds to the amount of light emitted into, and reflected from, the atmosphere. Therefore, energy loss calculated from the night time sky brightness measurements such as those reported here will be a minimum since the light directly transmitted to the outside of Earth's atmosphere and atmospheric absorption are not taken into account: It should be noted that around sixty to eighty percent (depending on the region) of the light directly transmitted to the outside of Earth's atmosphere for the spectral range of our interest [6]. On the other hand, measured values include the natural sky background but this is small enough to ignore for the present purpose.

Considering the total luminous flux calculated above, $\sim 1.03 \times 10^7$ lm, and the fact that the population of the Eskisehir Metropolitan Municipality is around 650.000 [7], the energy loss (in terms of luminous flux) due to the light pollution is found to be 15.85 lumens per person at an instant of a time. This value corresponds to ~0.144 megalumen-hour per person per year: It is approximately equivalent to a 100W incandescent lamp operated for 5-hours per day for a month if the lamp is assumed to have a efficacy of ~10 lm/W [8, 9]. It is known that different types of light sources (e.g. incandescent, fluorescent, sodium vapor pressure, light emitting diode, etc.) are used for outdoor lighting and that each has different efficacies ranging from 7 to 180 lm/W [8, 9]. Assuming, however, that the average efficacy for electric light sources in the Eskisehir city center is ~60 lm/W and the average electricity consumption for a household per month is 180 kWh [10], we have calculated that the total energy loss is equivalent to the total electricity consumption of ~680 households for a month. As of March 2013, the unit price without service charges and taxes for the electricity is ~0.1 €/kWh; this means that a total of about €155.000 is wasted annually from the Eskisehir city center.

4 Conclusions

Night sky brightness mapping and modeling of Eskisehir city center and its surroundings are realized as a pilot project for rendering the Turkey's night sky brightness map. This detailed study was carried out by means of RS & GIS techniques. Total energy loss for the city center due to light pollution has been estimated by a numerical method applied to the night sky brightness measurements as function of zenith distance. The ratio between the total luminous flux based on the observed sky brightness as a function of the zenith distance and that based on the total luminous flux at the zenith only is calculated at a selected point in the city. It is suggested that this ratio may be used to estimate the total luminous flux per unit area from the SQM reading at the zenith at other points in the city. The total energy loss for Eskisehir city center is found to be ~0.144 megalumen-hour per person per year and it is worth about €155.000 annually.

Acknowledgements

Authors would like to thank Anadolu University Earth and Space Sciences Institute, and Istanbul Kultur University for their financial support and for providing the measuring devices.

References

[1] Z. Aslan, O. Gölbaşı, D. Koçer, Z. Tunca, E. Işık, A. T. Yelkenci, D. Bağdaş, A. Devlen, T. Özdemir, T. Özışık, K. Yelkenci, T. Demirciler, U. İkizler, A. Karamahmutoğlu, M. Koçer, M. Mutlu, Ü. F. Özyar, H. Yüzer, (2011): Measuring Light Pollution in Turkey in the proceedings of 8th National Meeting on Illumination, April 14-15, 2011, İstanbul, pp 69–74 , ISBN: 978-975-561-392-5 (in Turkish).

[2] G. Wahba (1990): Spline Models for Observational Data. **59**. SIAM. p. 162.

[3] H. Bayraktar, F. S. Turalioglu (2005): A Kriging-based approach for locating a sampling site—in the assessment of air quality, SERRA, 19 (4), 301-305.

[4] P. Cinzano (2005): Night Sky Photometry with Sky Quality Meter. First draft, ISTIL Internal Report n. 9, v.1.4, ISTIL, Thiene, http://unihedron.com/projects/darksky/sqmreport_v1p4.pdf

[5] http://unihedron.com/projects/darksky/magconv.php

[6] T. G. Kyle (1993): Atmospheric Transmission, Emission and Scattering (Pergamon)

[7] Turkish Statistical Institute, 2012 (http://www.tuik.gov.tr)

[8] D. Schreuder (2008): Outdoor Lighting: Physics, Vision and Perception (Springer)

[9] N. Lechner (2009): Heating, Cooling, Lighting: Sustainable Design Methods for Architects (John Wiley & Sons)

[10] Osmangazi Electricity Distribution Corporation (http://www.osmangaziedas.com.tr) by personal contact.

An online mapping of sky radiance contribution and sensitivity from sky radiance model ILLUMINA

Martin Aubé[1]

[1] *Cégep de Sherbrooke, Sherbrooke J1E 4K1, Canada*
tel: +819 564-6350-4146, e-mail: martin.aube@cegepsherbrooke.qc.ca

Abstract

Propagation of light pollution in the atmosphere is a complex and non-linear process because of the relative complexity of the surrounding environment. This propagation is dependent on inhomogeneities in the light fixture inventory (radiant power, angular photometry, lamp pole height), on the spatial variability of the spectral ground reflectance and on the topography. It is also sensitive to the aerosol atmospheric content (concentration, types, vertical profile) and to the presence of small obstacles like trees and buildings. We have shown in our previous works that in many situations, 2nd order scattering is important. To solve explicitly such a complex problem, we designed a numerical model and after an extensive validation process, this model is now mature to be used as a high level decision tool to help scientists or local authorities to restrict or reduce sky brightness over their sites. In that paper we will show you the potentiality of two very innovative output maps generated by the model. The first gives the relative contribution of each part of a territory to the sky brightness at a given site and line of sight. The second map give the most sensitive places where any light fixture removal will have an important reduction effect. The maps are now available on an interactive web geoserver and we will use this system to show you maps for Observatorio del Teide in the Canary Islands , Spain.

1 Introduction

In this study we used the model ILLUMINA [1] [2] to compute the sky radiance at a given observing site for many viewing angles and wavelength including the 2nd order of scattering. We also calculated with the same model, two maps for each angle and wavelength: 1- the spatial origin or contribution of the calculated radiance, 2- the spatial sensitivity which is the ratio of the first map over the local radiant power. In the following sections, we will give some details about the model and the web portal which is used to access model outputs.

2 Input data

Basically the model consider the spatial heterogeneity of the ground and light inventory properties, and is calculating 1st & 2nd order of scattering from molecules and aerosols with and without reflection on the ground. The model requires many input data and some of them are coming from satellite imagery product. Some others are single parameters, and some need the help of a local expert who has a good knowledge of the typical light fixtures used as a function of the territory parts. Satellite imagery is used to determine the ground reflectances, the upward radiance and the topography. Reflectance is extracted from MODIS satellite sensor [3], upward radiance is measured with the DMSP-OLS satellite [4], and the data from the Shuttle Radar Topography Mission [5] (SRTM) data provides the topography. We are also using the MODIS data for distinguishing between ground and water surfaces. By combining the ground reflectance, the DMSP-OLS radiance, the uplight fraction, the zenith light output pattern value, and the spectral type from the typical mix of luminaires for each part of the territory, we can get a good estimate of the gridded spectral radiant power with the help of equation 1.

$$\Phi = R_\lambda \left(\frac{I_{OLS}}{\frac{1}{\pi}\left(1 - F_{up}\right)\rho + LOP(0)} \right) \quad (1)$$

Where Φ is the spectral radiant power (W/nm), R_λ is the calibration constant for each spectral line considered, I_{OLS} is the OLS radiance, F_{up} is the upward flux fraction, ρ is the ground reflectance, and $LOP(0)$ is the value of the light output pattern toward zenith. Figure 1 show the original DMSP-OLS radiance map (pane (a)) and the MODIS band 4 reflectance (pane (b)). Panes (c) and (d) of the same figure is showing two radiant power maps (respectively for Hg 546 nm line and Na 569 nm line) derived from equation 1. Note that the the total radiant power given by equation 1 is splitted in two submaps, one for Hg lines and the other for Na lines and the fraction attributed to each submap is estimated with the help of a local expert who has a good idea of the proportion of mercury/metal halides lamps vs sodium lamps all over the territory. In the case shown below the expert identified 3 caracteristic zones with different LOPs and Hg over Na ratio (La Palma, Tenerife west, and all other places). The important variability in the characteristics of the light inventory between these 3 zones is the result of a local abatement to protect the sky quality of Observatorio del Roque de los Muchachos on the La Palma island (Ley del cielo). In fact no Hg-based lamps can be installed on the La Palma

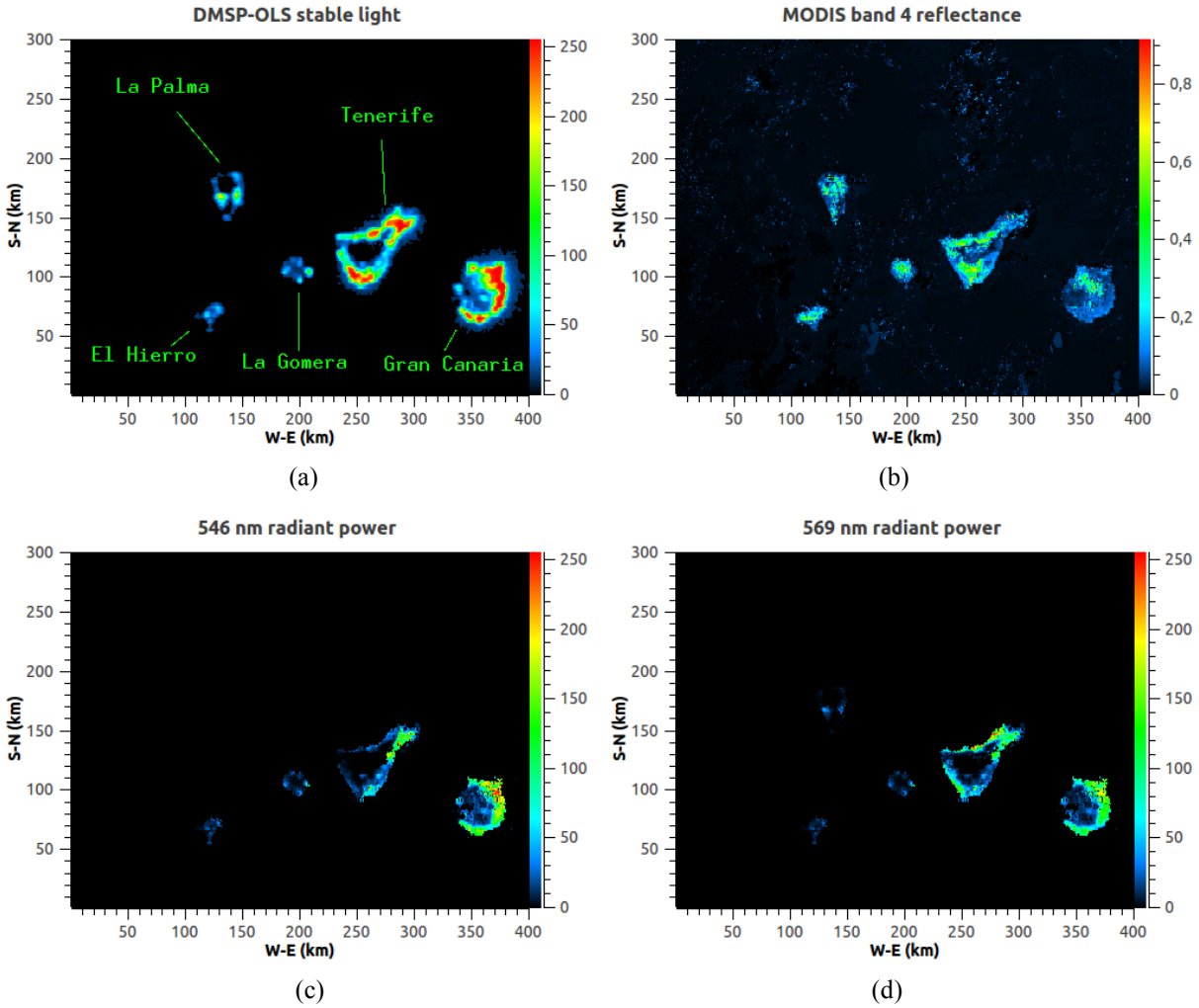


Figure 1: Example of gridded input data. (a) DMSP-OLS 2009 stable light, (b) MODIS bans 4 reflectance, (c) lamp radiant power per km2 in the Hg 546 nm line, (d) lamp radiant power per km2 in the Na 569 nm line

island and their number are highly reduced on the western side of Tenerife Island (part of Tenerife facing La Palma). This difference in the light inventory can be clearly seen if we compare visually panes (c) and (d) of figure 1. Simulations have also been conducted for two periods (before and after midnight). As DMSP-OLS data are acquired before midnight we used again the information given by the local expert to estimate the after midnight reduction of the radiant power for each zone.

In the model calculation process, the MODIS reflectance is used to calculate the contribution of the light reflected by the ground. As other input data, we need to know the ground level air pressure, the aerosol mix (maritime, rural, or urban according to [6]), the relative humidity, the typical distance between subgrid obstacles and typical obstacles height. These latest information are determined with the help of a local expert that has a good knowledge of the ground reality. More details about model input data can be found in [7].

3 Modeling parameters

Our model is only capable of determining indirect light from the scattering atmospheric elements. To simulate the sky spectral radiance for a given observation site and viewing angles, the calculation acts similarly to a ray tracing software. For each ground grid element, the total spectral radiant power in a given spectral line is calculated from the light inventory. The average light output pattern is also computed. Then many light rays leave this grid cell to finally reach the observer line of sight after experiencing 1- first order scattering, 2- second order scattering, 3- first order scattering after reflexion on the ground, and 4- second order scattering after reflexion on the ground. The second order scattering is time consuming, and then we are restricting this calculation in a 4 km action radius with respect to the line going from the ground element to a scattering cell of the line of sight. As this radius is outlining a volume, the number of calculation is considerably increased so that we need to optimize the calculation by selecting randomly a subset of the volume elements that has to be computed (for the standard model product we are using a ratio of 1 voxel over 71). But even if this statistical and spatial selection of scattering cell allow a significant reduction the computing time, this time remains very long. So that we also implemented a statistical selection of the ground elements that have to be computed. This selection is based on a weight function which is proportional to the radiant power of the ground element radiant and inversely proportional to r^2, the distance between the ground element and the observer. But inside a radius of 25 km to the observer, all the ground elements are considered to insure a better accuracy in this critical region. When a ground element is retained for calculation, we are considering a cluster of adjacent cells, which number is increasing with the distance and with the reduction of local radiant power. Then we are combining their radiant power values in order to make only one computation for all adjacent cells. This statistical selection reduces the computation time by a factor of ~100 so that a complete calculation over a domain of $\sim 10^5$ km^2 takes about 2-3 days. For comparison, the complete calculation takes only a few seconds when we neglect the 2nd

Table 1: Standard parameters set use for the web portal database

Parameter	Values	Units
Relative humidity	70	%
Ground pressure	101.3	kPa
Spectral line	436, 498, 546, 569, 616	nm
Aerosol optical depth	0.05, 0.1, 0.2, 0.5, 1.0	-
Elevation angle	15, 20, 30, 40, 60, 90	Deg.
Azimuth angle	0, 15, 30, 45, 60, 75, 90, 105, 120, 135, 150, 165, 180, 195, 210, 225, 240, 255, 270, 285, 300, 315, 330, 345	Deg.
Grid mesh	1	km
Typical domain size	~100 000	km^2

order of scattering. The standard ground resolution is 1 km. Default values for the ground level pressure is 101.3 kPa and we are using 70% as a standard relative humidity. For a given observing site, the model is doing a complete run for 6 zenith angles, 24 azimuthal angles, 5 Aerosol Optical Depth (AOD) and 5 spectral lines. The standard parameters used for the system are summarized in table 1. The computation for a given site and period require around 9000 days on a single CPU. Hopefully, we have an easy access to Calcul Canada high performance computing infrastructure to calculate such experiment.

4 Model output and web portal

As stated earlier, the model is calculating a value of the sky radiance for each site, viewing angle, aerosol optical depth, and wavelength. But unfortunately, this value is not calibrated by default. This is because that the DMSP-OLS data used are not calibrated. To overcome this problem, one possible way is to acquire many sky spectral radiance measurement for a given site and the establish a calibration coefficient for each wavelength. That kind of calibration process consumes a lot of time so that it is not done by default. For that reason we decided to not display this value for the first release of the web portal (version 1). Figure 2 show a screenshot of the portal web interface. This interface requires the selection by the user of the map type (contribution or sensitivity), the site/period desired,

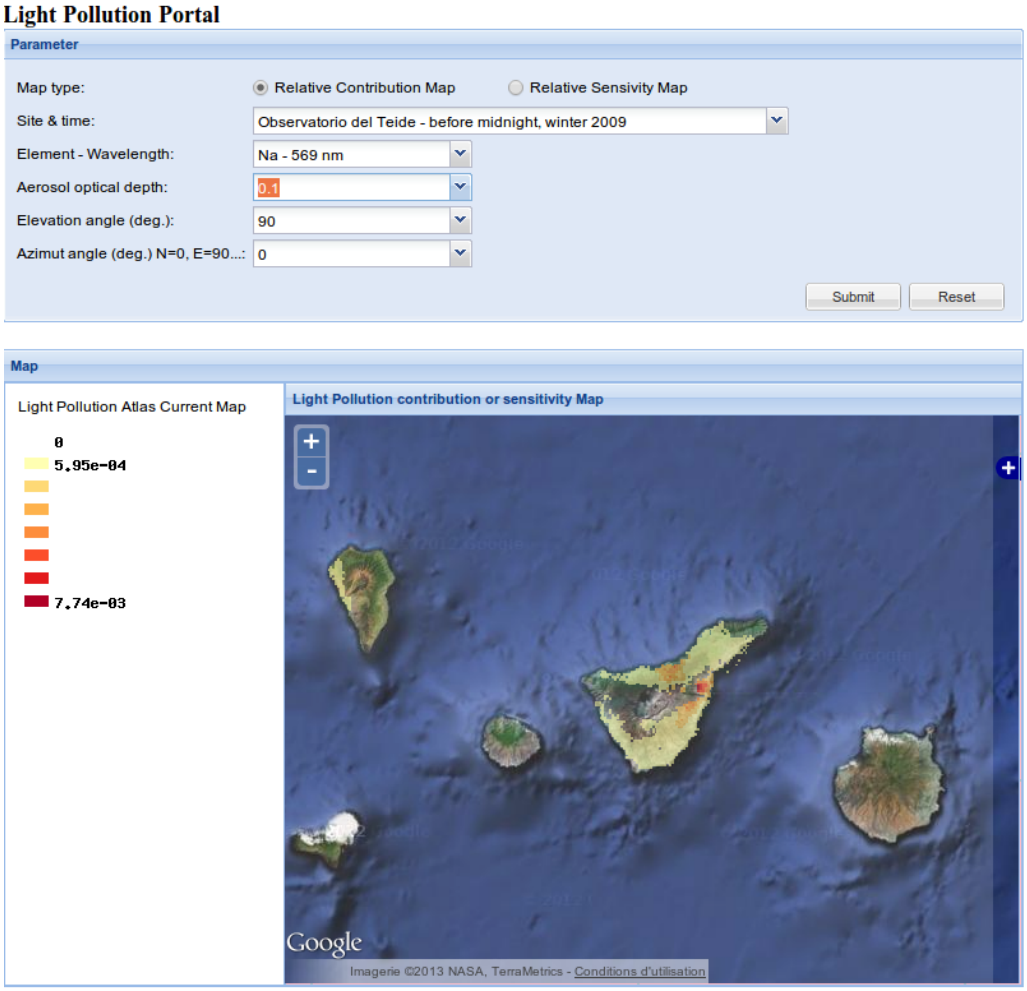
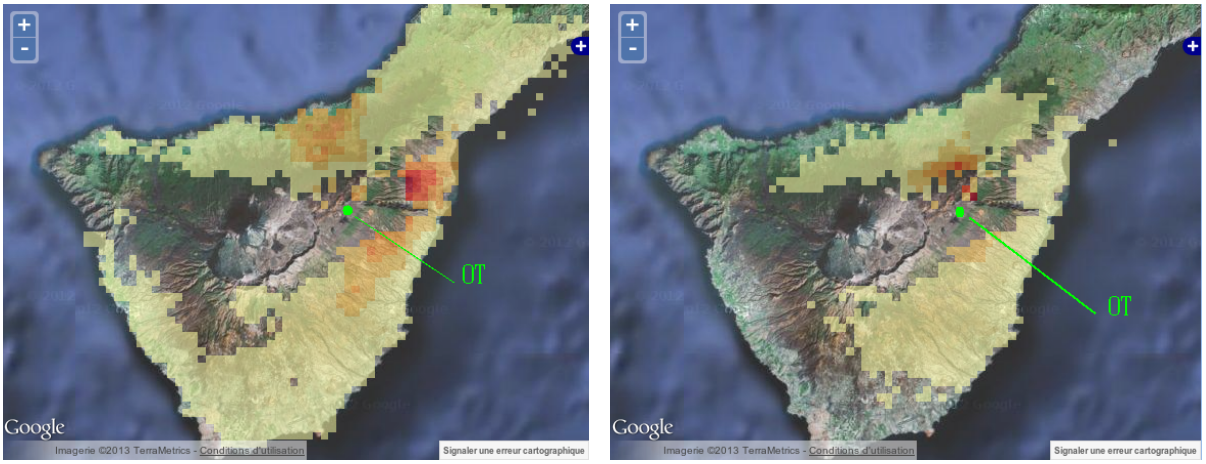


Figure 2: Online web portal interface version 1. The map show here is the before midnight contribution map for zenith at OT with an AOD of 0.1 and for the Na 569 nm spectral line. The map is an overlayed on the google maps satellite imagery.

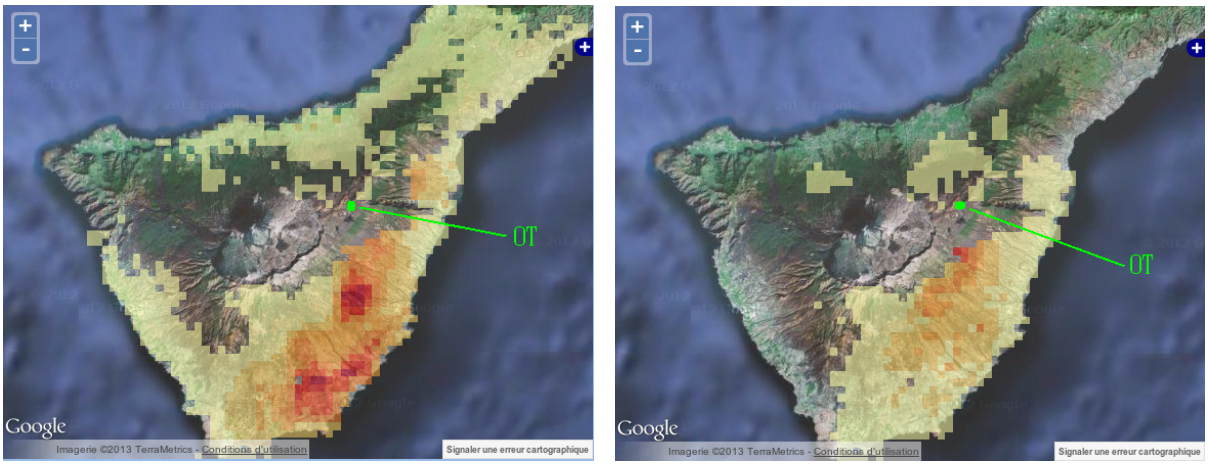
the wavelength, the aerosol optical depth, and the elevation and azimuth angles.

The portal is located at URL http://galileo.graphycs.cegepsherbrooke.qc.ca/atlas/. Up to now we have three site covered by the portal: 1- Observatorio del Teide (OT) and 2- Observatorio del Roque de los Muchachos (ORM) in Canary Islands, along with 3- Observatoire du Mont-Mégantic (OMM) in Québec, Canada. For the first two observatories we already know the relevant calibration coefficient that have been determined during a sky spectral radiance monitoring experiment made in 2010 with the Spectrometer for Aerosol Night Detection (SAND) [7]. We do not have the same database for OMM. It is in our objective to add the feature of displaying the calibration coefficient, along with the non calibrated radiances, on the web portal (version 2). In its current version 1, the portal displays only 2 maps for each site, period, viewing angle, wavelength and aerosol optical depth. As stated before the first map is the contribution map giving the relative contribution of each grid element to the modeled radiance. This map says from where, and in which proportion, the modeled radiance is coming from. The second map is obtained by taking the ratio of the contribution map over the original installed radiant power. We called this map the sensitivity map. In fact this map tells us the relative contribution per unit of power of each ground element to the sky radiance. This map is very useful because the highest values are the places for which a light fixture addition or removal will have the largest impact on the resultant sky radiance. So it is a very powerful tool for local authorities in order to identify the place they have to focus on when it is time to protect the sky quality or to enhance it by the removal of



(a) (b)

Figure 3: Before midnight zenith 569 nm contribution (a) and sensitivity (b) maps for OT with AOD=0.1.



(a) (b)

Figure 4: Same as fig. 3 but at an elevation angle of 20 deg. toward south (azimuth 180).

some lighting devices. As an example, if a limited amount of money is available to proceed to a light fixture removal or replacement, the removal/replacement must begin in priority on the site showing the highest value on the sensitivity map (red pixel on panes (b) of figures 3 and 4). That way, the sky brightness reduction is optimized inside the financial limits available.

Figure 3 and 4 are showing typical maps for the contribution (a) and the sensitivity (b). Both figures correspond to Observatorio del Teide (OT) at Na 569 nm line. Figure 3 is for a zenith observation while fig. 4 correspond to a line of sight at 20 degree above horizon toward south. By comparing equivalent panes of fig 3 and 4 it is easy to see that, when the observer is observing nearer to the horizon, the highest values on the maps appear concentrated on the side corresponding to the observing orientation.

5 Conclusion

The aim of this paper was to inform the scientific community about the availability of a high level decision tool in order to protect the night sky quality. This tool is now freely accessible via a web interactive mapping portal. The data product is now available thanks to many years of research spent to implement and validate a sky brightness simulation model. Up to now only 3 sites are available on the portal but as time will go on, many other sites will be added to the system. In order of priority, we are presently working on maps generation for the region of 400 km x 300 km centered on Madrid, Spain. Once completed, we will continue with Mount Palomar Observatory, USA, and with the Berlin area, Germany. In the future, we plan to add as much sites as possible and we invite scientists to make suggestions for the addition of new sites by contacting us. Suggestions should be accompagnied of a scientific justification in order to help us to determine the execution priority. The availability of a sky brightness measurement database for the proposed site is clearly an advantage.

Acknowledgments

We want to thank Jean-Denis Giguère who helped a lot in designing the web portal engine, and Javier Díaz Castro who was our local expert for the Canary Islands. Without their contributions, this work had not been possible.

References

[1] M. Aubé, L. Franchomme-Fossé, P. Robert-Staehler, V. Houle (2005): Light Pollution Modeling and detection in a heterogeneous environment: Toward a Night Time Aerosol Optical Depth Retreival Method, Proceedings of SPIE, 5890, 248-256.

[2] M. Aubé (2007): Light Pollution Modeling and detection in a heterogeneous environment, Proceedings of Starlight a common heritage, 351-358.M. Aubé, and M. Kocifaj

[3] E. F. Vermote and A. Vermeulen (1999): Atmospheric correction algorithm: Spectral reflectances (MOD09), ATBD version 4.0., NASA contract NAS5-96062, http://modis-sr.ltdri.org/MAIN_PUBLICATIONS/Papers/atbd_mod09.pdf

[4] ngdc.noaa (2010) http://www.ngdc.noaa.gov/dmsp/downloadV4composites.html

[5] T. G. Farr, P. A. Rosen, E. Caro, R. Crippen, R. Duren, S. Hensley, M. Kobrick, M. Paller, E. Rodriguez, L. Roth, D. Seal, S. Shaffer, J. Shimada, J. Umland, M. Werner, M. Oskin, D. Burbank, D. Alsdorf, (2007): The Shuttle Radar Topography Mission, Reviews of geophysics, vol. 45, 33 pp.

[6] E. P. Shettle and R. W. Fenn (1979): AFGL-TR-79-0214, Environmental Research Papers No. 676.

[7] M. Aubé, and M. Kocifaj (2012): Using two light-pollution models to investigate artificial sky radiances at Canary Islands observatories, Mon. Not. R. Astron. Soc. 422, 819–830.

Modelling sky glow from luminaire designs

Chris Baddiley

Scientific Advisor to the British Astronomical Association Campaign for Dark Skies.
Ferney Cottage, Mathon, WR13 5PP, UK. e-mail:cj.baddiley@physics.org

Abstract

In the UK, Skyglow illuminates the sky right into the rural environment between one town and the next. Most of this is caused by streetlights. Until this voluntary work, done over a period up to 2007 , the UK lighting industry was unaware of the physics of light scattering and how it can be controlled by specific streetlight luminaire design. A mathematical model was written by the author that reads industry standard photometry files of streetlight designs and calculates reflections and scattering off road and surrounds, including verges etc, into the sky. It then calculated the downward scattering integrated along the observer's viewpath, as Skyglow. It gives results for any atmospheric visibility, view distance, view elevation and azimuth angle. Different luminaires were compared in similar circumstances and conclusions drawn about the benefit of certain designs. Studies include tilted Low Pressure Sodium SOX, Cut Off High Pressure Sodium SON in both polycarbonate and curved tempered glass types, Full cutoff flat glass SON, and the effect of changing to white light sources. Critically, light is scattered by aerosols predominantly in the forwards direction, and lesser but still importantly for lighting design, in the reverse direction, while very little sideways. Low angle light above the horizontal, has the largest distance to travel through the lower atmosphere and scatter, and so is dominating light pollution, and yet could be easily controlled. With careful adherence to the design principles suggested by this work, the industry could incrementally raise lighting control standards, and so there could be a return of dark skies in rural and suburban areas. A Guidance note 'Towards Understanding Skyglow' based on this work, was published by the Institution of Lighting Engineers in 2007, at their conference. The work presented here covers some of the modelling work by the author that led to that document, and how now guideline photometry distribution tables are being considered by some lighting designers. The UK Highways Agency incorporated these ideas in their policies. The author has recently done a dark sky survey study for an area of outstanding natural beauty which appears to confirm the principles of the modelling work.

1 Introduction

Over the UK, skyglow from streetlights is the background to the sky right into the rural environment between one town and the next. Figure1 is a view north-east towards Worcester and Droitwich from the Wyche cutting on the Malvern Hills, showing streetlights and some other lighting with significant components above horizontal. This unwanted and unnecessary lighting above the horizontal scatters forwards over large distances into the rural countryside, and here is illuminating the sky over the far side of hill from which this image was taken. This can be seen in subsequent all sky images in the survey section of this paper, taken from that far side.

This paper outlines the skyglow modelling program designed to compare the skyglow from different designs of luminaires at rural distances as a function of view angle on the sky. The results of this work in various forms has been presented at a number of European and other international conferences on light pollution and can be found in several proceedings and on the Internet. (Annex 2a, refs 1-6). Primarily, it was a used as the basis of a guidance note 'Towards Understanding Skyglow' (ref 4), which was published by the Institution of Lighting Engineers in the autumn of 2007. For this reason, the physics is described for each part of the program, but not the standard equations and tracing and integrating code in detail.



Figure 1. View north-east towards Worcester and Droitwich from The Wyche cutting on the Malvern Hills, showing streetlights and some playing field lights all illuminating above horizontal.

2 Description of the model

This section describes the various components of the model. A full list of the model inputs and outputs is covered in annex 1.

2.1 File reading and surface descriptions

The model reads lighting industry-standard photometry files in several possible file formats. The sources used for its development listed at the end of this paper (Annex 2b). It takes three luminaire designs at a time for comparison purposes. The program traces rays from the selected luminaire interpolating the photometry datafiles. It determines the light path for each facet angle on the ground. It finds the surface reflection value for the incident and reflection angle and the amount of scatter.

2.2 Surface reflections and scattering

Surface reflections increase away from normal incidence . The peak specular reflection angle is equal to that of the angle of incidence, with a small spread from variation of angle of small surface facets from the normal. All surfaces become highly reflective close to grazing angle. There is also small back scatter peak at the same angle. The scattering off surfaces does effectively the reverse, having a cosine distribution peaking at normal incidence and falling to zero at grazing incidence, see figure 2. This effectively follows the projection of a surface area into the view direction. The combination as a function of incidence angle is the bi-reflection distribution function (BRDF), shown in figure 3.

The program ray traces the emergent beam back to the sky for each possible skyward gamma angle and C angle. Three routes are shown in figure 4. Direct upward, ground reflected, and back ground with wall reflected, paths. Only the specular reflection angle routes are calculated. It was not practical to include all possible scatter routes (such as the thin dotted path) caused by scatter facet angle distributions as a convolution would not be expected to change the overall distant view total result.

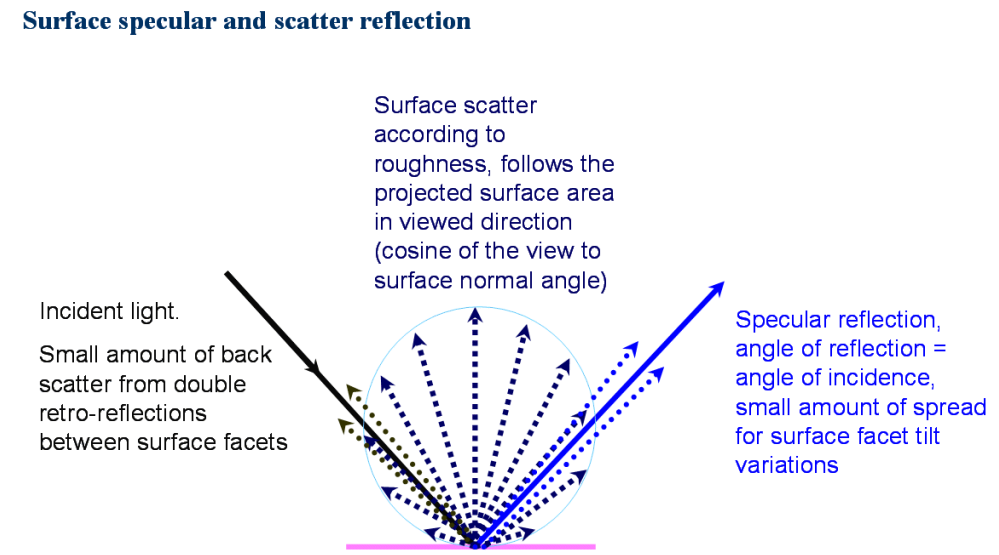


Figure 2. Scatter with reflection has several components . Specular reflection angle of reflection = angle of incidence, with a small amount of spread for surface facet tilt variations. A small amount of back scatter from double retro-reflections between surface facets. Surface scatter according to roughness, follows the projected surface area in the viewed direction (cosine of the view to surface normal angle).

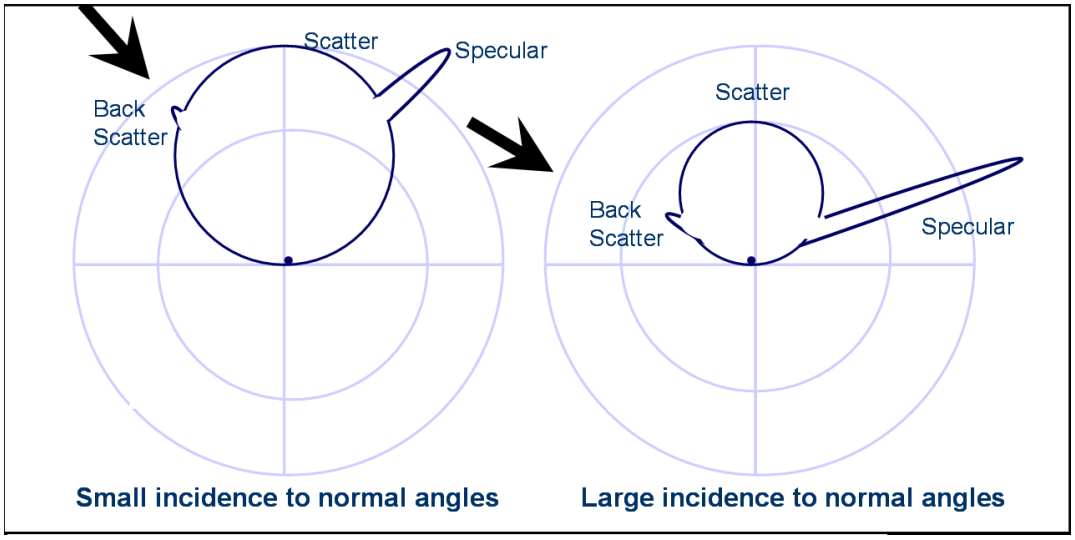


Figure 3. Bi-directional Reflectance Distribution Function, showing dependence of scatter on cosine of incidence and cosine of view projection angle (near Lambertian), and specular dependence on incidence angle increasing towards grazing angle.

The program adds in any direct radiance from the luminaire to the sky at that same angle. Two surfaces are allowed in the horizontal plane, namely a road of given reflectivity and surface roughness, and a grass surround of given reflectivity and roughness, but various surfaces can be substituted. If buildings are present, then reflections off vertical surfaces in combination, and obstructions are included in the trace.

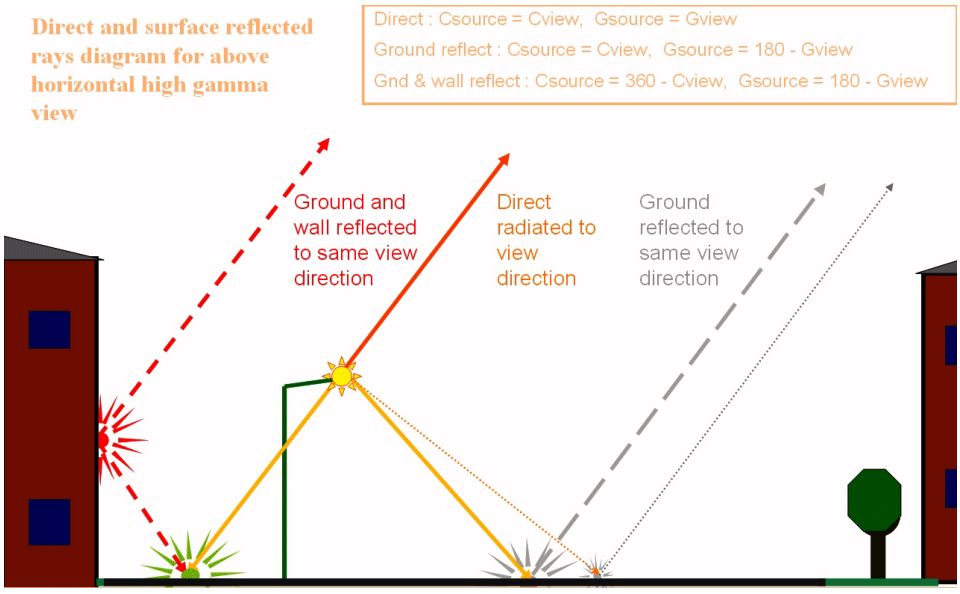
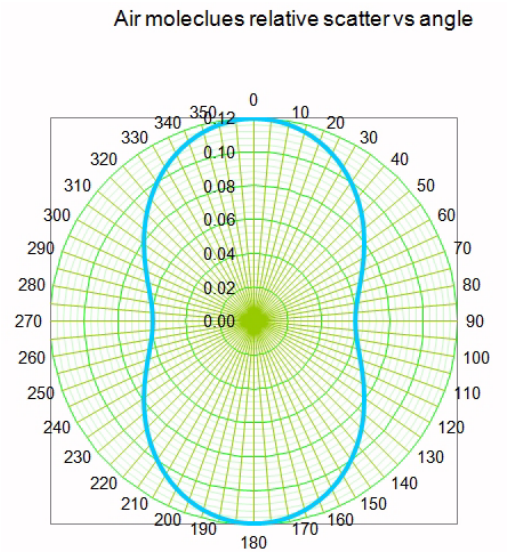


Figure 4. Direct and surface reflected rays diagram for above horizontal high gamma view. Three routes are shown. Direct upward, ground reflected, and back ground with wall reflected, paths. Only the specular reflection angle routes are calculated.

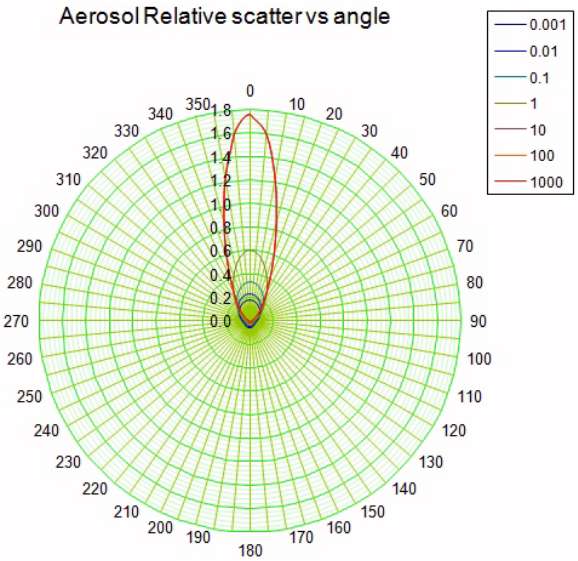
2.3 Atmospheric scattering mechanisms

Rayleigh scattering applies to air molecules, being smaller than the wavelength of light. They have equal probability of scatter forwards and backwards, with a lower figure sideways, as shown in figure 5. It is strongly wavelength dependent, predominantly in the blue (reciprocal wavelength to the fourth power), accounting for the blue daylight sky.



$$P(\psi) = (3/(16\pi)(1+\cos^2\vartheta)$$

Figure 5. Rayleigh scattering. In this diagram the light path is in the zero direction. The scattering is predominantly forwards and backwards with some sideways. It is strongly blue wavelength biased.



$$P(\vartheta) = (1-g^2)\left[\frac{1}{(1+g^2)-2g\mu)^{3/2}} + f\frac{(3\mu^2-1)/2}{(1+g^2)^{3/2}}\right]$$

Figure 6. Mie scattering. In this diagram the light path is in the zero direction. The larger the scatter particle, the more forwards the scatter beam becomes. It is not wavelength biased.

Mie scattering from Aerosols (dust and water droplets) is not wavelength dependent, (as seen in clouds or from snow). The particle size determines the nature of the scattering. The larger the particle, the more the scattering is in the forwards direction. Large aerosols such as water droplets mostly scatter in the forward direction, with a small amount backwards, and very little sideways, figure 6.

Water droplets forming clouds are dominant in the lower atmosphere up to a few kilometers, while dust and ice based Aerosols continue higher, falling exponentially with molecular density. By 10 km, the atmospheric density is only a third of that above ground level. The model takes this scaling of molecular and aerosol scattering densities along the view path.

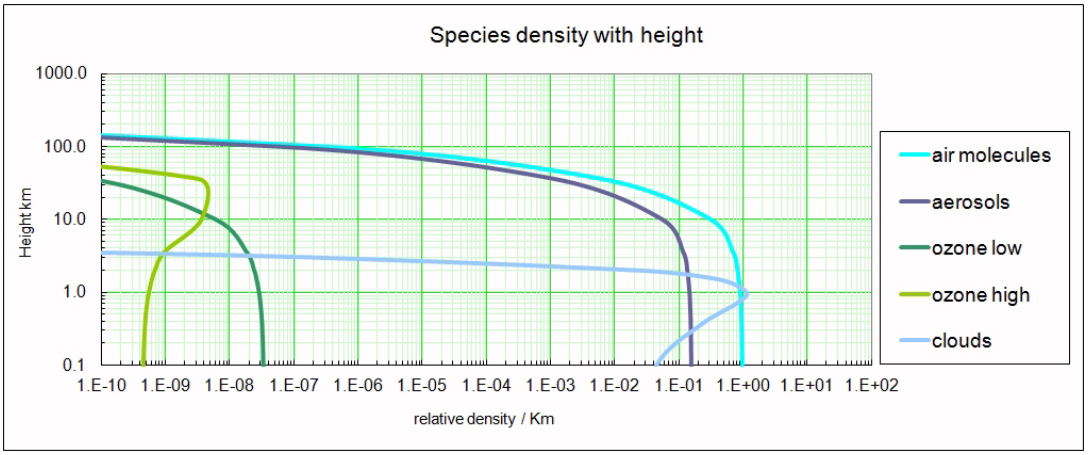


Figure 7. Species density variation with altitude, Showing cloud forming water droplets, general aerosol and molecular density.

2.4 Sky viewpath scatter path and geometry

The combined light from these various routes at a given elevation to the sky is then propagated to the point where it intersects the line of view to the sky of the observer, figure 8. The scattering in the unit cell at that location is calculated, based on the molecular and aerosol densities for that altitude. Also calculated, are the scattering probabilities for the air molecules and aerosols for that scatter angle into the view direction cone. The components per unit view distance along the view path at a given view elevation are plotted and then summed to give the total contribution of luminance to the observer.

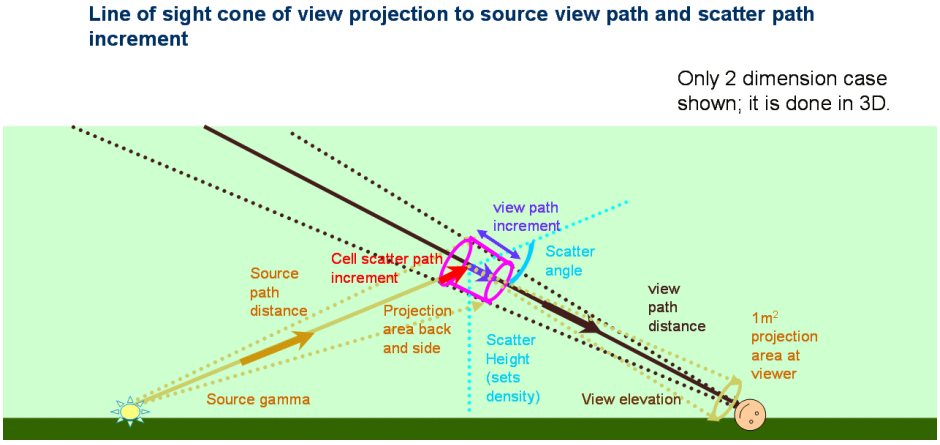


Fig.8, Line of sight cone of view projection to source view path and scatter path increment. A unit cell in a cone of sky from the viewer is seen to project side and front to the source, according to the scatter point location.

For a given view elevation and azimuth and path distance and source distance …. all the other distances and angles can be calculated, that is … the source path distance, the scatter point height, the source or reflected gamma and C angle of the light, and the scatter angle. The solid angle subtended by the cell at the source in terms of that for the viewer can be calculated. That times the scatter probability into the view direction for unit ground area gives the sky luminance for that increment after allowing for the source and viewer path extinction.

Figure 9 shows the relative contributions ground reflection, and of direct radiance and molecular and aerosol scattering for each section of the view path. The contribution of all increments along the viewpath are summed,. Due to the limited height of atmosphere, the path geometry is dominated by shallow angles. Aerosols scatter efficiently at shallow angles. While at the zenith of the view location, the scatter is at right angles where aerosols do not scatter, and so scattering is then due to air molecules.

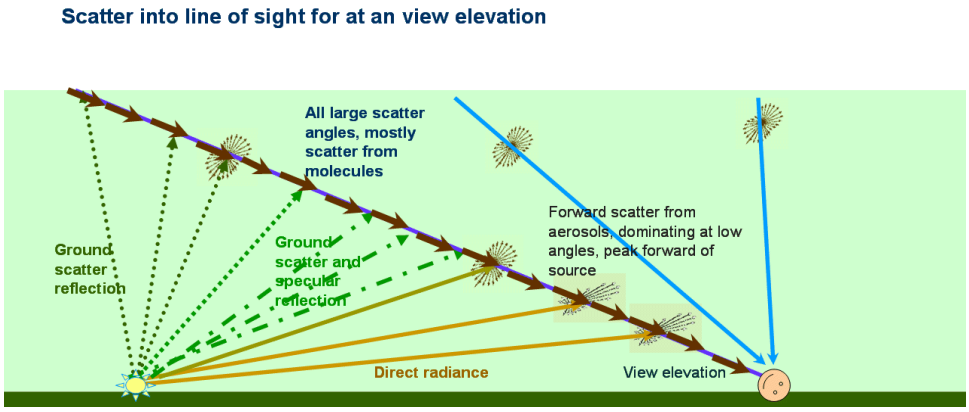


Figure 9. All increments along the viewpath are summed. Molecular scattering from ground reflection dominates over the source, while aerosol scattering of direct luminaire upward components scattered through narrow angles in the lower atmosphere dominates further down a long the view path.

2.5 The effect of long-distance path geometry and atmospheric tunneling

Viewing from a rural location, a distant light source, atmosphere has a tunnel effect. The scatter path geometry is mostly determined in the lower atmosphere, emphasising the contribution from luminaire gamma angles just above the horizontal, through the long scatter path lengths of the lower atmosphere. See figure 10. So this effectively puts a weighting factor for angles just above the horizontal.

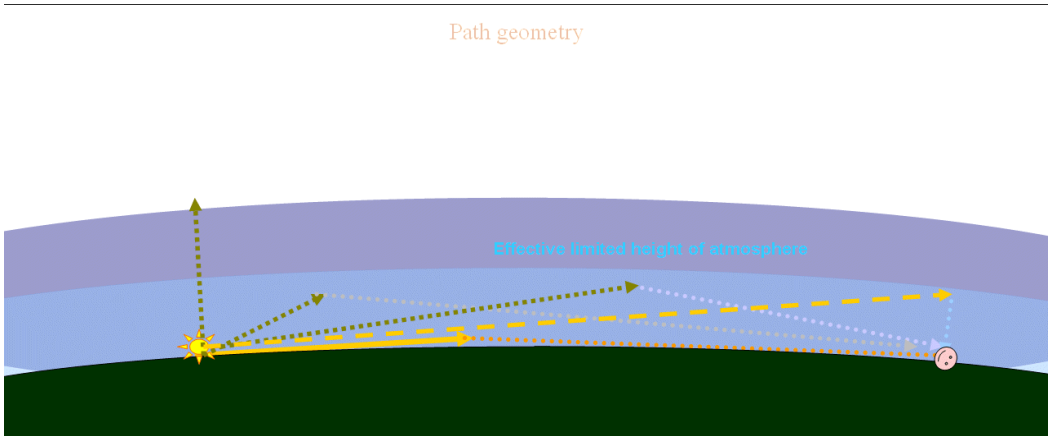


Fig.10, Viewing from a distance (10's of Km). Due to the limited height of atmosphere, the path geometry is dominated by shallow angles. Aerosols scatter efficiently at shallow angles. While at the zenith of the view location, the scatter is at right angles where aerosols do not scatter, and so scattering is then due to air molecules.

3 Output plot results

Outputs for the specific cases are described below. The implications of these are then discussed. Studies include tilted Low Pressure Sodium SOX, Cut Off High Pressure Sodium SON in both polycarbonate and curved tempered glass types, Full cutoff flat glass SON, and the effect of changing to white light sources.

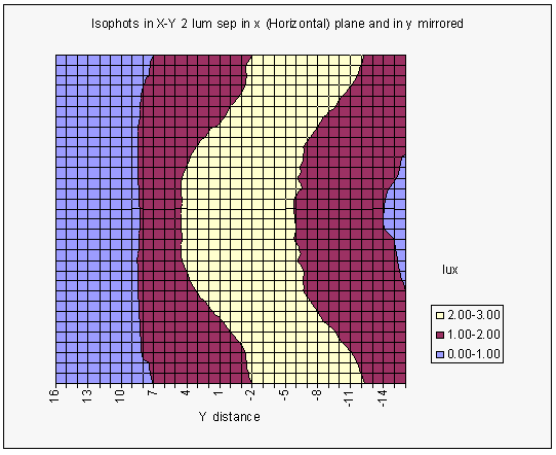
The Results from the cases considered are shown in the form of plots and tables of predicted Skyglow seen at a range of distances and view elevation angles from test cases of road lighting, these being

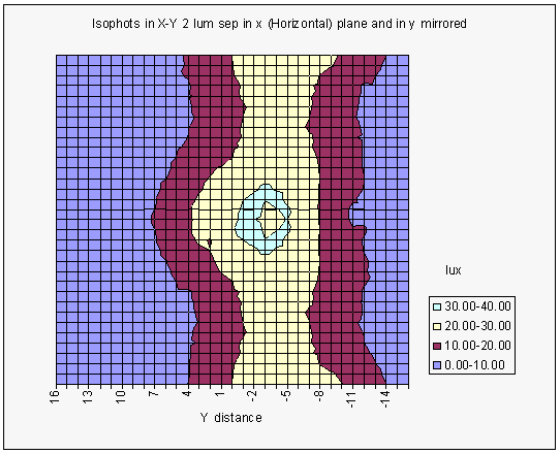
1. A comparison between a SOX luminaire tilted at 5°, a cut-off SON luminaire, and a full cut-off SON luminaire; all with the same illuminance at 30° gamma on the road, for a given pole height and roadwidth and grass surround.
2. Comparisons between curved shallow glass bowl, and polycarbonate bowl, with reference to full cut-off Flat glass.
3. A comparison between flat glass luminaire with peak spectral output at standard sodium D wavelength of 590 nm, then 550 nm corresponding to a white light source, and 500 nm with additional blue content.

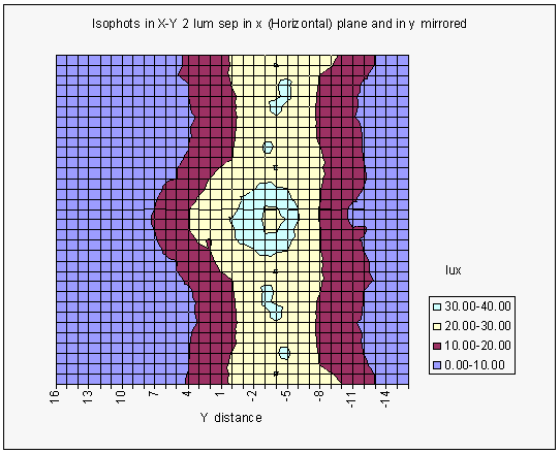
3.1 Output plots for SOX, shallow bowl cut off SON, and full cut off SON

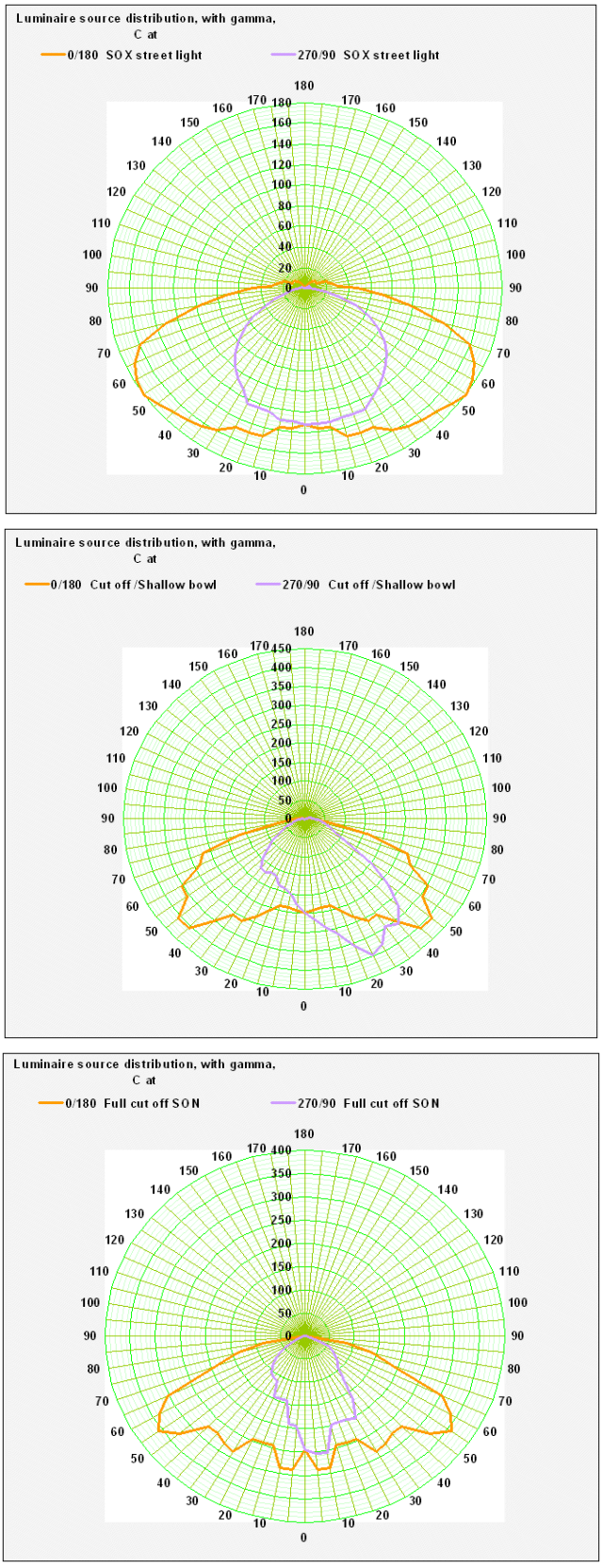
Plots 1 to 6 are a comparison study between a SOX luminaire tilted at 5°, a cut-off SON luminaire, and a full cut-off SON luminaire; all with the same illuminance at 30° gamma on the road, for a given pole height and roadwidth and grass surround. The descriptions are in the legends.

Plot 1. Ground photometric road contours (Lux) for typically spaced oppositely staggered layouts:- a, low pressure sodium SOX, b, high-pressure sodium cut-off SON, and c, high-pressure sodium full cut-off luminaires.

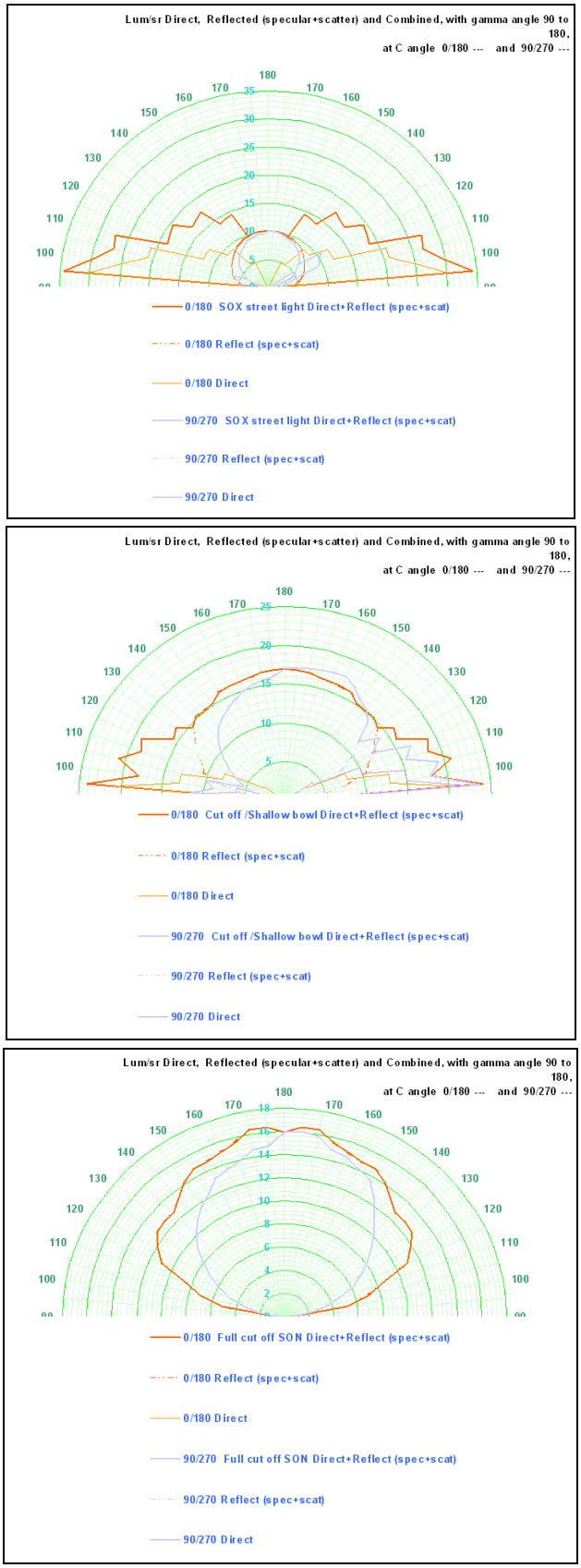




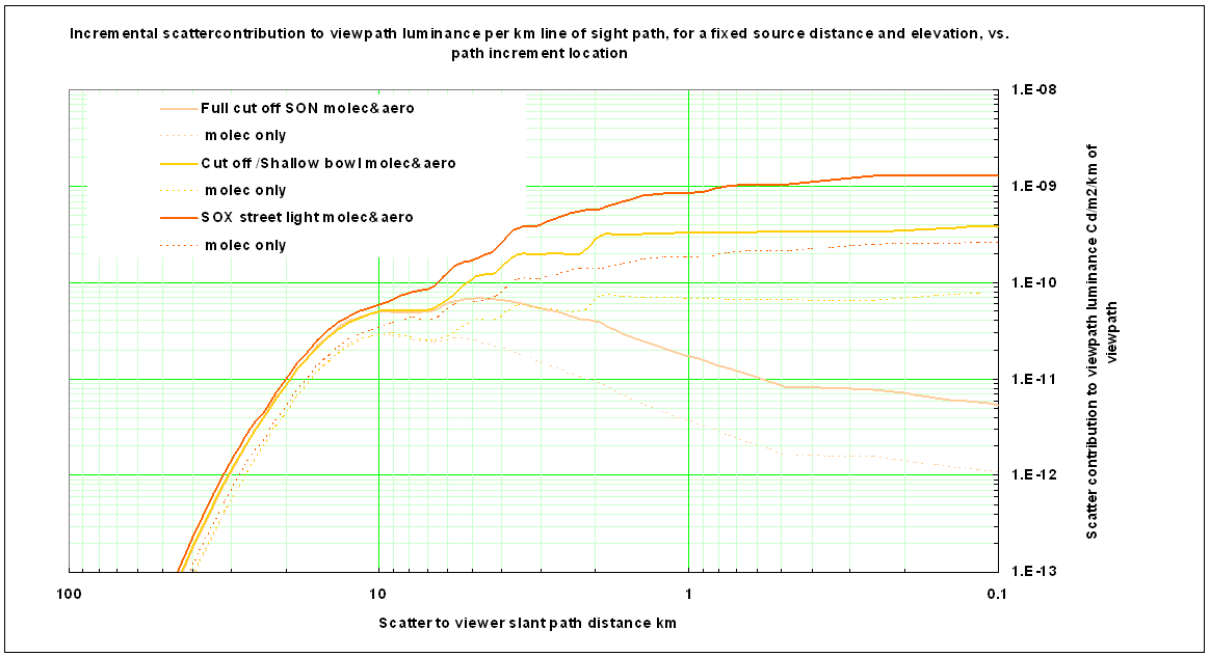




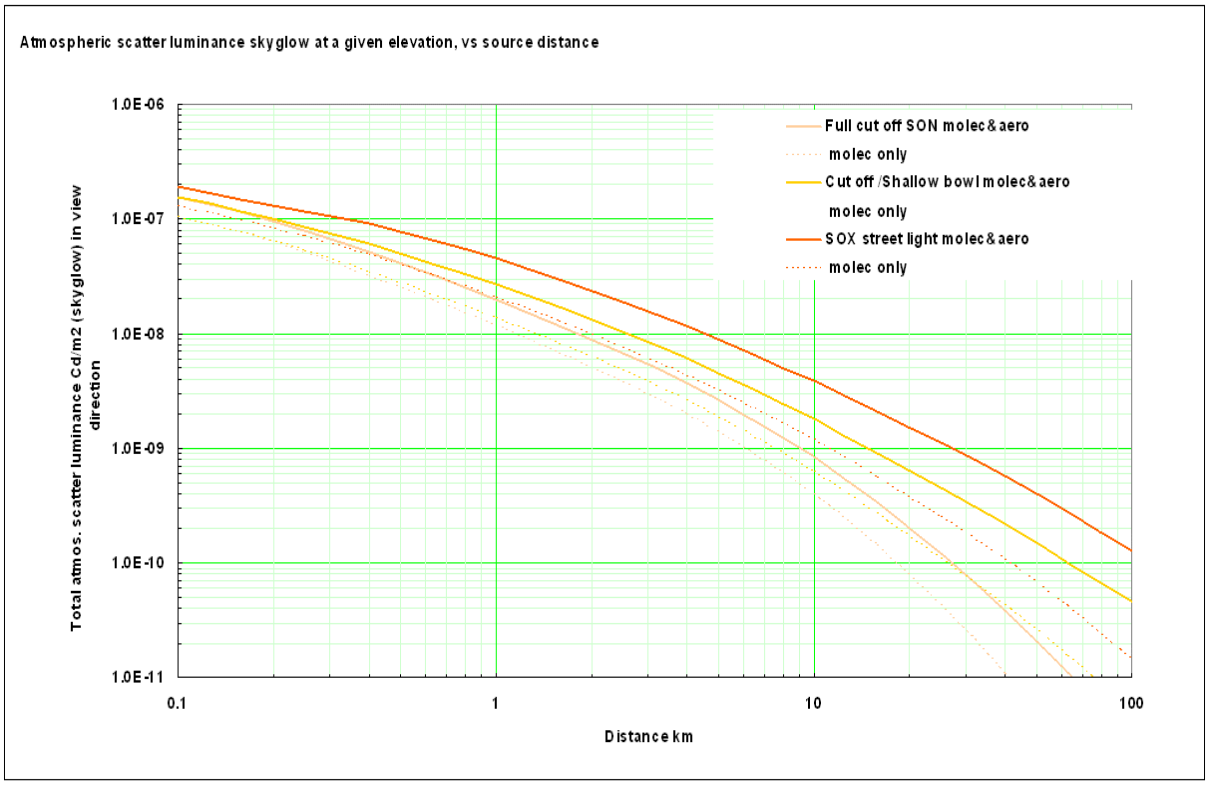
Plot 2. Gamma angle photometry for long and across the road for the cases of a, low pressure sodium SOX, b, high-pressure sodium cut-off SON, and c, high-pressure sodium full cut-off luminaires.



Plot 3. Gamma angle photometry above the horizontal for long and across the road for the cases of a, low pressure sodium SOX, b, high-pressure sodium cut-off SON, and c, high-pressure sodium full cut-off luminaires



Plot 4. This plot shows the scattered light input per km path length, into the line of sight along a viewing path at 45° elevation, measured from the viewer, for each increment along the path. The source is at 10 km distance from the viewer. The viewer is at the right, and the source is far left of centre. Units of cd/m2 for a single luminaire.



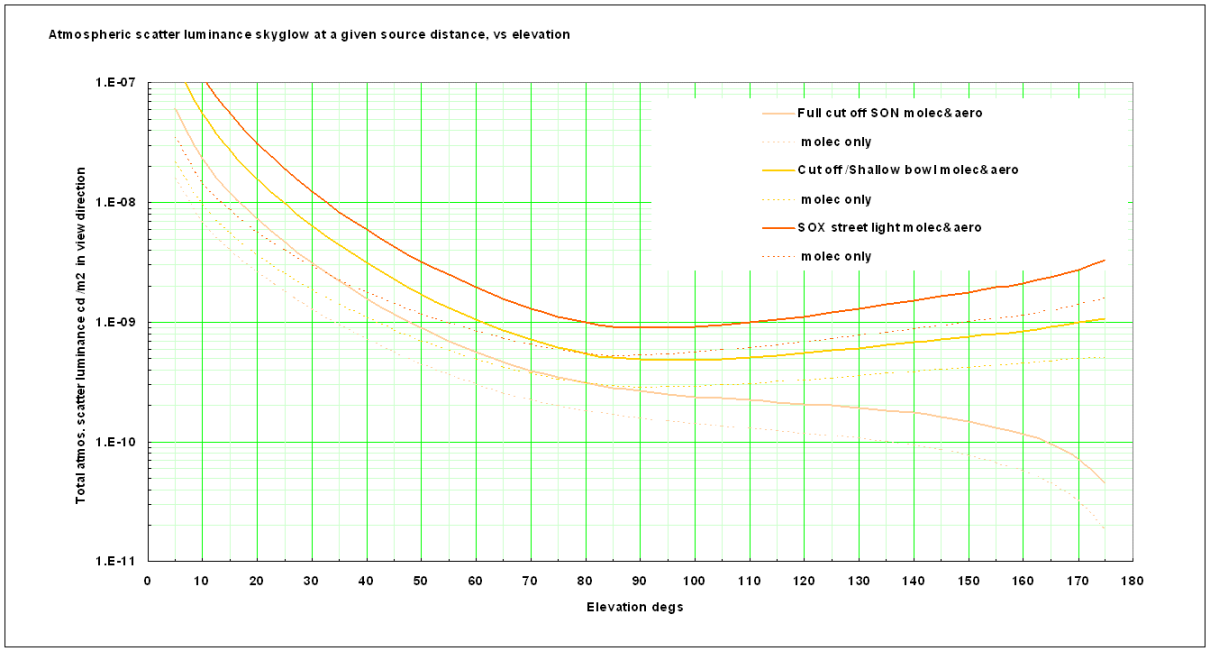
Plot 5. This plot shows the relative total skyglow luminance at a 45 degrees elevation view path, as a function of distance of source to observer. The source is on the left. The observer moves from there to the right. Units of cd/m2 for a single luminaire.

Plot 4 shows the relative contributions of each increment of view path, as the scattered light input per km path length, into the line of sightfor a 45° elevation view path. For scattering in air just above the source, most of the luminance is from ground reflection, while at distances of 5 km beyond much of the sky luminance at lower elevation view angles is from direct luminance to the sky.

On the left of plot 4 shows the back scatter from the atmosphere for scatter points beyond the source. At 14 km along the inclined viewing path, the scatter point is directly over the source and the scattering is near orthogonal and mostly from air molecules. This is the first peak on the left, for all three sources. The illumination of the scatter point is then ground reflection. The rising line to the viewer for the SOX luminaire (deep orange), is the effect of its direct radiance to the sky, causing excessive scattering in the lower atmosphere, due to its badly controlled output above the horizontal, scattered particularly by aerosols.

Note for the molecular scattering only component (thin dotted curves), the SOX case has a peak then falls. The full cut off luminaire (pink) with no direct radiance, shows no forward scatter peak at all. The shallow bowl cut off design curve lies above the full cut off curve most noticeably at the nearer distances to the viewer. For all the luminaires, the luminance at a fixed gamma angle along the road was scaled to the same.

Plot 5 shows the sky luminance at a 45° angle elevation at increasing distances. Notice that SOX (deep orange) creates significantly more skyglow than the cut off case (pink) at all ranges, especially at large distances beyond 10 km. It is visible after cut off (light orange) and full cut off (pink) SON are no longer contributing significant skyglow. The excess from the shallow bowl cut off luminaire (light orange) is also clearly seen.



Plot 6. This plot shows the relative skyglow luminance for all elevations, 0 to 180 degrees over the sky, from horizon to horizon, into the angle of view, by SOX (deep orange) and cut off (light orange) and full cut off (pink) SON lighting. The viewer is 10 km from the source. Units of cd/m2 for a single luminaire.

Plots 6 shows the contributions seen at a distance are 10 km from the luminaire at viewing elevations from directly towards the luminaire, through the zenith, to the opposite direction. Notice that although at small viewing elevations all have major impact; while at all other viewing elevations, it is the SOX luminaires that are contributing by far the most to the skyglow. The least is full cut off SON. Further work has shown that the effect of buildings about the road is to reduce the skyglow a

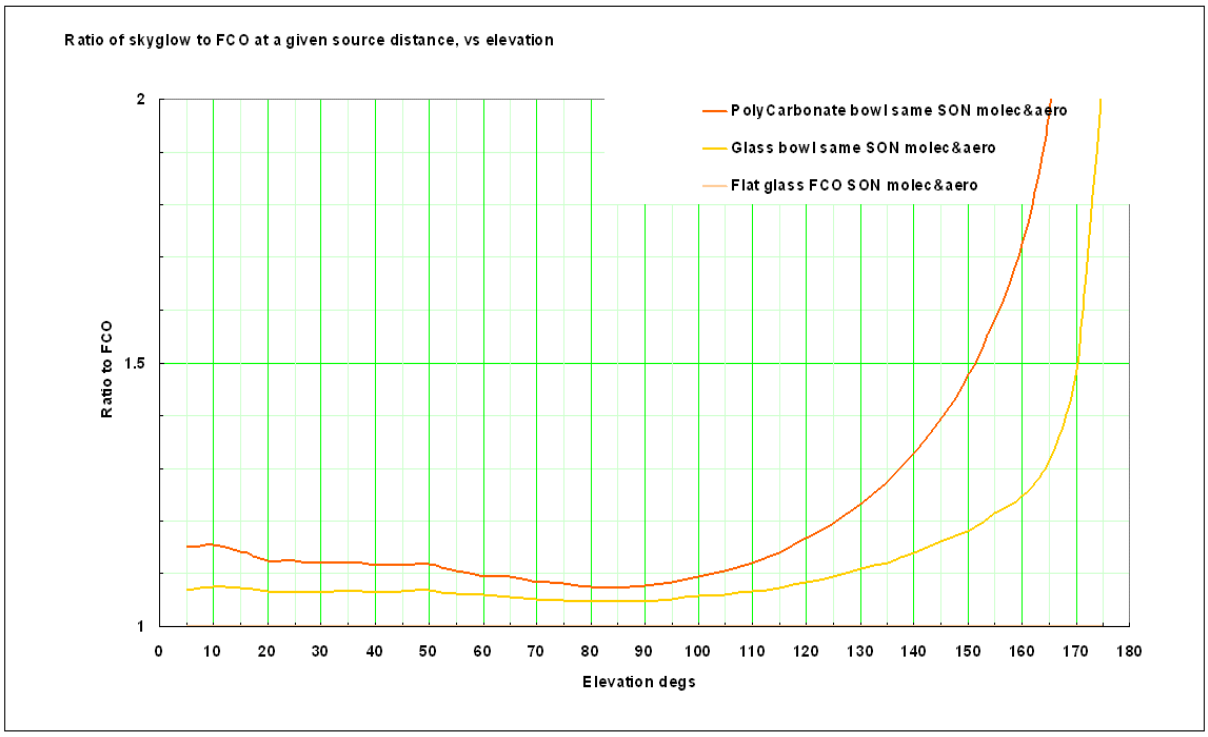
little from obstructions, and at the same time significantly flatten the curve, though vertical surface reflections. At closer distances, the curves are more flattened, as skyglow spreads through reflections to all elevations.

Note the very large differences between SOX, SON and FCO luminaires at all sky view angles. The differences increase with elevation angle and even more so in the opposite direction where the illuminance is in backscatter. Full cut-off whiting has no horizontal component or above and so it is purely scattered ground reflection.

Critically, light is scattered by aerosols predominantly in the forwards direction, and lesser but still importantly for lighting design, in the reverse direction, while very little sideways. Low angle light above the horizontal has the largest distance to travel through the lower atmosphere and scatter, and so is dominating light pollution, and yet could be easily controlled.

3.2 Comparison Output plots for shallow glass bowl, and polycarbonate bowl SON, with respect to full cut-off flat glass SON

Plot 7 shows the relative skyglow luminance view at 10km distance, for cases of polycarbonate bowl (deep orange), and Glass bowl (orange) with the same luminaire compared with flat glass full cut-off. The differences are between 10% and in the forwards direction and 25% to 100% in the away direction. Plot 8 shows the relative skyglow luminance to Flat Glass at 45 degs view as a function of distance. Cases of polycarbonate bowl (deep orange), and Glass bowl (orange) with the same luminaire. The differences are between 8% and in the forwards direction and 100% in the away direction.



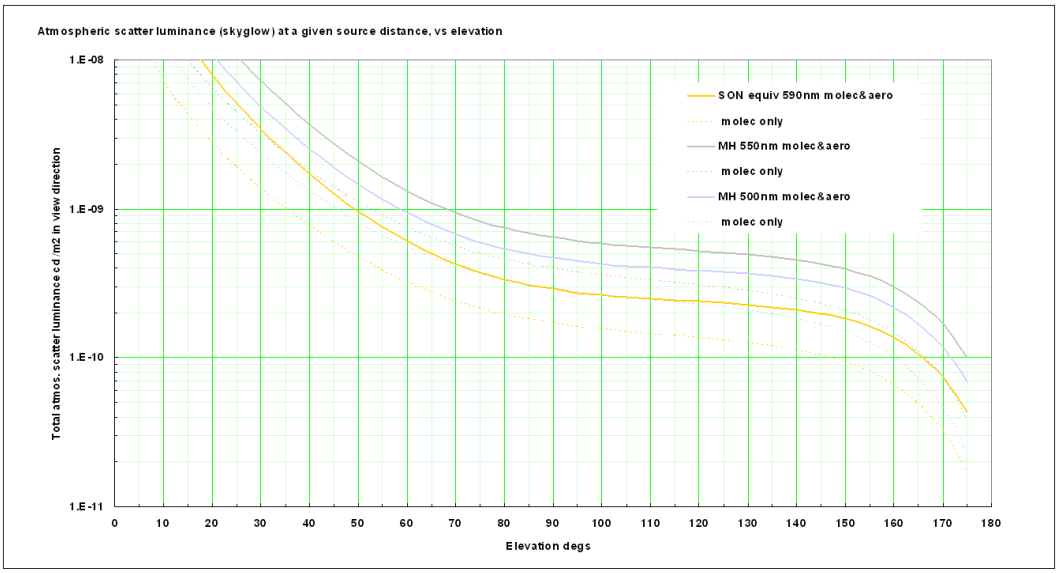
Plot 7. This plot on a linear vertical scale, shows the relative skyglow into the angle of view at 10km distance for cases of polycarbonate bowl (deep orange), and Glass bowl (orange) with the same luminaire, with respect to full cut-off Flat glass. The differences are between 10% and in the forwards direction and 25% to 100% in the away direction.



Plot 8 This plot on a linear vertical scale, shows the relative skyglow luminance at 45 degs view as a function of distance for cases of polycarbonate bowl (deep orange), and Glass bowl (orange) with the same luminaire, with respect to full cut-off Flat Glass. The differences are between 8% and in the forwards direction and 100% in the away direction.

3.3 Comparison Output plots for flat glass luminaire peaking in wavelength at 590nm, 550nm, and 500nm

The case is shown here to illustrate the effect of broadening the wavelength from sodium D to include high-pressure sodium with a yellow pink component and for fall white light with a blue component. The cases are for a glass luminaire with peak spectral output at standard sodium D wavelength of 590 nm, then 550 nm corresponding to a pink-white light source, and 500 nm with additional blue content.



Plot 9. This plot shows the relative skyglow luminance for all elevations, 0 to 180 degrees over the sky, from horizon to horizon, into the angle of view at 10km distance, by an FCO flat glass full cut-off luminaire peaking at 590nm (pink), 550nm (grey) and 500 nm. (blue). Units of cd/m2 for a single luminaire.

Plot 9 shows increase in skyglow at 550 nm for enhanced reflection from green grass on verges and especially atmospheric scattering. Note the smaller skyglow at bluer wavelengths.

Skyglow at high elevations, increases in the green by a factor of at least two, due to the much greater reflection from vegetation, particularly grass. It is less dominant in the blue, but then molecular scattering is much greater. The observer also sees more scotopic matching to the celestial background, hence less contrast.

4 Accumulated effect of many luminaires and the visibility of the The Milky Way

For large built-up areas with many streets of luminaires, the buildings retain heat at night more so than flat ground which radiates directly to the sky. This results in a microclimate of warm air and accumulated aerosols in up currents leading to enhanced dust. The warm rising air cools resulting in local condensation, even in conditions of otherwise clear visibility. This has not been modelled but will enhance scattering in all directions towards the horizon for distant views. And it's quite often visible when looking from high ground towards towns at a distance. Tall buildings in central towns block sideways lighting directly channelling it upwards, but the suburbs with more open spaces continue to radiate sideways.

The Milky Way surface luminance was calculated to be about 8.4 x10^-5 cd/m2. From plot 6, for 1,000 SOX lumianires sky glow at 30° elevation becomes 1E-4cd/m2 which swamps the Milky way, while for FCOs in the away direction it is much lower, making the Milky Way visible. Rural sky glow in the UK is typically similar surface brightness as many Messier catalogue nebulae. A reduction in sky glow by just one magnitude (40%), increases the number of stars visible by 300%.

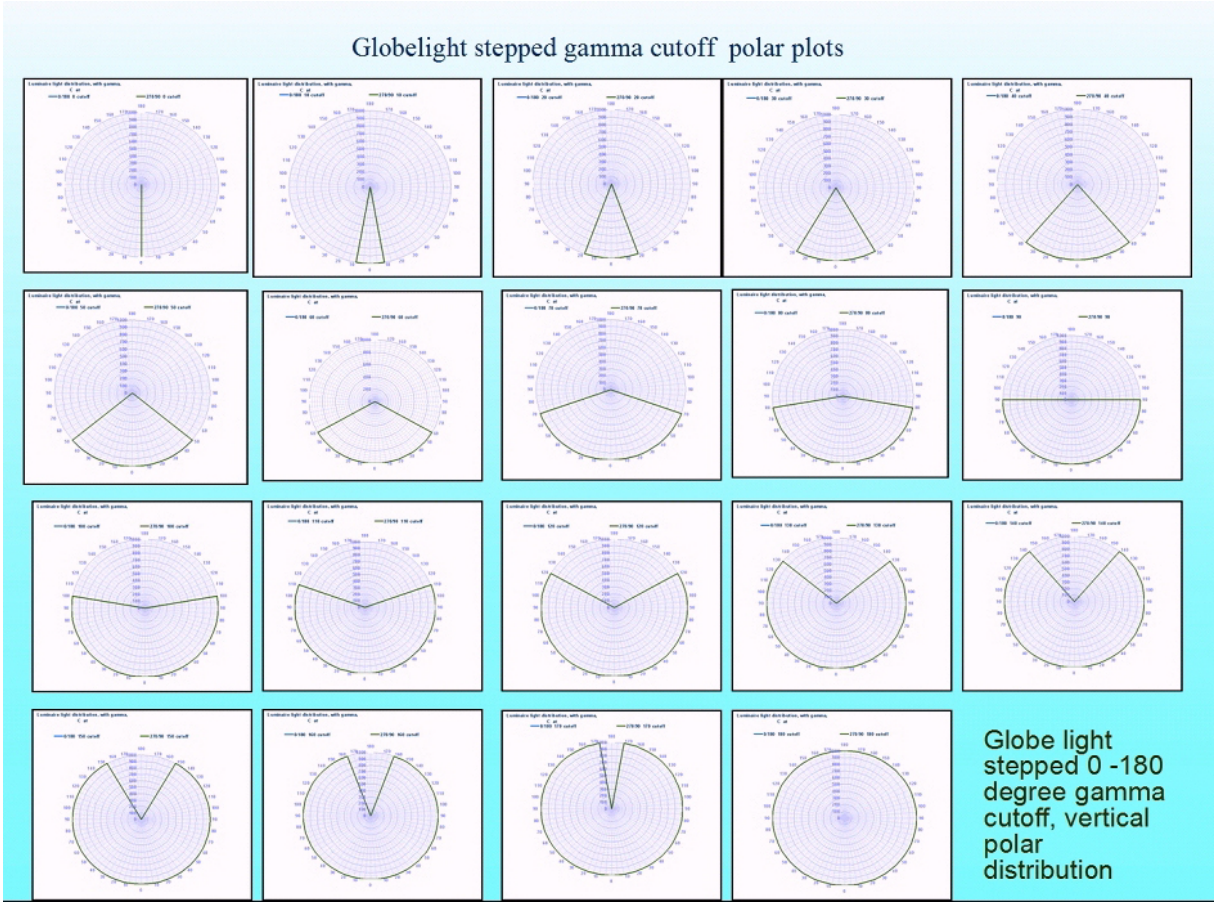


Figure 11. A globe light of stepped gamma cutoff 0° to 180° gamma.

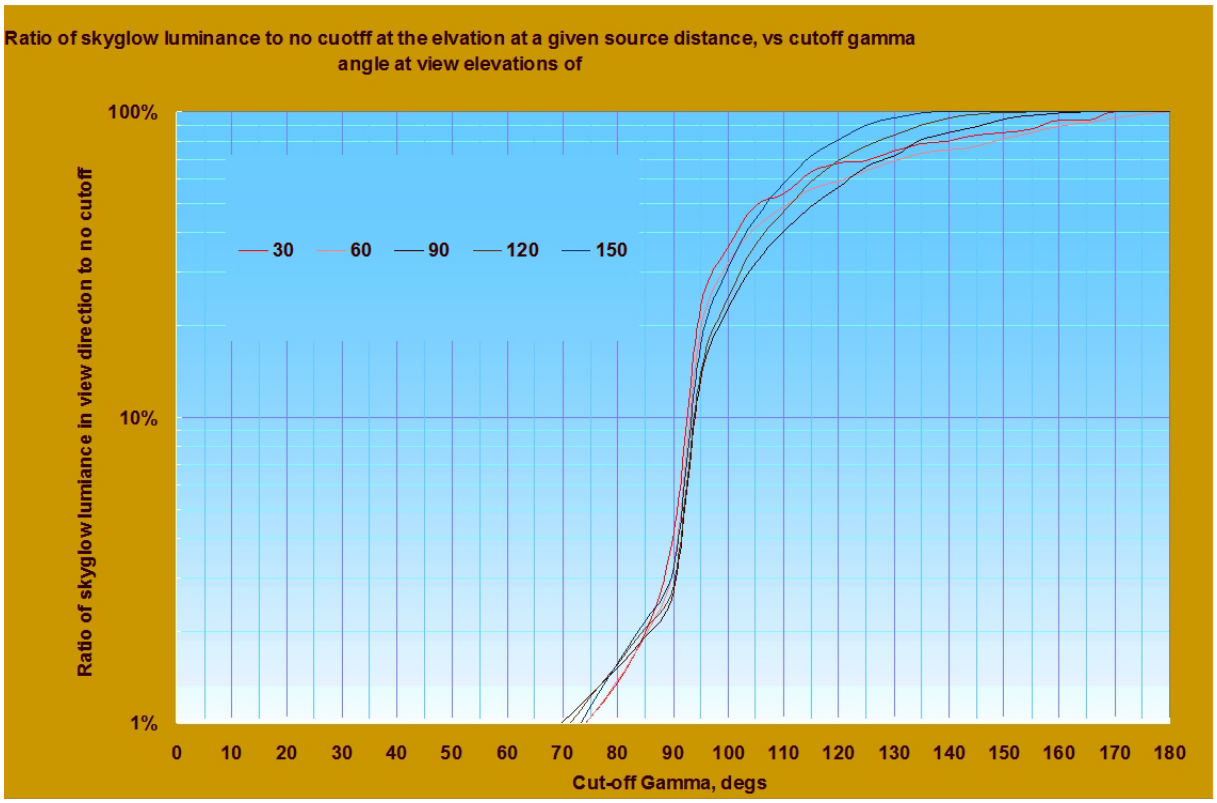
5 Variable gamma cutoff angle Globelight

5.1 Range of cut-off angles

In this study, and evenly illuminating globe light was modelled with stepped cut-off gamma angles from narrow angle downwards through the horizontal to none, shown in figure 11.

5.2 Results: View averaged normalised gamma Cutofff

Plot 8 below shows the relative sky brightness for a globe light on open ground with different angles. The cases are for from 10 km in good atmospheric conditions; at view elevations 30, 60,90, 120, 150. The curves are all the same shape but differ in scale according to view elevation angle, and so it was practical to normalize. They are all normalised to 100% regardless of view angle for the case of no cut-off.



Plot 10, Relative sky luminance for a globe light of stepped gamma cutoff to no cutoff 30° 60° 90° 120° and 150° view elevations. These were all normalised to 100% at no cutoff, for each view elevations. It is a logarithmic percentage scale.

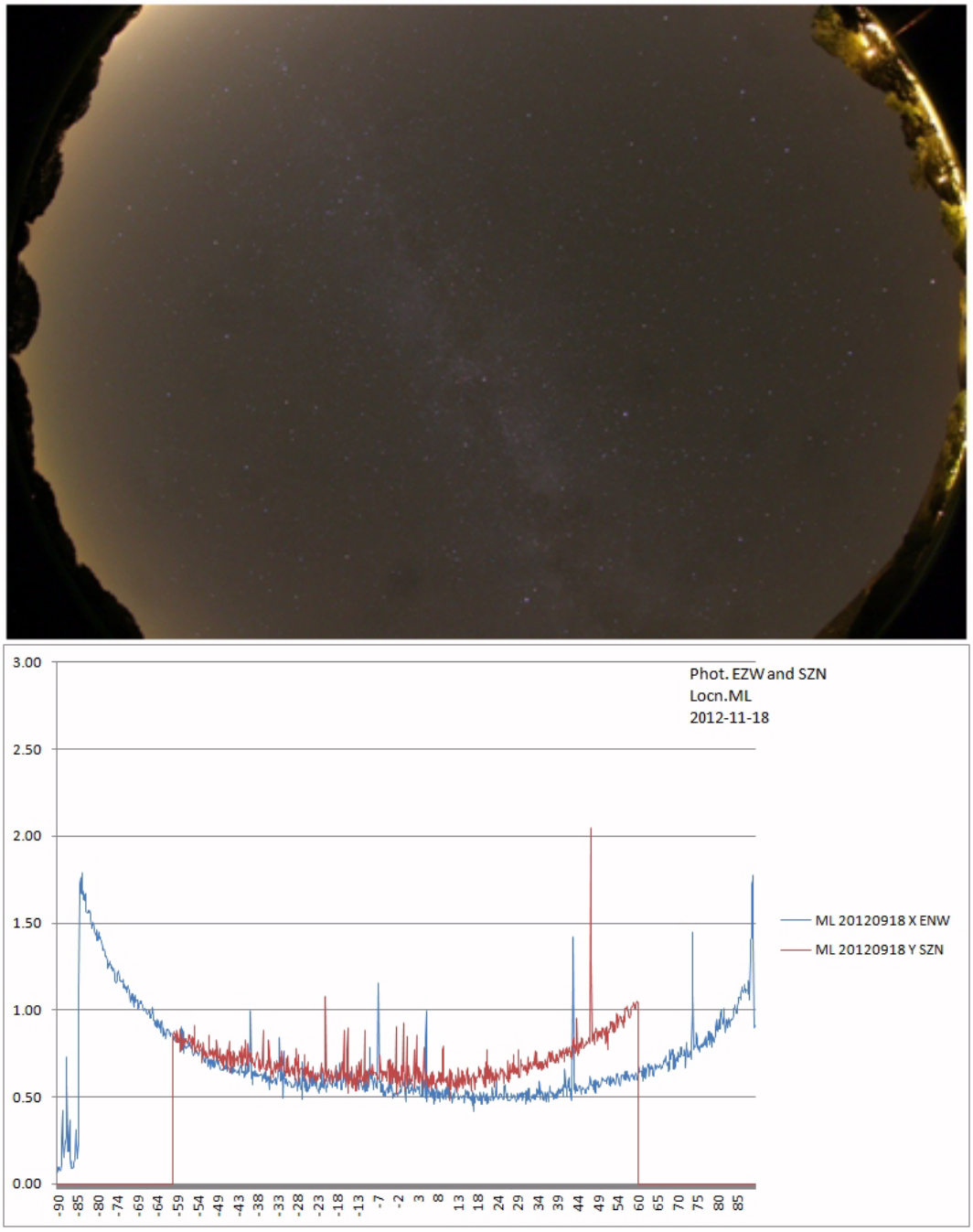
Plot 10 is logarithmic percentage . It clearly shows the large increase in sky glow for cut-off gamma angles of 70° and above, that is 30° below horizontal and above. But this is the course where illumination on the ground is least. The curves are for different view angles on the sky, all normalised to give the same maximum. Note they are all following similar shape.

6 Comparison with a recent AONB dark sky survey

These are the results of a study by the author of the Malvern Hills area of outstanding natural beauty (AONB) between 2011 September to December, for Malvern Hills AONB authorities, published with permission. This included photometry from all sky images of clear sky. In the darkest rural locations,

they showed a typical photometry range of over 6 to 1 from a few degrees above the horizon to zenith.

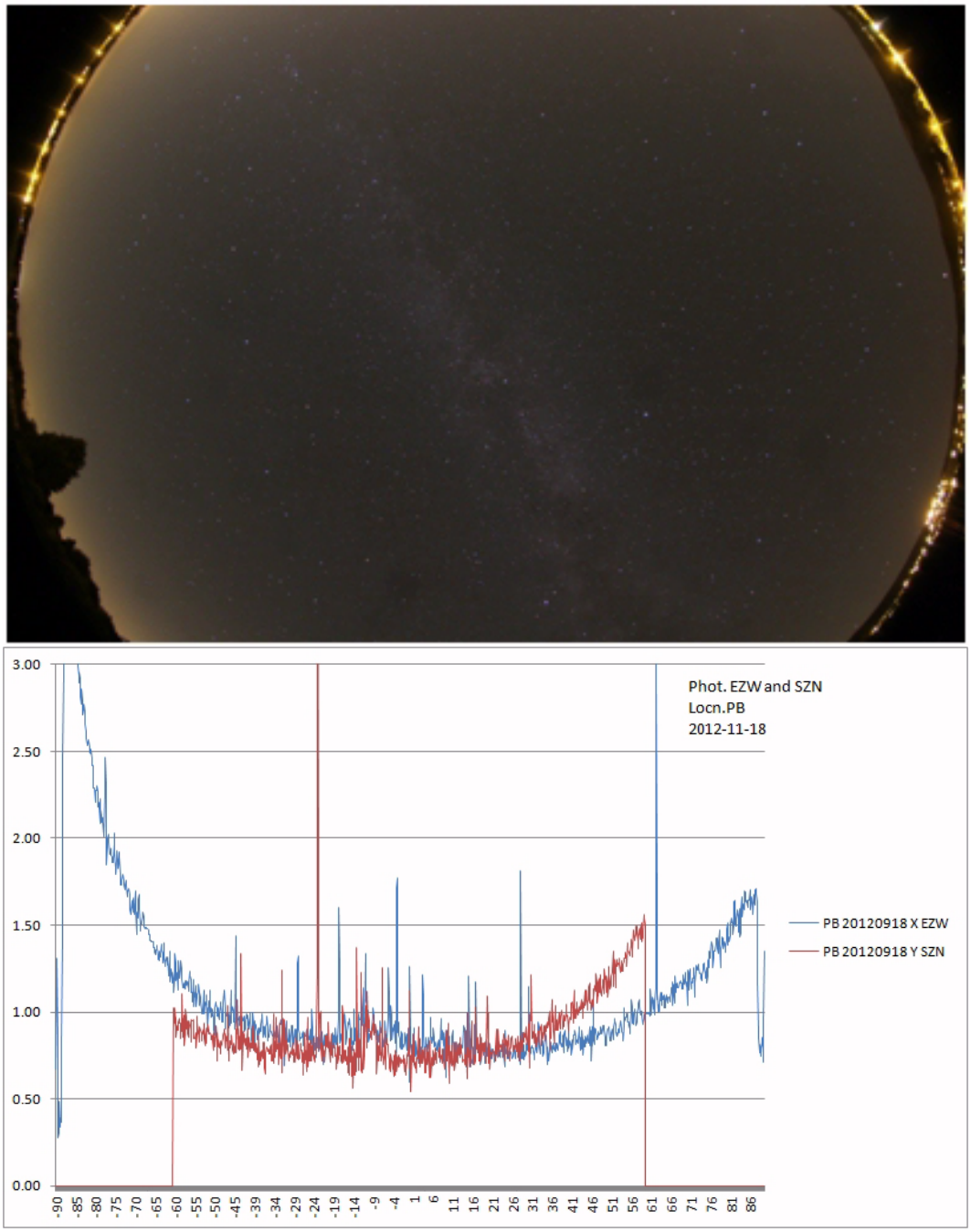
Zenith readings were taken on successive dark of the Moon periods each month on the clearest and most deadly night successive months. Typical range of sky brightness was in town 20.5 magnitudes per square second (0.5 Milli candelas per square metre) ,and at its edge 20.7 (80%), and a few kilometres from it 21.0 (63%) also in all other rural areas at a few kilometres. There were variations month-to-month, see later.



Plot 11a. Malvern link common all sky image (no vignetting correction), and Photometric profile plots for East-Zenith-West (blue) and South-Zenith-North (red), centred mid frame from the above image, corrected for vignetting. Photometry Units mill Candelas per square metre for degrees from Zenith . Spikes are individual stars. Dates shown next to the plots. Data was calibrated with SQM Zenith readings.

Image and photometry plot 11a are from Malvern Lin common, surrounded by Malvern town. Details are given in the Legends.

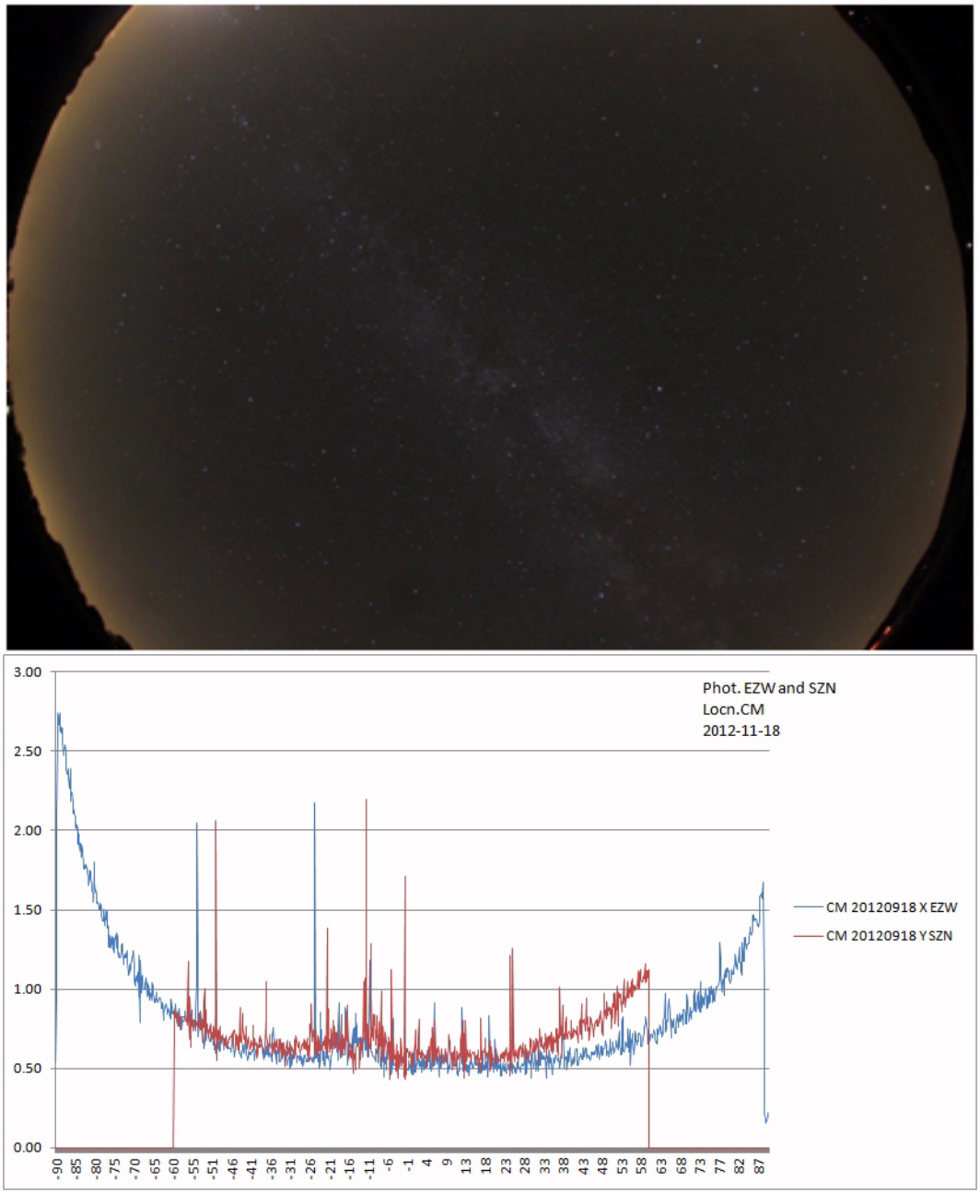
Pool Brook common is on the south edge of Malvern, so Malvern town light contribution dominates to the north, and Worcester to a north-east, but there is still a sharp rise to the East which is more from all of the river Severn valley area even where there are no towns.



Plot 11b. Pool Brook common all sky image (no vignetting correction), and Photometric profile plots for East-Zenith-West (blue) and South-Zenith-North (red), centred mid frame from the above image, corrected for vignetting. Photometry Units mill Candelas per square metre for degrees from Zenith. Spikes are individual stars. Dates shown next to the plots. Data was calibrated with SQM Zenith readings.

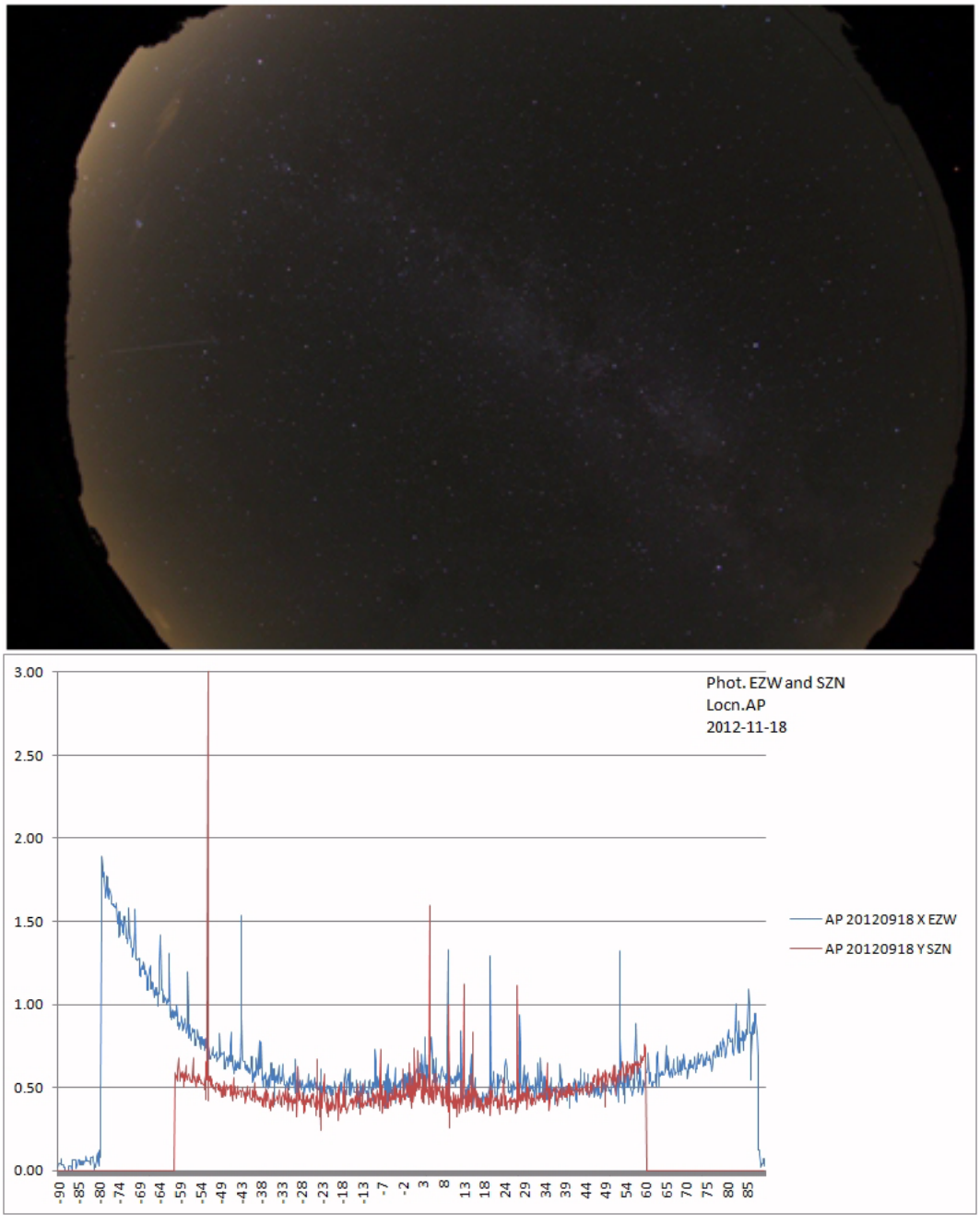
Castlemorton common in plot 11c is about 3 km to the south of Malvern town and the rise to the north is clearly visible, and yet there is still a strong rise to the East with no obvious town in that direction. This is from all the lighting in the Severn valley to the East. This location is generally thought to be a very dark area but in fact it's no darker than any other location well away from towns. It is just that the horizon is relatively flat without any significant habitation except just to the north.

Alfrick Pound in plot 11d, clearly shows a very high rise to the East which is the city of Worcester but otherwise has a fairly dark horizon. Several other locations were similarly imaged and analysed. Those shown here were of special interest as described.



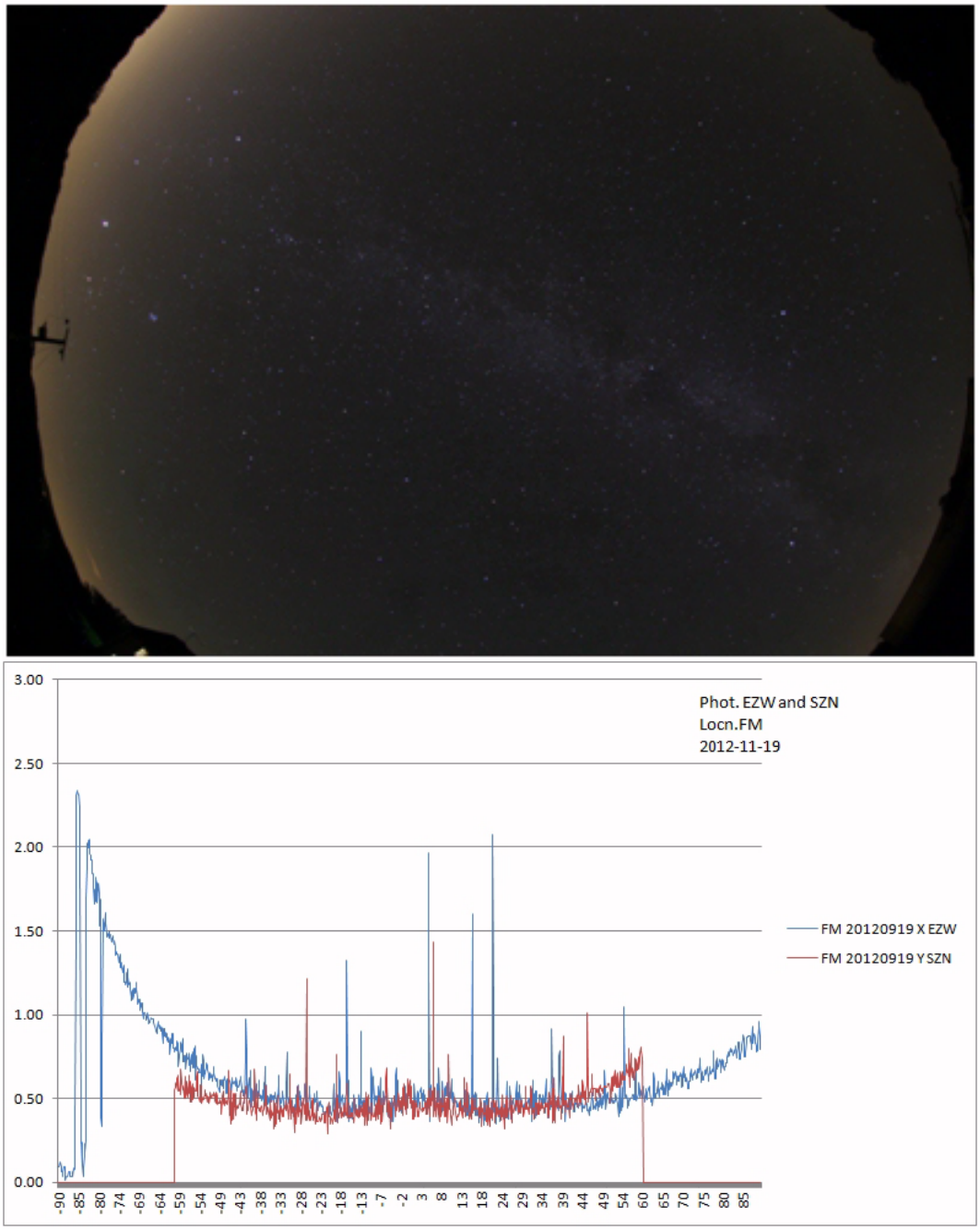
Plot 11c. Castle Moreton common all sky image (no vignetting correction), and Photometric profile plots for East-Zenith-West (blue) and South-Zenith-North (red), centred mid frame from the above image, corrected for vignetting. Photometry Units mill Candelas per square metre for degrees from Zenith. Spikes are individual stars. Dates shown next to the plots. Data was calibrated with SQM Zenith readings. .

The image and its associated photometry plot 11e is for the Mathon Observatory, west of the Malvern Hills, one of the darkest locations in the area, and is regularly monitored. The rise to the east is partially due to Malvern town but also due to the many distributed lights of the Severn Valley and beyond as has been shown from the various other locations where a Malvern town is not to the East. The valley is on the far side of the Malvern Hills that only provides a block for the very low elevation light. While in the opposite direction, right to the West is more rural Herefordshire and then Wales which can be seen to me much darker. Spikes are individual stars.

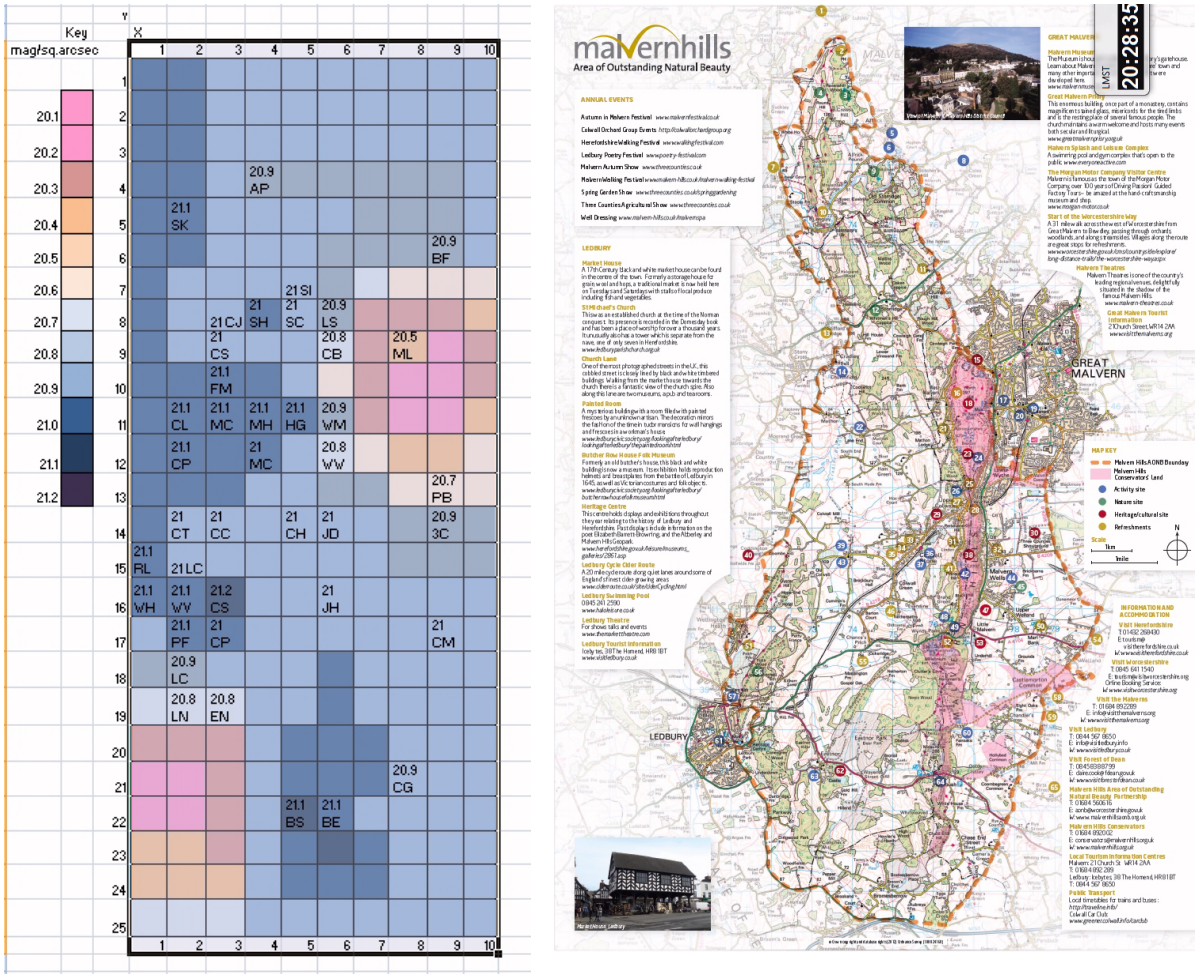


Plot 11d. Alfrick Pound all sky image (no vignetting correction), and Photometric profile plots for East-Zenith-West (blue) and South-Zenith-North (red), centred mid frame from the above image, corrected for vignetting. Photometry Units mill Candelas per square metre for degrees from Zenith . Spikes are individual stars. Dates shown next to the plots. Data was calibrated with SQM Zenith readings.

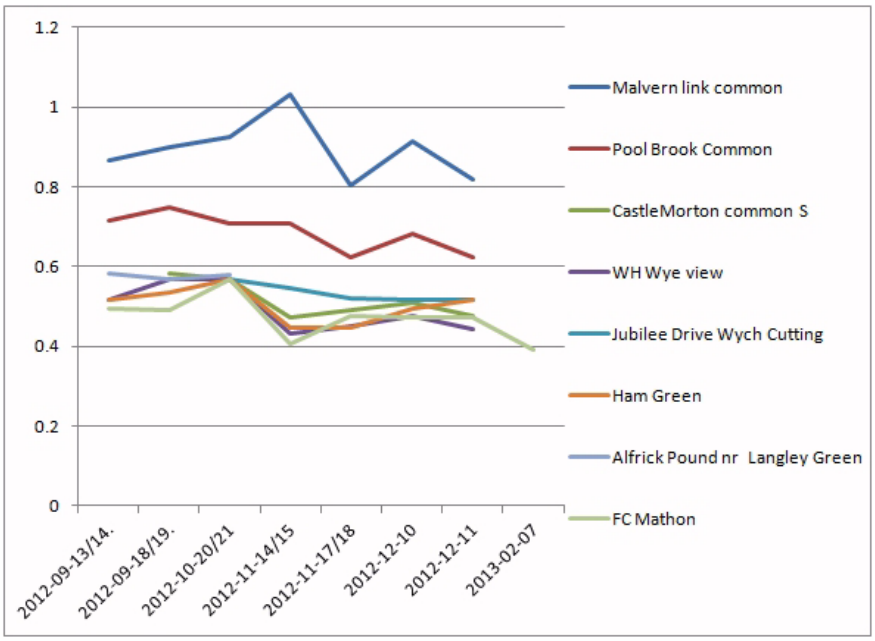
Plot 13 shows the sampled survey 1 km grid Zenith photometry for one of the darker nights. The overall background level is set by many towns tens of kilometres distant and more distant cities, which is typical of the UK. The typical figure of 21.0 consistent with dark sky studies in the UK. The darker values are obtained from raw isolated locations, especially with sea on one side such as in some national parks. These can achieve a magnitude darker. Some of these have applied for or gained International dark sky status.



Plot 11e. All sky image of a dark sky, (no vignetting correction) from Mathon Observatory, a rural area west of the Malvern Hills, UK. Together with the photometric profile plots for East-Zenith-West (blue) and South-Zenith-North (red), centred mid frame from the above image, corrected for vignetting. Photometry Units mill Candelas per square metre for degrees from Zenith. Spikes are individual stars. Dates shown in next to the plots. Data was calibrated with SQM Zenith readings. .



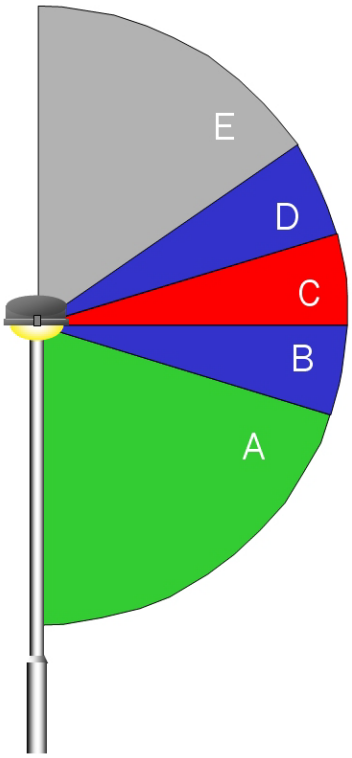
Plot 13. One square kilometre grid colour-coded dark sky survey SQM data. Zenith magnitudes per square arc second. Also showing a map of the AONB.



Plot 14. Variation for selected locations from one month to the next in similar dark sky conditions. Units of cd/m2

Plot 14 shows the variation from one month to the next on selected locations. These figures were affected by the Milky Way overhead at this particular time of year (15%) as shown in the all sky plots. Local atmospheric conditions produce a 15% reduction in sky glow on some occasions on later months into March, and can vary by several percent over a few minutes. The lowest sky brightness figure recorded was 21.2 magnitude per square arc second, in March of the following year. This was expected. Variations in the winter on the darkest of nights can be over a few minutes and vary from location to location in any a few hundred metres. This is due to humidity and water or ice condensation due to the temperature reaching local dewpoint. Some nights can be dark with very little star visibility. Geographic obstruction such as shadowing by trees some distance away on high ground can affect even overhead readings locally, over a few hundred metres. These conditions were avoided.

7 Lighting engineer's guide on Skyglow and cut-off angle



E 100–180° Critical area for skyglow experience from within urban and all areas but proportionally less impact to rural areas.

D 95–100° Significant contributor to skyglow, especially in rural areas where it is most aerosol dependent. Less likely to be obstructed.

C 90–95° Critical zone for skyglow and obtrusion seen at 10s of km (in rural areas) where it is strongly dependent on aerosol scattering.

B 85–90° Significant contributor to skyglow seen at a distance through reflection but reflected light more likely to be obstructed by buildings, trees and topography.

A 0–85° Ideal light distribution.

This diagram was prepared as a simple guide to lighting engineers together with a description of the previous work it was published by the Institute of Lighting Engineers (now Institute of Lighting Professionals), as Towards Understanding Skyglow.

The UK highways agency has already adopted a full cut off flat glass luminaire policy for its roads, partially based on this work. The British standards Institute lighting guide for rural roundabouts adopted this many years ago.

A meeting with the lighting engineers came up with a possible way of setting standards . Photometric curves are currently available for most luminaire designs. Using the cut-off angle data, it is possible to set a high standard criterion for the more controlled units. The idea was to adopt effective control cut-off that gave a 50% pass rate for current production for the best designs. This would encourage the lighting engineers to improve lighting control to get a higher pass rate. After a while this could be further adjusted to get back to the 50% pass rate, and so the criterion is raised.

8 General summary

The program was designed the just dark clear nights where atmospheric scattering is limited to single scattering, but that is realistic for star visibility.

Vertical beams scatter little at right angles into the view direction, especially at high source direction elevations. Close to towns, ground reflection dominates skyglow. The reflected light is

mostly from the surrounding surfaces to the roads, - grass in suburban areas. At a distance from towns, skyglow is dominated at low to mid elevation angles by direct radiance above the horizontal. Maximum scatter is at some distance in front of the source, from enhanced aerosol scatter at shallow angles.

In moving to white light, skyglow at high elevations, increases strongly into the green due to the much greater reflection from vegetation, particularly grass. It is less dominant if Green is absent and blue is dominant , but then molecular scattering is much greater. With whiter light, the observer also sees more scotopic matching to the celestial background, hence less contrast.

Shallow bowl luminaires were originally thought by the lighting industry to cause less sky glow than full cut-off types, due to lower numbers per given road length. While cut-off shallow bowls allow light to shine directly into the sky with their higher beaming angles and side emission, and the higher reflectivity of surfaces at these angles enhances this, so causing more skyglow. For the same luminaire source but differing front optical window, the polycarbonate shallow bowl has significantly more contribution to Skyglow away from source direction, and very slightly less from shallow glass bowls; as compared with flat glass, which has none.

The presence of tall buildings generally causes low angle direct light close to the horizon to be blocked, and higher elevation direct radiance to be reflected more towards the vertical, and in all reducing the effect from Skyglow by a factor of two or so. The difference between different luminaire types remain, and so it is still important to have well controlled lighting.

The author is unaware of any lighting industry environmental illumination impact programs using atmospheric modeling. And yet it is critical to the environmental effect. The industry continues use direct illuminance at all angles to the sky directly over the source without angular discrimination. Standards of lighting intrusion are based on industry decided population usage zones and only local to the source. While light has no respect of zones whatsoever and has environmental impact over great distances.

The use of better control cut-off angle is often negated by still using 5° tilted units to provide water run-off and directed illumination away from the pavement. Also particularly the common use of brighter and whiter light. For reasons explained previously, this is counter-productive. They also propagate the idea that whiter light is better environmentally, but for most fauna and flora the opposite is the case.

Light pollution continues to dominate the skies of the UK and is predicted to do so. Local councils are now switching out some lighting during hours of low traffic in selected areas for energy economy. It is only this that is likely to have an effect on sky glow reduction, but at present is very limited. Most of the young generation have never seen the Milky Way in a dark sky, but used to inspire people to take up science and engineering, and yet it is the ultimate area of outstanding natural beauty, with no protection in law.

9 Essential points for good practice

1 All lighting should be shielded from horizontal view.

2 The reduction in skyglow by universally adopting full horizontal cutoff lighting in all areas outside of town centres can be a factor of 3 to 5 according to elevation and distance of view.

3 Shallow bowls can cause more skyglow than equivalent FCOs, and are visually more obtrusive. They should not be used in open areas and should be restricted to town centres.

4 All measures are needed, such as dimming, as is now being tried, and switching off when not necessary.

Private funding initiatives are available for improved quality lighting but then the lighting is installed to the cheapest specification and is locked in for at least 30 years with no practical improvement. Generally there is is more and more lighting for town centres, new housing and amenities.

Using FCOs alone may not reduce sky glow sufficiently, against the growing amount of lighting in the UK

Above all else, this paper has shown that the lighting industry needs to move away from its current means of modelling assessment, and onto an atmospheric base model to work out proper impact through illuminance angles and over large distances.

Annex 1

A list of the features of the Skyglow model

- The Skyglow model runs in Excel spreadsheets, calling VBA function to generate tables that are plotted. It reads industry photometry files in the three common formats (CIB,IES, INR), directly creating an intermediate random access file including an inverse angle look up table, that is then re-read in. It then plots luminance distribution polar diagrams in gamma angles, along road C angle= 0/180 and across road C= 90/270. It also does polar plot photometry in C angle 0-360 degrees, for stepped gamma angles 0-90. It also plots road lux distribution given pole spacing one sided and alternate sided staggered, as colour coded surface plots, for horizontal surfaces (on and off road), also in vertical planes across road, behind parallel to road and in front as specified. It calculates horizontal plane surface uniformity.
- The program calculates integrated sphere lumens or for part sphere up to a given gamma angle, and at a given angle band, also plots these and as a fraction of the whole, over all gamma angles.
- It plots BRDFs... bi directional reflectivity distribution functions for a single source, both specular and scatter components and combined. These plots of reflectivity are polar maps in gamma angle across a road inc surrounds, and along a road, also around in C angle at stepped gammas for 90 to 180 degs (above horizontal). This is for specular and scatter parts or combined, also for each view path or direct. For vertical surfaces, this includes all reflections and obstructions, according to view angle. Reflectivity of each surface can be specified in cell input, also roughness, and spectral type ... for road, concrete, walls, trees, grass etc is referred to by a type number.
- Three surfaces are allowed for now, but this may be expanded to mixes of several. The three are 1 = road (asphalt or whatever), 2 = surround (grass or whatever), 3 = vertical (either concrete or brick wall, or trees of several types). If vertical surfaces are include they are modelled as continuous and two sided about the road. i.e. a simple trough geometry, using basic corner reflection optics rules.
- Luminous reflection plots are shown in the same format as the specular and scatter reflectivity plots, but are then with the given incident luminaire source distribution.
- These are then integrated for all C angles values for a sphere or part sphere to a given gamma angle and fraction of the whole, also plotted for gamma angle, as was the luminaire distribution. The atmospheric model is fixed as standard but aerosols can be switched on or off, both shown on the output atmospheric scatter plots. The atmospheric scatter plots are all dome for three comparison luminaires simultaneously, as selected from file.
- At a given distance from the source specified, the incremental contribution of scatter per km of view path into a given observer view direction at a given view elevation angle to the sky, is plotted for all atmospheric view path increments along the view direction to the sky, for molecular and aerosol particle view paths and surfaces. The integrated path scatter for view elevation is plotted for all elevations, (for three lumimaire designs in parallel with and co plotted) with and without aerosol scatter. The plots can be based on the luminous output of each luminaire rescaled to a common total, or not as selected, for comparison of optical design.
- The skyglow at a given view elevation is also plotted for increasing source distance up to 100 km distance. A curved Earth surface is used. Path distances are calculated and displayed logarithmi-cally.
- The full atmospheric scatter program runs in about 2 minutes on a 3GHz PC. Three luminaire light distributions are read in and also plotted.

Annex 2a

Related publications and conference proceedings by the author

[1] Memorandum to the Parliamentary science and technology committee investigation into light pollution.2003.

[2] Proceedings of the European dark sky symposium Portsmouth 2006.

[3] Modelling from luminaire designs for Skyglow, La Palma Starlight conference 2007.

[4] Towards understanding sky glow, Institute of lighting engineers 2007.

[5] Modelling from luminaire designs, Towards Understanding Skyglow, IDA AGM 2008.

[6] Towards sky-luminance based lighting standards, EDS Vienna 2008.

[7] Modelling light pollution for sky-luminance reduction based lighting standards, JENAM 2009.

Annex 2b

Sources used for developing the model

1 NOAA UK isophotic data for 1993 and 2000 (NOAA/ CPRE)

2 British standards on road lighting BS5489 and EN 13201

3 “Guidance Notes for the Reduction of Light Pollution”, Institution of Lighting Engineers.

4 “Parliamentary Science and Technology Committee report on light pollution and astronomy”. HMSO. 2003

5 P. Cinzano, F. Falchi, C. D. Elvidge (2001): “The first world atlas of the artificial night sky brightness” Monthly Notices of the Royal Astronomical Society, 328, 689-707.

6 P. Cinzano, F. Falchi, C. D. Elvidge (2001): “Naked eye star visibility and limiting magnitude mapped from DMSP-OLS satellite data” Monthly Notices of the Royal Astronomical Society, 323, 34-46.

7 P. Cinzano, F. J. Diaz Castro (2000): “The artificial sky luminance and the emission angles of the upward light flux”, Measuring and Modelling Light Pollution, ed. P. Cinzano, vol.71, 251-256 - submitted May 1998.

8 R. H. Garstang (1986): "Model for Artificial Night-Sky Illumination,", Pub. Astron. Soc. Pacific 98, 364.

9 R. H. Garstang (1987): "Modelling Man made Night-Sky Illumination,", in Identification, Optimization and Protection of Optical Telescope Sites (eds. R. L. Millis, O. G. Franz, H. D. Ables, C. C. Dahn, Lowell Observatory, Flagstaff, Ariz.), 199.

10 F. Riewe, A. E. S. Green (1978): “Scatter phase functions” From Applied optics vol. 17 no 11 1978/June

11 webexhibits.org, http://webexhibits.org/causesofcolor/14B.html

Windows in buildings: potential source of light pollution

Stanislav Darula

Institute of Construction and Architecture, Slovak Academy of Sciences, Dúbravská cesta 9, 845 04 Bratislava, Slovak Republic
tel:+421 2 59309267, fax: +421 2 5477 3548, e-mail: usarsdar@savba.sk

Abstract

Activities of people have been shifting significantly from daytime into night-time during the last 100 years. This fact results in applications of solutions for illumination of work places in the exterior and interior, of street lighting and illumination other exterior objects in cities. All night artificial light sources produce also light propagated through the atmosphere. A large-scale experiment of switching off street lighting shows that windows in buildings can significantly contribute to light pollution. This paper discusses subjects associated with artificial light emitted by windows.

1 Introduction

In the urban spaces can be identified several sources of light pollution in the night: luminaires of public lighting and in the open areas, windows and skylights of various type buildings, headlights for illumination of building façades and monuments, headlights of cars, trams or trains eventually of billboards, etc. [1 - 3].

Increasing quantity of artificial light in the atmosphere influences the lives of people, animals and plants in the nature and in urban spaces during night. Moreover, during clear nights astronomical observations close cities with densely built-up locations are impossible.

Influence of street lighting on the light pollution is currently presented as the most important effect during clear night [4, 5]. Modeling of light emissions from these sources is relatively well described [6]. Street lighting system is characterized by its stable location on the ground and constant light intensity during the whole time of operation. Determination of position of this source is simple and its directional light emissivity can be modeled after a light emission function, e.g. in [7].

People provide various activities also during night. After sunset they can work, have a rest or health care in building interiors illuminated by electric lighting. The same indoor spaces are illuminated by natural light through windows or skylights during the day. Generally, it can be noticed that windows have two functions: they deliver natural light in the interiors during day-time and emit artificial light into atmosphere during night-time when interiors are occupied by people.

Windows in building façades and skylights on building roof tops produce light of lower intensity but from a very large area. Various spectrums of light and light of various intensities are emitted from windows and their time variability of the switch on regime are basic properties of this source. If windows are in vertical position, predominantly horizontal direction of light propagation can be expected. In the case of skylight, this direction is changed to vertical direction with very high impact on the upper part of the atmosphere. Luminance of windows depends also on the construction of shading devices installed in the aperture, quantity and position of luminaires in the rooms, reflectance of indoor surfaces, optical glazing properties and presence or absence of curtains [2]. In Figure 1 is presented night view on the façade with windows of various light emission and related luminance map.

Paper discusses various situations of light escaping from windows in the Section 2, measurements of window illuminance in Section 3 and reports findings of time changes of light emission from windows in Section 4.



A. B.

Figure 1: A building façade. A. The luminous windows, B. Related luminance map

2 Light escaping from windows

Windows in the buildings are generally designed in vertical position and with various dimensions and shapes. The double clear glazing is applied in transparent part of windows built in buildings in Slovakia. Shading devices like jalousies, curtains or louvers can be mounted outside or inside of the room. If electric lighting system is switched on in the room luminaires placed on the ceiling illuminate indoor surface, i.e. walls, floor, ceiling and furniture from top. This results artificial light source which potentially influences light pollution. Light escaping from windows consists from two parts. The first is direct light, penetrated glazing directly from luminaires to outside. The second part is diffuse light as product of multiple light reflections from indoor surfaces. If luminaires are embedded on the ceiling, direct light is effective in the bottom part of outside open space, Figure 2. If luminaires are located below window lintel direct light penetrates through glazing also in the upper part of hemisphere and significantly influences light pollution.

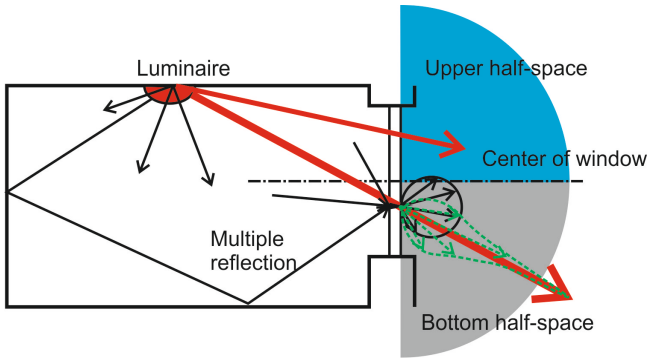


Figure 2: Scheme of the direct and indirect light escaping from window

Modeling of light emitted from windows in the atmosphere is more complex problem. This requires to determine: – indoor luminous conditions; - optical properties of window elements and mounted devices. Light reaching inner window pane is a product of artificial sources and multi-reflection of light from interior surfaces and can be modeled by luminous flux Φ consisting of two direct and diffuse components:

$$\Phi = \Phi_{dir} + \Phi_{dif}\,, \tag{1}$$

where Φ_{dir} direct luminous flux,
Φ_{dif} diffuse luminous flux.

It can be assumed that luminous flux leaving clear unshielded window glazing will be preferable directed downwards and portion of light emitted upwards will be significantly lower due to absence of direct component. Intensity of emitted light from window in this case will differ because various artificial sources with various luminous intensities are installed in rooms which can differ in dimensions and color of surfaces. Rooms in buildings are not empty but occupied by humans therefore location of furniture on the floor can change proportion of light emitted downwards and upwards.

Very complicated situations can occur when windows are equipped by shading devices like jalousies, louvers, curtains etc. Generally, lamellas of these devices are adjustable from horizontal to near vertical position. In dependence on the setting of lamellas the luminous flux leaving window pane can be directed upwards to the sky, downwards to the ground or horizontally. Examples in the Figure 3 present case when jalousies are located inside the space of the window glazing and only direct component of indoor light is investigated. The maximum light is redirected in the upper space when position of lamellas is as in Figure 3.A. When lamellas are in opposite position, Figure 3.C, the rays are directed downwards and influence on the increasing of light pollution is minimal in this case. Intensity of the light penetrated through window system depends on the luminous intensity of light sources, optical properties of jalousies and their momentary setting.

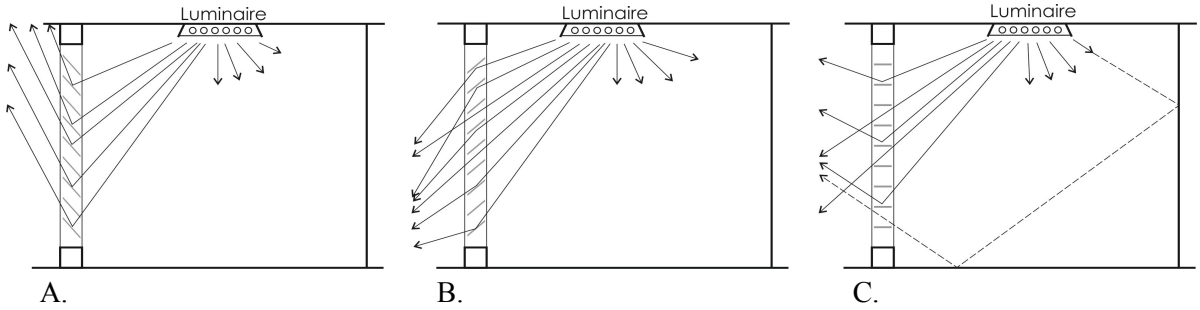


Figure 3: Light propagation from interior to exterior through window with jalousie. A. Luminous flux redirected upwards, B. Luminous flux redirected downwards, C. Case with lamellas in horizontal position

The windows are often covered by curtains at homes, flats and rooms in residential buildings. Curtain material and system with its manipulation result a lot of situations for penetration of light from interior to exterior. Light reaching curtain is scattered and through glazing penetrate outside, Figure 4. If density of curtain material is higher also diffusivity of light leaving the window pane is higher. Windows covered by curtains emit diffuse light of lower intensity without direct light or with small fraction of direct light.

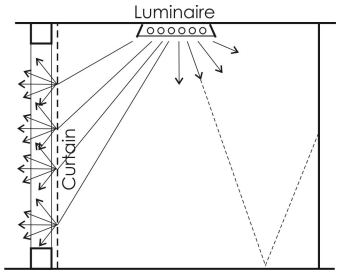


Figure 4: Light propagation from interior to exterior through window equipped by curtain.

3 Luminance of windows

Information about luminance, luminous intensity and photometric characteristics of windows during night time is published scarcely [1]. Authors measured luminance of windows and building façades in

Veszprém and found out luminance of 107 cd.m^{-2} at the unshaded window and 1,2 cd.m^{-2} at the shaded window. Published values of luminance of façades in the city vary between 0,2 cd.m^{-2} to 569 cd.m^{-2}. The lowest value was measured on the dark building wall while common illuminated surfaces had luminance close 18 cd.m^{-2} and luminance of bright façades can rise to 600 cd.m^{-2}.

Night luminance of widows can be measured by luminance meter or CCD camera. Very important is position of the luminance meter to the window normal. If measurements will be carried out from the ground the information about light emission to upper space will miss. Assuming, that luminous intensity curve of light emitted from window is rotary symmetrical it is possible to measure luminance of window also in upper half-space from an opposite high building. Such measurements were carried out in Bratislava on 19th July 2009. This night was clear sky without cloudiness with observable more brightness stars. Luminance of selected windows in residential building was measured by luminance meter Minolta 1° from ground (bottom half-space) and from roof of opposite building (upper half-space). Distance between both buildings were 54 m. This distance is too long for covering only glazing of the 0,9 m wide window by solid angle of used luminance meter. In this case the luminance of window L_w was calculated as weighted mean value of measured luminance L_m and luminance of supplementary façade area. The façade luminance of 0,05 cd.m^{-2} was considered in all calculations. Obtained results are shown in Table 1.

Table 1 Night luminance of window with various shading devices

Window dimensions	Window luminance				Description
	L_m	L_w	L_m	L_w	
M	cd.m^{-2}		cd.m^{-2}		
Width × Height	Measured from upper half-space		Measured from upper bottom-space		
0.9×1.5	3.5	5.01	1.2	1.72	Without curtain
0.9×1.5	1.2	1.67	1.1	1.63	With curtain
0.9×1.5	2.6	3.59	1.7	2.57	Half part of window covered with curtain
0.9×1.5	24.2	32.97	12.4	19.64	Fluorescent lamp in kitchen
2.4×1.5	0.4	0.50	0.5	0.62	Jalousie

4 Time luminance changes of the building façade

Measurements of window luminance have showed high variability of room occupation in building. If people are in the interior the electric lighting is switched on. If rooms are empty interiors are dark and no emission of artificial light in the exterior is observed. Night occupation of interiors by people is irregular.

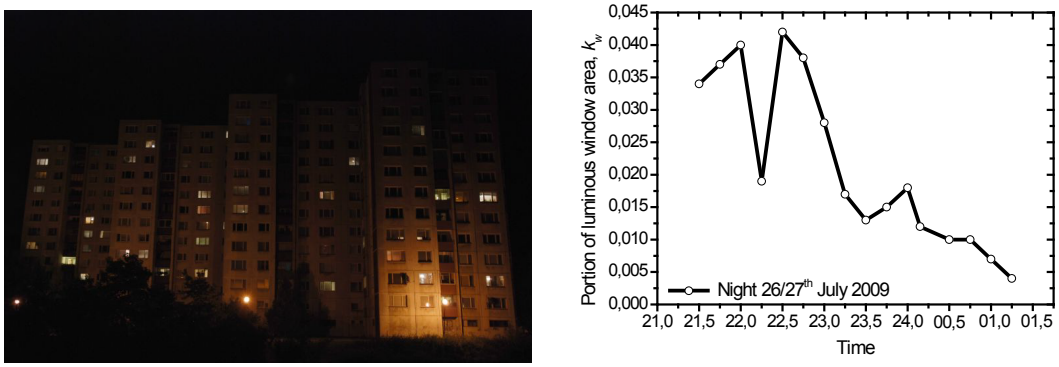
The CCD camera method was applied to study time changes of light emission from windows of a typical residential building, Figure 5.A, in the Bratislava urban space during a night. Changes of the portion k_w of total windows area emitting light S_{wi} to the whole façade area S were investigated, i.e. $k_w = \sum S_{wi}/S$. As the length of day also changes during the year, a different quantity of emitted light in the period between sunset and midnight can be expected. People are generally at home after 18:00 and the electric lighting is switched on mostly during winter period. Summer days are longer therefore shorter period from sunset to midnight results lower effects of artificial lighting emission to the outdoor space.

Determination of window luminance and all of façade areas in urban spaces is practically impossible, therefore it would be useful to derive the average façade luminance and luminous intensity curve representing typical situations occurring in the cities. If luminance of façade $L_{F,j}$ and window L_{wi} is determined, e.g by measurements or calculations, and area of the façade $S_{F,j}$ is known then the average façade luminance L_F can be expressed as follow:

$$L_F = \frac{\sum_i^n L_{w,i}\, S_{w,i} + \sum_j^m L_{F,j}\, S_{F,j}}{\sum_i^n S_{w,i} + \sum_j^m S_{F,j}} = \frac{\sum_i^n L_{w,i}\, S_{w,i} + \sum_j^m L_{F,j}\, S_{F,j}}{S}, \quad (2)$$

where $S_{F,j}$ area of the façade with luminance $L_{F,j}$.

The parameter k_w is logically decreasing towards the midnight. Its maximum value was found at 22:30 when 4,2 % façade area emitted light in the atmosphere, Figure 5.B.



A. B.

Figure 5: Changes of luminous windows. A. View on the investigated façade of typical residential building in Bratislava at 22:30. B. Changes of windows area emitting artificial light expressed by k_w

5 Conclusions

It was found that luminance of windows can be higher than 100 cd.m^{-2}, depending on the window shading system. Interior electric lighting is switched on irregularly during night-time with decreasing impact on the light pollution from sunset to midnight. Windows can contribute significantly to decreasing light pollution in the densely built-up urban spaces.

Precise modeling of luminous flux leaving window glazing with shading devices is practically impossible for all spaces in building. It should be useful to calculate average luminance values and luminous intensity curve of building façades and to consider their changes during the night.

Acknowledgment

This paper was written under the support of grant VEGA 2/0029/11.

References

[1] B. Kránicz, Z. Kollath, V. Gyutai (2008): Measuring Light Pollution. CD Proc. Conf. Lumen V4, Szczyrk.

[2] S. Darula, M. Kocifaj (2010): Svetlo produkované oknami budov a jeho šírenie v atmosfére v noci (Light emitted by windows and it propagation in the night atmosphere). Proc. Conf. Light influence on the night environment, Jablonec nad Nisou, p. 74-81.

[3] T. Novák, K. Sokanský, P. Závada, D. Diviš (2011). Analysis and evaluation of lighting parameters measuring of the night sky. Proc Conf. CIE 27th Session, Sun City, p. 144-150.

[4] A.J. Cabello, C.F. Kirschbaum (2002): Modeling of urban light pollution: Seasonal and environmental influence, Journal of the Illuminating Engineering Society **30** 142-151.

[5] F. Falchi (2011): Campaign of sky brightness and extinction measurements using a portable CCD camera. Mon. Not. R. Astron. Soc. **412** 33–48.

[5] M. Kocifaj (2011): A numerical experiment on light pollution from distant sources. Mon. Not. R. Astron. Soc., **415** 3609-3615.

[7] R.H. Garstang (1986): Model for artificial night-sky illumination, PASP, 98, p. 364-375.

Applied scotobiology in luminaire design

Robert Dick

Canadian Scotobiology Group, and
The Royal Astronomical Society of Canada
tel: 1-613-7815, fax: 1-613-283-0362, e-mail: rdick@csbg.ca

Abstract

Studies of our illuminated environment demonstrate the importance of light to humans, who by evolution are essentially daytime creatures. However the study of behaviour and the biology that occurs during the night has clearly shown the importance of darkness for both human and ecological health. Since humans are expanding their activity throughout the night and across the countryside, is there a compromise between the human desire for light and the need for darkness? Although there is no substitute for darkness, we have applied the findings of scotobiology to develop outdoor lighting that minimizes the disruption of artificial light at night (ALAN) on the natural environment and on human health. By limiting the brightness, extent, degree of glare, spectrum and duration of the emitted light, we have developed a luminaire that bridges these two solitudes to provide sufficient light for human activity while minimizing its impact on the environment.

1 Introduction

The ecosystem does not need or want any more light than is provided by natural means. All life has evolved and adapted to the natural levels, even humans. The levels and periodicity of light affect behaviour and biochemistry in profound ways through our circadian and circannual rhythms [1]. However increase in nighttime human activity since the industrial revolution and the recent development of 24/7 life styles, has increased the human desire for nocturnal lighting.

The ecological balance is based on the interrelationships between diverse species in a wide range of habitats. Wildlife, to some degree, occupies every niche on this planet. Although not obvious to most people, nocturnal creatures balance out the day-night ecosystem. About 30% of vertebrates and 60% of invertebrates are nocturnal [2], and it has even been proposed that mammals began as nocturnal animals hundreds of millions of years ago [3], and some of them have evolved into daytime creatures since then.

Although there is no single illuminated condition that represents all niches across a region, we can identify five attributes that are critical to quantifying its characteristics:

1 Brightness level of illumination,

2 Extent of the illuminated area,

3 Degree of glare,

4 Spectrum of light used, and

5 Duration of the illumination.

The original goal of this work was to determine what characteristics of artificial light at night (ALAN) have dominant effects on the ecosystem, and how much they can be reduced while still providing sufficient illumination for basic human activity. This required the study of scotobiology.

Scotobiology is the study of the need for periods of darkness. The study is complicated by the range in tolerance that the multitude of life forms have for nocturnal lighting. Since they have evolved to fill neighbouring, and in many cases overlapping, niches and that they can exercise very different behaviours, a single illuminated, or dark condition is not ideally suited for all nocturnal animals. Also other environmental factors such as activity levels and food supply that skew the data. However, a

general pattern does appear with the natural cycles of day and night when coupled with the affects of twilight and the monthly appearance of the Moon. And, these provide insights into the effects of ALAN.

1.1 Brightness Level

The natural night is rarely very dark. Twilight and dusk provide a gradual transition between daylight and nighttime. Only under thick cloud cover can it be so dark we cannot see anything, otherwise illumination by starlight, about 0.001-lux, contributes enough light for humans to walk around, and the Moon can illuminate the countryside up to 0.27-lux for a period of time each month. All life on the Earth has evolved, or adapted their behaviour to accommodate this range in nighttime illumination.

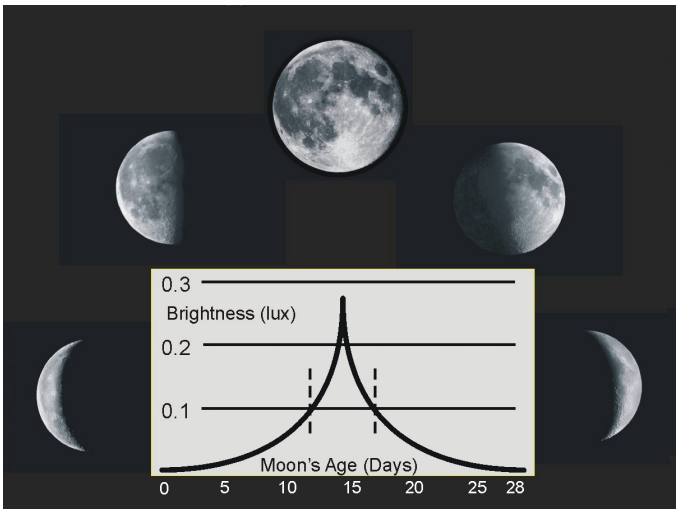


Figure 1- Moon Phases: The Moon dominates the night sky for about a week centred on the ull moon. At other times, its phase is much thinner, and it sets soon after the Sun at night and rises just before the Sun in the morning.

Although Moonlight has been a nocturnal light source since the Earth formed 4.5-billion years ago, it still disrupts the activity of wildlife with its monthly brightening. For example, nocturnal foraging species alter the extent of their travels under the light of the full Moon [4], and some zooplanktons restrict the vertical migration in the water column during times of natural lighting [5,6]. These species then compensate for the dietary loss during the relative dark of the rest of the month.

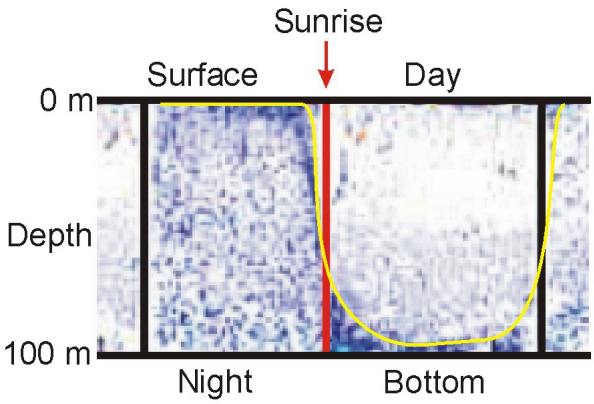


Figure 2 – Diel Vertical Migration of Zooplankton recorded in Saanich British Columbia [7]. It shows the relatively rapid descent of zooplankton during dawn. These records were made during a three-day old moon (crescent in evening sky) and does not show any significance effect of the lunar phases.

Historically human activity has been pedestrian with a casual walking speed up to about a meter per second. For a relatively flat landscape starlight is sufficient to provide visibility for a few physical hazards. However humans are not primarily creatures of the night and the visibility needed for greater activity requires more illumination - greater than the full moon. Personal tests under a range of illumination levels suggest that very little extra artificial light is needed for good visibility. Without glare, 1-lux is quite adequate to easily see hazards on the ground and at 3-lux we could read a newspaper.

We are living longer than our ancestors and this exposes us to the degradation of our vision and biochemistry. The eyes of senior citizens become more opaque with age and less responsive to light, especially at short wavelengths [8]. Our cognitive functions change if we are not exposed to bright light during the day [9] and sleep in dark enough quarters to provide a contrast in the flow of melatonin [10]. The hormone melatonin is needed to help us sleep and get the most out of our time at rest. In healthy humans 7 to 17 lux is sufficient to reduce our nighttime levels of melatonin [11,12]. However, the amount of the melatonin decreases as we age so lower levels of illumination can have more severe effects than for younger subjects. Animal studies show that illumination as low as 0.2-lux will affect melatonin secretion [13].

Modern mechanized human activity is much faster than a walking pace. Hazards are increased with fast vehicles in close proximity to pedestrians and require decisions to be made much more quickly than in the past. These require higher illumination levels for visibility.

Our response to visual stimuli above a threshold illumination level follows an ogive curve that levels out with decreasing benefits with greater illumination levels [14]. Some of the complicating factors for a quantitative study of this type are the effects of: hazard size, colour and contrast; the person's age, visual acuity and degree of alertness, which is affected by the time of day; the brightness, colour and associated glare of the illumination and the contribution of other light sources (car headlights). It also depends on how quickly the detection of a hazard should be made, which depends on the nature of the hazard. For this last point a person walking can take many seconds to react after seeing a hazard whereas a driver may have only a few seconds to make a decision. Therefore the results of a complete study may not be very helpful in determining the best illumination level unless it is expanded to include the probabilities of these conditions and presents the results in a statistical format. This can be justified by accepting that life has risks that can be addressed with statistics.

Higher illumination levels are used on roads with higher speeds and traffic densities. Based on pathway and roadway measurements in 2011 of existing illumination in the City of Ottawa, Canada, collector roads are illuminated to a maximum of about 17-lux with non-uniformities of 3:1, and older residential streets and pathways are lit to a maximum of 20-lux with non-uniformities of more than

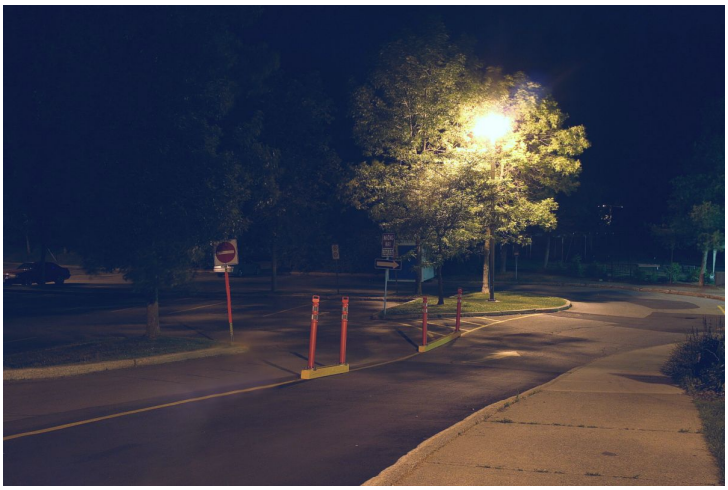


Figure 3 – Residential Street with large range in illumination level. The illumination from a lamppost is used as "marker light" rather than for visibility.

10:1

Even pedestrian traffic with illumination levels of about 1-lux is in conflict with the ecosystem in rural areas and the human desire to be mobile at night. Although the full moon provides some illumination, it is not a constant source over the month and vegetative cover limits its general usefulness along pathways. Therefore, some artificial lighting can be helpful but at the cost of affecting the natural environment. If we are to be sensitive to the needs of the environment, a compromise is needed.

We conclude that 1-lux is sufficient for pedestrian traffic along pathways but with qualification. This illumination level must be restricted to the area for pedestrians. The extent of this area depends on the overall human use of the area and the level of priority given to wildlife.

1.2 Extent of the Illumination

There are several reasons for limiting the extent of an illuminated area. It reduces light trespass and it focuses the light within the target area, so less light is needed for the purpose. This is usually achieved with "full cut-off" (FCO) light fixtures that do not directly shine any light above a horizontal plane that passes through the bottom of the fixture. However this permits light that shines slightly below the horizon, which can cast shadows and compromise night vision several hundred meters away.

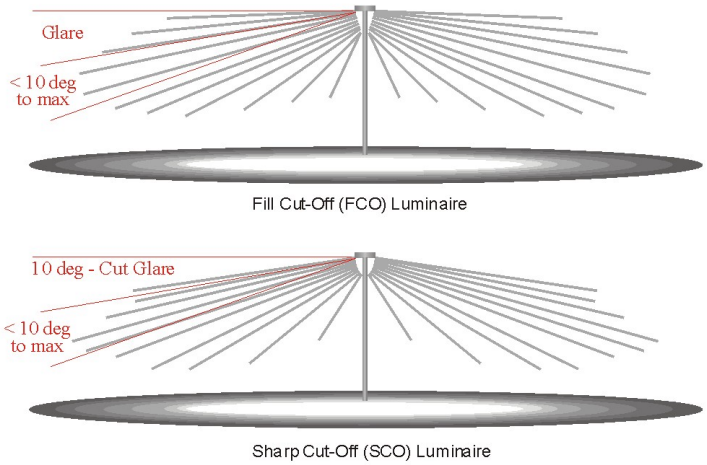


Figure 4 – Comparison between the shielding of Full Cut-off (FCO) and Sharp Cut-off (SCO) luminaires. SCO luminaires reduce the amount of light that shines within the 10-degree band below the horizon.

It is impossible to completely shield a luminaire. The lamp must be visible in order to illuminate the ground. However a more restrictive shielding requirement will reduce the apparent brightness of the lamp when viewed from the periphery of the target area. In the 1990's some manufacturers (Mouldcast, Inc. for example) produced luminaires with "sharp" cut-off (SCO) shielding that restricted the emission of light within the 10-degree band below the horizon. This characteristic did not become popular and we now have the more lenient FCO classification. The performance of the FCO optics allowed a wider light distribution and fewer mounting poles, which are the main cost of installing artificial lighting. However, FCO luminaires also create the direct view from the ground of the lamp from a considerable distance (about 10x the mounting height), even though the ground illumination level at that distance is negligible (less than 10% maximum) and insufficient due the impact of the glare from the lamp. So, the light that shines beyond the target area creates glare, without the benefit of illumination. In order to more tightly contain the illuminated area more aggressive SCO shielding is needed.

The target area should be restricted to less than the foraging range of the local animals. This allows the animal to detour around the affected area. However, determining the foraging range is complicated

by the number of different species that inhabit the area. The foraging range is very roughly a function of the size of the animal [15] and can exceed a hectare. Therefore, it is not possible to prevent all impact without setting aside large areas in which no light should be permitted. This has been done to some degree with Canadian Dark Sky Preserves and more effectively in the new RASC Nocturnal Preserve Program.

The best we can do is design luminaires with restrictive shielding to limit the extent of the contamination and use visual barriers (buildings, berms or bushes) to reduce the light that scatters out of the target area. So as not to affect foraging patterns we prefer not to use physical barriers.

1.3 Degree of Glare

The definition of glare is complicated by our need to quantify it and its effects. In this context, glare will refer to a light source or surface that compromises visibility. Visibility can be compromised by the direct view of the light-emitting component, which can bleach a portion of the retina or cause us to squint. A bright point or surface can also cause our iris to close down – letting less night into our eyes. And it can affect our photochemical night vision so we cannot see into less illuminated areas. These are made worse by imperfect eyes and the additional scattering of light by airborne particles, weathered windows and scratched eyeglasses. Animals with similar eye structures should also be subject to some of these debilitating effects of glare.

To reduce the effect of a point source, the light must be diffused over a large area. Most roadway luminaires use refractors to scatter the light. FCO luminaires use internal mirrors that reflect the light onto the road, but the bright surface of the lamp is visible from below the fixture. The new LED luminaires have small lenses mounted on each LED and these focus the light on to the target, so we can see the individual LED emitters by looking up from under the fixture. The intense brightness of the LED emitter is roughly the brightness of a tungsten filament in a clear incandescent bulb - causing temporary blind spots in our field of view and potential eye damage [16].

A lesser effect occurs with bright light sources in the distance. Distant light sources can be distracting and make the foreground illumination seem ineffective.



Figure 5 – Re-lamping a major collector roadway demonstrates the reduction in glare and improvement in visibility (near field) compared to the section with semi-cut-off luminaires (distant). Images of high contrast scenes cannot show the real effects of glare because of the limited dynamic range of the image.

Non-uniform illumination on the ground can produce a form of glare. It is caused by the combined effects of the "inverse square law", where the illumination level decreases by $1/r^2$, where the distance from the source is r, and the "cosine law" where the illumination level decreases with the angle of the incident light from vertical (θ), or cosine θ. The combined effect makes the area at nadir (under the luminaire) appear much brighter than the periphery. Unless five times more light is projected to the periphery of the target area than the nadir there will be a significant illumination gradient. For some

luminaires this illumination gradient is so steep that the nadir illumination will overwhelm that of the periphery.

1.4 Light Spectrum

Most of our sensory input comes from our vision, and most of that is encoded in colour. All surfaces reflect different colours of light. Unless a surface is incandescent, we can only see it by the incident light. In order recognize the surface colour the spectrum of the incident light must be familiar and cover a broad spectral range. An incident spectrum covering less than the solar spectrum will result in poor colour recognition. However, a broad spectrum of ALAN will mask the more general cues than a changing illumination spectrum provides.

The colour of daylight is not constant, and is used by animals to determine the time of day. For most of the day, the sky is dominated by the sunlight, which for the most part is white. The slight variation in the Sun's spectrum does not seem to affect our judgement of the colour. However in the evening the low Sun causes more of its blue light to be scattered across the sky making the sun's disk appear more orange. As it sets, the predominantly yellow coloured disk of the Sun disappears and a major yellow component of the light is reduced.

In the evening the dominant colours are red on the horizon near sunset and blue from the scattered light that remains across the sky. As the Sun's disk continues below the horizon, the blue sky fades below our visual threshold and the sky appears dark. The reverse happens at dawn.

This transition in colour is detected by the photosensitive cells in our eyes. Our retina has two types of visual light detection cells: cone cells that are used during the bright daytime, and rod cells that are about 1,000 times more sensitive that are used at night. The rod cells are sensitive to a broad spectral band of light centred on 508 nm. Our daytime photopic spectrum peaks at 555 nm - towards the yellow from our night vision. By limiting the emitted spectrum of ALAN to the longer wavelengths, we can preserve our night vision. Ideally, red LEDs can be used because their emission is almost out of the spectral sensitivity of our rod cells.

Just after sunset, the blue of twilight illuminates the ground as the daylight creatures retire and the

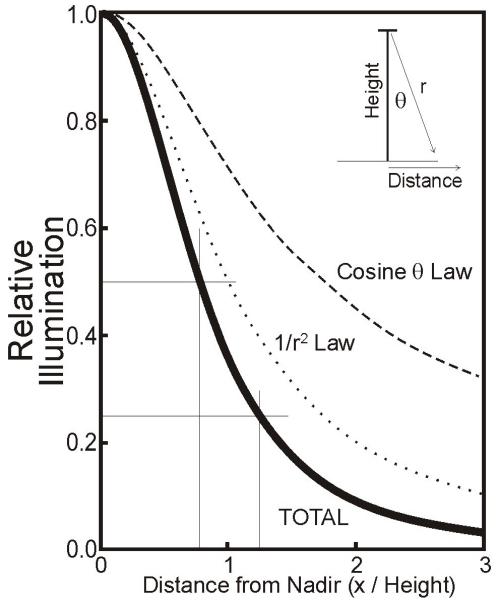


Figure 6: The cumulative decrease in illumination with distance due to the inverse square law and cosine law. About 5 to 10 times more light must be projected to the edge of the target area to reduce the natural non-uniformity of illumination.

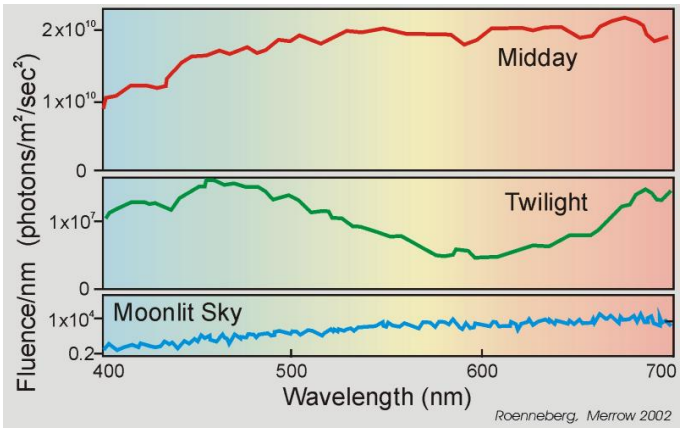


Figure 7: The change in spectral properties of the sky from daylight, through twilight [17]. Yellow light decreases with twilight as the Sun's disk sets below the horizon.

nocturnal animals come out to forage. The illuminated blue sky can extend daylight past sunset by over 30-minutes at the beginning of string, and longer in the summer. Our ability to see by this light is a survival advantage for daytime animals like humans because it offers an extended period of safety while beginning to settle down to sleep, but it also has a biochemical function. During twilight the illumination levels are high enough to delay our circadian rhythm in so far as indicated by delaying the release of the hormone melatonin [18].

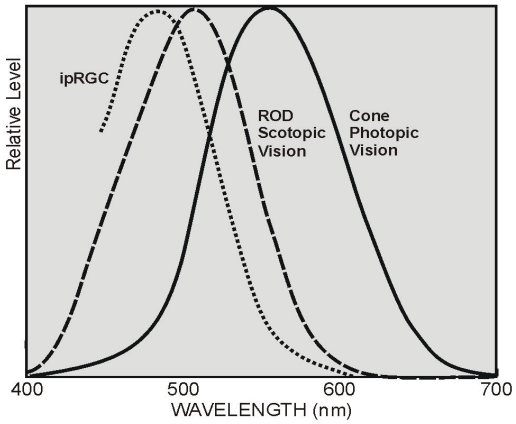


Figure 8: The spectral sensitivity of the two visual detector cells in our retina: rod cells for our night scotopic vision, and cone cells for our daytime photopic vision. The intrinsically photosensitive Retinal Ganglion Cells (ipRGCs) are used to "detect" nighttime when the blue light of twilight falls below their detection threshold.

The biochemistry and behaviour of animals is controlled by the circadian rhythm, which is kept in synchrony with their active lives by the detection of blue light by non-visual intrinsically photosensitive Retinal Ganglion Cells (ipRGCs) in our retina.

These cells are most sensitive to the spectrum of light centred about the wavelength of 480 nm and together their network has a threshold sensitivity of very approximately 1 to 10 lux [19] and a more general review of the literature suggests as low as 0.1 lux [20]. Sensitivities at the single photon level have been reported that seem due to their biochemistry and neuron logic [21]. As the sky darkens below about two lux, these cells are not able to confirm it is still twilight. In response, hormones are released to reduce our metabolism and put us to sleep.

This detection of nightfall also enables the release of other hormones that repair damaged tissue and fight infection [22]. They are created in late afternoon in preparation for their release, but they begin to break down several hours later and are re-absorbed. Therefore their release must be well timed with our rest period. If the release of these hormones is delayed then the benefits of our rest and resulting health is compromised.

It is important that ALAN not contain short wavelength light that will be detected by our ipRGC cells, even though this will alter our recognition of colour.

1.5 Duration

The natural environment is not static. Life uses its plasticity to adapt to changes. One of these is the duration of daylight, and darkness. Only on the equator are the day and night of equal length throughout the year. The length of day and night cycle with increasing amplitude towards the north and south poles that results in the seasons. At the mid latitudes daylight can range between 8 and 16 hours.

The lengthening period of daylight in the spring, and shortening in the autumn is used by wildlife and plants as an indication of the time of year. Plants generally bloom in spring and drop their leaves in late autumn. Animals prepare for hibernation or migration late in the year. Disrupting the perceived length of the day, or more precisely, the length of night can confuse these visual cues and leave some animals and plants ill-prepared for winter.

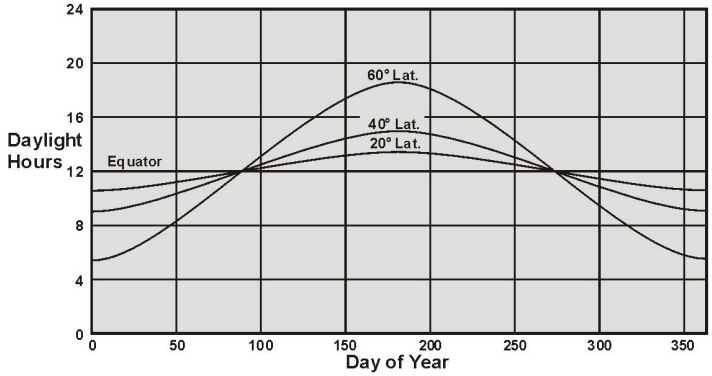


Figure 9 – The length of daylight for different latitudes [23]. The range in daylight hours increases with latitude and increases the importance of length of natural daylight for knowing the time of the season.

Determining the duration of ALAN after sunset, and before sunrise to permit illumination does not suggest that it is a "good idea". Any ALAN that extends into the night will advance preparations during spring for summer and delay those in autumn for winter. This could place animals at a disadvantage if their need for food is in advance of, or too late for its supply.

Nature's tolerance to the length of night before it has a significant impact on the ecosystem has never been studied, but that does not mean we cannot deduce some guidelines. Although light indicates the season, the temperature and snow cover, at mid and high latitudes, stresses the environment. Temperatures vary considerably from year to year, delaying snowfall for over a month or more. The corresponding difference in day length over a month in spring and autumn is approximately an hour in the morning and an hour in the evening. Twilight blurs the transition to nighttime by an additional 30 minutes or so, though at least it is predicable.

Recognizing the effects of cloud cover, and local shading due to vegetation it seems reasonable to round up the tolerance to nightfall to about 2-hours in the evening and again in the morning, after sunset and before sunrise. Switching the ALAN on and off at specific times (for example turning it off at 11 pm every night) is not sufficient since it does not recognize the seasonal shift in the time of sunrise and unset, which provides the temporal cues.

Since ALAN is only used to assist human activity, the illumination level should match this activity. Although many people have embraced 24/7 lifestyles, traffic records for major cities indicate that most people do not. High-speed roadways have the greatest use for ALAN due to the need for short reaction

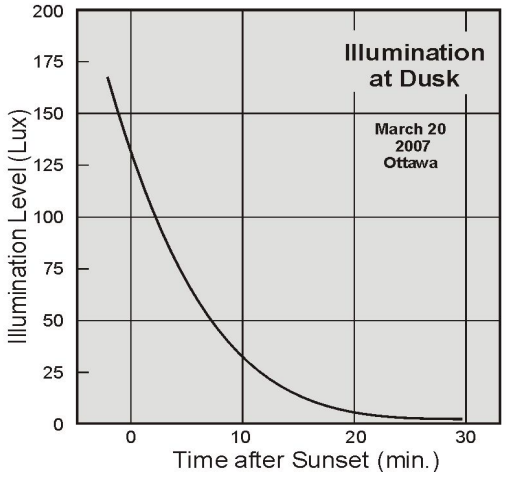


Figure 10 – From sunset until it is no longer easy to see can be more than half an hour as the upper atmosphere eventually enters the Earth's shadow. This significantly extends the length of useable daylight.

times of motorists. Studying traffic records show a clear pattern of high-density traffic during the day and very little traffic at night. During spring, summer and autumn, the periods of greatest traffic volume are during daylight.

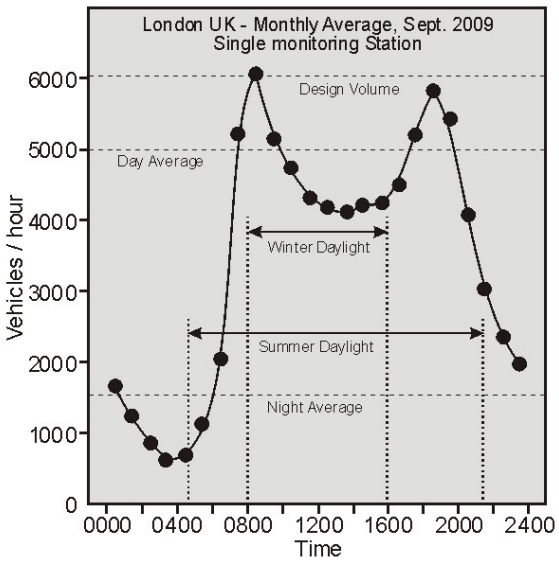


Figure 11 – Traffic density along a major roadway in London, UK [24]. Although winter rush hour traffic occurs in relative darkness, summer daylight encompasses rush hour traffic.

Only in the winter months does this traffic, bounded by morning and evening rush hours, extend well into night. Reducing the illumination levels, or turning-off the lights, within 2 hours of sunset during summer and most of the spring and autumn (the most ecologically sensitive seasons) will not affect most commuters. Leaving the lights fully on throughout the night is therefore a decision based on politics and aesthetics.

2 Luminaire Specification and Performance

Existing luminaires have significant environmental impact. They have been developed for the major urban markets and provide illumination for our less sensitive photopic vision that uses our cone cells. By addressing the vision thresholds of wildlife, and the characteristics of our ipRGC, we have developed a luminaire that is suitable for ALAN in ecologically sensitive areas - preserving night vision for many mammals and having reduced impact on their circadian rhythm and health. It can also be used in urban areas to reduce the impact of ALAN on parklands and residential neighbourhoods.
In this section we will summarize the specification and performance of this luminaire, which holds a provisional patent in the United States.

The luminaire has a weatherproof aluminium enclosure $20 \times 20 \times 8$ centimetres that connects directly to 110vac, 220vac or 277vac power and existing lighting controls. It uses light-emitting diodes that consume less than 15-watts at maximum light output, and more typically less than 12-watts making it appropriate for off grid lighting and solar power applications.

Unlike all previous lighting technologies, LEDs must be kept cool – ideally near room temperature. The optical and mechanical design passively maintains the junction temperature of the LEDs to less than 50C above the ambient air temperature at maximum light output, and more typically less than 30C above ambient. We have maximized the heat transfer areas, minimized the number of thermal interfaces and made the convection surfaces vertical. Maintaining a minimal temperature difference is critical for long life of the LED and surface phosphor. Plastic lenses become less transparent at high temperature, though our design does not use them.

The cost of the luminaire is greater than typical consumer light fixtures, but is less expensive than most LED luminaires that are marketed for similar applications.



Figure 12 – The Canadian Scotobiology Group (CSbG) luminaire is compact unit with LED light sources powers through a current course from 110 vac, 220vac or 277vac. The thermal design maintains the LED junction temperature to less than 50 C above ambient air temperature.

2.1 Illumination Level

The luminaire is designed for a maximum of 3-lux, though higher levels are achieved when mounted at a lower height. This is adjustable over a range of about 5:1 to compensate for various mounting heights and applications. This illumination level can be reduced to 1-lux, or lower for pedestrian areas.

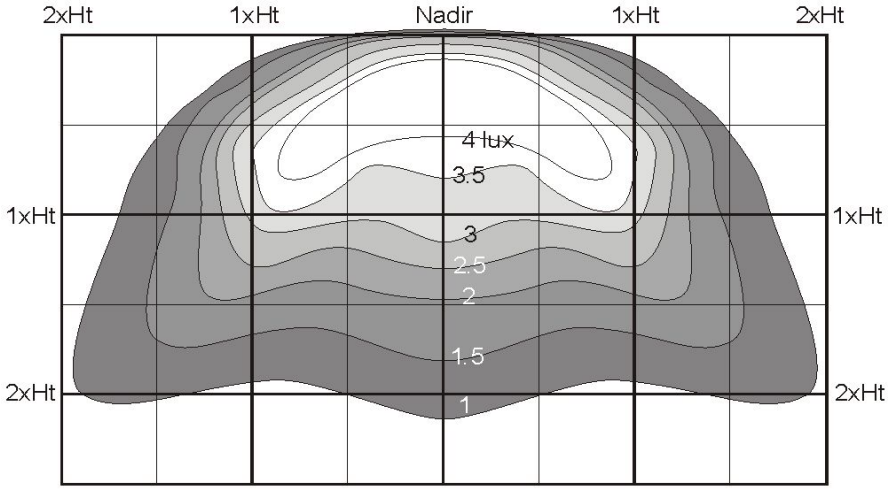


Figure 13: The CSbG luminaire provides relatively uniform illumination over an area more than 3 × 1.5 times its mounting height. The field adjustable light output allows the brightness to be reduced for lower mounting heights. These values are for a mounting height of 4.9 meters and about 13-watts. The illumination pattern can be shaped by adjusting the angle of the mirrors, and the illumination level can be reduced in the field by adjusting the current. The illumination level was reduced to less than 0.1 lux at 3×2 times mounting height from the nadir.

During testing in a dark rural setting, 1 to 3 lux is more than sufficient to provide illumination around automobiles, for loading and unloading gear and finding dropped articles in the grass. The uniform illumination across the target area of about 3 × 1.5 times the mounting height is within 3:1 to minimize bright spots in the field of view and to maximize the target area for a given amount of power.

The specified target area is sufficient for most applications requiring illumination, such as the area around buildings, stairs and doorways, kiosks, pathways, patios, parking lots and low speed roadways. There is a graceful dimming of the illuminated area beyond the target area. When mounted in a string for pathway and roadway lighting, the spacing can be about 3 pole heights, or more if non-uniformity requirement can be relaxed.

The optical design minimizes the amount of backlight that shines behind the luminaire. This prevents significant light trespass and reduces vertical-surface glare if it is wall-mounted.

2.2 Degree of Glare

All components fit inside the enclosure to produce a full cut-off fixture. The interior optics further reduces the amount of light below the horizon to approximate a sharp cut-off luminaire.

Reflective baffles direct light from the LED emitters towards main mirror, and prevent the direct view of the LED emitters from outside the luminaire. The main mirror serves three functions. It is curved to expand the light into a broad uniform pattern. It expands the light of the LEDs so they appear as diffuse light sources. The textured main mirror increases the effective surface area of the light sources - reducing the apparent intensity of the emitters to about 3% of the original LEDs. This texture also prevents patterns of light, from optical artefacts, being projected onto the ground.

The mirror-like sidewalls direct light into the periphery to make the illumination distribution larger and more uniform. Additional reflective shielding prevents glare for people leaving a building when the luminaire isused as a doorway and porch light.

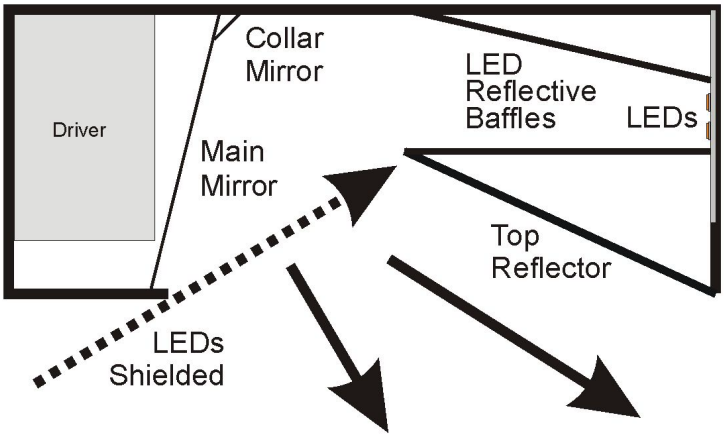


Figure 14: The internal reflective baffles prevent the direct view of the LED emitters to prevent eye damage. They also minimize the backlight. When mounted as an egress light fixture, these baffles prevent the light that would shine into the eyes of people leaving a building and that would create light trespass when used near a property line.

2.3 Light Spectrum

Non-white LEDs are used to minimize the impact of blue light on wildlife and human health. The LEDs are fully phosphor converted that emit no light at wavelengths shorter than 500 nm. Although they have to be tested, the restricted light spectrum resembles the spectrum of “Bug Lights” that have a significantly reduced attraction for mosquitoes, a known vector for infectious diseases [25].

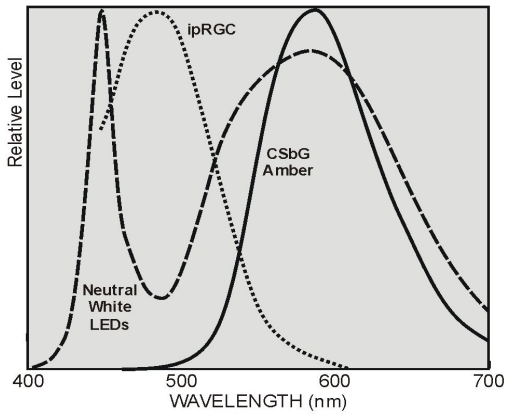


Figure 15: The CSbG Amber spectrum is compared to that of a white LED, and the sensitivity of our intrinsically photosensitive Retinal Ganglion Cells. There is only about 11% overlap of the amber light with the ipRGC sensitivity.

2.4 Duration

The current driver for the LED can uses either a 0-10vdc, or variable resistor to control the brightness of the target area. The luminaire may be dimmed either abruptly, or gradually under the command of the central control circuit, depending on the complexity of the control circuitry.
Including a photo sensor and timer in every luminaire increases complexity, failure modes and cost to a luminaire. It is recommended that all luminaires in an area use a reliable (redundant) control circuit to control the string of luminaires.

A light sensor should detect the approximate time of sunset to turn-on the luminaire. A timer should turn-off the luminaire about two hours later, or reduce its output to a minimal level. The timer should turn the luminaire on, or increase the output in the morning, and the light sensor should turn it off before sunrise. Depending on the application, the facility manager may deviate from these guidelines, but regardless the luminaire is designed to minimize the impact of the ALAN on the environment.

If deemed appropriate by managers, a presence detector can be added to turn-on the luminaire during the off-period for a short period of time.

3 Summary

The study of scotobiology has been used to develop rational limits for artificial light at night. To the best of our knowledge there is no commercially available luminaire that can achieve these specifications. We developed this luminaire to be a viable alternative for ecologically sensitive areas, and to reduce light pollution in other places. Although any ALAN will impact the environment, our luminaire minimizes these impacts at a reasonable cost while providing sufficient illumination for human activity.

Acknowledgements

I am grateful for the support of Dr. Roseann Runte, President of Carleton University, Ottawa, Canada for use of their academic library and access to their eJournals.

References

[1] W. Koukkari, R. Sothern (2006): Introducing Biological Rhythms (Springer Science).

[2] F. Hölker, C. Wolter, E. K. Perkin, K. Tockner (2010): Light pollution as a biodiversity threat. Trends in Ecology and Evolution 25(12): 681-682, doi: 10.1016/j.tree.2010.09.007.

[3] M. Menkar, L. Moreira, G. Tosini (1997): Evolution of Circadian Organization in Vertebrates, Brazilian Journal of Medical and Biological Research 30: 305-313.

[4] P. Beier (2006): Effects of Artificial Night Lighting on Terrestrial Mammals, Chapter 2, Ecological Consequences of Artificial Night Lighting, C. Rich, T. Longcore, Ed. (Island Press).

[5] J. Ringelber (2010): Diel Vertical Migration of Zooplankton in Lakes and Oceans, Chapter 9, (Springer Science B.V.), doi: 10.1007/978-90-481-3093-1_9.

[6] S. Dodson (1990): Predicting Diel Vertical Migration of Zooplankton, Lmnol. Oceanogr., 35(5), 1195-1200.

[7] http://venus.uvic.ca/2007/11/zooplankton-the-mighty-migrators-in-saanich-inlet/. Zooplankton: the Mighty Migrators in Saanich Inlet, Accessed March 24, 2013.

[8] W. Charman (2003): Age, Lens Transmittance, and the Possible Effects of Light on Melatonin Suppression, Ophthal.Physiol. Opt. 23: pp181–187.

[9] B. Myers, P. Badia (1995): Changes in Circadian Rhythms and Sleep Quality with Aging: Mechanisms and Interventions, Neuroscience and Biobehavioral Reviews, Vol. 19, No. 4, pp. 553-571.

[10] D. Blask (2009): Melatonin, Sleep Disturbance and Cancer Risk, Sleep Medicine Reviews 13257–264

[11] G. Brainard, M. D. Rollag, J. P. Hanifin (1997): Photic regulation of melatonin in humans: ocular and neural signal transduction, Journal of Biological Rhythms, Vol. 12 No. 6, pp. 537–546.

[12] J. M. Zeitzer, D.-J. Dijk, R. E. Kronauer, E. N. Brown, Ch. A. Czeisler (2000): Sensitivity of the human circadian pacemaker to nocturnal light: melatonin phase resetting and suppression, Journal of Physiology, 526.3, pp.695–702.

[13] R. T. Dauchy (1997): Light contamination During Dark Phase in Photoperiodically Controlled Animal Rooms, Effect on Tumor Growth and Metabolism in Rats, Laboratory Animal Science, 47(5): 511-8.

[14] R. Blackwell (1959): Specification of Interior Illumination levels on the basis of Performance Data, Illumination Engineering Institute, June 1959.

[15] R. K. Swihart, N. A. Slade, B. J. Bergstrom (1988): Relating Body Size to the Rate of Home Range use in Mammals, Ecology, 69(2), pp. 393–399, Ecological Society of America

[16] Effets sanitaires des systèmes d'éclairage utilisant des diodes électroluminescentes (LED), Agence nationale de sécurité sanitaire de l'alimentation, de l'environnement et du travail, Saisine n° 2008-SA-0408, 19 octobre 2010

[17] T. Roenneberg, M. Merrow (2002): Light Reception: Discovering the Clock-Eye in Mammals, Current Biology, Vol. 12, R163–R165.

[18] J. M. Zeitzer, D.-J. Dijk, R. E. Kronauer, E. N. Brown, Ch. A. Czeisler (2000): Sensitivity of the human circadian pacemaker to nocturnal light: melatonin phase resetting and suppression, Journal of Physiology, 526.3, pp.695–702.

[19] K. E. West, M. R. Jablonski, B. Warfield, K. S. Cecil, M. James, M. A. Ayers, J. Maida, C. Bowen, D. H. Sliney, M. D. Rollag, J. P. Hanifin, G. C. Brainard (2011): Blue light from light-emitting diodes elicits a dose-dependent suppression of melatonin in humans, Journal of Applied Physiology 110: pp. 619–626, Figure 4.

[20] S. Pauley (2004): Lighting for the Human Circadian Clock: Recent Research Indicates that Lighting has become a Public Health Issue, Medical Hypotheses 63, pp. 588–596

[21] M. T. H. Do, S. H. Kang, T. Xue, H. Zhong, H.-W. Liao, D. E. Bergles, K.-W. Yau (2009): Photon capture and signalling by melanopsin retinal ganglion cells, Nature 457, 281-287, doi: 10.1038/nature07682.

[22] W. Koukkari, R. Sothern (2006): Introducing Biological Rhythms, Chapters 10 and 11 (Springer Science).

[23] http://www.gandraxa.com/length_of_day.xml, Accessed March 26, 2013.

[24] http://trads.hatris.co.uk, Accessed May 17, 2012.

[25] A. Barghini, B. A. S. de Medeiros (2010): Artificial Lighting as a Vector Attractant and Cause of Disease Diffusion, National Institute for Environmental Health Perspectives, doi: 10.1289/ehp.1002115 (available at http://dx.doi.org/), Online 1 August 2010

Light pollution measurements in Ireland

Brian Espey[1,2,3] and Joe McCauley[1,3]

[1] *School of Physics, Trinity College Dublin, College Green, Dublin, 2, Ireland*
[2] *School of Cosmic Physics, Dublin Institute for Advanced Studies, 31 Fitzwilliam Place, Dublin, 2, Ireland*
3 Royal Irish Academy Sub-committee on Light Pollution
tel: +353 1 896 1675, fax: +353 1 671 1759, e-mail: brian.espey@tcd.ie

Abstract

We report on our work towards the first ever ground-based survey of light pollution in the island of Ireland. The aim of this work is to establish a database of information to serve as a reference to monitor future changes, to compare with in-orbit measurements, to study the potential impact on the environment, and to permit the calculation of the effects of future changes in lighting usage and patterns. During the era of the Celtic Tiger economy, there has been a large growth in the development of rural areas, together with the associated spread of lighting into these environments. We report on the results of our work, the current status to establish an International Dark Sky Reserve in one of the darkest areas of the country, and our efforts to develop tools to support our work. Additionally, we report on the development of a stand-alone measurement

1 Introduction

Until recently there was no systematic effort to obtain data and monitor the night sky brightness and to establish the health or otherwise of the sky over the entire island of Ireland. Spurred by the meeting in Armagh on the occasion of the International Year of Astronomy in 2009, a number of Unihedron Sky Quality Meters [1] were provided by Armagh Observatory with additional instruments supplied by the International Dark Sky Associaton, and Günther Wuchterl [2]. We have amassed roughly 400 manual measurements from individual sites around the country made with SQM and SQM-L instruments, and also roughly 13,500 automated observations, predominantly made with Wuchterl lightmeters.

Observation of the Irish night sky, even from rural locations, tends to identify the presence of scattered light from sodium public lighting. Lamp types for public lighting in the Irish Republic are roughly equally split between low pressure and high pressure sodium lights, with only a small proportion (~3%) of mercury lamps, and roughly 625,000 luminaires on the entire island. Since the building boom of the late 1990s to mid-2000s, there has been in an increase in the number of houses built in Ireland, including in smaller rural locations. As a result, large parts of the country have seen an increase in lighting levels brought about by improved roads as well as housing developments, as shown in the latest data from the NASA SUOMI satellite [3] (Figure 1).

There are still areas of the country where there dark skies are still obtainable, particularly in the West of the country, facing towards the Atlantic Ocean, but also areas where the influence of our nearest neighbour – the United Kingdom – can be measured. Figure 1 shows images obtained in diametrically opposite parts of the country, with similarly opposed light pollution issues. Note that, despite the presence of a few local sources of light, the view from the southwest clearly shows the Milky Way, and this is an area of the country where further surveys are planned in order to delineate a region which can be developed as an International Dark Skies Association Dark Sky Reserve. At the other end of the country, the light from Glasgow in Scotland creates a large light dome which is readily visible 150km away, and which casts an intervening island and famous bird sanctuary into silhouette.



Figure 1: The good and the bad – two images illustrating the range of sky conditions away from local sources displayed beside an image obtained with the NASA Suomi satellite obtained in March 2012. Top right shows an image from the North-East of Ireland with an obvious sky dome from Glasgow, Scotland nearly 150km away. Visible in the original image is the silhouette of an island that lies between the two countries. Bottom left shows an image from a near-pristine region of the country, looking out to sea. Note that the brightness has been exaggerated to facilitate reproduction. It is hoped that an area in this region may be developed as an IDSA Dark Sky Reserve. Images supplied by Terry Moseley (Irish Astronomical Association) and Julie Ormonde (South Kerry Astronomy Society)

2 Light Pollution Measurement

We have performed measurements in many parts of the country, but have concentrated on measurements of the diffuse zenithal background rather than of local sources of light. The aim of this work has been to identify the general state of health of the sky, rather than to make measurements which would be more indicative of local conditions rather than the general condition.

One of our findings has been that Dublin (the largest city in the Republic, with roughly one quarter of the entire population), has a big effect on both its local and more general environment and its effects are visible even in the Wicklow Mountains National Park, away from local light sources. Figure 2 shows some of the results from this work, obtained both within and outside the metropolitan area. Due to the presence of the Wicklow Mountains, urban development is constrained to ~10km from the city centre and beyond that point generally obtained from along a country road which runs along the spine of the hills. At larger distances (and generally lower elevations), measurement areas are limited by topographical features and the presence of forestry, but the influence of local population centres can also be seen.

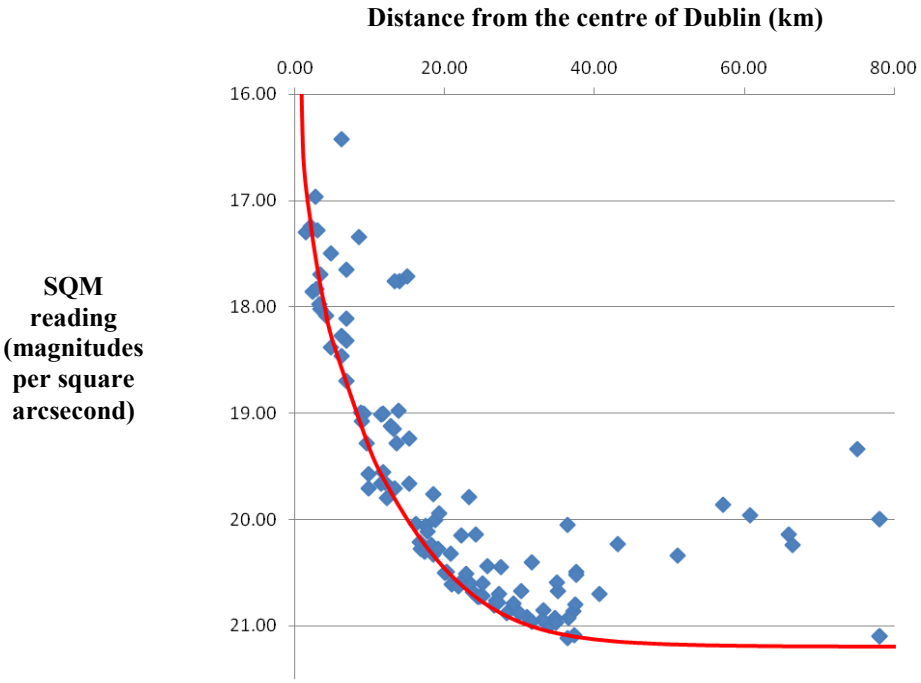


Figure 2: Measurements of zenithal night-sky brightness measured southwards from Dublin: most measurements were obtained along a mountainous route in a rural location in the Wicklow Mountains National Park, so are representative of the light from the capital city rather than of local light sources. As a guide, the popular tourist location of Glendalough lies at 50km from the city. The solid line is a simple approximation to the lower limits at each point, and it normalised to the darkest Irish night sky. Note that the model trend differs from the commonly-used Walker model.

We have performed other surveys, mainly in the Dublin/Wicklow area due to accessibility, and also as we received joint funding from the national Department of the Environment, as well as Wicklow County Council, and we have also collected spot readings from other areas around the country contributed by volunteers. So far, the two darkest locations appear to be in the west and southwest of the country, and both have SQM readings of just below 21 magnitudes per square arcsecond. The quality of the night sky is likely to be due to the rural location coupled with a limited contribution from larger population centres because of the blocking effect of mountains on both light and development, as well as the proximity of the Atlantic Ocean. Further work is ongoing, and we plan on obtaining data for other likely locations where conditions are expected to be good, such as in Donegal in the north-west of island.

3 Development of a new detector

3.1 Overview

We have focussed our measurements on zenithal sky brightness observations which are indicative of the general, rather than the local environment (such as wide-angle readings that take into account the light falling on the surface), and which do not have too strong a dependence on the contribution of sky background at large zenith angles, which is sensitive to the contributions from different airmasses. As a result, we have come to favour the Unihedron SQM-L meter, and have provided some units for use by people interested in assisting our work (e.g., through loans of instruments to students of Trinity College Dublin when they visit various parts of the country). One disadvantage we have found, however, relates to the difficulty in obtaining accurate positions and/or timings of observations, and the necessity to obtain multiple readings (we normally request 6 separate readings at each location) and device temperatures in order to try to obtain a reliable estimate of conditions.

In light of these factors, we have developed a sky brightness measurement and data acquisition unit which can be vehicle mounted or permanently set up and left unattended to record sky brightness for a period of time. It consists of a sensor head unit and a microcontroller based data logging unit connected by roughly 2m of cable, enabling the system to be placed on a car roof mounting yet remain operable from inside the vehicle.

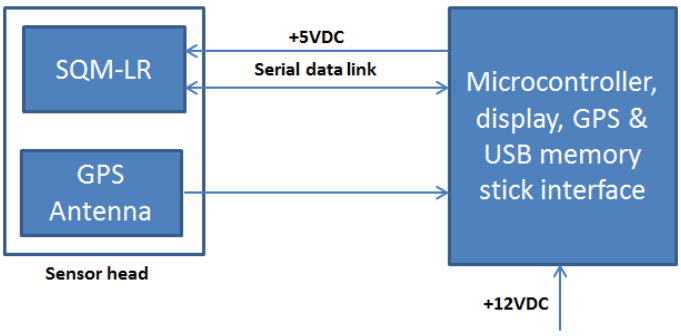


Figure 3: Block diagram of the layout of the basic components of the automated sensor (see photograph for actual construction). The sensor head is a waterproof box that also contains a GPS unit to log both time and location is designed to be placed up to 2m from the microcontroller box.

3.2 The sensor head

Referring to the block diagram above, the sensor head on the left contains a light detector and a GPS antenna. The light sensor is a stripped down SQM-LR unit [4] chosen for its ease of integration with serial devices such as the stand-alone microcontroller used here. Unlike the requirements of a new detection element, the Unihedron SQM-LE unit incorporates all the functionality needed without having to re-develop code and also, particularly, the optical parts and detector needed to acquire the data. The FWHM of the unit is 24 degrees which is compatible with the manual SQM-L units used, and has proved more convenient than whole-sky monitoring equipment which can be affected by neighbouring light sources. The output is a serial data stream in RS232 framing format which may be easily read. This output is in ASCII format and contains sky brightness readings in magnitudes per square arcsecond and system temperature for each reading. The unit has been modified to operate from a +5VDC supply. The sensor head also contains a GPS antenna unit so that readings from the SQM-LR may be correlated with geographic location and given a timestamp with Universal Time.

3.3 The control box

The microcontroller is a PIC24FJ256GB106 which performs all the data acquisition and storage functions, and which resides in a box that also supplies the detector head unit with +5V DC. The

interface consists of a basic menu driven display for the user, and stores the data on a FAT16 formatted USB memory drive of up to 2GB storage. The unit will operate from 8 – 15V DC, allowing it to be powered from the 12V socket of a car for mobile operation, or where operation away from local power sources is required, such as when running as an unattended base monitoring station when surveys are being conducted. The microcontroller can also apply a filter so that readings above a certain level are ignored to avoid recording daytime data when run in standalone mode.

3.4 Data acquisition

There are 2 modes of data acquisition:

1. Manual mode: The system only stores data when a button is pressed. This allows the user to choose what data to store having regard for local conditions such as nearby car headlights etc.
2. Automatic mode: The system may be set up ant left unattended acquiring data at a pre-set fixed interval.

In both modes of operation, it is possible to setup an option where the stored reading consists of the average of a pre-set number of readings.

3.5 Data storage

Data is stored to the USB stick formatted to FAT16 in standard ASCII comma-separated (CSV) format. A typical data line is shown below:

53.28697N,6.24708W,01/12/2012 02:54:43UT,17.12,17.12,17.12,18.3,1,Fix: 3D

Fields 1 and 2 contain the latitude & longitude the reading was recorded at, Field 3 contains the date and time (note that this has an explicit UT indication). Fields 4, 5 & 6 contain the averaged reading, and both the highest and lowest reading in the measurement. Data is stored in this fashion for ease of programming. Field 7 contains the temperature (in degrees Celsius). Field 8, in this case a "1", indicated how many measurements were averaged (in this case max and min are still reported, but with have the same value) . Field 9 contains information about the quality of the GPS fix, providing criteria for rejecting a reading later (uncertainty of timing or position). Although memory sticks of greater than 2GB capacity are cheap, this limit is imposed by the FAT16 format used by our hardware choices. However, despite this restriction, at approximately 75 bytes per line of data, there is room for more than 28 million readings. With a sample rate of one output every 10 seconds (the fastest allowed by the system), this equates to a continuous data readout of over 8.5 years and so is well suited to providing storage for unattended operation.

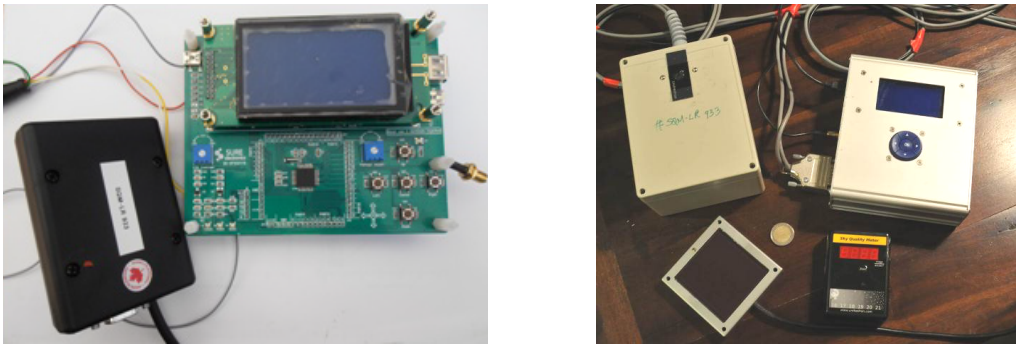


Figure 4: Left: The SQM-LR unit and microcontroller board with integral LCD display. Right: An illustration of the new automated system based around a Unihedron SQM-LR device (detector head at top left, microcomputer and data display at top right. Other systems shown are a Wuchterl IYA lightmeter (bottom left), and an unmodified SQM-LR device (bottom right). A €2 coin is also shown for size comparison.

3.6 Initial results with the instrument

The new instrument has been compared with our existing manual SQM units, and is working nominally, although there is a slight offset in readings due to the different window used. We are also currently experimenting with the use of filters, initially with a Wratten 44A cyan (minus red) filter which has been used in amateur astronomy circles as it excludes most of the emission from the main public lighting luminaires, with a passband (FWHM) of ~440 – 530nm, lying between the blue and peak of the green-yellow emission features. Measurements taken in a location in suburban Dublin shows a drop in intensity of roughly 2 magnitudes in either partial cloud or totally clear sky: from 18.6 to 20.5 magnitudes per square arcsecond in the latter case. The blue portion of the Wratten filter's response sits inside that of the standard Johnson B filter, and so our results are crudely consistent with those of Kyba et al. [5], but with the advantage of a more affordable filter.

4 Future Work

Work is continuing to produce a more comprehensive assessment of light pollution over the entire island and to identify areas which currently have low light backgrounds, but which may be at future risk. We plan on undertaking a series of co-ordinated campaigns, with many measurements being made by mobile volunteers within a well-defined area, with this work supported by observations from a base site in the middle of the region of study to monitor for changes in conditions. Future work will include filtered measurements in order to quantify the nature of the light sources, as well as digital images to obtain whole-sky colour imaging and to quantify the location of contributors to the light pollution burden.

Acknowledgments

We would like to thank the Irish Department of the Environment and Wicklow County Council for providing some funding via. the Local Agenda 21 Programme.

References

[1] http://www.unihedron.com/

[2] http://lightmeter.astronomy2009.at/

[3] http://www.nasa.gov/mission_pages/NPP/mission_overview/index.html

[4] http://www.unihedron.com/projects/sqm-lr/

[5] C. C. M. Kyba, T. Ruhtz, J. Fischer, F. Hölker (2012): Red is the new black: how the colour of urban skyglow varies with cloud cover, Mon. Not. R. Astron. Soc. 425, 701–708.

Dark sky conservation in Sierra Sur range (Spain): The astronomy as a tool of social revitalization and environmental conservation

J. Jiménez[1], F. Martín[2]

[1] *Asociación Astronómica Hubble. Cadiz st. 14 23600 Martos (Jaén) Spain*
[2] *Iberus Medio Ambiente S.L. Av. Granada 35, 1ºA 23003 Jaén. Spain*

Abstract

"Sierra Sur" is a region located in the province of Jaen (Southern Spain) Its geography is characterized by an extremely steep terrain, with mountains that reach nearly the 2,000 meters (approx. 6,560 feet) over the sea level, with narrow valleys and deep cliffs going trough. These hard conditions have contributed to a low density of population which has helped Sierra Sur to preserve one of the darkest skies in Southern Spain. Nowadays, there is a growing interest in the value of this fabulous sky, not only because we have a moral responsibility to preserve and enjoy our starry nights, but also because it helps revitalize the economy of our region.

1 Introduction

From the scientific community we are not may right selling our activity as a resource that promotes the economic and cultural development of people who live in those places that share their lifes with a sky full of stars. In the last years, some progress have been done in scientific and astronomical divulgation and nowadays, the interest on science in general is increasing, thanks in part for the role of astronomical societies and some programs to bring closer the science to the general public.

However, not many efforts have been done to make the people consider that the conservation of the dark sky is, in addition a necessity to study and understand our place in the universe, a chance to better know the relation between it and our physic environment, for learning how to manage the resources we need for our current life, and also as a resource that give us the chance of generate certain social activity based on astronomical tourism, nature tourism (depending in part of the quality of some dark sky parameters) or economic activity generated around scientific research. And the most important, a resource to be proud of, as the truth is that it sadly is a scant resource.

The region of Sierra Sur, in the province of Jaen, has decided to promote its environmental and astronomical heritage by integrating between its fundamental principles, the conservation of the dark sky as another tool more to manage its nature, its culture and its own history at the same time that it set the bases to promoted the economic reactivation of the region from the basic of the respect to the nature in all its facets.

In our region we want to speak about light pollution and night sky conservation considering all the aspects, many local authorities want to bet for the scientific research investing in infrastructures like the recently opened Astronomical Observatory in La Pedriza (Alcalá la Real), it's wanted to bet for the environmental conservation considering the alterations that night lighting is causing to the local biodiversity, and we want all this to suppose a real benefit for the habitants of the region attracting tourism and encouraging the investment with the obtaining of a Starlight certification by the Starlight Foundation. We want the Sierra Sur region to be a referent of a place where dark sky conservation was faced as an opportunity of development and nature conservation as well.

2 Astronomy: promoter of the innovation, development and conservation in Sierra Sur

We can proudly say that in our region we are betting on the use of science in general and the astronomy in particular to make this place a world reference in combining research and social-

economical development with the respect to our natural heritage. Above our mountains and valleys we have all a spectacle, and being aware of it, during the last times some interesting step have been given by local authorities and many other entities with something to say in the development of the region.

Among our biggest achievements we can talk about the Hubble Astronomy Association, placed in the town of Martos considered one of the most relevant astronomy associations in Spain in the last years with more than 10.000 registered persons in their website and more than a million visits every month! With the help of the local authorities this society organized one of the most important meetings on astronomy every year, this event is called "Astromartos". Likewise the Andalusian Astronomy Observatory has been recently inaugurated in Alcalá la Real, this observatory is going to collaborate with many important research and educational programs and aspires to be an important focus of economical activity in the nearby surroundings.

And probably the most important, ADSUR (Association for the Rural Development of Sierra Sur) is going to start the formalities to get the certificate of Starlight Reserve for the region, one of the most valuable certifications around the world in this matter and that will be the final colophon to a complete strategy to do from the astronomy one of the references of this beautiful region.

2.1. Starry nights in Sierra Sur range

In spite of growing Spanish population, our country is still one of the less densely populated in all Europe, in part because of the important movement of concentration around big cities like Madrid (already with more than 7,3 millions of persons in its metropolitan area), while in the other hand Spain preserves a huge surface of rural areas almost depopulated. Thanks to this, Spain has one of the darkest skies in all the continent, which means than in addition of the clime, the conditions for the observation of the night sky are actually excellent.

However, we also have signals that show us that our skies are losing its darkness. During the last 10 years the light pollution monitoring works show that residual illumination is starting to be common even in some isolated areas. Therefore we are in time to change the direction of our night lighting model to avoid to waste energy, disturb the wildlife and prevent the loss of part of our heritage at the same time we use this resource to promote the scientific research as a tool of social development in our region. We must to consider the investment that astronomy means for a region, commonly rural areas where an important part of the economy is based in a good conservation of the environmental factors, like the tourism of nature or agriculture for example. It is important to make the population understand that they have a limited resource that many people are willing to enjoy or use to their research, that this resource has an important value and that they must to protect and use as a way for the development and innovation.

2.2. Biodiversity depending on dark sky in Sierra Sur

Sierra Sur is home to many important species from the point of view of biodiversity conservation. Despite the fact that it didn't use to be considered as a factor, nowadays we know that the artificial night lighting can be behind the decline of some fauna and flora species. Some studies shows that the presence of light in natural habitats can alter some natural conditionals for amphibians and birds for example, being one of the most important factors that determine the presence or absence of some species.

In this region there are important species, some of them with certain degree of threat of extinction. During the last years some efforts have been taken from the administration to protect and preserve those species, but without considering the disturbances that light pollution is probably causing on them. It is very important to have a good understanding of how lights affect the vital cycle of this threatened animals, for implementing new standards in their conservation programs considering some actions directly focused in alleviate these problems due to light pollution.

The dark sky conservation must be considered also as an important tool to understand and manage the whole scheme where those important species live, promoting the comprehensive attention to every single factor to ensure the environmental conservation.



Figure 1: Typical Sierra Sur landscape.



Figure 2: Night view at Sierra Sur.

3 New achievements to preserve the dark sky and to develop the region

From all those considerations we are willing to make a reality. Some entities are starting to share efforts to demand a general strategy for our region that involve the use of our resources linked with the astronomy and the dark sky conservation to make of Sierra Sur Range a demonstrative lab where to show how to involve all the actors of a region to achieve a social, cultural and economical develop-

ment based on the respect to our common heritage, the wish of study and discover our universe and our role in it.

During the last years, and without any established purpose previously, Sierra Sur and the south of the province of Jaen in general is starting to have a place in the scientific community, due to some important and independents circumstances like the creation of one of the most important astronomy associations in the whole country or the recent inauguration of the Astronomy Observatory of La Pedriza. Probably all those actions are taking place because of that we are simply in the right place, our people is made to look up and see a brilliant sky from horizon to horizon. But now we are starting to understand that with the right agreement of local authorities we can combine all those initiative to aspire to a real revitalization of the region with the astronomy and the science as references.

Our main purpose nowadays is to create a net of local entities related with the scientific community and environmental conservation to develop new ideas to make of the Sierra Sur Range an international reference in the dark sky conservation and enjoyment.

4 Conclusion

During the next years Sierra Sur is going to mark a new way for itself. Here we are willing to undertake the challenge of designing the actions aimed to do of the region a world reference in development based in science and astronomy, with the unquestionable premise of the conservation of the night sky as our main concern. Currently, some local entities are starting to share their efforts to encourage local authorities to notice the connection between sky conservation and socio-economical development.

Acknowledgments

We would like to officially thanks to all this persons and entities that have collaborated during years with the Hubble Astronomy Association in our hundreds of activities and also to all these persons concerned about the conservation of our natural heritage. We have a rich region in culture, environment, gastronomy, traditions and it is very well known for it, thanks to all these people interesting in add the astronomy and the dark sky to the previous list, in particularly to IAJ (Instituto Andaluz de la Juventud), Diputación Provincial de Jaén, local authorites from Martos, Alcalá la Real, Valdepeñas de Jaén, Los Villares, Frailes, Alcaudete, Castillo de Locubin, Fuensanta, Jamilena and Torredelcampo, ADSUR, Einstein Astronomy Society and many others private individuals. Thanks from Hubble Astronomy Association and Iberus Medio Ambiente S.L.

References

[1] R. Catherine (2006): Ecological Consequences of Artificial Night Lighting.

[2] B. W. Buchanan (1993): Effects of enhanced lighting on the behavior of nocturnal frog. Animal Behavior 45:898–899.

[3] A. R. Upgren (1996): Night blindness: light pollution is changing astronomy, the environment, and our experience of nature. Amicus Journal 17 (4): 22–25.

[4] A. Wilson (1998): Light pollution: efforts to bring back the night sky. Enviromental Building News 7 (8):1, 8–14.

[5] K. W. Riegel (1973): Light pollution: outdoor lighting is a growing threat to astronomy. Science 179: 1285–1291.

[6] Health Council of the Netherlands (2000): Impacts of outdoor lighting on man and nature. Publication No. 2000/25E. Health Council of the Netherlands, the Hague.

[7] L. Acharya, M. B. Fenton (1999): Bat attacks and moth defensive behaviour around street lights. Canadian journal of Zoology 77:27–33.

[8] Sociedad Española de Ornitología (2006): El águila perdicera en España: Población en 2005 y método de censo. Seguimiento de Aves No 9. P.42–46.

[9] ADSUR (2010): Guía Básica de Información Turística. Guía y Mapa de la Comarca con ubicación de los recursos turísticos más relevantes.

[10] ADSUR (2008): Nueva Estrategia Rural de la Sierra Sur de Jaén, NERA.

[11] Decreto 357/2010, de 3 de agosto, por el que se aprueba el Reglamento para la Protección de la Calidad del Cielo Nocturno frente a la contaminación lumínica y el establecimiento de medidas de ahorro y eficiencia energética.

[12] Consejería de Medio Ambiente. Junta de Andalucia. Protección del Cielo Nocturno.

[13] Consejería de Medio Ambiente. Junta de Andalucia. (2011). Guía técnica de adaptación de las instalaciones de alumbrado exterior al decreto 357/2010 de 3 de agosto.

[14] Asociación contra la Contaminación Lumínica: http://www.celfosc.org

[15] International Dark Sky Association: http://www.darksky.org

An improved scattered moonlight model for the sky background

Amy Jones[1], Stefan Noll[1], Stefan Kimeswenger[1], Wolfgang Kausch[1] and Cesary Szyszka[1]

[1] *Institue for Astro- and Particle Physics, University of Innsbruck, Technikerstrasse 25, Innsbruck, Austria*

tel: +43 512 507 52046, fax: +43 512 507 52099, e-mail: Amy.Jones@uibk.ac.at

Abstract

The largest natural source of light pollution in the optical at night is the Moon, and it is the major contributor to the astronomical sky background. Being able to accurately predict the sky background including the scattered moonlight is important for estimating and scheduling astronomical observations. We have an improved scattered moonlight model, where the components are computed with a better physical understanding rather than a simple empirical fit between 0.3 and 1.0 micron. This is the first moon model that we know of which is this physical. With the new scattered moonlight model, our current sky background model has a lower uncertainty, $\sigma \sim 0.2$ [mag], compared with our previous one, $\sigma \sim 0.3$ [mag]. In extension to the original astronomical purpose, since the model is more physical, we can use the scattered moonlight to probe the properties of the atmosphere, such as the distribution of aerosols.

1 Introduction

As part of the Austrian ascension to the European Southern Observatory, we developed a model to predict the sky background for the Exposure Time Calculator for Cerro Paranal. This will allow a better estimation of the amount of time needed for an astronomical observation to attain the desired signal to noise ratio. This sky model has been designed for the observatory at Cerro Paranal and the nearby future site of the E-ELT (European Extremely Large Telescope).

There are several components that contribute to the sky background between 0.3 and 30 micron. The brightest component in the optical regime is scattered moonlight. There have been surprisingly few studies on this. Our original scattered moonlight model was a further parametrized version of Krisciunas and Schaefer (1991) V band model [1] that was extended to all optical wavelengths based on data obtained with the optical low-resolution spectrograph FORS1 mounted at the Very Large Telescope (VLT) of over 1100 spectra (247 with the Moon above the horizon) [2]. This previous model is described in Noll, et. al. (2012) [3]. We have now greatly improved this model, by making it more realistic. It is based more on physical processes and observational data than empirical parametrization. It can be used to predict the amount of scattered moonlight for a given astronomical observation, where the overall uncertainty of the full sky model is only $\sigma \sim 0.2$ [mag]. Because our model is more physical, it can be used with sky observations to characterize the nocturnal atmosphere.

2 Model Description

To accurately calculate the scattered moonlight, there are several components that must be considered. The source of the scattered moonlight is the Sun and we use the solar spectrum from Colina, et al. (1996) [4]. Then the light is reflected by the Moon which depends on the lunar albedo. We use the fit from data of the ROLO survey [5], which gives the albedo at certain wavelengths based on the lunar phase and selenographic latitude and longitude. We interpolated the fit between the given wavelengths and extrapolated it to all lunar phases to have a lunar albedo for all the possible phases and wavelengths needed for our sky model. Next, the moonlight enters the Earth's atmosphere, where it is scattered by molecules (Rayleigh) and aerosols (Mie), and absorbed. The single and double scattering is modeled by using a fully 3-D code, with an extrapolation to higher orders, and includes a wavelength-dependent ground reflectance, for typical particle distributions in the atmosphere above

Cerro Paranal. The Rayleigh scattering extinction is given by Liou (2002) [6], and we use the analytical solution for the phase function. The Mie scattering is calculated using the size distributions for remote continental and stratospheric aerosols [7] scaled to the Mie extinction curve given in Patat, et al. (2011) [8] (Figure 1). The Mie phase functions are then determined by a code based on Bohren and Huffman (1983) [9]. Our scattering intensities were verified by comparing it with the radiative transfer code package libRadtran [10]. For the absorption, we use a merged atmospheric profile from the MIPAS equatorial standard atmosphere, the global GDAS weather model, and a local meteorological station to scale it to the location of Cerro Paranal [11]. With our atmospheric profile, we use the radiative transfer code LBLRTM to determine the amount of absorption [12].

The scattered moonlight model depends on the lunar phase and the positions of the Moon and target. The FORS1 spectra were spread over several years through all seasons and various weather conditions, and variations in the atmospheric particles have been seen on timescales of hours to months.

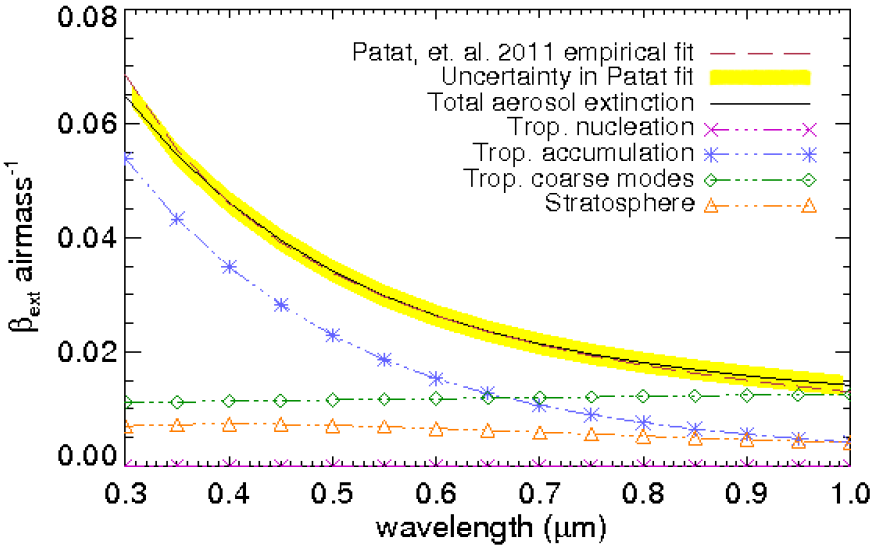


Figure 1: The composition of Mie scattering. The extinction from four different types of aerosols are shown. The total extinction from Mie scattering, where the various types are summed, along with an empirical fit from data. The yellow band shows the uncertainty in the Patat fit which corresponds to ~10% variation of the total aerosol extinction. By comparing the moon model and observations, we can estimate the properties (type and size distribution) of the aerosols in the Earth's atmosphere.

3 Results and Applications

We have compared our model with a data set of over 1100 optical spectra, 247 of which have a moon above the horizon, and 141 also have good weather conditions [2]. An example of a typical spectrum with moderate moonlight is shown in Figure 2, overlaid with the full sky background model developed in the framework of our project [3] and moon model spectrum. There is excellent agreement between the modeled and observed spectrum. Our moon model overall has an uncertainty of ~0.2 mag. This is a definite improvement over previous models, which have an uncertainty of more than 0.3 mag [1, 3]. Figure 3 shows the average value of the difference between the observed sky spectrum and modeled one in several narrow continuum windows, with error bars showing the one sigma spread. The model is more uncertain at redder wavelengths because of the airglow emission lines. There also seem to be systematic uncertainties in the flux calibration of the various FORS1 data sets, which can be seen in the jump of the mean and sigma values around 500 nm.

Soon we will verify our model with data taken by a high resolution, UV to infrared, spectrograph X-Shooter on the VLT, which will be observed during this summer semester. With this new data set,

we will also be able to extend our model into the infrared. This will be the first model of the moonlight in the infrared.

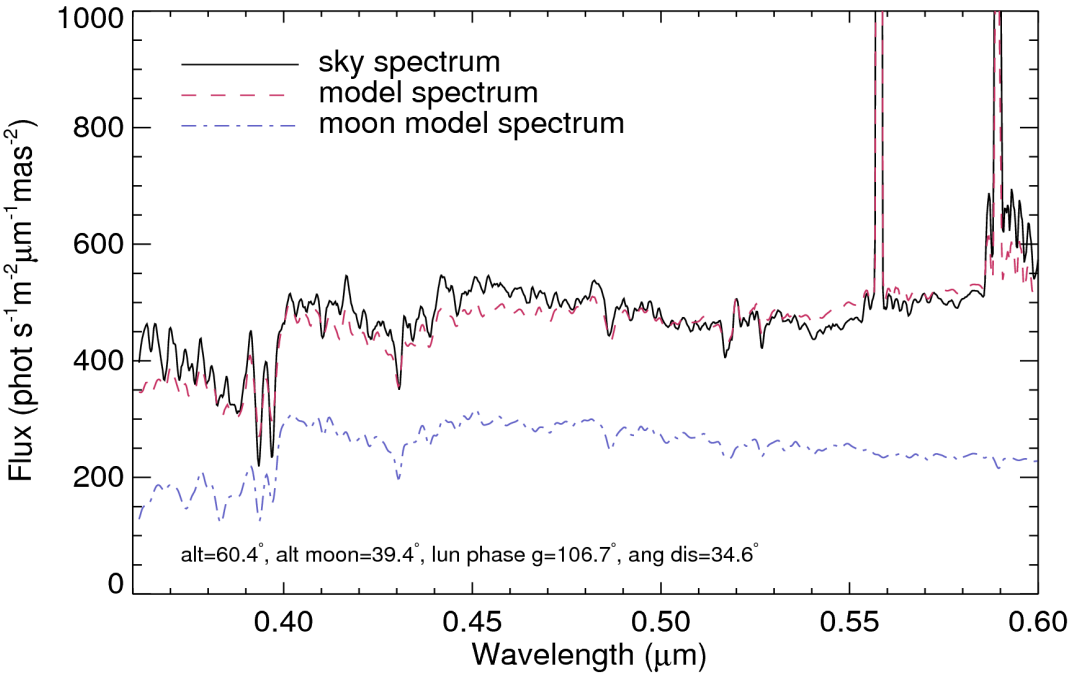


Figure 2: Typical FORS1 spectrum with moderate moonlight. The full sky model and moon model spectrum are also plotted. Even with only moderate moonlight (near first quarter), about half of the background flux is from the Moon. The sky model is in excellent agreement with the observed spectrum.

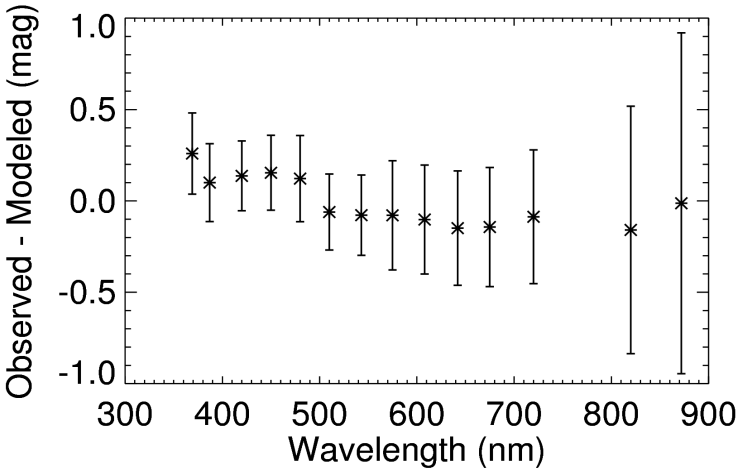


Figure 3: The mean of the difference between the observed sky spectra [2] and modeled ones for several continuum windows of the data with good weather conditions and flux greater than 100. The error bars show the one sigma spread. The uncertainty increases at redder wavelengths due to the airglow emission. There are also systematic uncertainties in the flux calibration of the different data sets, which can be seen in the jump of the mean around 500 nm. This will soon be resolved with our guaranteed X-Shooter data. Overall our scattered moonlight model has an uncertainty of ~ 0.2 mag.

Our model is the most physical, to our knowledge, compared to previous ones that were mostly parametrizations [1]. Our model is based on the observational data of the lunar albedo, optimized atmospheric profiles, and typical size distributions of atmospheric particles.

We can use the Moon as a beacon to approximate the properties of the aerosols in the Earth's atmosphere, since the model is mostly physical. The moon model, especially at wavelengths greater than 0.8 microns, is sensitive to the various mixtures and amounts of aerosols. It can also be used to determine the presence of haze or a nearly invisible cloud layer and explore the nocturnal atmospheric properties. With our upcoming X-Shooter data, this will be investigated. Since there are observatories around the world that collect data almost nightly, this method could yield some important results for atmospheric science.

Our improved scattered moonlight model will not only enhance telescope scheduling and efficiency and provide a physical understanding of scattered moonlight, but can also be used to derive aerosol properties for atmospheric science.

References

[1] K. Krisciunas, B. Schaefer (1991): A model of the brightness of moonlight, PASP, 103, 1033.

[2] F. Patat (2008): The dancing sky: 6 years of night-sky observations at Cerro Paranal, A&A, 481, 575.

[3] S. Noll, W. Kausch, M. Barden, A. M. Jones, C. Szyszka, S. Kimeswenger, J. Vinther (2012): An atmospheric radiation model for Cerro Paranal, A&A, 543, A92.

[4] L. Colina, R. C. Bohlin, F. Castelli (1996): The 0.12-2.5 micron Absolute Flux Distribution of the Sun for Comparison With Solar Analog Stars, AJ, 112, 307.

[5] H. Kieffer, T. Stone (2005): The spectral irradiance of the moon, AJ, 129, 2887.

[6] K. N. Liou (2002): An introduction to atmospheric radiation, 2nd edn., Academic Press.

[7] P. Warneck, J. Williams (2012): The Atmospheric Chemist's Companion, Springer.

[8] F. Patat, S. Moehler, K. O'Brien, E. Pompei, T. Bensby, G. Carraro, A. de Ugarte Postigo, A. Fox, I. Gavignaud, G. James, H. Korhonen, C. Ledoux, S. Randall, H. Sana, J. Smoker, S. Stefl, T. Szeifert (2011): Optical atmospheric extinction over Cerro Paranal, A&A, 527, A91.

[9] C. Bohren, D. Huffman (1983): Absorption and scattering of light by small particles, Wiley.

[10] B. Mayer, A. Kylling (2005): Technical note: The libRadtran software package for radiative transfer calculations-description and examples of use, Atmos. Chem. Phys., 5, 1855-1877

[11] A. Seifahrt, H. U. Käufl, G. Zängl, J. L. Bean, M. J. Richter, R. Siebenmorgen (2010): Synthesising, using, and correcting for telluric features in high-resolution astronomical spectra. A near infrared case study using CRIRES, A&A, 524, 11.

[12] S. A. Clough, M. W. Shephard, E. J. Mlawer, J. S. Delamere, M. J. Iacono, K. Cady-Pereira, S. Boukabara, P. D. Brown (2005): Atmospheric radiative transfer modeling: a summary of the AER codes, JQRST, 91, 233.

Optimized optical filter for LED lighting

Jean-Pierre Lavallée, P.Eng, D.S.A.[1] and Martin Aubé[2]

[1] *Ledtech International, 3100 Industrial Boul., Sherbrooke, J1L 1V8*
tel: 1-877-418-3244, e-mail: jplavallee@ledtechcanada.com
[2] *Cégep de Sherbrooke, Sherbrooke J1E 4K1, Canada*
tel: +819 564-6350-4146, e-mail: martin.aube@cegepsherbrooke.qc.ca

Abstract

In conjunction with the Mont-Mégantic Dark Sky Reserve and the Cégep de Sherbrooke, LEDTECH International has developed a working technology for filtering white light-emitting diodes (LED) regarding unwanted potential health and environmental impacts. A multi-layer optical interference filter has been designed to filter out the undesirable wavelength while preserving the maximal colour rendering. The filter spectral transmittance has been optimized to restrict potential interference with the human circadian cycle but efforts have been made to also reduce sky brightness for astronomers and nocturnal photosynthesis to preserve environmental integrity.

1 Introduction

The arrival of light-emitting diodes (LEDs) in the field of lighting is a technological revolution. LED technology has several advantages over traditional lighting technology. One of the major advantage is its long lasting life, thus reducing maintenance costs associated with its use. LEDs are also easy to control and modulate. They provide good luminous efficacy, at least equivalent to traditional technologies like High Pressure Sodium.

Currently, light output is maximized for LEDs emitting in the blue part of the visual spectrum. To produce white light based on LED technology, the most efficient approach is to stimulate a layer of phosphor using blue LEDs. The phosphor converts a large part of the blue light into yellow light. The electromagnetic spectrum of white LEDs can be described as the superposition of a yellow spectrum produced by the phosphor covering a large part of the visual spectrum with a peak of blue that succeeds in passing through the phosphor (see the peaked curve in Figure 1).

The presence of this blue peak in the resulting spectrum poses a significant problem in terms of the environment, road safety, and human health. First, blue light scatter more efficiently in the atmosphere than yellow or red light. This is why the sky is blue. This ability to scatter more efficiently in the atmosphere means that blue light has a tendency to produce more astronomic light pollution than any other colour with a longer wave length for an observer near the source of light. When the observer is far from the source, the atmospheric extinction removes more efficiently the blue then reduces the gain from higher scatterers efficiency. Over large distances, the spectrum is very similar to the original lamp spectrum. Another reason to reduce the amount of blue light is related to the phenomenon of glare. With the aging of the population, scattering inside the eye increases because an aging eye becomes less and less transparent [4],[5]. Glare could be a cause of traffic accidents [6],[7]. Less blue is also less attractive to insects. This filter should therefore considerably reduce insect mortality around streetlamps. The mean number of insects killed at a streetlamp per night is estimated at 150 for high-pressure mercury vapour lamps (blue-enriched white light) and 60 per night for high-pressure sodium vapour lamps (yellowish lamp) [3].

Blue light plays an important role in regulating the circadian cycle (biological clock) in many animal species, including humans. In the latter, the regulation is ensured by a photoreceptor in the retina of the eye, but which does not participate in vision. When the photoreceptor is stimulated, the production of melatonin is suppressed, thus conditioning the wake cycle. In the reverse case, without blue, melatonin is secreted, putting the organism in rest mode.

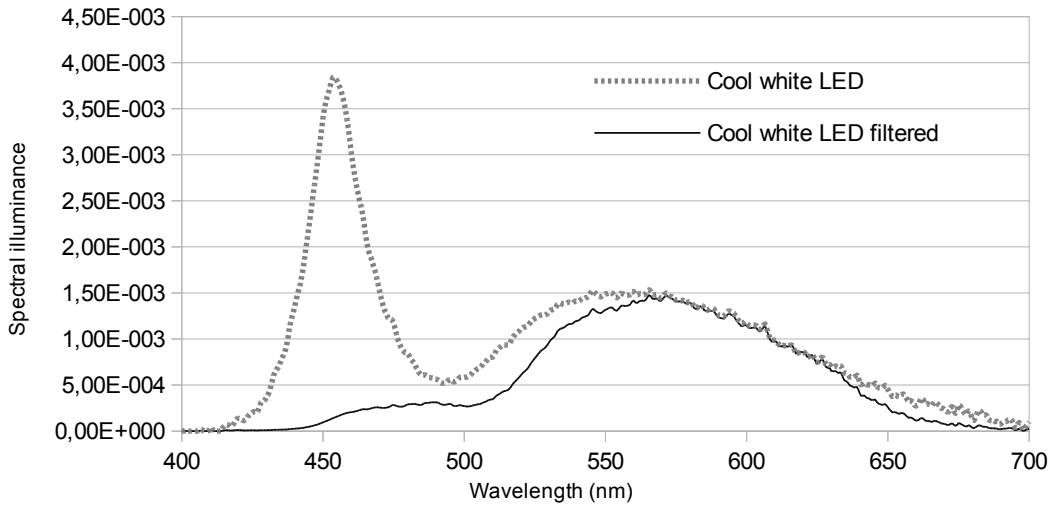


Figure 1: Example of Spectral Power Distribution for a cool white LED with and without our LEDTECH *Equilib* filter at a normal incidence (nadir).

2 Method

Brainard *et al.* 2001 [1] and Thapan *et al.* 2001 [2] have succeeded in characterizing the spectral response of melatonin suppression. This dependency is called the Melatonin Suppression Action Spectrum (MSAS). For this article, we combined the independent data measured by the two teams (squares in Figure 1) and made a mathematical adjustment of the sum of two asymmetrical log-normal profiles to determine an analytical equation that would characterize in spectral terms the MSAS at all wavelengths. The equation is illustrated in Figure 2 (orange curve), and we have identified it as $MSAS_a$. Figure 2 shows the quality of the mathematical data adjustment with the analytical model adopted.

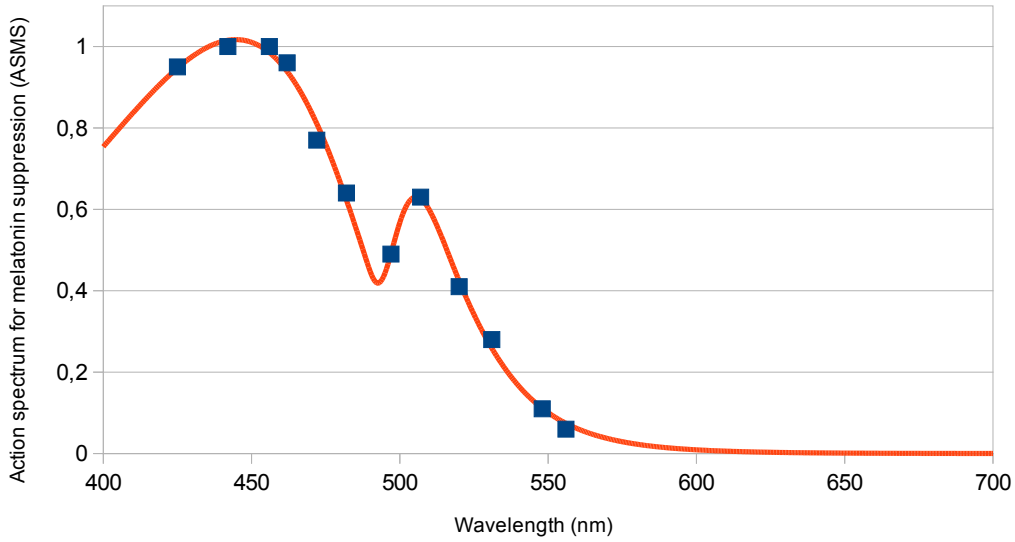


Figure 2: Melatonin Suppression Action Spectrum (MSAS). The squares are measures from Brainard et al. 2001 and Thapan et al. 2001, while the curve is an adjustment of the two asymmetrical log-normal curves.

The thrust of the filter rests largely on the analytical adjustment of the MSAS. To reduce the undesirable effects of blue light as mentioned above, but more importantly on the possible disruption

of melatonin cycle, we produced an interferential optic filter with a spectral transmittance between 400 nm and 600 nm that closely follows the curve obtained (T_i) by using the following equation:

$$T_i = 1 - MSAS_a \quad (1)$$

Equation 1 is plotted in Figure 3.

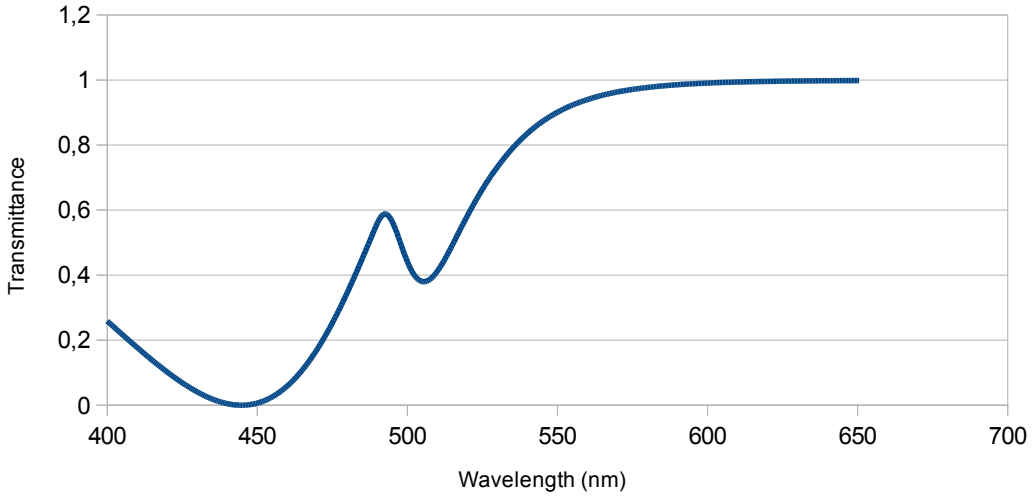


Figure 3: Spectral transmittance T_i respecting equation 1. This curve is optimized to minimize the impact of nocturnal light on the human circadian cycle.

In addition to the constraint to minimize the negative impact of blue light on human health and a starry sky, we added an additional constraint to reduce by at least half the amount of light transmitted by the filter beyond 650 nm. This constraint was intended to reduce the disturbance of nocturnal light on terrestrial and aquatic vegetation located near lighting equipment. The modified transmittance curve (Te) is shown in Figure 4. The rationale for this modification is that chlorophyll-a, which is the most common and abundant type of chlorophyll found in vegetation, has two visible absorption peaks: the first around 430 nm and the other around 660 nm. While the peak at 430 nm is already filtered by the Ti transmittance, the peak at 660 nm is not. By adding the gradual decrease of transmittance before reaching 650 nm, we reduced the impact on the peak at 660 nm. Thus, vegetation located near lighting equipment that has been fitted with this filter will be less affected at night.

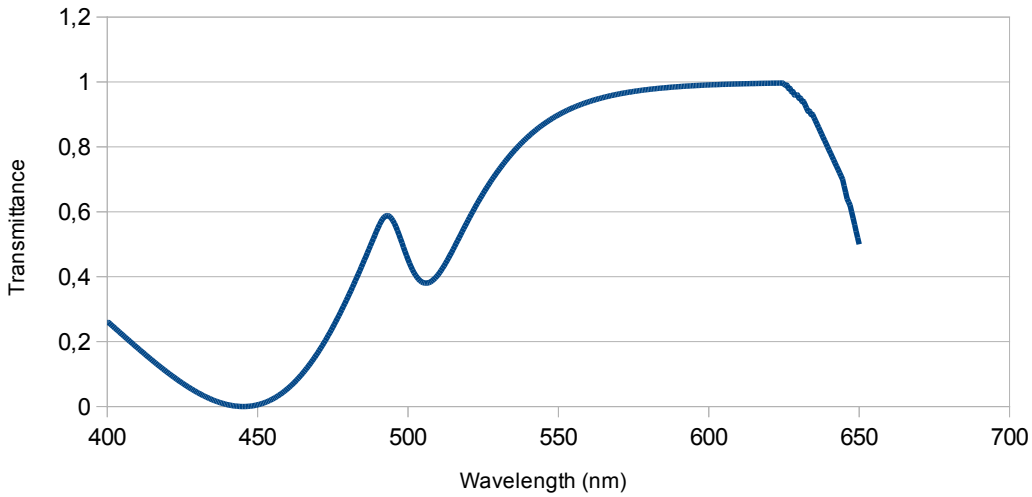


Figure 4: Desired spectral transmittance T_e. This curve corresponds exactly to the curve in the 400- to 650-nm range in Figure 1. A decline in transmittance is then imposed to reach a value of 0.5 to 650 nm.

3 Results

Up until now, the filter has been available on a substrate that can be placed in front of any streetlamp as long as it can be cut and adjusted to the casing in question. Since streetlights often have type II or type III light distributions, most of the light emitted from such lamps does not cross the filter with zero angle of incidence and so the filter's optical performance is greatly reduced. The filter, in its current form, is better adapted to lighting equipment that has a forward oriented light distribution like type V or floodlights. The result obtained with a Type V fixture is shown in Figure 5. This spectrum is an average over the sphere. The blue peak of the spectral power distribution (SPD) was reduced by the filter. The SPD with the filter shows a ratio of the contribution between 405 nm and 530 nm reported to the contribution from 380 nm to 730 nm of 9%. For the non-filtered SPD, we obtain 17%. But if we look closer to the region for which the MSAS is maximal, between 425 nm and 475 nm, the filtered luminaires have an integrated contribution of 7% while the non-filtered have 15%. This later result shows how the filter is optimized to reduce impact on melatonin suppression even if the light is not crossing the filter at normal incidence. For normal incidence, the integral between 405 nm and 530 nm is only 4% while it is less than 3% between 425 nm and 475 nm. Basically, this means that the light emitted at large nadir angles is whiter, but fortunately part of this light will be absorbed by nearby obstacles like trees or buildings and then will be rapidly removed from the radiative budget. Lastly, it is important to note that the non zero filter's spectral transmittance in the blue, reduces the yellowing effect in comparison to a simple high-pass filter. In other words, when a complete reduction in the blue is not achieved, we can maintain a good colour rendering while significantly reducing the blue component of the spectrum.

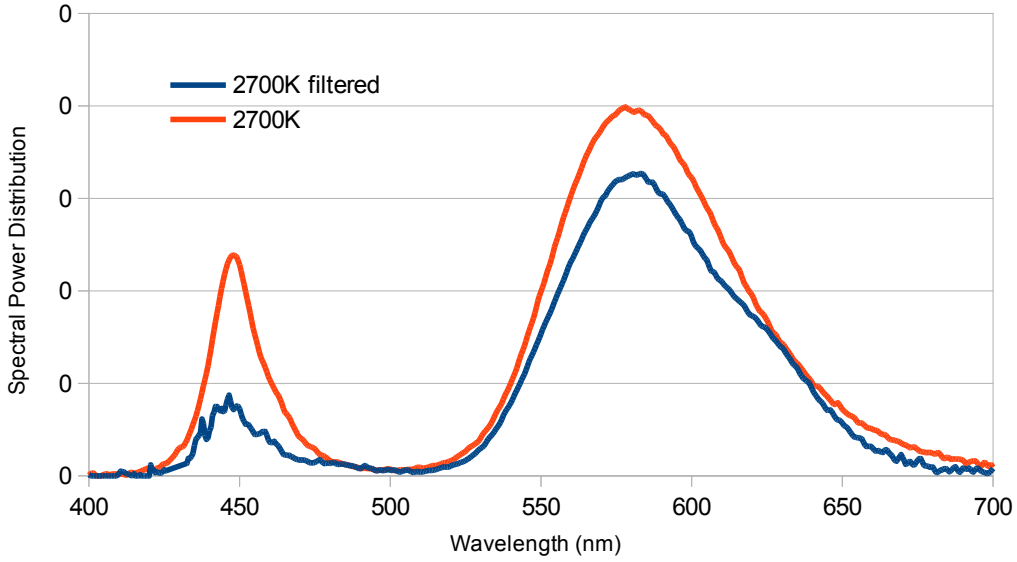


Figure 5: Spectral power distributions of a Bridgelux 2700K LED Type V luminaire with and without LEDTECH's Equilib filter.

4 Conclusion

Even if our filter performs well for Type V or floodlight, it is not optimized for most common light distributions used in street lighting (Type II and III). We are currently working on a different way to make the multi-layer deposit right on the LED optics, and if successful our filter will be able to be used on any type of photometric distribution. This new version of the filter should be validated by the end of April 2013.

References

[1] G. C. Brainard, J. P. Hanifin, J. M. Greeson, B. Byrne, G. Glickman, E. Gerner, M. D. Rollag (2001): Action Spectrum for Melatonin Regulation in Humans: Evidence for a Novel Circadian Photoreceptor, The Journal of Neuroscience, 21(16): 6405–6412.

[2] K. Thapan, J. Arendt, D. J. Skene (2001): Rapid Report – An action spectrum for melatonin suppression: evidence for a novel non-rod, non-cone photoreceptor system in humans, Journal of Physiology, 535.1: 261–267.

[2] C. F. Bohren, D. R. Huffman (1983): Absorption and Scattering of Light by Small Particles (Wiley, New York).

[3] G. Eisenbeis (2006): Artificial Night Lighting and Insects: Attraction of Insects to Streetlamps in a Rural Setting in Germany, in: C. Richt, T. Longcore (Eds), Ecological consequences of artificial night lighting. Island Press, Washington D.C. pp. 281–304.

[4] J. J. Vos (1984): Disability glare – a state of the art report. Commission International de l'Eclairage Journal; 3:39–53.

[5] T. van den Berg (1986): Importance of pathological intraocular light scatter for visual disability. Doc Ophthalmol; 61: 327–333.

[6] M. A. Babizhayev (2003): Glare disability and driving safety. Ophthalm Res 35, 19–25.

[7] T. van den Berg, J. van Rijn, G. Grabner, H. Wilhelm, G. C. de Wit, R Kaper-Bongers, C. Nischler, D. Gamer, L. Franssen, D. J. Vonhoff, M. Emesz, A. Schuster, J. E. Coppens, H. J. Völker-Dieben (2003): Assessment of visual function of driving-licence holders. Joint research EU project: I-TREN E, 3(200):7.

How effective are lighting codes?

Christian B. Luginbuhl

U.S. Naval Observatory Flagstaff Station, 10391 W Naval Observatory Rd, Flagstaff AZ 86001
tel: 928-779-5132, e-mail: cbl@nofs.navy.mil

Abstract

If we hope to reduce sky glow through regulations ("lighting codes"), it is critical to understand what standards are effective. I present a metric called the Sky Glow Index (SGI) that allows comparison of the amount of sky glow (visible or radiometric) arising from lighting following standards that specify maximum lighting amounts, shielding characteristics, and lamp spectrum. The SGI is used to evaluate the effectiveness of the IDA Pattern Outdoor Lighting Code, the Joint IDA-IES Model Lighting Ordinance, and compare common roadway lighting practices.

1 Introduction

Though there are many obtrusive effects arising from the use of outdoor lighting, a principal concern of astronomers, both professional and amateur, is the increased luminance of the night sky caused by the scattering of light from molecules and aerosols in the atmosphere – sky glow, or more correctly anthropogenic sky glow.

Regulations intended to reduce anthropogenic sky glow have been devised and implemented in the U.S. since the late 1950s. Most of these regulations set restrictions on light fixture shielding characteristics, i.e. on the fraction of light that can be emitted above the horizontal. Many specify preferred or required lamp sources, such as limiting the use of white sources (e.g. metal halide, fluorescent) to applications where color perception is paramount. A few address total amounts of light permitted, either through general or non-use-specific limits on the amount of light per unit area, or through a requirement that lighting amounts not exceed lighting industry "standards" or "norms" for specific lighting uses or applications.

The questions arise as to whether particular standards will actually decrease the expected sky glow, and if so by how much. In this paper I propose a new metric that allows comparison of the relative sky glow impact of different lighting standards. For example applications I use this metric to compare the sky glow control effectiveness of the 2011 Joint International Dark-Sky Association / Illuminating Engineering Society of North America Model Lighting Ordinance (IDA-IES MLO, [1]) with the 2000 IDA Pattern Outdoor Lighting Code (POLC, [2]), and shielded vs. unshielded roadway lighting.

2 The Sky Glow Index

Light reaching the sky arises from light emitted *directly upward* from incompletely shielded fixtures, as well as from light *reflected upward* from the ground or other surfaces. These two components, however, do not have equal impact on sky glow, because in general they are headed in different directions. Light emitted directly upward from incompletely shielded fixtures is usually concentrated at angles near the horizontal, while light reflected from horizontal surfaces is more strongly concentrated toward the zenith (see Figure 1). Though interaction with objects (buildings, vegetation) near the ground can significantly decrease intensity at large zenith angles [3], research has shown [4, 5, 6] that light propagating upward but at a small angle relative to the horizon has an impact on sky glow two to over 100 times greater than light reflected from a horizontal ground surface, with the enhancement ratio increasing strongly with distance from the light source. When viewed from more than a few kilometers distance, a lumen emitted directly upward in general has a much greater impact on sky glow than a lumen reflected upward.

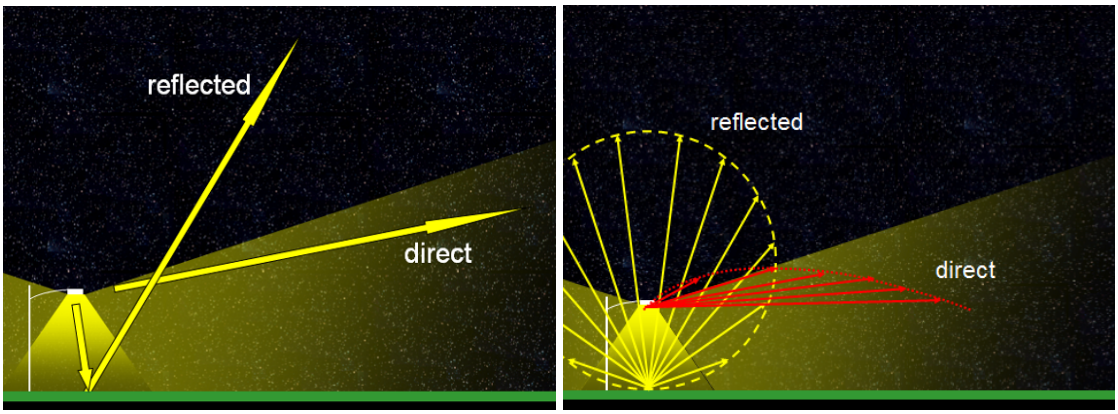


Figure 1: Sources (left) and representative angular intensity distributions (right) for light reflected upward from a horizontal surface and light emitted directly upward from an incompletely shielded fixture. Actual distributions will depend on many factors such as blocking, fixture photometric characteristics, and mounting details.

Another factor influencing sky glow is the spectral content of the light source. Though the scattering cross-sections of the aerosol and particularly the molecular components of the atmosphere are wavelength dependent, this dependence only weakly influences sky glow due to the balance between increased scattering and increased extinction [7]. However, the visual brightness of sky glow is strongly influenced by the spectral characteristics of the light source due to the Purkinje shift [8]. Under dark-adapted or scotopic conditions (i.e., luminance $L_V \leq 0.001$ cd/m^2) blue-rich light sources have a dramatically increased visual brightness compared to yellow-rich sources. Under conditions with intermediate light adaptation appropriate for consideration in urban environments, ($0.001 \leq L_V \leq 3$ cd/m^2) this effect is decreased as the luminance increases.

The Sky Glow Index (SGI) is a proposed metric that takes angular intensity distribution and spectral sensitivity effects into account. The SGI is defined as:

$$\begin{aligned} \text{SGI} &= \text{S/P} \times [\text{reflected upward lumens} + \text{direct upward lumens} \times \text{UIF}] \\ &= \text{S/P} \times [(\text{LL} - \text{UL}) \times \text{G} + \text{UL} \times \text{UIF}] \end{aligned}$$

where S/P is the scotopic/photopic ratio of the light source, G is the ground reflectivity (assumed independent of wavelength), LL is the luminaire lumens, and UL is the direct uplight lumens. In this analysis I will assume that ground reflectivity is 0.15; when comparing lighting codes I will consider the lumens (LL and UL) per square meter. The UIF term represents the uplight impact factor, or the ratio of the sky glow impact of direct upward emissions compared to light reflected from a horizontal ground surface. In this analysis I will use UIF of 5, which is a conservative figure for areas within suburban environments or within several kilometers of the light sources. In circumstances where sky glow viewed from locations very close to the light sources (within about 1km) is to be evaluated a UIF of 1 is more appropriate; in circumstances where sky glow at large distances from the lighting is to be evaluated (at distances over about 20km, such as at astronomical observatory sites or rural parks) a UIF of 10, 20 or more should be used.

When evaluating the SGI for two less common lighting applications not well described by the above discussion – façade floodlighting and lighting under canopies – SGI is evaluated as follows. For façade floodlighting, I assume that all light strikes the building face with reflectivity H, and that 50% of the reflected light propagates upward with UIF of 5:

$$\text{SGI}_{\text{façade}} = \text{S/P} \times [(\text{LL} - \text{UL}) \times \text{G} + (\text{UL} \times \text{H} \times 0.5) \times 5]$$

For lighting under canopies (such as is common at American service stations), I assume that all lighting is fully shielded (*i.e.* UL = 0), that the ground surface is concrete with reflectivity 0.25, and that the canopy blocks 75% of the reflected light from reaching the sky:

$$SGI_{canopy} = S/P \times LL \times 0.25 \times 0.25$$

Finally scotopic to photopic ratios of representative light sources are shown in Table 1.

Table 1. Representative S/P ratios for area lighting sources

Lamp Type	S/P
LPS	0.25
HPS	0.65
MH	1.5
LED 4300K	2.0

I note the purposeful lack of sensitivity of the SGI to distance. The *absolute* impact of a given lighting installation on the sky glow at an observation point will vary overall approximately as the inverse 2.5 power of the distance. Reasonably accurate predictions of absolute sky glow levels must include a treatment of specific circumstances and factors, including lighting fixture locations, specific photometric details concerning shielding and blocking, and accurate information concerning atmospheric conditions. The SGI as formulated here is intended only to evaluate the *relative* impacts of lighting installations with differing total amounts of light and shielding characteristics. From any particular observation point, a given lighting installation with an SGI of 30 will have approximately twice the sky glow impact of the same installation in the same location with an SGI of 15.

At times (i.e. when considering the effects of sky glow on astronomical measurement, or on human circadian disruption) it may be appropriate to consider a radiant sky glow index, or a sky glow index including the circadian response function, instead of the visual sky glow index defined here. Under such circumstances we suggest using the terms such as vSGI, rSGI or cSGI to distinguish sky glow indices that include visual S/P ratio, no spectral factor, or a "circadian to photopic" ratio of the light sources. Other response ratios relating lumen (photopic) output of lamps to the response of the affected system or organism may be used in appropriate circumstances and for particular purposes

3 The effectiveness of the POLC and the MLO in limiting sky glow

3.1 Summary of relevant control standards

As a basis for evaluating SGI under existing U.S. "state-of-the-art" dark sky lighting codes, I will use the IDA Pattern Outdoor Lighting Code [2], with several updates as reflected in the Coconino County, Arizona outdoor lighting code [9]. Besides strict standards for "fully shielded" fixtures (i.e. no direct uplight), as an explicit means of limiting sky glow these codes limit total site lighting to 4.3, 8.6 and 17 lm/m^2 in three Lighting Zones (LZ1, 2, 3). It is important to note that these allowances are applied has an average over the entire site, and not applied to portions of a parcel or each square meter – they are a means to limit total lighting use and thus sky glow, and not metrics for lighting design. Canopy lighting is limited to 140, 280 and 280 lm/m^2 in LZ1, 2 and 3. (These figures are the equivalent fixture lumens – these codes use "lamp lumens," with nominal values of 25, 50 and 100 klm/acre and 20, 40 and 40 lm/ft^2.) Based on rough estimates of reduced sky glow impacts of lighting mounted under canopies, canopy lighting counts toward the site lumen allowance 100% when located 1.5m (5ft) or less from the canopy edge, 25% when 1.5 – 3m (5 – 10ft), and 10% when over 3m (10ft). The Coconino code also allows a maximum of 0/0.5/0.5 lm/m^2 (0/2.1/2.1 klm/acre) in unshielded fixtures in LZ1/2/3; the maximum output of such a fixture is 1750 lm. the Coconino lighting code also has restrictions on lamp types, requiring the use of low-pressure sodium (or narrow-spectrum amber LED) for general area illumination such as for parking lots and roadways. As general area illumination dominates outdoor lighting, the implications of general illumination lamp type standards for visual sky glow brightness can be dramatic. These standards will be referred to as the "POLC" in this analysis.

In contrast to the POLC, the MLO is more complex, with many more standards affecting SGI. The principal methods used to regulate outdoor lighting in MLO are 1) five lighting zones, 2) lumen allowances based on lighting zone, lighting use, and various measures of use area, 3) control of direct uplight through luminaire shielding standards following the Luminaire Classification System (LCS) BUG standards [10], or limitation of measures termed "off-site" impacts, and 4) after-hours lighting reductions. There are three separate methods (and two "options") for setting allowances and determining compliance, called the Prescriptive Parking Space Method, Prescriptive Hardscape Area Method and the Performance Method.

I will not attempt to summarize all of the relevant standards and numbers needed to evaluate the SGI under MLO lighting designs, but instead refer the reader to the MLO itself. It is important to recognize that there are no luminaire shielding standards at all under one option of the MLO Performance Method. Further, since all methods/options are available to all lighting designers/projects, I will gauge the SGI following the regulatory options that yield the greatest impact.

3.2 SGI for commercial lighting

The maximum SGI under POLC standards is determined by only the lighting zone when canopy lighting is not included, and is shown in Table 2. I assume 50% of the unshielded allowance is directed upward. The last line in this table indicates the SGI per square meter for unregulated lighting (installed before the current lighting code) on 32 commercial sites as observed in Flagstaff, Arizona [11], where 38 lm/m^2 (155 klm/acre) with 8% direct up was determined; HPS lighting with S/P = 0.65 is assumed.

Table 2. SGI and related values for commercial lighting regulated following POLC standards, and unregulated commercial lighting observed in Flagstaff Arizona.

		LZ 1	**LZ 2**	**LZ 3**
POLC				
Total allowance (LL)	lm/m^2	4.3	8.6	17
Unshielded allowance	lm/m^2	0	0.52	0.52
Direct uplight (UL)	lm/m^2	0	0.27	0.27
SGI/m^2 (LPS)		0.16	0.65	0.96
SGI/m^2 (HPS)		0.42	1.7	2.5
SGI/m^2 (LED)		1.3	5.2	7.7
Unregulated (Flagstaff, AZ)				
SGI/m^2 (HPS)			21	

Determining the SGI under MLO standards requires specific lighting designs, as the lighting allowances are based on specific lighting uses and the associated areas, and maximum "off-site" impacts must be evaluated using sophisticated illuminance calculation software including inter-reflections between surfaces both on and off the site. Specific designs conforming to the MLO Performance Method Option B in MLO LZ 2 were developed following three specific site plans, including an auto dealer, motel, and a bank. The average SGI/m2 and associated values are listed in Table 3.

Table 3. Average SGI and related values for three lighting designs meeting MLO Performance Method Option B standards for LZ2.

		LZ 2
Total allowance (LL)	lm/m^2	36
Direct uplight (UL)	lm/m^2	8.0
SGI/m^2 (LPS)		11
SGI/m^2 (HPS)		29
SGI/m^2 (LED)		88

4 Roadway Lighting

Without attempting to delineate the myriad practices for roadway lighting, the SGI metric allows an approximate quantification of the sky glow consequences of some common choices made concerning lamp type and uplight fraction. Besides the question of lamp spectral power distribution and its attendant S/P ratio, discussions are commonly presented by the lighting professions concerning the fraction of direct uplight, the attendant pole spacing and therefore lumens per area of roadway, and the relative impact of these competing factors (increased direct uplight and decreased total and therefore reflected uplight) on sky glow. Though specific figures depend on the circumstances, the suggestion is commonly made that allowing a few percent of uplight permits a 10 – 20% wider spacing of poles, thus reducing the total number of lumens used per unit length of roadway. A switch from HPS to white LED is a topic of much recent interests. Assuming these figures, estimated SGIs per unit length of roadway are summarized in Table 4.

Table 4. SGI and related values for roadway lighting as described in the text.

Condition	**SGI**
Fully shielded (HPS)	0.098
3% direct up (HPS)	0.19
3% direct up, LL reduced 20% (HPS)	0.15
3% direct up, LL reduced 20% (LED)	0.47

5 Conclusion

The sky glow index provides a simple way to evaluate the relative sky glow impacts of lighting regulations and specific lighting designs, including a treatment of the increased impact of direct upward emissions compared to reflected upward flux, and accounting for the brightness of different light sources to the dark-adapted eye.

Using the SGI to compare the effectiveness of the 2000 IDA Pattern Outdoor Lighting Code (POLC) and the newer Joint IDA-IES Model Lighting Ordinance (MLO), I show that the POLC reduces the expected sky glow increase to 1/10 or less that observed from a limited sample of unregulated lighting practice, assuming no change from the current mixture of light sources. Including the specification for low-pressure sodium (LPS) lighting contained in some implementations of the POLC, sky glow impacts can be reduced to 1/20 or less of unregulated (assumed to be principally HPS) lighting.

Comparing the effectiveness of the POLC to the MLO, the estimated sky glow impacts of lighting under POLC are 1/4 to 1/35 that expected under MLO standards for LZ 2; the reductions compared to the higher numbered MLO LZ's would be expected to be much larger still. Lighting under MLO standards appears to represent a drastic step backward in sky glow limitation compared to the older POLC standards, and is not appear effective at reducing sky glow impacts even compared to the limited measures of unregulated lighting as observed in Flagstaff, Arizona.

For roadway lighting using drop-lens fixtures with 3% direct uplight, sky glow impacts can be expected to increase by nearly a factor of two compared to fully shielded designs if the total number of lumens per unit length of roadway remains unchanged. If improved light distribution available with such fixtures allows a 20% increase in pole spacing, the sky glow increase is reduced to approximately 50% over the fully shielded design. A switch from the now common HPS to white LED can be expected to increase visible sky glow approximately 200% if no overall lumen density reduction is achieved; even if the total installed lumens of an LED system could be reduced to one half that of an equivalent HPS system, the visible sky glow would still be expected to double.

References

[1] International Dark-Sky Association / Illuminating Engineering Society of North America (2011): Joint IDA-IES Model Lighting Ordinance.

[2] International Dark-Sky Association (2000): IDA Outdoor Lighting Code Handbook and Pattern Code.

[3] C. B. Luginbuhl, D. M. Duriscoe, C. W. Moore, A. Richman, G. W. Lockwood, D. R. Davis (2009): From the Ground Up II: Sky Glow and Near-Ground Artificial Light Propagation in Flagstaff, Arizona, PASP 121:204.

[4] P. Cinzano, F. J. Diaz Castro (2000): The Artificial Sky Luminance and the Emission Angles of the Upward Light Flux, MSAIt 71:251.

[5] C. B. Luginbuhl, C. E. Walker, R. J. Wainscoat (2009): Lighting and Astronomy, Physics Today 62:32.

[6] F. Falchi, (2011): Campaign of Sky Brightness and Extinction Measurements Using a Portable CCD Camera, MNRAS 412:33.

[7] C. B. Luginbuhl, P. A. Boley, D. R. Davis, D. Duriscoe (2013): The Effects of Lamp Spectral Distribution on Sky Glow over Observatories, Proceedings of the IAU Gen. Assembly XXVIII, in press.

[8] C. B. Luginbuhl, P. Boley, D. R. Davis, D. M. Keith, C. A. Moore (2013): The Impact of Light Source Spectral Power Distribution on Sky Glow, this conference.

[9] Coconino County Zoning Ordinance, Chapter 17. As of 15 November 2012 available at http://www2.coconino.az.gov/uploadedFiles/Community_Development/Section17.pdf

[10] Illuminating Engineering Society of North America, (2011): TM-15-11: Luminaire Classification System for Outdoor Luminaires.

[11] C. B. Luginbuhl, G. W. Lockwood, D. R. Davis, K. Pick, J. Selders (2009): From the Ground Up I: Light Pollution Sources in Flagstaff, Arizona, PASP 121:185.

A new definition of light pollution based on the status of light pollution in Iran

Seyed Hamed Mirzakhalil

A member of Davtalaban-e Sabz-e Iran (Green Volunteers Society),
An Iranian non-governmental and non-profit organization
Tel:+989124354092, e-mail: info@lightpollution.ir

Abstract

In Iran, the discussion of light pollution theory has been proposed less than 10 years by Noor-e-Shab group (under my management) which is the member of an environmental non-governmental and non-profit organization (NGO). This article has been written to explain this group's activities found new definition of light pollution by their observations and studies in Iran and holding 300 persons/hours seminars. National and international studies and classification of 1300 photos of different samples of light pollution in big cities of Iran could attain aforementioned definition for this group. The plan of this definition resulted in fundamental transformations in the field of outdoor lighting and astronomers' attitude in Iran. In this article, in addition to explanation of light pollution's new definition, has been studied some parts of the most important achievements of this group attained through last 8 years, despite existing problems and restrictions such as short of funds, lack of attention of urban managers and urban numerous problems, lack of educational and informative centers or organizations.

1 Introduction

As you know, each country has its own behavior related to the light, based on its approach to lighting. For this reason, the definition of light pollution may belong to the same country. These definitions are sometimes such a way that if an enthusiastic person, in another corner of the world, wants to know what the light pollution is, doesn't understand or hardly understands it. This makes my group and me (Messrs Hadi Kashani and Parham Mirzakhalili, Mrs. Sara Bagheri) gathered more accurate and more pictures to find a definition of existing light pollution in Iran and offer a new definition for it.

The definition of pollution or an issue should be comprehensive, inclusive and exclusive, perfect and also have the ability of quantitative and qualitative measurement. Many years ago, when I started my studies about light pollution, I didn't find any definition contains all items and my observations in Iran, such as wasting energy and its destructions affect sky and environment. Definitions mainly were as examples to explain some events can destroy sky or environment by light. It could be proper studying examples for an expert and someone who is familiar with this issue but not for beginners. It is useful in short-term activities and just for familiarizing or superficial study of a student, but if this person wants to found and manage an association in the field of light pollution or make an academic study or lobby authorities, after a while, both self and his target society get confused.

In my opinion, according to following reasons it is difficult to understand what the light pollution is for an ordinary person in Iran; therefore to find pollution reduction methods for each society, having primary knowledge of pollution is as a priority to control it.

1 We were born in an environment where taught us a very simple way to escape fear of darkness which is pushing the button and turning the light on. It is obvious that our understanding of darkness is different from our predecessors' understanding, before light invention. In this condition which artificial light is a part of human culture and behavior, it is somehow difficult to discuss about control and standard of light and to understand this subject by audience.

2 Discussion about some materials such as saving energy and wasting energy by lighting is not understandable for people and authorities given no attention and credit to it, in such countries

like Iran which energies are not still expensive and everybody can choose his lighting among different kinds of energies and electricity. Incidentally, people don't pay high charges for using energy as lighting.

3 In Iran, More severe pollutions such as air pollution have attracted the attention of most urban authorities and managers. Air pollution has triggered shutting down many days through each year and caused 20 more people die, on air pollution crisis compared with ordinary days, because of stroke or heart attack leading death in Tehran, the capital of Iran [1]. According to this, it is unprofitable to discuss about wasting energy, faint stars, going wrong astronomers' observations or disturbing biological clock of citizens' bodies, and we could see less co-operation of authorities.

4 Some other reasons such as economic pressure on people and paying attention to basic needs like food and clothing have caused that people think less about environmental issues or sacrifice environment for their lives.

5 As mentioned before, cheapness of energy in Iran has triggered the managers have no serious and codified planning in the field of optimal use of light in cities and this caused an approach led by taste towards the subject of urban lighting, and contractors and authorities' being unfamiliar with standards.

6 Lack of academic fields or widespread governmental or non-governmental educational centers has triggered taste attitude, wasting energy by disregarding standards and then lack of understanding of light pollution concept.

7 Another reason for appearing taste attitude in the authorities and contractors' projects is lack of specified and rigid rules at the country level about lighting or light pollution.

We mention the state constitutions hint light pollution: Article 1 of protect and improve the environment code (adopted 17,June,1974 and modified 15,November,1992) states: «protect and improve the environment and to prevent and avoid any type of contamination and destructive action which disturb environment's balance and proportion are considered as Environmental Protection Agency's tasks.»

Article 9 of protect and improve the environment code states: «Preceding any activity that bringing environmental contamination is prohibited.

Environmental contamination refers to distribution or combination of foreign substance with water or air, soil or land to the extent that its physical or chemical or biological quality transforms which could be detrimental to human being or other live creatures and or plants and or buildings. »

Article 2 of prevention method of air pollution (adopted 23, April, 1995) states: «Preceding any activity that bringing air pollution is prohibited.

Air pollution refers to existence and distribution of one or more solid, liquid, gas, radioactive and non-radioactive radiation pollutant in open-air in the amount and length of time enough to transform its quality which could be detrimental to human being and or other live creatures and or plants and or buildings.»

But the history of the first direct rules related to light pollution was on November, 2008 which the City Council of Tehran obliged Municipality of Tehran to control light pollution and provide comprehensive plan of light and lighting of Tehran urban spaces, and also Municipality was obliged to use colored flags instead of lighting in National Celebrations but this rule was not executed for a long time. (It should be said that the country had faced an energy crisis in that year.)

Tehran is as a pattern for other cities of Iran; this has caused them to sit on their hands and keep their eyes on capital which Tehran becomes their pattern for new and creative plans. Also, about lighting and light pollution, Tehran has leading role in urban spaces lighting and use of non-standard decorative lights (sphere model), this caused to unofficially issue the license of using non-standard lights in the whole country and everybody knows these lights as beautiful ones without paying attention to citizens' taste and poll.

In the country, there are just a handful of non-governmental organizations and institutions interested in the topics of light and lighting and control of light pollution; based on this fact, the capacity of specialist manpower has been low at the country level and confined funds of these organizations has lost the power and opportunity of propaganda and giving information or holding a conference or workshop for interested or ordinary people. In this situation, confined students of some academic fields related to these subjects, temporarily consider this matter or learn from experience of experts.

Existence of perfect definition of light pollution which contains all side-effects (comprehensively) of it, can direct individuals interested in opposing light pollution to a single way. Lack of specified definition, in a country and or in the world, has triggered an approach led by taste for using the light and sometimes may confuse urban management officials and sometimes imperfect definition distracts their attention from light pollution identification, as a result it causes no single system to plan a solving program. Also, it is difficult to find a national common solution when the problem should be solved but there is no single definition because people and groups of experts of a society think, conclude and represent solution based on their enthusiasm and knowledge of a phenomenon. Different attitudes in a society follow different solutions; as a result it needs more time to find a desired conclusion such as pollution reduction or knowledge increase of a society. A unified definition can adopt a unified policy in the society; otherwise there will not be collaborative and worldwide work.

Based on aforementioned reasons, my group, at the beginning of its activity, took action to determine a definition for Iran's light pollution. The other reason was deficiency of the other definitions of light pollution. For example, Department for Environment, Food and Rural Affairs of England (DEFRA) (2005) presented the following definition:

"Light pollution is the adverse effects of artificial light. Adverse effects can include sky glow, glare, and light trespass. Sky glow is the glow that appears due to scattered artificial lights caused by dust particles and water droplets in the sky. Glare occurs when bright light clashes with a dark background. Light trespass is when light goes beyond the property on which the light is located. Types of artificial lighting that commonly causes light pollution are street lighting, security lights in gardens and flood lighting used for sporting events."

In this definition there is no hint to spectrum of a lamp. For example, most of lamps have ultra violet (UV) and adverse effects for environment and human beings if they use at inappropriate time.

International Dark Sky Association has presented following definition: "Any adverse effect of artificial light, including sky glow, glare, light trespass, light clutter, decreased visibility at night and energy waste." Also, this definition has not mentioned at the quality and spectrum of lamp light in different usage of light in urban life. Or for example Ministry of the Environment of Japan (MOE) (2006) presents this definition: "light pollution as any adverse effect and disturbance by light trespass as a result of the improper use of artificial light." It is sometimes happened no light trespass or somebody feels no adverse effect, but choosing an improper light for a place doesn't need it causes light pollution unwillingly.

The following definition is presented by Oxford Dictionary: "Brightening of the night sky that inhibits the observation of stars and planets, caused by street lights and other man-made" [2]. Also, this definition just hints at inhibiting the observation of stars and doesn't say anything about the other [adverse] effects.

Another definition says: "Degradation of photic habitat by artificial light" [3]. You may use artificial light at home and don't degrade any habitat but the improper usage of artificial light would leave adverse effects with your family and you.

"Light pollution is the alteration of light levels in the outdoor environment (from those present naturally) due to man-made sources of light. Indoor light pollution is such alteration of light levels in the indoor environment due to sources of light, which compromises human health." [4].

Deficiency of this definition is paying no attention to indoor environment, which may be light-polluted, although no live creature commutes. In fact, we shouldn't assume that there are just adverse effects of light pollution in environments which a live creature definitely commutes. You may produce light pollution in the environment that there is no one in but in the other environment, its adverse

effects would happen. According to aforementioned reasons, it seems following definition contains, based on its new classification, the most reasons and effects of light pollution.

2 Definition of light pollution

Artificial lights which, in improper time and place, deviate from their standard, and hurt and pollute environment and night sky by adverse quality. In this definition, 3 words of time, place and quality are especially important, therefore we discuss them more.

Improper time: It may be used artificial light through some hours of a day which is not necessary. It may occur while indoor environment of building is bright enough by sunshine; our wrong habit makes us to increase indoor lighting by artificial lights. Another situation is in parking and corridor which all the time several lights are on; although there is rarely commute.

Lighting engineering forms when there aren't natural light sources like sun, or they don't light our desired environment enough. Therefore, if through a day, there are enough light and also light lamps, it is as an improper time.

Improper place: In modern world it will be done accurate calculation to use many kinks of energy such as electric power which are very important. There are also some defined standards about the use of artificial light sources at homes, public places, shops, hospitals, restaurants and etc and health of human, especially his vision, was highlighted by researchers. According to the type of each place, some standards of lighting level are defined for everyone planned for a special activity normally; it will cause light pollution if these standards not to be considered and taste attitude manages the use of lights. Actually, we can properly use energy and protect ourselves against harms with this attitude that represents how much light is needed for each activity and places. For example it is needed 100 lux of light for bedroom, 500 lux for classroom and 1000 lux for technical drawing room [5]. Therefore extra use of light, in each place, causes light pollution. Now here we can hint at intercity and transit bus parking that has been lit with extreme lights and these reflect extra lights to the space and causes light pollution. Another problem of using light at improper places is entry the light to the private environment of people such as home and especially bedroom. Brightness of bedroom in the middle of night causes a disorder of melatonin hormone release and thus disturbs body's biological clock and triggers stress, anxiety, concentration decrease and etc [6]. It could be surely said the most residents of Tehran Metropolis sleep in a light polluted environment and just their physical bodies sleep not their minds principally. This is because of severe light pollution of this city and existence of turtle lights with glass shell lamp in narrow alleys and high streets, even near the house windows.

For example, amount of light pollution of Tehran Metropolis has been calculated in a suburb observatory of this city [7]. Study of the amount of light pollution based on Walker Model

$$I = CPD^{02.5}$$

In this model, C is constant factor of each city's pollution, P is the amount of resident population, and D is distance from observed point to city center. Study of the amount of I for Maranjab Caravansary observing place. This place is located 47 km of Kashan city (with a population of 253500). Thus:

$$I = 0.01 \times 253500 \times 47^{-2.5} = 0.16 \quad > \quad I = 16\%$$

Also, from a distance of 160 km and direction of northwest of Tehran (with a population of 7,500,000), it affects on this city and the amount of I is:

$$I = 0.01 \times 7500000 \times 160^{-2.5} = 0.23 \quad > \quad I = 23\%$$

Adverse quality: the quality of light is very important in light engineering. As light should be used in proper time and space, the quality of light is very important for medical and health attitude. Each lamp, based on its process of light production, has especial quality, light color, and spectrum. For example, in astronomers' opinion, the light of low-pressure sodium lamp is so suitable because it is easily possible to hide and cover its light from the view of astronomical instruments with special filters. The light of this lamp just lights yellow spectrum and has no other spectrum, therefore can be

easily omitted by a filter. Unfortunately, sodium lights are no panacea. Some animals, it turns out, fare no better with narrow-spectrum, yellow light than with any more traditional artificial lights. Some even seem to fare worse [8]. So it is better to specify the kind of the light according to the environmental function.

3 Conclusion

Today, lighting designing is very important besides lighting engineering and necessity of paying attention to this subject gradually increases besides the other elements of urban architecture and even urban furniture. Experts' attempt to define beauty in this field and paying attention to psychology and social behavioral science which lead to peace in different environments prove the importance of them in this world; although lighting designing is almost a matter of taste and gets away with formulas and calculations of light engineering.

References

[1] Director of Behesht-e-Zahra Cemetery in the meeting of Tehran environmental condition survey, Environment Committee of City Council of Tehran, 10, December, 2012.

[2] http://oxforddictionaries.com

[3] F. J. Verheijen, (1985). Photopollution: Artificial light optic spatial control systems fail to cope with. Incidents, causation, remedies. Experimental biology 44 (1): 1–18. PMID 3896840.

[4] J. Hollan (2009): What is light pollution, and how do we quantify it? Darksky 2008 conference paper, Vienna, August 2008. Updated April 2009.

[5] H. Kalhor: 1386. Lighting engineering. Enteshar Publication Company.

[6] T. Gallaway, R. N. Olsen, D. M. Mitchell (2009): The economics of global light pollution, Ecological Economics J, 26 November 2009, p 659.

[7] S. Alidoosti, (2011): Special booklet for Astronomy Club Isfahan, 26, June, 2011, p11.

[8] B. Harder (2002): Deprived of Darkness: The unnatural ecology of artificial light at night, Science News, Vol. 161, No. 16, April 20, 2002, p. 248

Night sky brightness measurements and night sky spectroscopy performed at the Vienna University Observatory

Thomas Posch[1], Johannes Puschnig[1], and Stefan Uttenthaler[1]

[1] *Department of Astrophysics, University of Vienna, Türkenschanzstraße 17, A-1180 Wien, Austria*
tel: +43 1 4277 538 00, fax: +43 1 4277-9518, e-mail: thomas.posch@univie.ac.at

Abstract

We present a series of automated measurements of the night sky brightness performed at the Vienna University Observatory (IfA) and at the Leopold-Figl-Observatorium für Astrophysik (LFOA). The latter is located about 35km to the southwest of Vienna at an altitude of 880m. Our measurements have been performed with Sky Quality Meters, made by Unihedron, Inc. The measurements cover a time span of one year. They have been carried out every night, with a sampling rate of 7 seconds, resulting in a large data set which has been evaluated statistically. The mean zenithal night sky brightness at IfA is currently found to be in the range between 15 … 19.5 mag SQM / arcsec^2; at LFOA, it is in the range from 17 … 21 mag SQM / arcsec^2 with a strong circalunar periodicity. Furthermore, we took spectra of the night sky in Vienna, using an 80cm telescope. The goal of these spectroscopic measurements was to identify the main types of light sources and the spectral lines which cause the light pollution in Vienna.

1 Introduction

Up to now, astronomers have mainly been measuring the brightness of the night sky (in magnitudes per arcsec²) at dark sites, especially at modern mountain observatories, or at potential observatory sites as a part of site-testing and site-monitoring. Within the past few years, it has become evident that increasing night sky brightness (henceforth: NSB) and light pollution have far-reaching consequences for human health as well as wildlife [1].

Therefore, it is desirable to measure and monitor the night sky brightness not only at remote mountaintop observatory locations (as done, e.g., by Patat [2]), but also close to the centers of modern civilization, and to do so every night, in a reproducible way, with the aim of performing long-term studies. Only in this way, the impact of night sky brightness with respect on biological rhythms and on animal behavior and human health can be assessed.

2 Measurement sites

The two sites at which we have performed systematic measurements were the Vienna University Observatory (in the following: IfA – short for *Institut für Astrophysik*) and *Leopold-Figl-Observatorium für Astrophysik* (in the following: LFOA).

The observing conditions and the night sky at IfA are typical for a large city. We show in detail what this means in terms of night sky brightness values. Visual night sky observations by the authors at IfA revealed that the Milky Way can be seen only very few times a year near the zenith under exceptional meteorological conditions there. At LFOA, in contrast, the Milky Way can be clearly observed during every clear and moonless night, and not only near the zenith, but also close to the horizon. We consider night sky at LFOA as typical for a rural region with only a little amount of (local) light pollution. The altitudes above sea level and coordinates and of our measurement sites are summarized in Table 1. The distance between IfA and the city centre of Vienna is about 3km, while the distance between LFOA and the city centre amouts to ~35km (air line). Vienna has about 1.7 million inhabitants.

Table 1: Our measurement sites.

Location (altitude)	Longitude	Latitude
IfA (240m)	16°20'03''	48°13'54''
LFOA (880m)	15°55'24''	48°05'03''

3 Method of night sky brightness measurements

For our NSB measurements, we used "Sky Quality Meters" (SQMs) made by the Canadian company Unihedron. The specific model we used is called SQM-LE. It is equipped with a lens in order to detect only radiation from a limited solid angle. According to the manufacturer's manual, the integrated lens restricts the SQM's field of view to ~20° full width at half maximum (FWHM). The sensitivity then decreases rapidly, so that a point source located ~19° off-axis contributes 10 times less to the measured brightness than a spot directly on-axis. We have chosen the version with a lens because we use one of the devices in an urban region where the field of view is limited due to surrounding buildings anyway. Furthermore a wide beam width would result in lower accuracy due to possibly scattered light. All our measurements have been performed with the SQMs pointing toward the zenith.

We chose a sampling rate of 0,143 Hz (i.e., every seven seconds, a measurement is stored) and invested a substantial efforts in creating tools for the statistical analysis of the large amount of resulting data. A graphical interface was also created, which generates plots of the SQM results automatically every night. The plots and statistics can be downloaded at the following URL: http://astro.univie.ac.at/institut/lichtverschmutzung/.

Figure 1 shows an example of an automatically generated SQM light curve, measured at IfA during a full moon night (from 1st Aug. to 2nd Aug. 2012).

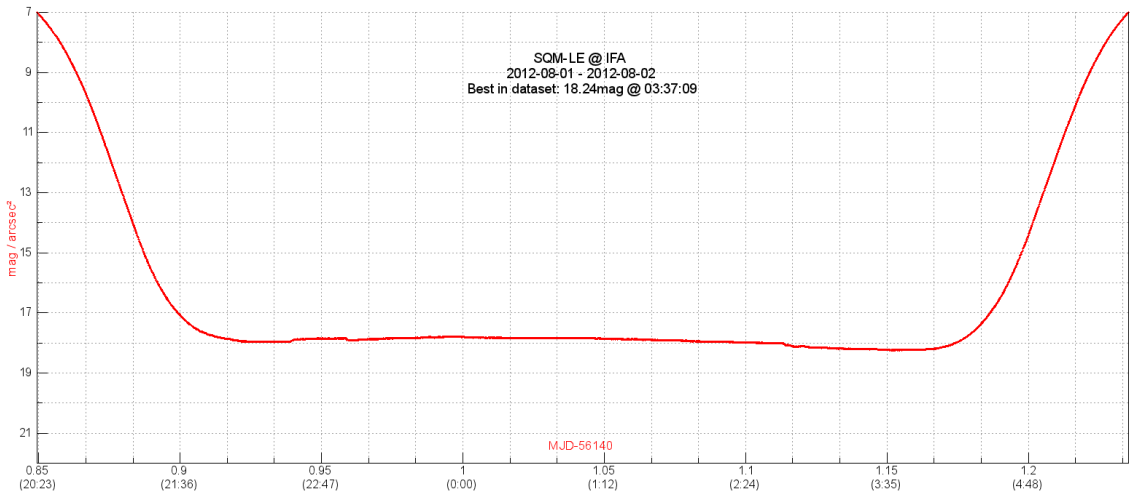


Figure 1: SQM-LE light curve measured at IfA during a clear full moon night. The mean sky brightness during this night was 17.95 mag_{SQM}/arcsec². The best value during this night was 18.24 mag_{SQM}/arcsec².

It should be noted that SQMs, as they are delivered, are not equipped with Johnson V filters. This is because the spectral response function of the detector inside an SQM differs from the transmittance of a Johnson V filter. Previous reports indicated that the night sky brightness values measured by SQMs do not differ strongly from those from systems equipped with a V filter. Nevertheless, given that SQM magnitudes are not the same as V magnitudes, we will use the unit "mag $_{SQM}$/arcsec²" throughout this paper in order to make this difference clear.

The spectral sensitivity of the SQM was measured by P. Cinzano [3]. A comparison between the SQM response function and the Johnson V band shows that the SQM is much more sensitive to light

at λ < 520nm. At a first glance the difference seems to make a comparison between the Johnson V band and the SQM response function very difficult, but considering the spectral distribution of the night sky over Vienna – which is dominated by emission lines at λ > 525nm, as will be shown below – we presume that a constant offset can be found for a comparison to the Johnson V band.

Figure 2 shows the spectral response function of an SQM as measured by Cinzano and compares it to the Johnson V filter profile.

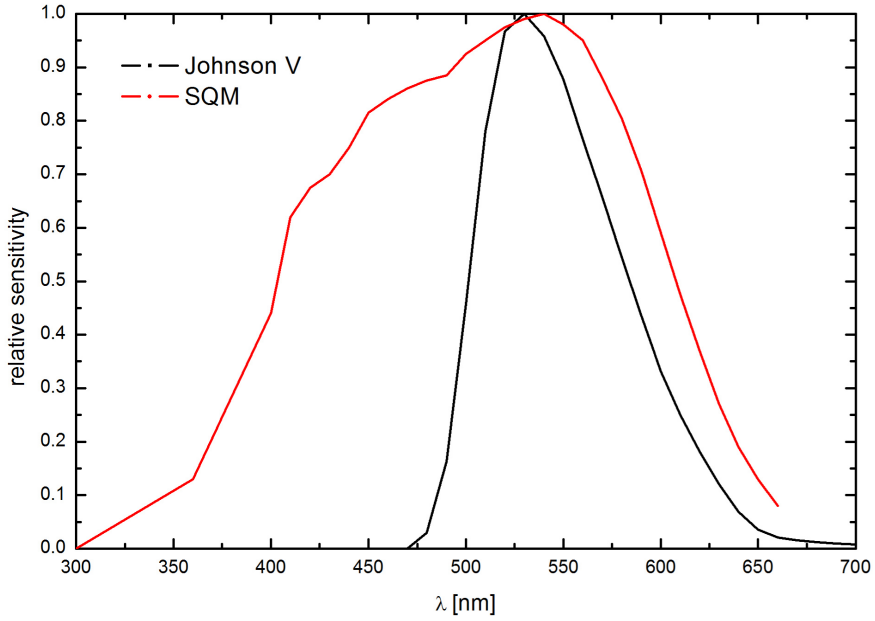


Fig. 2: Sensitivity of the SQM as a function of the wavelength (red line, [3]) compared to the transmittance of a Johnson V filter (black line).

4 Variation of the *mean* night sky brightness within a year; searching for a circalunar rhythm

As mentioned above, our measurements meanwhile cover a period of one year. We were therefore interested in the behavior of the *mean* night sky brightness at IfA and at LFOA during this period (March 2012 – March 2013). Mean NSB values were calculated by averaging each night's NSB values from the end of the astronomical twilight to its beginning in the early morning.

At a rural site, a strong influence of the lunar phase on the NSB is expected: full moon nights should be recognizable by much brighter night skies, especially for clear sky conditions. In contrast, nights around new moon should be much darker. Since LFOA is a rural site, this pattern can is indeed detected and a beautiful circalunar periodicity of the mean NSB becomes evident (see Fig. 3).

The NSB data from Vienna show a completely different picture. *Instead of the moon, the degree of cloudiness has the strongest influence on the NSB in Vienna*. The more clouds over a big city, the stronger the backscattering of urban light. But of course, the degree of cloudiness does not follow any strict periodicity. Therefore, the mean NSB measured in Vienna seems to oscillate in a stochastic way. *The circalunar rhythm has gone into extinction here.*

5 How bright and how dark does the night get? The range of measured (mean) night sky brightness values

We now turn to the question of the ranges of mean nocturnal sky brightness values that we found by analyzing our one year time series. Figures 5 and 6 present the answer to this question.

As these figures show, the mean zenithal NSB values in Vienna (location IfA) are in the range *between 15 mag $_{SQM}$ / arcsec^2 and 19.5 mag $_{SQM}$ / arcsec^2*. The black vertical line represents a sky brightness of 18.9 mag $_{SQM}$ / arcsec^2. This corresponds to a luminance of 3 x 10^{-3} cd/m^2 or 3 mcd/m². We take this value as the lower limit of the cones in human vision. At smaller luminances, the color-insensitive rods entirely dominate our vision. If the NSB is brighter than 18.9 mag $_{SQM}$ / arcsec^2, the adaptation of the human eye to darkness is very incomplete. The partial visibility of our Milky Way at least near the zenith requires a value which is reported to be close to 18.9 mag $_{SQM}$ / arcsec^2 as well. *According to Fig. 6, almost 90% of all nights at IfA are characterized by mean zenithal NSBs larger than the "18.9mag" threshold:* during the vast majority of all nights, therefore, entirely rod-dominated vision as well as Milky Way visibility is not reached.

At our rural, 880m-above-sea-level observing station LFOA, in contrast, only 20% of all nights

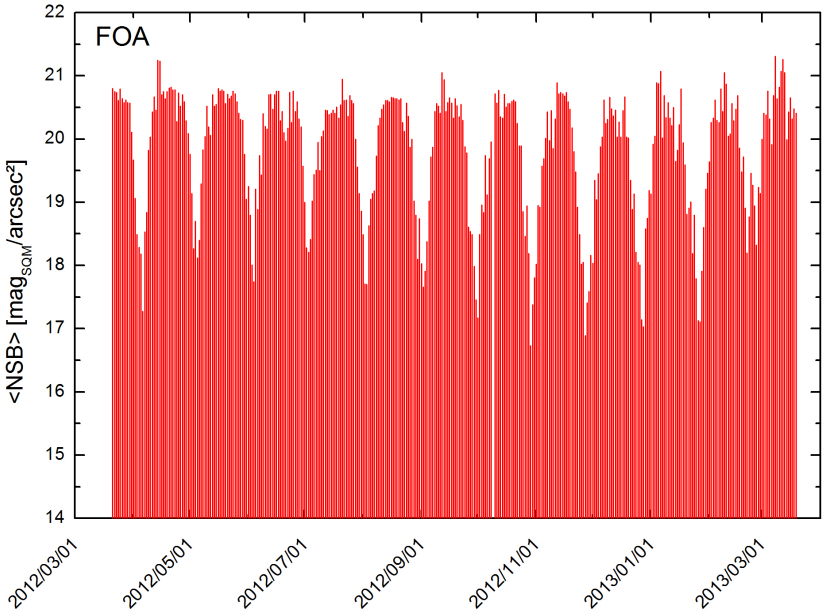


Figure 3: Mean NSB values calculated from our LFOA data from (end of) March 2012 to March 2013.

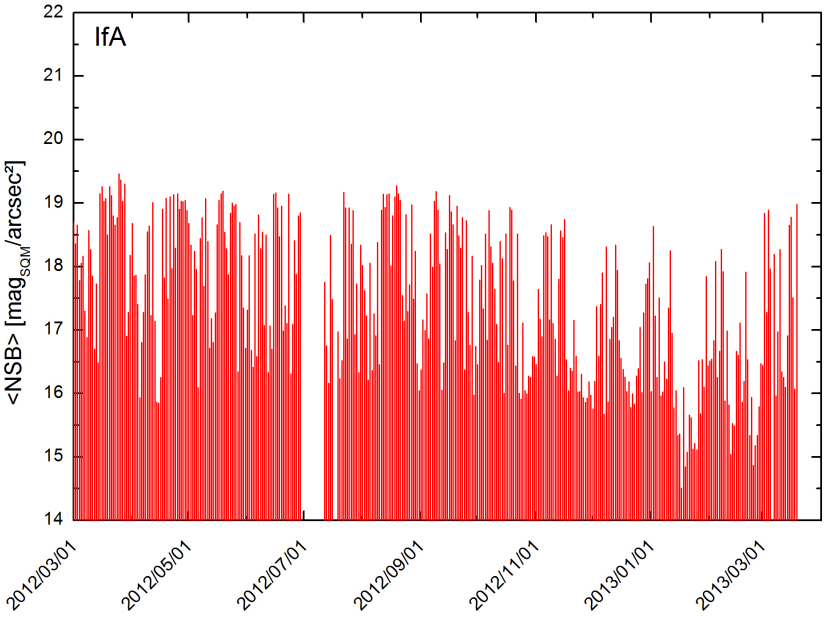


Figure 4: Mean NSB values calculated from our IFA data from March 2012 to March 2013.

have mean zenithal NSB values brighter than 18.9 mag $_{SQM}$ / arcsec^2. The full range of mean NSBs at LFOA is 17 mag $_{SQM}$ / arcsec^2 to 21 mag $_{SQM}$ / arcsec^2. Note that even the latter value is still about 0.7 magnitudes above the natural night sky brightness.

6 The effect of the 11 p.m. curfew on the night sky brightness

The city of Vienna partially reduces the brightness of its street lighting at 11 p.m. (also called curfew – in the following: 'C'). Main roads, however, are still kept at constant luminance throughout the whole night. At 12 p.m., most of the decorative façade illuminations is switched off (this effect is labelled 'F' below). Our sky brightness curves, therefore, show two discontinuous steps at 11 and 12 p.m., of which the first one is larger. This is shown in Figure 7.

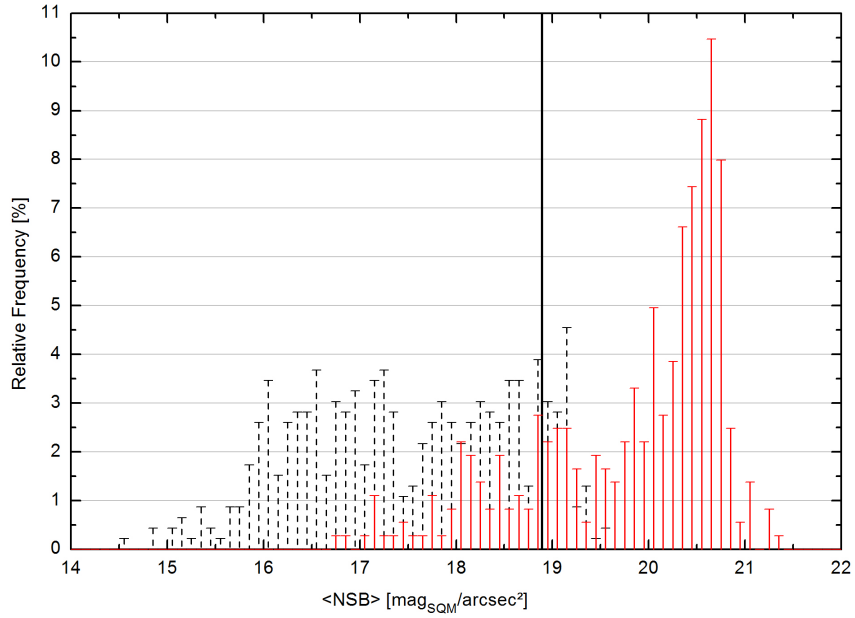


Figure 5: Distribution of the mean NSB values at IfA-Vienna (black) and at LFOA (red).

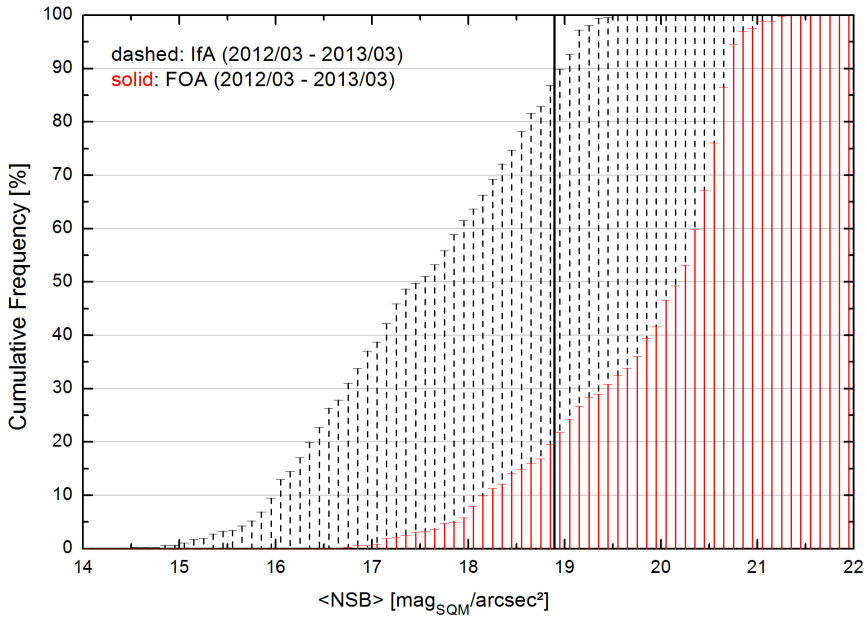


Figure 6: Same as Fig. 5, but with mean NSB values plotted cumulatively. See text for details.

On average, step C results in a night sky brightness decrease by 0.18 mag $_{SQM}$ / arcsec^2, while step F leads to a decrease (=improvement of the sky quality) by 0.09 mag $_{SQM}$ / arcsec^2.

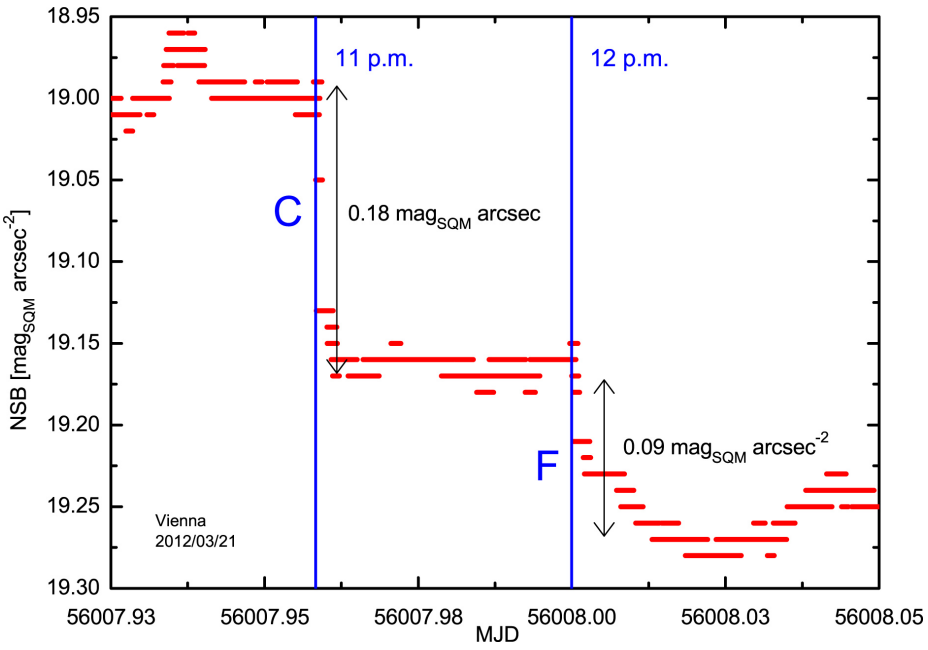


Fig. 7: Effect of the 11 p.m. curfew and of switching off many façade illuminations in the city of Vienna on the night sky brightness as detected in one of our SQM-LE light curves (from March 21st, 2012).

7 Spectral lines detected in the light-polluted night sky of Vienna

As mentioned above, we complemented our photometric observations of the night sky with spectroscopic measurements. These measurements were done with an 80 cm Cassegrain telescope in the North Dome of the IfA. Its focal length amounts to 6.7m. A spectrograph "DSS-7" produced by SBIG was attached to the telescope. DSS-7 is a grating spectrograph offering five slits with different widths, the narrowest of which provides for a dispersion of ~0.55nm/pixel, corresponding to a spectral resolving power of about 500. An ST-7 CCD camera, also made by SBIG, was connected to the spectrograph to acquire the spectra. With this camera, the wavelength coverage is approximately 450-850nm (with some small variations between the observing runs). The chip of the CCD camera was cooled down to -10°C during the observations.

To record the spectra of the night sky, the telescope at IfA was pointed to the south or to the south-east (i.e. towards the city centre of Vienna) at an elevation of ~45°. Frames of 300s integration time were obtained. All spectroscopic observations were carried out during the evening hours. Some of our night sky spectra were obtained as dedicated observations; others were extracted as a by-product of stellar spectroscopy, in which case they were subtracted as background. The 2D raw spectra were dark-subtracted and flat-fielded with dome flats (using light bulbs mounted on the telescope). To extract the 1D spectra, all pixel rows that were illuminated by the narrowest slit were summed up along the slit direction. The wavelength calibration was done using the sky emission lines themselves by adopting a second-order polynomial to map pixel positions to wavelength values.

Figure 8 shows one of several spectra that we took.

The strongest spectral line that we detected in the light-polluted night sky over Vienna peaks at 544nm. This sharp line is due to fluorescent lamps (FL), which are currently the most common type of lighting in Vienna, escpecially in residential areas. The second strongest spectral feature that we find in our night sky spectra is centered at 611 nm. Its origin is a combination of fluorescent lamps (main contribution) and high pressure sodium (HPS) lamps. The latter are used to illuminate suburban highways, crossroads and main streets.

Between these two dominating peaks, a series of lines are detected, most of which can be identified as sodium lines (the three strongest peaks are at 569 nm, 588nm and 594nm. These peaks are due to scattered light from high pressure sodium (HPS) lamps. Beyond 800nm, namely at 819nm, we detect another, very strong HPS band in the sky background. Table 2 summarizes our results on spectral lines found in the night sky of Vienna. More detailed information on the emission lines of FL and HPS lamps can be found in Elvidge et al. [4].

The fact that FL spectral lines dominate our spectra is in accordance with the fact that 79.8% of all lamps used for Vienna's public lighting are of the FL type. The second most common lamp type is HPS with a percentage of 16.2 % (these numbers refer to the year 2009, but did not change significantly since then). Note that other types of lamps (mercury vapor lamps, metal halide lamps, LEDs etc.) add up to a residual contingent of only 4%.

Table 2: Selected strong spectral lines that we detected in the night sky of Vienna.

Peak position [nm]	Assignment (see text)	Remark
544	FL	
569/588/598	HPS	
611	FL	blend with HPS
819	HPS	

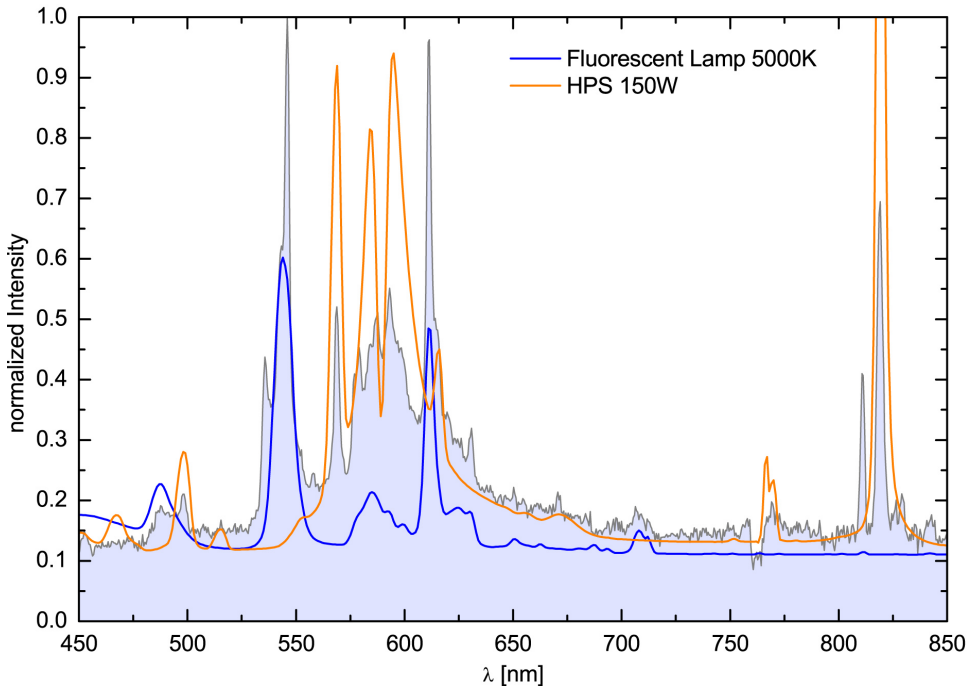


Figure 8: Spectral lines which we detected in the light-polluted night sky of Vienna with an 80cm telescope on Feb. 1st, 2012 (filled area) – and the origin of these lines (fluorescent lamps, in blue, and high pressure sodium lamps, in orange). Note that the fluorescent lamps used in the streets of Vienna actually have color temperatures < 5000K. Data from [5] have been used to produce this figure.

Acknowledgments

We thank Otto Beck, Erich Schäfer and Werner Zeilinger for their help with the installation of the SQMs in Vienna and especially at the LFOA. We gratefully acknowledge Stefan Meingast's help with the spectroscopic measurements. We also thank Gerald Pummer and Gerald Wötzl from the urban

administration, division "MA 33" for detailed information on the types of lamps currently used in Vienna and on their percentages.

References

[1] Th. Posch, A. Freyhoff, Th. Uhlmann (2010): *Das Ende der Nacht. Die globale Lichtverschmutzung und ihre Folgen* (Wiley, Weinheim).

[2] F. Patat (2008): The dancing sky: 6 years of night-sky observations at Cerro Paranal, Astron. Astrophys. **481**, 575-591.

[3] P. Cinzano, (2005): Night Sky Photometry with Sky Quality Meter, first draft, ISTIL Internal Report **9**, v. 1.4.

[4] C. D. Elvidge, D. M. Keith, B. T. Tuttle, K. E. Baugh, (2010):, Sensors **10**, 3961-3988.

[5] US Department of Commerce, NOAA, National Geophysics Data Center. Laboratory Spectra. URL: http://www.ngdc.noaa.gov/dmsp/spectra.html (last viewed 2013/03/30).

Measuring light pollution in Montsec: a protected area

Salvador J. Ribas,[1] Ramon Canal-Domingo,[1] and Catalan Light Pollution Official Service[2]

[1] *Parc Astronòmic Montsec, COU, Camí del coll d'Ares s/n, E-25691 Àger, Catalunya, Spain.*
[2] *Servei per a la Prevenció de la Contaminació Acústica i Lluminosa, Generalitat de Catalunya, Av.Diagonal 523-525, E-08029 Barcelona, Catalunya, Spain.*
tel: +34 973 455 246, e-mail: sjribas@montsec.cat

Abstract

Montsec Mountains are a special protected place in Catalonia (NE of Iberian Peninsula). Since mid-90's, this area was selected for amateur astronomers to install their astronomical observatories. In 2002 the Government of Catalonia started the project Parc Astronòmic Montsec with the aim to have two astronomical installations: one for research and the other for outreach and education. Dark skies are probably the most valuable thing in Montsec and for this reason this area is specially protected by Catalonian Laws. In 2012, Parc Astronomic Montsec and the official Catalan Service against Light Pollution have developed a measurement plan using different kind of data. The results of this study showed Montsec is one of the best places in Southern Europe with typical sky brightness better than 21.0 and in some places between 21.5 and 22.0.

1 Introduction

Montsec is a calcareous mountain range more than 40 kilometers long, covering an area of 18,696 hectares divided between Aragon and Catalonia in the North-East of Iberian Peninsula. The Catalan institutions since more than 10 years ago are working in the area to implement a regional development project, by taking advantage of its capabilities and potential helps to redirect and improve its socioeconomic situation.

Before of the 90's this area has been a reference observation point for amateur astronomers activities. In mid 90's these groups of amateur astronomers tried to promote the creation of a big astronomy project for observation and outreach. The Catalan scientist of NASA, Dr. Joan Oró, leaded the project and the Catalonian Government started the construction of Parc Astronòmic Montsec (PAM).

The PAM has two main parts: the Observatori Astronòmic del Montsec (OAdM) and the Centre d'Observació de l'Univers (COU). The OAdM is a professional observatory with an 80-cm catadioptric telescope (Joan Oró Telescope), this telescope is a robotic telescope that can be controlled from anywhere in the world via the Internet. The COU is a large multipurpose center which is intended to become an educational benchmark for teaching and communicate astronomy and other sciences in Catalonia.

Since the beginning of PAM project, Government of Catalonia starts to work in the protection of the dark sky of Montsec. Examples of this protection are the Catalonian Law (Law 6/2001), the first autonomic Law of Light Pollution in Spain, or its associate Measurement Plan (2000-2002) around Catalonia with special efforts in Montsec area. One of the topics of this Law is protect natural and astronomical sites, so the OAdM was defined as the reference point of Catalonia. Around 1600 km2 in the surroundings were established as maximum protection area.

In the last ten years, the Government of Catalonia has engaged many actions to improve Montsec night sky. One of these was the replacement of all the old lamps (white lamps) with sodium lamps of sixteen municipalities in the neighborhood of the Parc Astronòmic Montsec area. Recently the definition of reference point was changed to accept in the future the use of amber LEDs.

The Measurement Plan of the Law generates the first standard measures of Montsec sky. This old measures were made using astronomical photometry with telescope and CCD camera. The problem of this method is the large amount of time required for a 'pseudo all-sky' measure. After some years



Figure 1: Montsec night view with domes of PAM.

without new measures, in 2012 we started a new Measurement Plan with the agreement of Catalan Service against Light Pollution and Parc Astronòmic Montsec. This new measurements are made using the newest techniques available and has been used for the certification process of Montsec as Destination and Reserve Starlight. These new measures will be described in the next sections.

2 Measurement Techniques and Methodology

For this 2012 campaign we have used two main techniques, using two of the most common instruments currently available. In all the data the measures have been made under strict conditions (during astronomical night, without Moon, without clouds or fog, skipping high humidity levels or any other perturbation). We have obtained useful data of around 50 nights from February to November 2012.

SQM Photometry

We have used the most common instrument, Sky-Quality Meter (SQM) that allows us to obtain the sky brightness in magnitudes per square arcsecond (standard units in Astronomy). In our case we used SQM-LU that sends the data to a PC using USB port. In the same PC there is a GPS unit plugged and RoadRunner Software developed by Sociedad Malagueña de Astronomía. This system allows us to collect data of the sky brightness and position at the same time (see figure 2). So we can install it on a car and made moving measurements using roads and paths of the study area.

Around the methodology, we defined measurement routes that could be repeated in the future. These routes have an important coverage of the study area. We have defined 11 routes taking into account to cover the maximum area and the maximum of measurements (see figure 3)

Astronomical Photometry with ASTMON

The second method is the classical method of astronomical photometry taking as reference the magnitude of standard stars and taking measurements in the different directions of the night sky. Currently it is not necessary to use telescopes and CCD cameras, like in the 2000-2002 measurements, now we can use new systems using fisheye lens to provide easily an all-sky image.

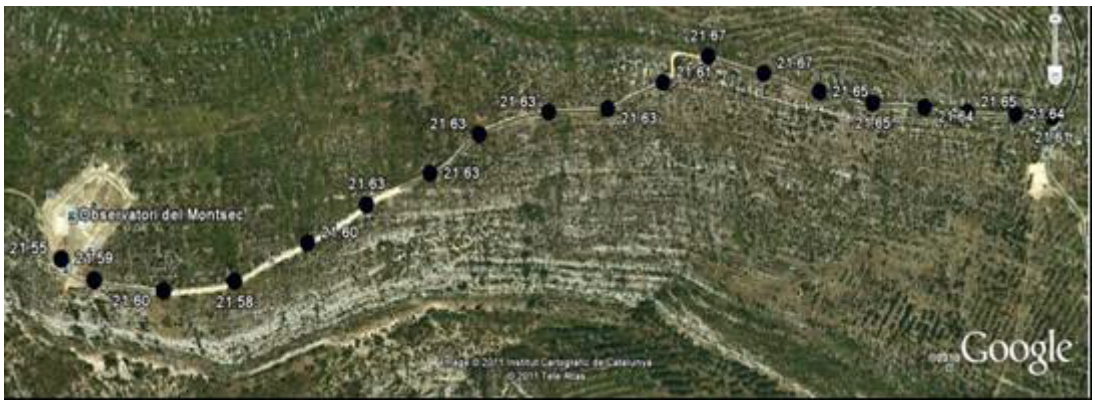


Figure 2: Example of results in a test measurement in Montsec.

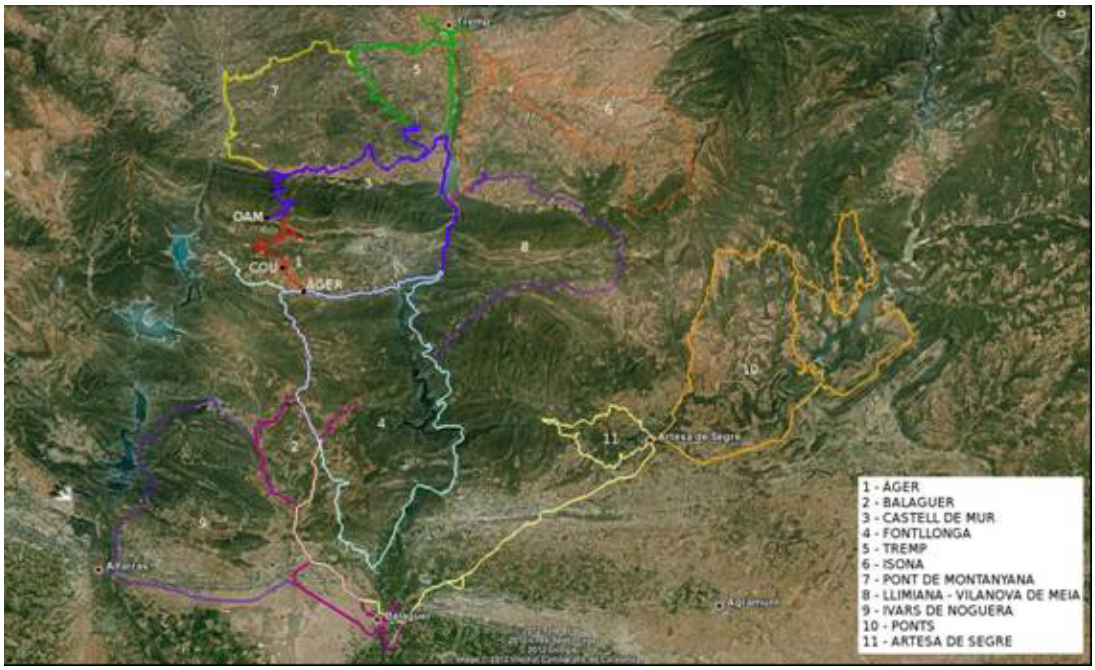


Figure 3: Map of the 11 routes defined in Montsec area.

We used an ASTMON Lite system developed by Itec Astronomica S.L. Company (http://astro-itec.com/). This is a portable version of ASTMON system installed on Calar Alto Observatory (Almeria, SPAIN) or National Park of Doñana (SPAIN). The system consists in an astronomical CCD camera with Johnson photometric filters and 8mm fisheye lens. The system is operated by a PC with specially designed software that could do the measurements and calibrations to get the all-sky map.

The methodology is more standard. Just we selected some positions of the study area and we took measures during 30-45 minutes approx. For this first campaign we selected 7 measurement sites.

Observation site	**GPS position**
A - Observatori Astronòmic del Montsec	42,050 N 0,716 E
B - Centre d'Observació de l'Univers	42,024 N 0,736 E
C - Port d'Àger	41,997 N 0,755 E
D - Balaguer	41,783 N 0,783 E
E - Isona	42,116 N 1,000 E
F - Castell de Mur	42,010 N 0,850 E
G - Alt de Fontllonga	41,950 N 0,850 E

3 Results and Conclusions

The current study allows us to test two techniques and to evaluate the status of Montsec night sky. So with this to kind of approaches we have obtained methodology results and evaluation of the sky results.



Figure 4: ASTMON Lite system.

Methodology conclusions

- SQM-Road Runner technique showed as the best option for a global study of an extended area, but it is necessary to define good route to cover it.
- The integration of SQM with GPS in a moving system give us the opportunity to take a lot of measurements and to repeat them for comparison
- It is very important to have a good knowledge of the area to prevent effects of vegetation, canyons, etc in the measures.
- ASTMON technique showed as the best for the detection of light emission areas because we obtain an all-sky map of the brightness.
- Using a fisheye lens is more efficient than the old techniques using telescopes. ASTMON give us a very accurate map in few minutes.
- Using all-sky techniques allow us to detect the emission areas and the altitude of their effect in the sky.

Evaluation of Montsec sky conclusions

- Confirm the sky of Montsec as one of the best skies in Southern Europe. Almost all the measurements outside villages are better than 21.00 mag in the zenith position.
- Detection of excellent areas with results better than 21.50 mag in the zenith. These areas are placed in the mountains and not so close to the towns and villages (see map in figure 5).

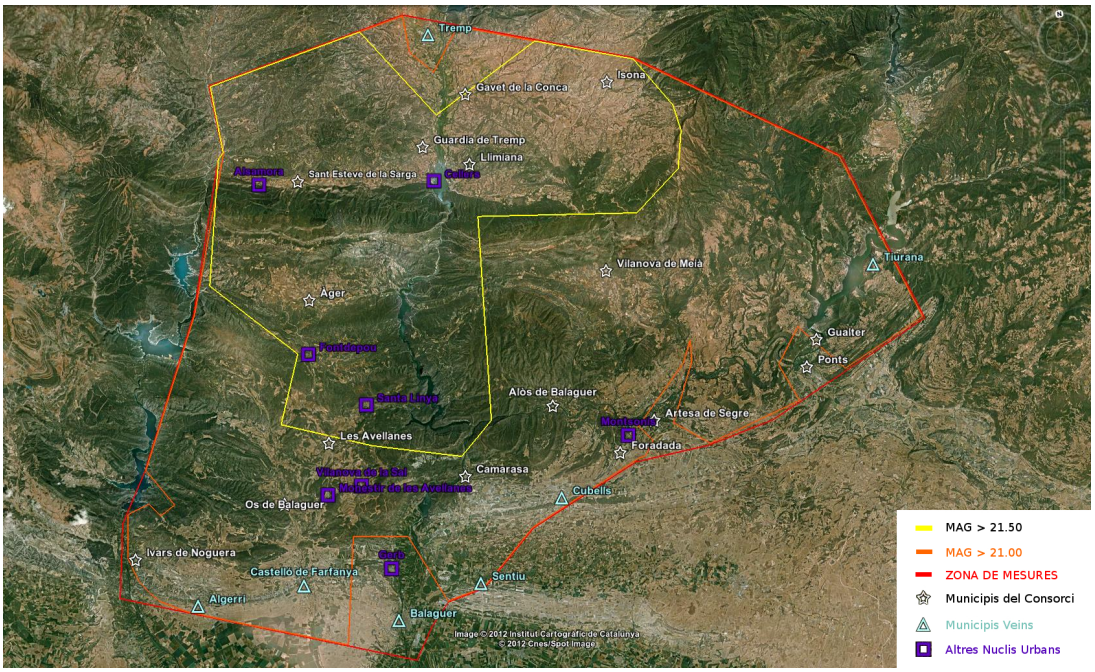


Figure 5: Map of Montsec area with the different kind of categories.

- Only few municipalities inside the area create notable light effects outside the urban area. These are Balaguer, Tremp, Ponts and Artesa de Segre, the bigger municipalities of the area.
- Direction analysis showed there are not notable influences of municipalities inside the Montsec area. Only border and external municipalities' effects have been detected.
- Large distances effects have been detected from Lleida (50km far), Barcelona and surroundings (more than 100km), Zaragoza (more than 100km) and Barbastro and Monzón (50 km). The most important effects are from Lleida. These effects have been detected in measurements made inside Balaguer city.
- The comparison of previous data showed us the central parts of the area have similar results. In some places now we obtain better results than in 2000-2002 due to the lamp replacement programs made in the last decade.

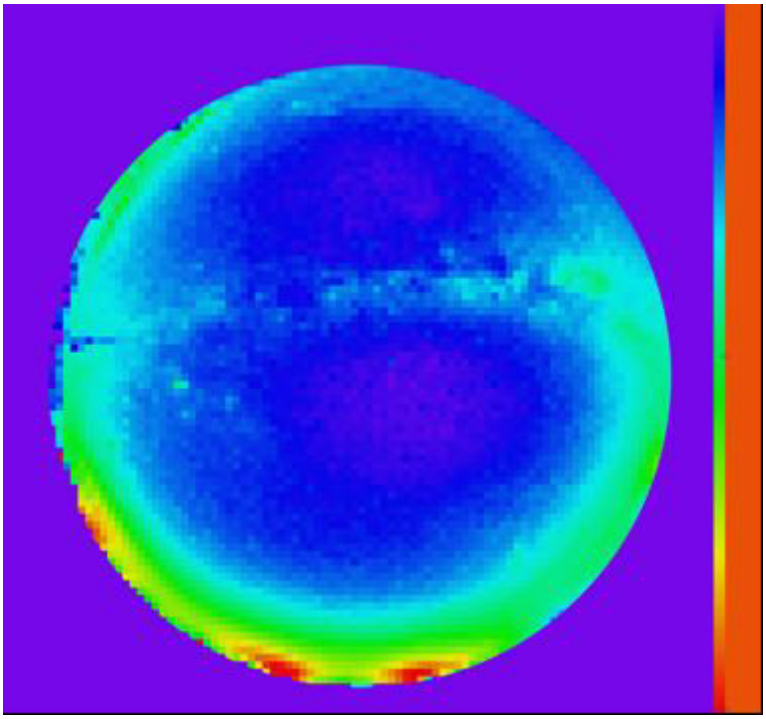


Figure 6: All-sky map obtained from Observatori Astronòmic del Montsec. The red spots in the lower part are Balaguer and Lleida. In the left there is the effect of Barcelona.

Acknowledgments

All the data are property of Servei per la Prevenció de la Contaminació Acústica i Lluminosa of Government of Catalonia.

Impact of light pollution before and after the creation of the first International Dark Sky Reserve, OMM, Quebec, Canada

Johanne Roby[1] and Martin Aubé[1]

[1] *Cégep de Sherbrooke, Sherbrooke J1E 4K1, Canada*
tel: +819-564-6350 poste:4118, e-mail: johanne.roby@cegepsherbrooke.qc.ca

Abstract

We used the ILLUMINA model to investigate the impact of light pollution on sky brightness before and after the establishment of the International Dark Sky Reserve (IDSR) at the Mt Megantic Observatory (MMO, located in Quebec, Canada).

1 Introduction

The light pollution shall be defined as any artificial light source in our environment. It causes bright haloes, harmful for sky observation. Night sky has been altered by the presence of light ever since humans invented outdoor lighting. It is now known as an occurrence of abnormal presence of light during the night and is due to human activities, mainly because of street lamps, advertising panels and lighted buildings. This kind of light affects fauna, flora and human health and are now well-documented. For example, recent studies have shown a significant correlation between artificial light at night and many diseases such as breast cancer [1], as well as obesity [2] and depression [3].

The streetlight has been identified as the primary source of brightness at night and light pollution could be reduced by improving the streetlamps performance. The transition from the Cobrahead model to the Helios model reduces the luminous flux to 1% above the horizon (5 % decreases). In 2007, the establishment of the International Dark Sky Reserve (IDSR [4]) at the Mt Megantic Observatory (MMO, located in Quebec, Canada) allowed to take a significant step forward in this direction by replacing all the street light within a 25 km radius of the observatory by the Helios model, reducing, at the same time, their brightness by almost half.

The research project is designed to point up the current incidence of light pollution, including the second order scattering, in the surrounding area of the MMO.

This will allow us to target the critical zones in term of sensitivity and contribution to sky brightness , then, to measure the impact of the IDSR creation by comparing the data of 2005 (before the creation of the IDSR) and those of 2009 (after the creation of the IDSR).

2 Results

In this paper, we will present how different parameters of light fixtures, urban and countryside environment, wavelength and atmospheric content may influence the level of light pollution as a function of the viewing angle before and after the creation of the IDSR. Sensitivity and contribution maps produced by the ILLUMINA model [5], allow us to represent as faithfully as possible the phenomenon of sky brightness detected from a standing point, which is in our case the MMO. The contribution maps illustrate how each km^2 of the region contributes to the sky brigtness detected at various viewing angles from MMO, according to a scale of relative importance. Furthermore, the sensitivity maps point up the impact of a typical streetlamp on sky brighness measured at the MMO, and this for each km^2 surrounding the observatory.

Contribution and sensitivity maps are then georeferenced and published in a web portal maintained by our group [6], so that it becomes easy to associate these observations with specific point on the ground. We are then able to know the places that are most damaging in terms of sky brightness. Our results are eventually designed to strategically minimize the impact of light pollution on the MMO astronomical activities and to efficiently control the addition of new streetlamps in the surroundings.

3 Conclusion

This study aim to provide some guidelines to help authorities to manage their lighting infrastructure in a way to reduce light pollution and its adverse effects.

Our experiment show that replacing all the street light within a 25 km radius around the observatory with Helios model and reducing to the half the installed luminous flux is a very efficient way to reduce sky brightness. Our results also highlight critical zones where any change in the lighting infrastructure has the more important impact on sky brightness at MMO. The results is now shared with MMO officials and used as a tool to improve sky quality at the observatory.

References

[1] I. Kloog, A. Haim, R. Stevens, M. Barchana, B. Portnov (2008): Light at Night Co-distribute with incident Breast but not Lung Cancer in the Female Population in Israël. Chronobiology International, 25(1): 65–81.

[2] L. K. Fonken, J. L. Workman, J. C. Walton, Z. M. Weil, J. S. Morris, A. Haim, R. J. Nelson (2010): Light at night increases body mass by shifting the time of food intake. Proc Natl Acad Sci U S A., 107:18664–9.

[3] T. A Bedrosian, Z. M. Weil, R. J. Nelson (2012): Chronic dim light at night provokes reversible depression-like phenotype: possible role for TNF, Molecular Psychiatry, doi:10.1038/mp.2012 .96.

[4] IDSR at MMO: http://www.astrolab-parc-national-mont-megantic.org/en/mt_megantic_international_dark_sky_reserve_idsr.what_is_an_idsr.htm

[5] M. Aubé, L. Franchomme-Fossé, P. Robert-Staehler (2005): Light Pollution Modelling and Detection in a Heterogeneous Environment: Toward at Night Time Aerosol Optical Depth Retriaval Method, SPIE'S Annual Meeting Proceedings, San Diego, CA (paper 5890-40, 1.1 Mb); M. Aubé (2010) Heterogeneous modeling of artificial sky luminance: http://www.cegep sherbrooke.qc.ca/~aubema/index.php/Prof/IllumEn

[6] Light Pollution Data Server: http://galileo.graphycs.cegepsherbrooke.qc.ca/lpds/index.php?n=Site.Products).

Evolution of the energy consumed by street lighting in Spain estimated with DMSP-OLS data

Alejandro Sánchez de Miguel[1], Jaime Zamorano[1], José Gómez Castaño[1], Sergio Pascual[1]

[1] *Dep. Astrofísica y CC. de la Atmósfera . Universidad Complutense de Madrid, Avd. Complutense s/n, Madrid, 28040 Spain*

tel: +34 91 394 52 38, fax: +34 91 394 4635, e-mail: alejasan@ucm.es

Abstract

We present the results of the analysis of satellite imagery to study light pollution in Spain. Both calibrated and non-calibrated DMSP-OLS images have been used. We describe the method to scale the uncalibrated DMSP-OLS images that allows us to use differential photometry techniques in order to study the evolution of the light pollution. Population data and DMSP-OLS satellite calibrated images for year 2006 have been compared to test the reliability of official statistics in public lighting consumption. We have found a relationship between population and consumed energy that is valid for several regions. Finally the real evolution of electricity consumption for street lighting in Spain from 1992 to 2010 have been derived. This calibration and our method might be used to estimate the evolution of the public lighting consumption around the world.

1 Introduction

Satellite images taken during the night have changed our image of the Earth and they are now one of the most efficient tools in the fight against light pollution. Many studies on the relationship between the amount of light registered by satellites, as DMSP with OLS, with parameters as population density and distribution, power consumption, and economic activities, to name but a few, have been published ([10][11][12][13][14][15], [37], [23]).

The relationship of this emission with light pollution is treated by Cinzano et al. [3][4][5][6][7][8]. The main contributor to light pollution is the public street lighting ([14], [22], [16]). This is why our group has been working during the last years with the aim of finding a procedure to estimate energy power consumption in public electric lighting using both statistics and satellite data ([25],[26],[27],[28],[29], [30]). This paper summarizes these works. We describe our method and results for Spain. Our final goal is to determine and compare energy efficiency for states of the European Union (EU) first and for the rest of the planet in a second phase. When color data of the light is available (with spectral data or at least with several photometric bands), information of the emitting sources can be obtained and that's necessary to have more accurate information about the real energy consumption and efficiency ([14],[18]).

Our method is based on empirical calibration of satellite data using statistics on power consumption. Total power consumption is ready available but the budget on electric power for public lighting is hard to find. We've only been able to access to VITO report ([32]), some sparse data for Italy ([24]), and official data from Spanish Ministry of Industry. With the Spanish data we calibrate the DMSP/OLS images and we estimate the evolution in power consumption for Spanish provinces, obtaining promising results that validate our method.

2 Data

2.1 DMPS/OLS images:

Our main source of satellite data is the radiance calibrated DMSP/OLS images corresponding to 1996-1997 ([13]) and 2006 ([36]), no calibrated DMSP/OLS images of 1992-2010 ([10], [13], [15] & [1]). Our future work will include data from Suomi NPP/VIIRS. All these data are provided by the Earth

Observation Group, NOAA National Geophysical Data Center. An additional source of information are the nocturnal pictures taken by astronauts aboard the International Space Station (ISS). These images taken with digital cameras have three color channels and they can be calibrated ([34], [30]). The data extraction was performed using GIS techniques, unlike in [29], where it was performed a manual extraction.

2.2 Available statistics data:

The Spanish Ministry of Industry, Energy and Tourism webpage publishes annual reports ("Estadísticas Eléctricas Anuales")[1] that provide information for each activity sector. National data from 1958 to 2007 are available, while they provide information for each Spanish province from 1975. As we have already shown in previous works, there are some discrepancies between official data and real power consumption (see figure 6 of [26]). Some provinces show weird decreasing values between 1985 y 1992 and the national power consumption seems to be stabilized before an increase from 1992 on. Using official data from the book "La Energía en España 2004"[2] and information for the years 1936 to 1957 collected at the Instituto Nacional de Estadística (INE) we rebuild the real evolution of electric power consumption in public lighting for Spain[27]. It has been done an exhaustive analysis of the statistics to find the source of those errors. The official data provided by the Spanish Ministry are already corrected of this error only for the year 2007 and so are some small provinces for all the years as it is easy to see in figure 10.

A test has been done to the official correction of the data. We performed a comparison between energy consumption and the cumulative radiance for 2007 following the prescriptions of [13]. We show in Figure 1 the goodness of the linear fit (R^2 =0.93).

Some provinces that do not follow the relationship of Figure 1 are also outliers in Figure 2. It seems that they have an excess of the measured flux from satellite or in power consumption. Probably the statistics for these provinces are not accurate.

The most populated provinces (Madrid, Barcelona o Valencia) have additional data available. For the region of Madrid we have analyzed the statistics for Comunidad de Madrid[3] (the whole region) and Madrid city[4]. We have been able to rebuild the real evolution of power consumption (see Figure

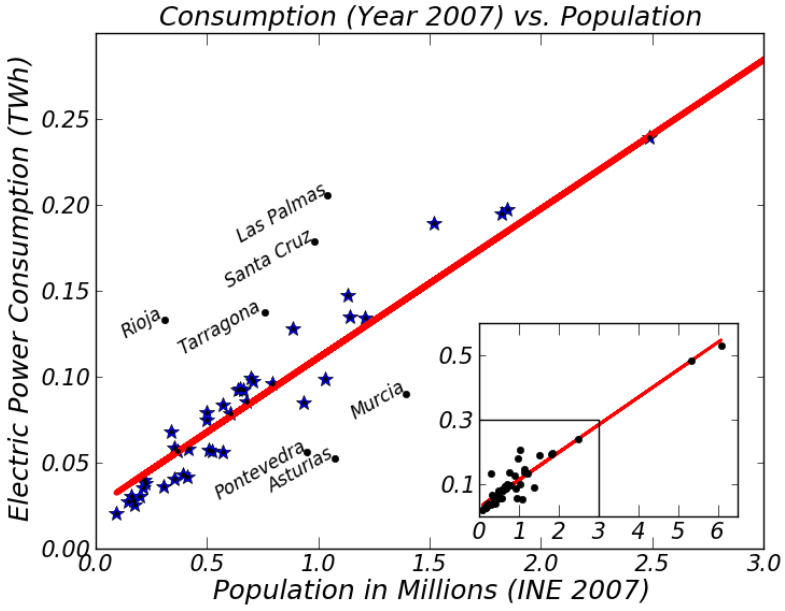


Figure 1: Power consumption in street lighting versus population.

[1] http://www.minetur.gob.es/energia/balances/Publicaciones/ElectricasAnuales/Paginas/ElectricasAnuales.aspx
[2] http://www.minetur.gob.es/energia/balances/Balances/LibrosEnergia/Energia_2004.pdf
[3] http://www.madrid.org/iestadis/fijas/estructu/general/anuario/descarga/anu12-2-3.xls
[4] http://www-2.munimadrid.es/CSE6/jsps/menuBancoDatos.jsp

3) using all the available data on 'official lighting', 'public lighting' and 'other types of lighting' and taking into account the different administration rules to archive power consumption data. The statistics for Madrid region (Ministry data) only includes power consumption for Comunidad de Madrid between 1986 and 2005 and not that corresponding to Madrid City. Data for Madrid city is divided in neighborhoods, lamp types and number of luminaries since the year 1975.

3 DMSP-OLS visible sources

Official statistics show that the electric power consumption increases in a monotone way. We expect that light emission vary in the same way. Most of the sources detected from space in the 0.3-0.9 microns range are public street lighting. Other sources of light are: (1) Ornamental or security lights (city centers, monuments, airports, open-air mineral extractions) and (2) Oil extractions and fires.

Light sources for group (1) are metal-halide lamps in Spain and they are easily found in DMSP/OLS images mainly in the city centers. They are usually excluded from statistics, as they appear saturated and their contribution varies during the night (Sánchez de Miguel in prep.).

Light sources of group (2) are also out of the official statistics but being no stable, they are not present in the final calibrated satellite DMSP/OLS images ([12]). They present spectra of black bodies of different temperatures.

4 Electric power consumption using satellite images.

4.1 Empical calibration using radiance calibrated satellite images.

We have obtained the cumulative radiance for the Spanish provinces following the methodology described by [13]. To compare with power consumption, we do not use total consumption but public street lighting, more related to the light emission detected by DMSP satellite. It should be ware in mind that the amount of light also depends on many other parameters as ground reflectivity, lamp efficiency, street design to name but a few. We have already shown in Figure 2 the relationship even using the no calibrated image.

The relationship between power consumption in street lighting and calibrated cumulative radiance is plotted in Figure 4. To reject outliers we use a roboust linear fit as explained in [33]. Next fit is

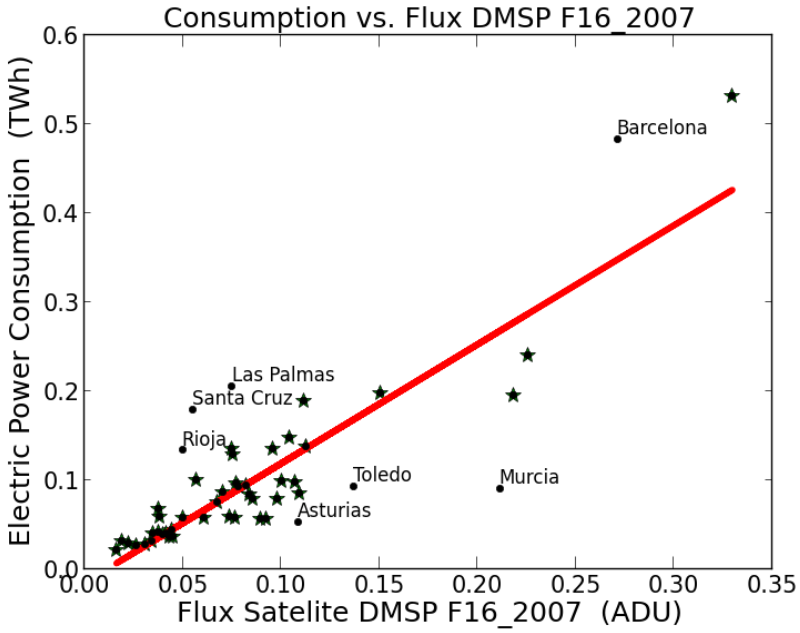


Figure 2: Electric Power Consumption in street lighting versus Flux F16_2007. Madrid and Barcelona, top right, are clearly saturated.

potencial log10(y) = m log10(x) + c.

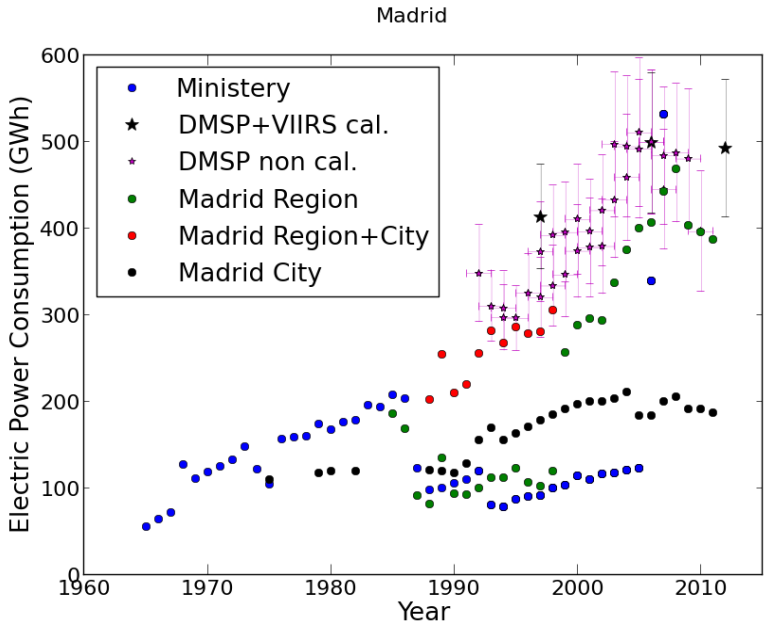


Figure 3: Madrid region electric power consumption for street lighting. In blue, the ministry data, in green, Comunidad de Madrid data, in black Madrid city data. In red, Comunidad de Madrid plus Madrid city between 1986 and 1999. Black stars, estimated consumption using radiance calibrated data, DMSP 1997, DMSP 2006 and testing 2012 VIIRS.

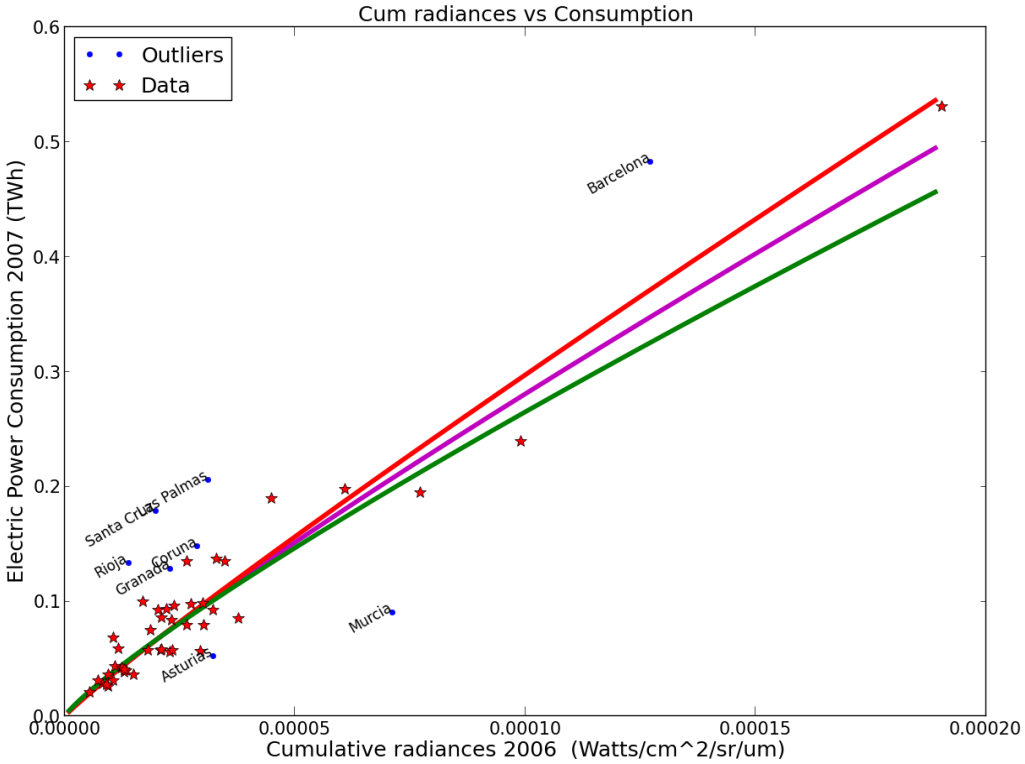


Figure 4: Fit to the power consumption in street lighting to cumulative radiances. Potencial fit to the data is shown in magenta.

To compare with previous pioneering works in this field we represent in Figure 5 our data with that of USA states from [13]. Power consumption for USA states has been divided by 100 to estimate

consumption in public lighting (around 1%) and a continuous line is obtained. Area correction (see [15], [19]) is not needed in this case as the differences for Iberian Peninsula are less than 10% and the latitude is similar to USA.

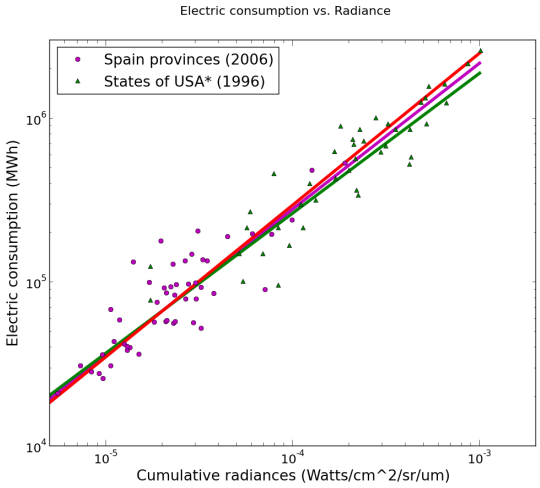


Figure 5: Comparison between the total power consumption in Elvidge et al. 1999 divided by factor 100, and the street light power consumption in Spain. The same lines as in fig. 4.

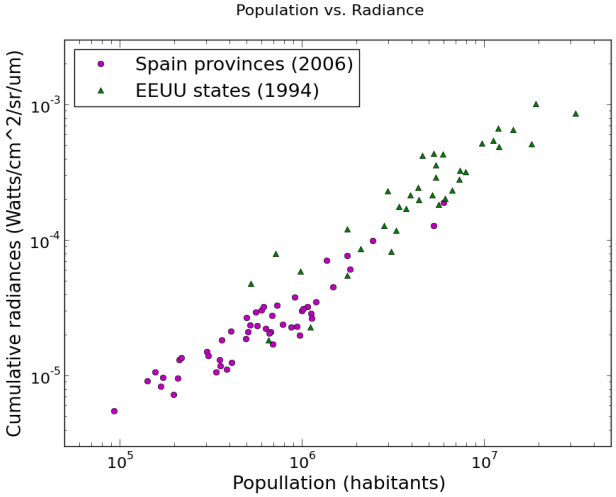


Figure 6: Population versus Cumulative radiance. USA by Elvidge et al. 1999, Spain this work.

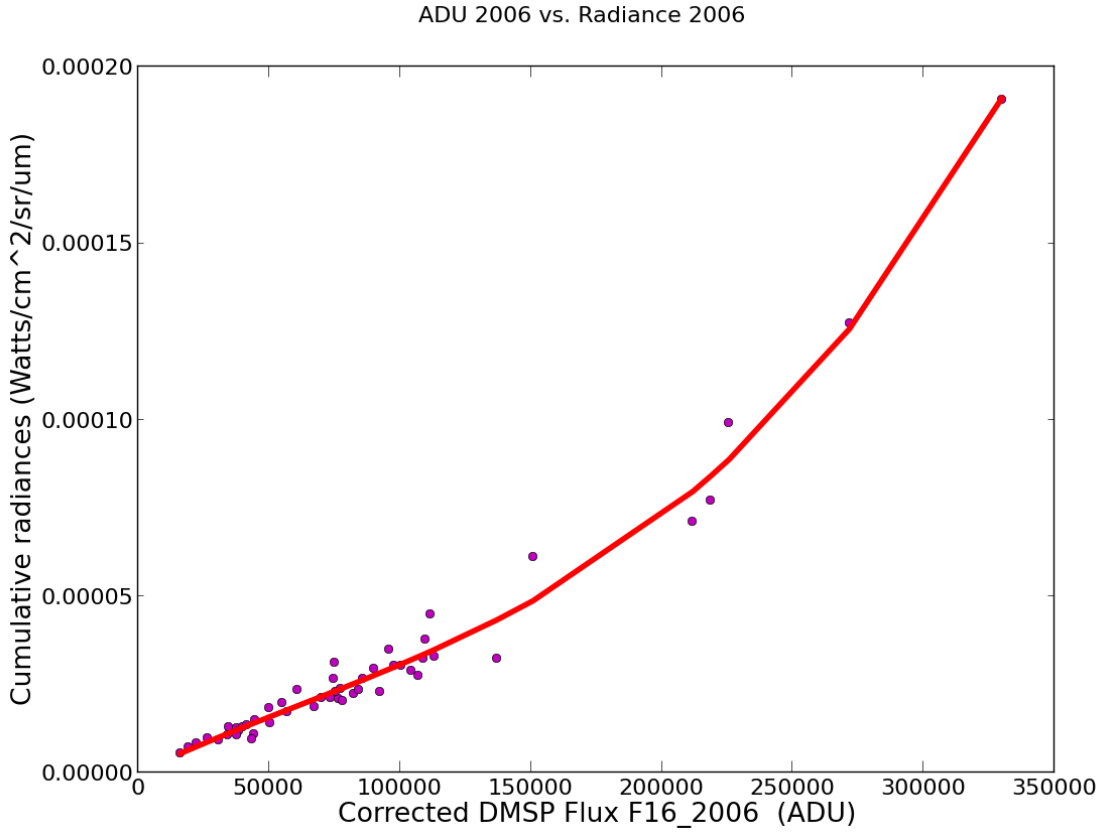


Figure 7: Relationship between the non-calibrated F16_2006 and the calibrated for Spanish provinces. Red line is a polynomial fit of order 4.

4.2 Crosscalibration of DMSP/OLS satellites

Radiance calibrated data is the key ingredient to study the evolution of electric power consumption in public lighting from satellite data. Some efforts have been made in the past to cross-calibrate DMSP/OLS data since there is an evident relationship between calibrated and non calibrated images as shown for instance by [13]. Our strategy consists in using data for Spanish provinces where there are almost no light sources of group (2) but many of group (1), mainly in the city centers. It is interesting to note that ornamental lights are variable (they are switched off during the night) and they appear with half the flux in DMSP/OLS images[1]. Pictures taken by astronauts from ISS show clearly this effect when images at different hours during the night are compared.

A polynomial fit of 4th order is enough to fit the cumulative radiances for Spanish provinces using calibrated data [36] and the flux in ADU of DMSP/OLS F16_2006 (see Figure 7). Elvidge et. al. 1999[13] explains how darker zones appear brighter due the diffuse lighting that originates in bright and saturated areas. We are working on this problem using nocturnal ISS pictures taken in HDR mode with increasing exposure times. It seems that this effect is real and not an artifact or instrumental problem ([34], [30], [31]).

There are systematic differences between DMSP satellites and over the years as shown by many authors (see Figure 14 of Falchi 2005 at [7], [15], [19], [23]). This is why it is not straightforward to apply this fit to all the satellite data. To sort this problem out, [15] analyses one region point by point. But there are differences between regions and we prefer to assume, as a first step, that there is a calibration for each region. If the results are consistent, the calibration could be used for any region in the world.

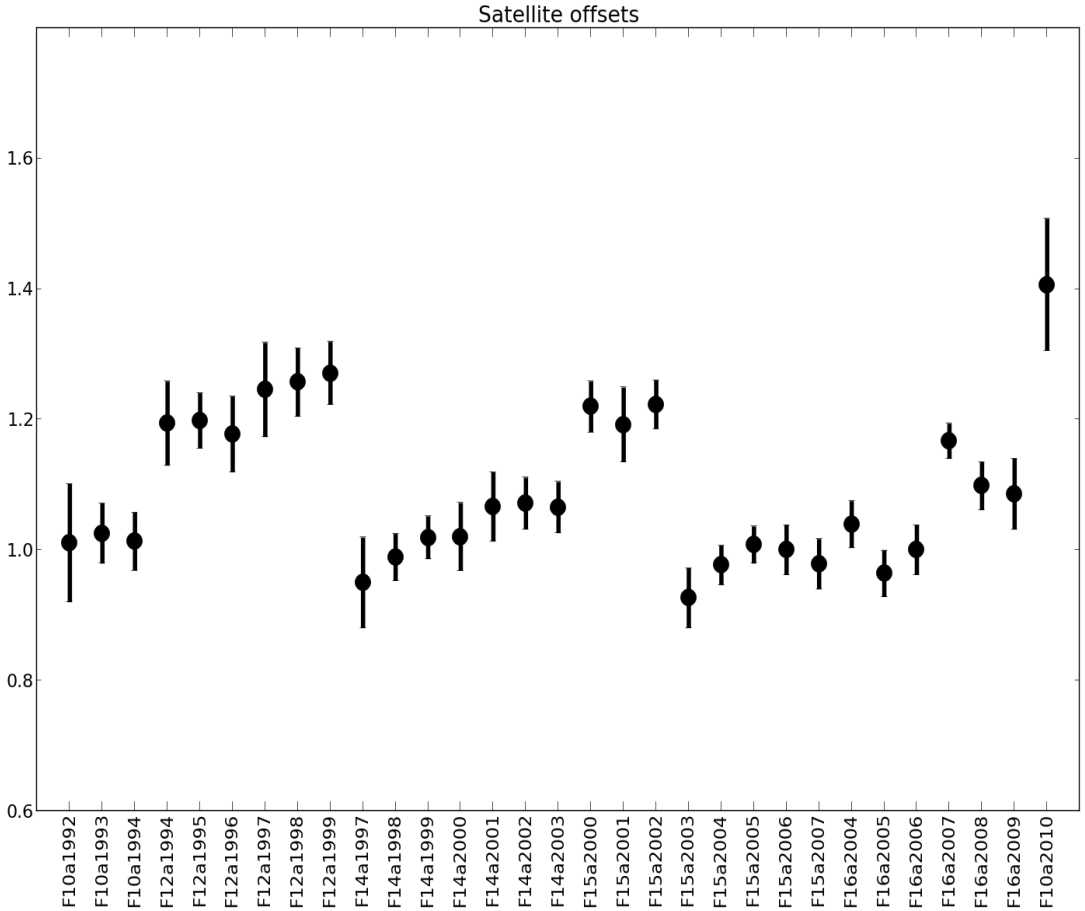


Figure 8: Offset between images and satellites. The F16_2006 has been set as reference. The error bar indicates the standard variation of the relative values of each region to the expected using the interpolation of DMSP calibrated images 1996-1997 and 2006.

Assuming a smooth evolution in light emission to the space, we use a linear fit to calibrated data for F12_1997 & F16_2006 and obtain a first estimate of the expected values for cumulative radiances for the years between 1992 y 2010 for each of the regions (up to 50 Spanish provinces). The residuals show the offset for each satellite/year with different dispersions that we consider a random error in flux. Thus we take F16_2006 as reference and use the mean values of these offsets to correct all the satellite data. The estimated cumulative radiance for each region is obtained using this empirical calibration on the non calibrated data. This procedure reduces data dispersion while keeping the evolution of each region.

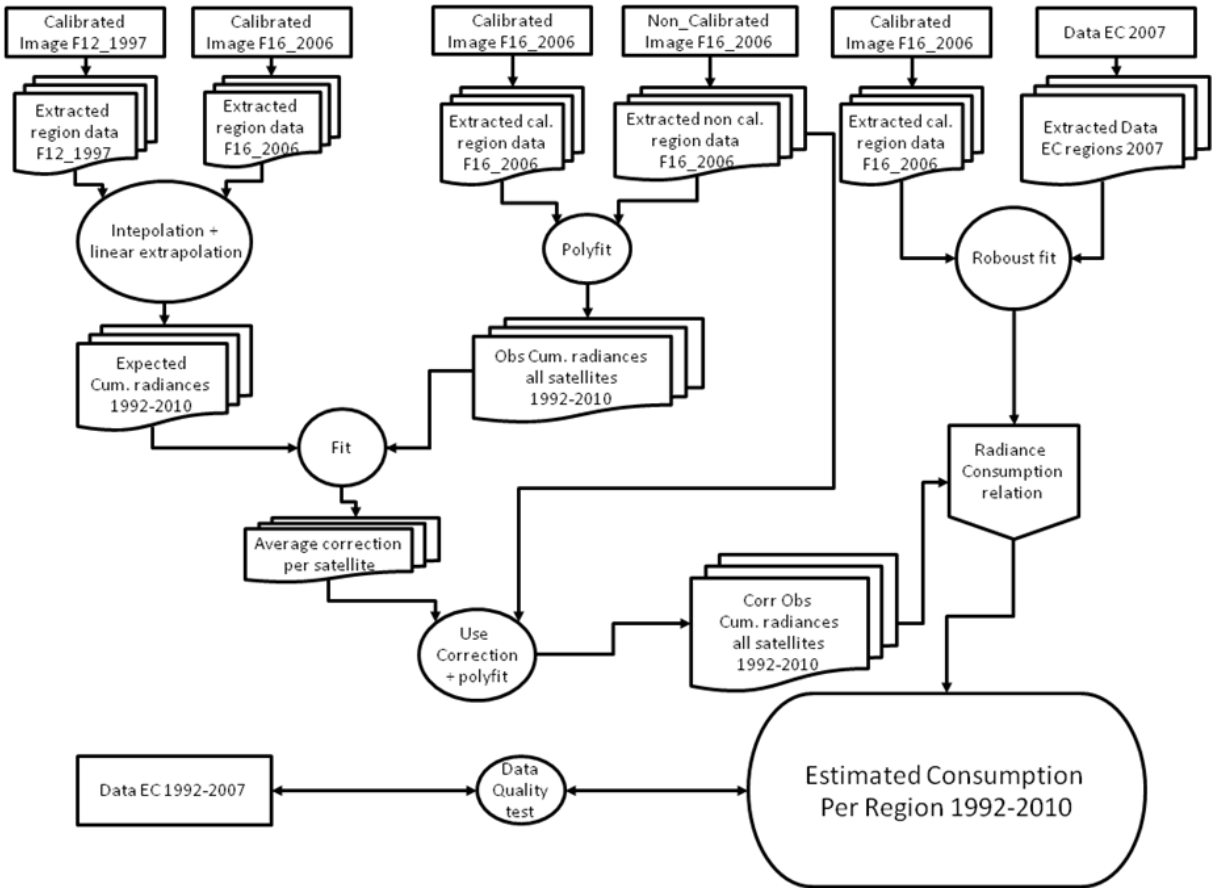


Figure 9: Calibration procedure.

4.3 Calibration of Electric power consumption in public lighting versus cumulative radiances

The quality of our empirical calibration could be tested by comparing the evolution of cumulative radiances for the region studied with the statistics in electric power consumption in public lighting as explained above. The panels of figure 10 show the plot for each one of the Spanish provinces.

The results are extremely good for the less populated provinces (i.e., Ávila, Cantabria, Burgos, Huesca, Soria, …) whose official statistics seems to be accurate. The inconsistencies found for the most populated provinces, where only for the last years power consumption is similar to that expected from satellite data) are due to the change in electric lighting statistics that was mentioned above for the case of Madrid.

For some provinces it seems that the evolution is recovered but with an offset. The differences could be due to poor empirical calibration but other explanations are possible as the fail to include some cities in the total power consumption statistics or the use of luminaries of different efficiencies.

We are working on a detailed study for the region of Madrid, where detailed official statistics data is available, using RGB color data from ISS nocturnal pictures, SUOMI-NPP/VIIRS and DMPS-OLS.

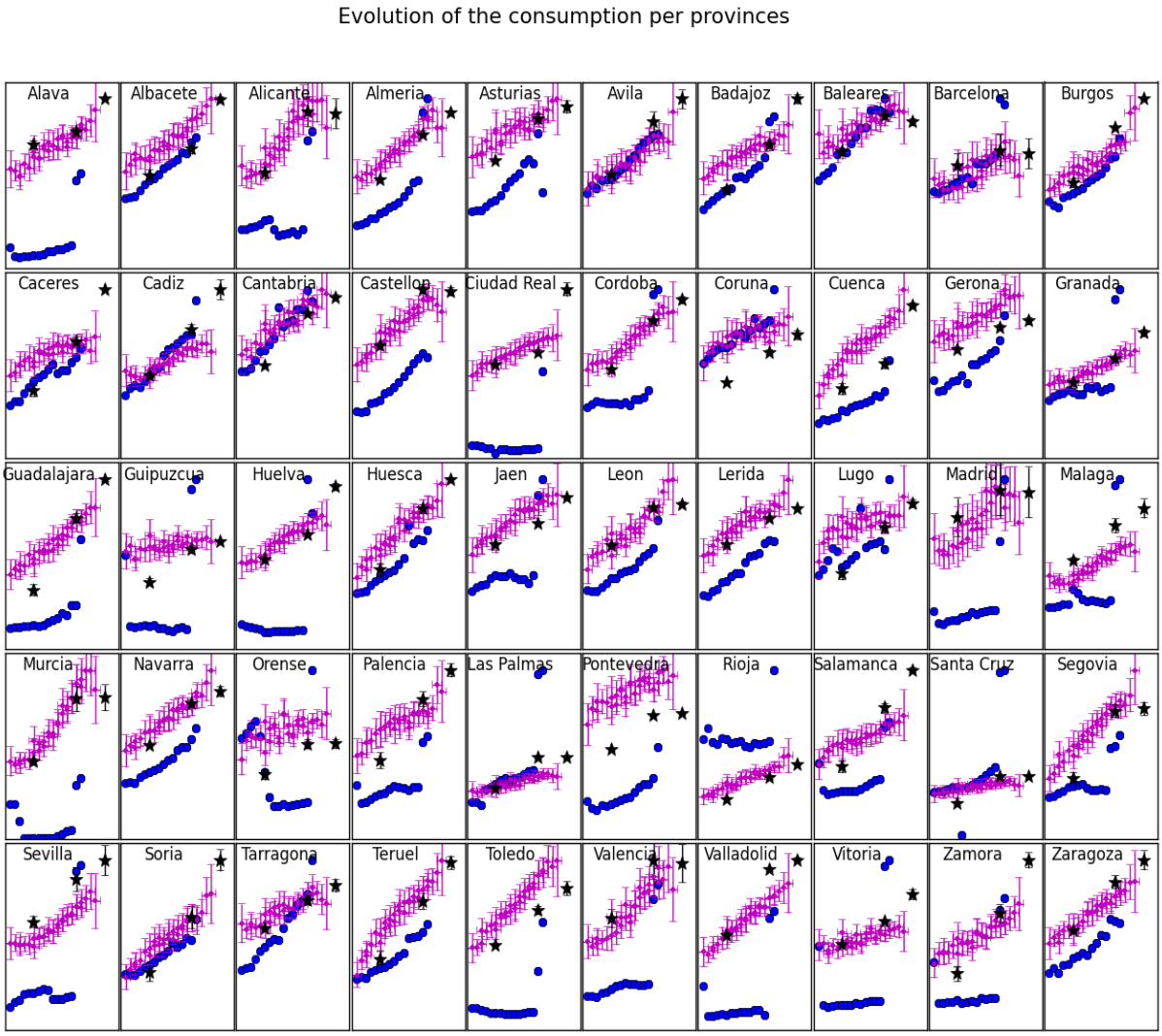


Figure 10: Evolution of the power consumption in street lighting. In blue dots, the official data. Pink dots, non-calibrated data. Black stars, calibrated data, 1996-1997 DMSP-OLS, 2006 DMSP-OLS and testing 2012 SUOMI-NPP/VIIRS. The black stars error bars have been calculated using the 90% confidence fit to the Power consumption vs radiance fit. The magenta error bars have been calculated using the satellite dispersion correction and the 90% confidence fit to the power consumption vs radiance fit.

5 Conclusions and results

We show how power consumption data agree with calibrated and uncalibrated radiance images. There is still great uncertainty for high radiance regions where there are many sources of error and they cannot be considered as stable sources. In spite of this, and the fact that these regions are saturated in uncalibrated images, they can be measured thanks to their contribution to diffuse light. The effect of projection has not been taken into account to make a correction on the area represented by each pixel in order to compare with the work of [13]. But an analysis is underway for Europe considering this effect without movintg the information as in [2] but using reprojection[15]. Most populated provinces

appear to start to stabilize the growth of spending on public lighting. However this does not happen in the smaller provinces that keep on growing at a similar rate in spite of the economic crisis.

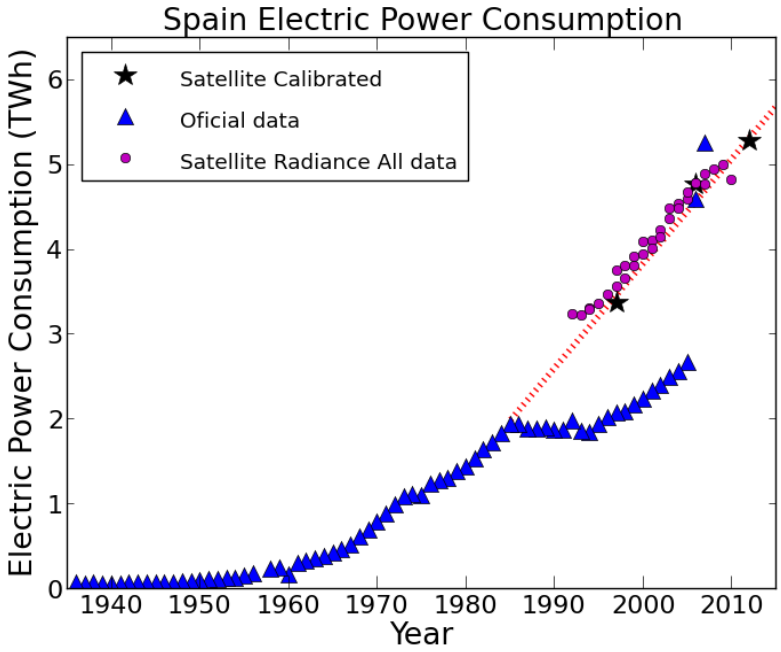


Figure 11: Evolution of the power consumption in street lighting in Spain. Official data, blue triangles. Pink dots, non-calibrated data DMSP. Black stars, 1996-1997 DMSP, 2006 DMSP, testing VIIRS.

Acknowledgments

This work has been partially funded by the Spanish MICINN (AYA2009-10368), by the Spanish programme of International Campus of Excellence Moncloa (CEI) and by the Madrid Regional Government through the AstroMadrid Project (CAM S2009/ESP-1496, http://www.laeff.cab.inta-csic.es/projects/astromadrid/main/index.php). Thanks also to Francisco Ocaña for the critical review of this text.

References

[1] K. Baugh, C. Elvidge, T. Ghosh, D. Ziskin (2011): Development of a 2009 Stable Lights Product using DMSPOLS data. Proceedings of the Asia Pacific Advanced Network.

[2] N. Cardiel,; J. Gorgas, J. Gallego, A. Serrano, J. Zamorano, M. García-Vargas, P. Gómez-Cambronero, J. M. Filgueira (2002): Proper handling of random errors and distortions in astronomical data analysis, Astronomical Data Analysis II. Edited by Starck, Jean-Luc; Murtagh, Fionn D. Proceedings of the SPIE, Volume 4847, pp. 297-304.

[3] P. Cinzano (2000): The growth of light pollution in north-eastern Italy from 1960 to 1995. Memorie della Società astronomica italiana, 71, 159.

[4] P. Cinzano, F. Falchi, C. D. Elvidge (2002): Naked-eye star visibility and limiting magnitude mapped from DMSP-OLS satellite data. Monthly Notices of the Royal Astronomical Society, 323(1), 34-46.

[5] P. Cinzano, F. Falchi, C. D. Elvidge (2002): The first world atlas of the artificial night sky brightness. Monthly Notices of the Royal Astronomical Society, 328(3), 689-707.

[6] P. Cinzano, F. Falchi, C. D. Elvidge, K. E. Baugh (2003): The artificial night sky brightness mapped from DMSP satellite Operational Linescan System measurements. Monthly Notices of the Royal Astronomical Society,318(3), 641-657.

[7] P. Cinzano, F. Falchi, C. D. Elvidge (2007): Recent progress on a second world atlas of the night-sky brightness, World Conference in Defence of the Night Sky and the Right to Observe the Stars, 20-23 april 2007, La Palma.

[8] P. Cinzano, F. Falchi (2012) : The propagation of light pollution in the atmosphere. arXiv preprint arXiv:1209.2031.

[9] C. Elvidge, D. Pettit, M. Imhoff, R. Nemani, D. Pack, P. Cinzano (2008, August): Observational considerations for moderate resolution nighttime lights. In Optical Engineering+ Applications (pp. 70810V-70810V). International Society for Optics and Photonics.

[10] C. D. Elvidge, K. E. Baugh, E. A. Kihn, H. W. Kroehl, E. R. Davis (1997): Mapping city lights with nighttime data from the DMSP Operational Linescan System. Photogrammetric Engineering and Remote Sensing, 63(6), 727-734.

[11] C. Elvidge, K. Baugh, V. Hobson, E. Kihn, H. Kroehl, E. Davis, D. Cocero (1997): Satellite inventory of human settlements using nocturnal radiation emissions: a contribution for the global toolchest. Global Change Biology, 3(5), 387-395.

[12] C. D. Elvidge, K. E. Baugh, E. A. Kihn, H. W. Kroehl, E. R. Davis, C. W. Davis (1997): Relation between satellite observed visible-near infrared emissions, population, economic activity and electric power consumption.International Journal of Remote Sensing, 18(6), 1373-1379.

[13] C. D. Elvidge, K. E. Baugh, J. B. Dietz, T. Bland, P. C. Sutton, H. W. Kroehl (1999): Radiance calibration of DMSP-OLS low-light imaging data of human settlements. Remote Sensing of Environment, 68(1), 77-88.

[14] C. D. Elvidge, P. Cinzano, D. R. Pettit, J. Arvesen, P. Sutton, C. Small, R. Nemani, T. Longcore, C. Rich, J. Safran, J. Weeks, S. Ebener (2007): The Nightsat mission concept. International Journal of Remote Sensing, 28(12), 2645-2670.

[15] C. D. Elvidge, D. Ziskin, K. E. Baugh, B. T. Tuttle, T. Ghosh, D. W. Pack, E. H. Erwin, M. Zhizhin (2009): A Fifteen Year Record of Global Natural Gas Flaring Derived from Satellite Data, Energies 2009, 2, 595-622; doi:10.3390/en20300595.

[16] T. Gallaway, R. N. Olsen, D. M. Mitchell (2010): The economics of global light pollution. Ecological Economics, 69(3), 658-665.

[17] C. Marín, J. Jafari, G. Orlando, J. A. Belmonte, L. C. Hernández, F. J. D. Castro, F. J. D., ... S. L. Tenydea, www. starlight2007. Net.

[18] J. P. Metcalf (2012): Detecting and Characterizing nighttime lighting using multispectral and hyperspectral imaging, Thesis, Naval Postgraduate school, Monterrey California, December 2012. http://calhoun.nps.edu/public/handle/10945/27869

[19] H. Letu, M. Hara, H. Yagi, K. Naoki, G. Tana, F. Nishio, O. Shuhiei (2010): Estimating energy consumption from night-time DMPS/OLS imagery after correcting for saturation effects, International Journal of Remote Sensing Vol. 31, No. 16, 20 August 2010, 4443–4458

[20] M. L. Imhoff, W. T. Lawrence, C. D. Elvidge, T. Paul, E. Levine, M. V. Privalsky, V. Brown (1997): Using nighttime DMSP/OLS images of city lights to estimate the impact of urban land use on soil resources in the United States.Remote Sensing of Environment, 59(1), 105-117.

[21] A. Jehl, T. Farges E. Blanc (2013) : Color pictures of sprites from non-dedicated observation on board the International Space Station. Journal of Geophysical Research: Space Physics.

[22] H. U. Kuechly, C. Kyba, T. Ruhtz, C. Lindemann, C. Wolter, J. Fischer, F. Hölker (2012): Aerial survey and spatial analysis of sources of light pollution in Berlin, Germany. Remote Sensing of Environment, 126, 39-50.

[23] B. Pandey, P. K. Joshi, K. C. Seto (2013): Monitoring urbanization dynamics in India using DMSP/OLS night time lights and SPOT-VGT data, International Journal of Applied Earth Observation and Geoinformation 23 (2013) 49–61.

[24] A. Pindar, M. Papetti (2002): Public Procurement of Energy Saving Technologies in Europe (PROST) Report on the Country Study for Italy: Task 2a – Current Public Sector Purchasing, Building, and Replacement Practices Task 4b – PICO Feasibility Study. February 2002, Politecnico di Milano.

[25] A. Sánchez de Miguel (2007): Differential Photometry Study of the European Light Emission to the Space. . In World Conference in Defence of the Night Sky and the Right to Observe the Stars, 20-23 april 2007, La Palma.

[26] A. Sánchez de Miguel, J. Zamorano Calvo (2008): Light pollution in Spain. An european perspective. Highlights of Spanish Astrophysics V. http://eprints.ucm.es/12281/.

[27] A. Sánchez de Miguel, J. Zamorano, B. Pila-Díez, J. Rubio, R. Ruiz, I. Rodríguez-Herranz, I., A. González-Pérez (2011, November): Light pollution in Spain 2010. In Highlights of Spanish Astrophysics VI (Vol. 1, pp. 784-784).

[28] A. Sánchez de Miguel, J. Zamorano (2011): Midiendo la contaminación del cielo desde el espacio. Física y sociedad, (21), 24-25.

[29] A. Sánchez de Miguel, J. Zamorano Calvo, J. Gómez Castaño, S. Pascual Ramírez, M. A. López Cayuela, J. Gallego Maestro, F. Ocaña González, G. Martín Martínez, C. Larrodera, B. Tinao, S. Oré, M. F. Palos, P. Challupner, (2012) : Contaminación Lumínica en España 2012: Light Pollution in Spain 2012. Highlights of Spanish Astrophysics VII. http://eprints.ucm.es/15970/.

[30] A. Sánchez de Miguel, J. Zamorano, S. Pascual, F. Ocaña, M. López Cayuela, P. Challupner, J. Gómez Castaño, A. Fernandez-Renau, J. A. Gómez, E. De Miguel, SpS17, Light Pollution: Protecting Astronomical Sites and Increasing Global Awareness through Education. Proceedings IAU Symposium, 2012 (in press).

[31] A. Sánchez de Miguel, J. Zamorano, F. Ocaña, J. Castaño (2013): El uso de imágenes de satélite para combatir la Contaminación Lumínica. (2013) in prep. AstronomíA.

[32] P. Van Tichelen, T. Geerken, B. Jansen, M. Vanden Bosch, V. Van Hoof, L Vanhooydonck, A. Vercalsteren, Final Report Lot 9: Public street lighting,2007/ETE/R/021.

[33] X. Li, X. Chen, Y. Zhao, J. Xu, F. Chen, H. Li (2013): Automatic intercalibration of night-time light imagery using robust regression, Remote Sensing Letters, 4:1, 45-54.

[34] J. Zamorano, A. Sánchez de Miguel, S. Pascual Ramírez, J. Gómez Castaño, P. Ramírez Moreta, P. Challupner (2011): ISS nocturnal images as a scientific tool against Light Pollution. LICA report, April 2011. Version 1.8, http://eprints.ucm.es/12729/.

[35] N. Zhao, T. Ghosh, E. L. Samson (2012): Mapping spatio-temporal changes of Chinese electric power consumption using night-time imagery, International Journal of Remote Sensing, 33:20, 6304-6320.

[36] D. Ziskin, K. Baugh, F. C. Hsu, T. Ghosh, C. Elvidge (2010): Methods Used For the 2006 Radiance Lights Proceedings of the 30th Asia-Pacific Advanced Network Meeting, August 9-13, Hanoi, Vietnam

[37] L. Zhuo, T. Ichinose, J. Zheng, J. Chen, P. J. Shi, X. Li (2009): Modelling the population density of China at the pixel level based on DMSP/OLS non-radiance-calibrated night-time light images International Journal of Remote Sensing Vol. 30, No. 4, 20 February 2009, 1003–1018.

A microcontroller based system for measurement skyglow levels with the use of DSLR cameras

Héctor Antonio Solano Lamphar[1], František Kundracik[2]

[1] *Institute of construction and architecture, Slovak academy of sciences, Dúbravská cesta 9, 845 04 Bratislava, Slovak Republic*
tel: +421 91 8224259, e-mail: lamphar@gmail.com
[2]*Department of experimental physics, 842 48 Bratislava 4, Mlynská dolina - pavilón F2*

Abstract

The authors propose a reliable low-cost platform developed with the intention of the study of skyglow levels. This equipment uses smart structures of software and hardware managed by an electronic controller, prepared with the objective of providing an automation of skyglow measurements. Specifically, the measures are made by a professional DSLR camera that changes the technical aspects with the use of the data that comes from an ambient light sensor. This automated system can measure the whole night with the objective of seeing the skyglow variations. All the data is automatically saved in a computer connected to the electronic controller via USB.

1 Introduction

The natural light has an enormous importance to the biological process of all living organisms, including the weather regulation, food production, biological functions, and the control of circadian rhythms. The artificial light has an importance too, because since its discovery a huge advance in history of humanity took place. However, the past decades have seen the rapid expansion of many countries due to urbanization, population density and economic development increasing the region influenced by artificial light that has become an unappreciated characteristic of cities, towns and transport networks worldwide. (Gallaway el al 2010) (Hunter and Crawford 1991). These rapid changes are having a serious effect in the environment and in all of the involved organisms (Rich and Longcore, 2006). Skyglow is well known for becoming a central environmental issue in the new global economy, having a significant increase in a short period of time. The problem occurs because of the interaction of mainly artificial light with the constituents of the atmosphere, aerosols and water molecules located basically at troposphere level. The principal origin of skyglow is an inefficient design of lighting system that sends light irradiation to zones in the sky where is not needed.

The possibility to perform adequate measurements of skyglow is frequently been limited to the use of appropriate measuring instruments. It is therefore necessary to consider tools that could be adapted to nocturnal measures, with a correct sensitivity, since during night time the illumination is much lower than during the day. The characteristics of the instruments are important components in the photometric measures of luminance, and for instance play a key role in skyglow analysis. Many of these instruments have been made with the purpose of lighting measurements in different environments to those found at night (radiometers, illuminance meters, luminace meters), and therefore often lack the necessary sensitivity and automation. As well, a small set of luminance cameras are manufactured with the aim of having a specialized light meter for specific tasks (video photometer with CCD technology). These instruments are often expensive or difficult to transfer to the measurement site.

It can be expected several variations in the intensity of skyglow during a single night. Previous studies have noted that the skyglow is directly related with atmospheric conditions at the point of study and that its levels could have identifiable variations depending on the time of analysis. For example, it has been suggested that clouds amplify the skyglow (Kyba et al 2012). In the present paper, the authors propose a microcontroller based system with the intention to enhance the

possibilities offered by the digital single-lens reflex cameras (DSLR) that are able to measure skyglow measurements considering a correct calibration. One of the most important orientations on measurements of skyglow is to collect data of luminance. The motivation of the work is to assessing the importance to measuring and spatially modelling the extent to which artificial light is manifesting in skyglow under different times and situations. The proposed system consists of a reliable and inexpensive platform, which is easy to prepare and control and which form the basis of spatial and temporal modelling of the light environment. The device was configured to quantify accurately and instantly SG levels taking all-sky images through the artificial brightness of sky background. The flexibility of the system can generate a wide range of measurement capabilities using an auto- mated data acquisition system. The digital single lens reflex cameras (DSLR) can be surely used in the measurements of luminance (Wuller and Gabele 2007). These cameras also provide a good opportunity in the study of light pollution and skyglow.

2 Experimental device

2.1 Hardware

An electronic controller, a servo, a light sensor and a professional reflex camera composed this device. The development board and all the system is based on the next components (see fig. 1):

- A laptop using a battery with a correct power and clocking control depending on the total time of the measure (at least 10 hours for the whole night).
- A single-board microcontroller.
- An ambient light sensor with a photocell resistance that varies with the amount of light.
- A remote control canon RS-60E3. When the camera is connected to the remote control can trigger the camera shutter button without touching it, so that it reduces the risk of camera shake in bulb exposures.
- A servo FUTABA S3003. This servo is basically a mechanical actuator based on a motor and a gear assembly, which allow us to multiply the torque of the final system. The servos are normally used in robotics. The action induced by the microcontroller permits movements in precise directions. Using an extension of light material and a special tissue, it is possible to open and close the lens.
- A fish-eye lenses Samyang 8 mm f/3.5 Aspherical IF MC with manual focus. Since this lenses are full frame and produced for cameras with the APS-C sensor, are more considered as ultra wide-angle lens having an angle of view of 167 degrees in Canon mounts (APS-C 1:1.6x). The lenses have 10 elements placed in 7 optical groups. The aperture consists of six diaphragms starting in f/3.5 and can be close to f/22.
- A DSLR camera Canon 60D with an APS-C (Advanced Photo System type-C) sized 18.0 Megapixel CMOS sensor. The sensor has a linear response.

As shown in Figure 1, (1) the laptop computer programmed the single-board microcontroller over USB using a program developed on Python (programming language). (2), (3) once programmed, (4) the microcontroller can independently control the sensor to make an ambient light measurement. The single-board microcontroller regulates the servo in order to close (5) and open (9) the camera lenses. (6), (10) The microcontroller control the camera using a wired remote control (7), (11) handle the exposure of the measures depending of the lecture of the light sensor. The camera is prepared to take RAW images (digital image format which allow to have data with minimum modification). The experimental progress is downloaded to the memory of the camera in a black image (8) and in a RAW image (12). The two images were taken considering the same camera settings in order to avoid saturated images. (13) The RAW image is downloaded to a computer and is processed by the LumiDISP software that allows us to calibrate the camera depending on its characteristics. 14 The

final product is a false colour image generated with the aim of representing visually the luminance data.

The sensitivity of the camera sensor, the ISO speed, is determined at the beginning of the observations. We used the maximum aperture that the lenses allowed and the focus is situated at infinite. Every shot is performed in bulb mode. We used a fisheye lens that permits us to obtain a hemispherical field of vision (167°). The ambient light sensor allows the automatic calibration of the camera changing the characteristics of the measurements. This sensor regulates the camera shutter; the time the camera sensor will be open or closed to incoming light from the camera lens. This time is determined depending of the ambient light that the sensor has measured.

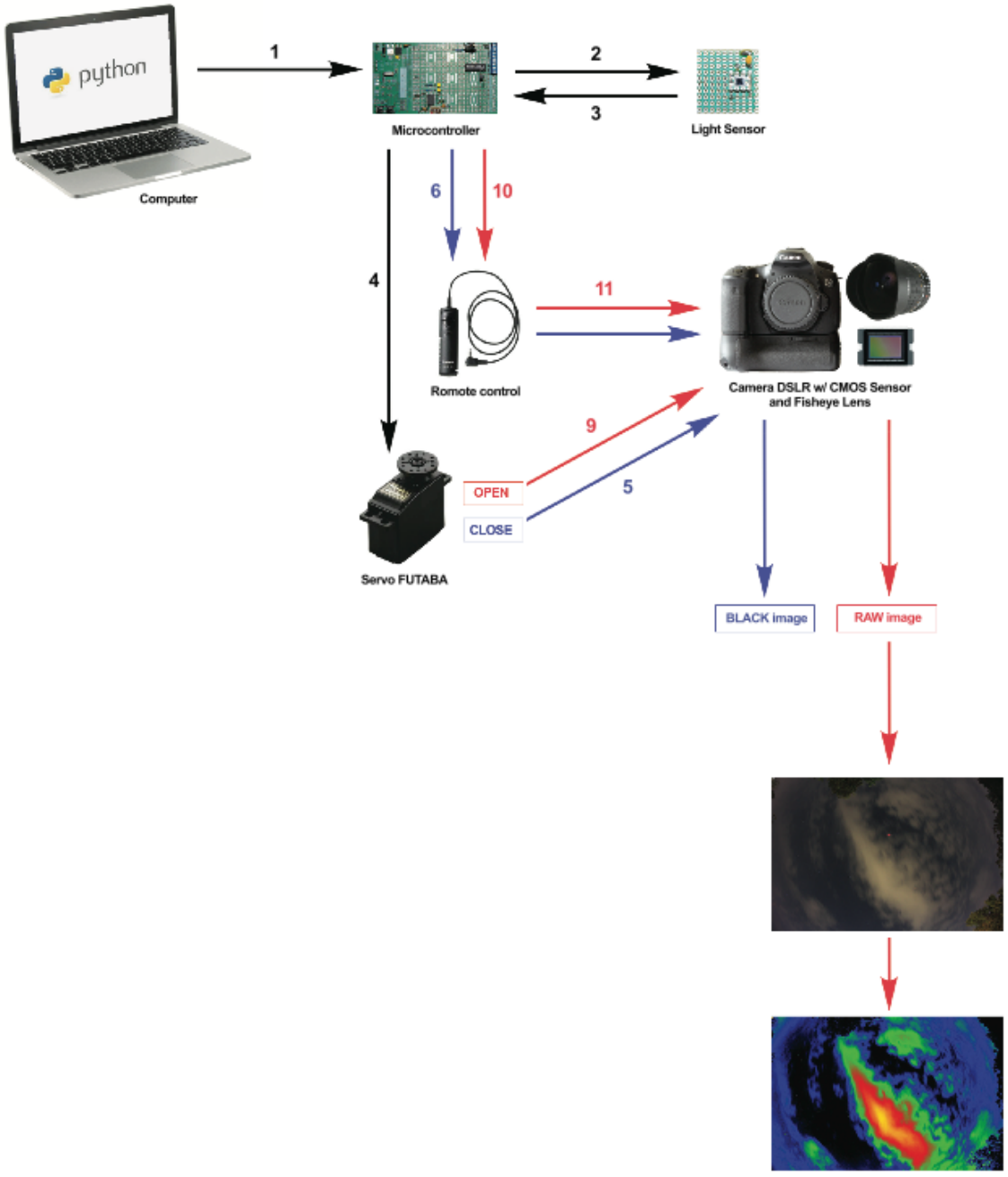


Fig. 1: Outline of the flow system.

2.2 Software

The programming language we used for serial communication is working on python. It is necessary to use a library called PySerial, to provide all the functions and methods required to establish a communication with the electronic controller. Data is to be logged and stores as a text to a computer connected to the electronic controller via USB. The software we used is prepared for the treatment of the images and allows us to make statistical analyses on the complete map or on a selected zone.

3 experiments

The tests were made over the course of a month, which permitted us to see the behaviour of the skyglow under different atmospheric conditions. We found that in one day the ambient night lighting could change several times and therefore the measure device should to be adapted to such variations.

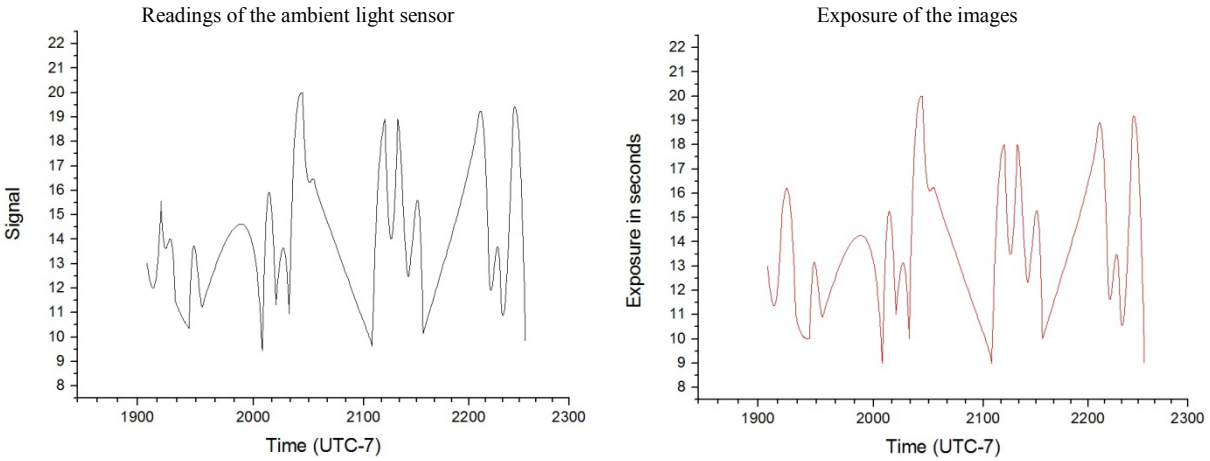


Fig. 2: Signal of the sensor in correlation to the exposure of the images (the measurements were taken on February 6th of 2013).

As can be seen from the Fig. 2 the sensor is allowed to identify the changes in the ambient light. With this information it is possible to allocated the exposure of the camera with precision. In the treatment of the images we have considered the colour space (CIELAB) recommended by the international commission on illumination. The CIELAB specifies a colour (L *, expressed from 0 black to 100 white) to the luminosity of every pixel in any image. With the CIELAB (using the L * value) it is possible to calibrate the camera studying the relation between the characteristics of the pixel and the features that any calibrated instrument is obtaining. The images were treated using the software lumiDISP, developed with the objective to process the images in RAW format to extract all the information we need to characterize the skyglow. The software converts the images in false colour images in order to see the distribution of the sky luminance. With the software is also possible to correct the effect of vignetting of the lens. The measurements were performed in two different regions during all the night. After the calibration of the camera, the images were processed by the software and were displayed on a false colour scale in order to identify the luminance distribution on the sky.

The Fig. 3 presents the results obtained from the preliminary analysis of skyglow. Through the use of the DSLR camera is possible to measure millions of points simultaneously, each pixel is represented by a colour according to their level of luminance. It is possible to see that the measurements were made in different locations, or even at the same location under different atmospheric conditions. The variation of skyglow during by day and time is extremely large.

The Fig. 4 illustrates the behaviour of skyglow in the same location, the same day, over 90 minutes. It is interesting to note that in such period of time is probable to find so many different conditions. These issues make difficult to make a proper characterization of skyglow if one does not have an automated system that detects changes in the ambient light and a control that manage the measurement characteristics according to those changes.

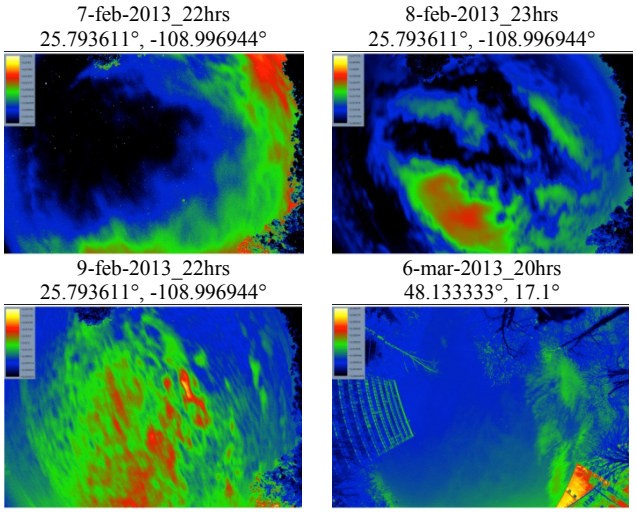


Fig. 3: Preliminary measurements in different days and locations.

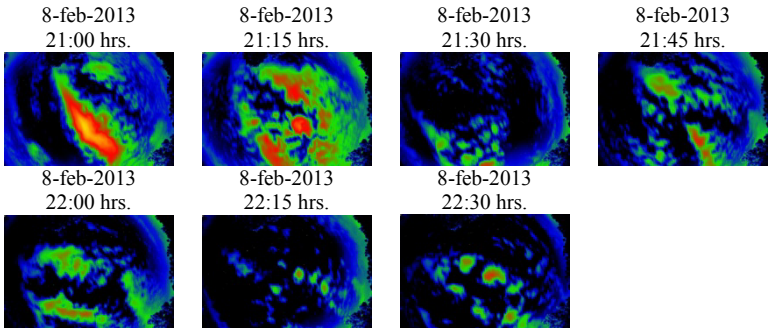


Fig. 4: Preliminary measurements performed in the same day (25.793611°, -108.996944°).

4 Conclusions

This study was carried out with the purpose to build an inexpensive microcontroller based system for measurement skyglow levels. The device is capable to make automated measures during the whole night. Specific researchers have conducted successful skyglow measurements using DSLR cameras previously; as well, the greatest contribution of this work was to automate the entire process.

In summary, the main findings of the work are.

- The development of an inexpensive automated device that permits to make skyglow measurements using DSLR cameras.
- The possibilities to have a control system in order to simplify the work during the measures and to optimize productivity.
- The opportunities to identify the night lighting variations and automatically calibrate the camera to perform the precise image.
- The possibilities to avoid saturation obtaining a black image and a RAW image.

Analyzing the preliminary results of the automated system proposed in this work, we determine that future applications can be identified and maybe open new lines of exploration. Future research should concentrate on the use of the results of the present study to compare them with mathematical models. This may be one of the important implications of the project for future practice.

Acknowledgments

This work was supported by The National Scholarship Programme of the Slovak Republic and by the Research & Development Operational Programme funded by ERDF supporting the project implementation 26240220002.

References

[1] T. Gallaway, R. N. Olsen, D. M. Mitchell (2010): The economics of global light pollution. Ecological Economics 69(3): 658-665.

[2] T. Hunter, D. Crawford (1991): The economics of light pollution. Light Pollution, Radio Interference, and Space Debris, ASP Conference Series, 17, 89-96.

[3] C. C. M. Kyba, T. Ruhtz, J. Fischer, F. Hölker (2012): Cloud coverage acts as an amplifier for ecological light pollution in urban ecosystems. PlosOne.

[4] C. Rich, T. Longcore, editors (2006): Ecological Consequences of Artificial Night Lighting. Island Press.

[5] D. Wuller, H. Gabele (2007): The usage of digital cameras as luminance meters. In Proceedings of the SPIE Digital Photography III Conference, San Jose, CA, US, Jan 29-30 2007.

Environmental zones classification in the Czech Republic

Petr Závada[1], Tomáš Novák[1] and Karel Sokanský[1]

[1] *VŠB-Technical University of Ostrava*
17. listopadu 15/2172, 708 33 Ostrava - Poruba, Czech Republic,
email: petr.zavada@vsb.cz, tomas.novak1@vsb.cz, karel.sokansky@vsb.cz

Abstract

Obtrusive light is discussed quite often nowadays and so this term became well-known not only for the professionals in the field of lighting but also for public, designers and administration. Quantification of obtrusive light depends on many factors. The biggest factor is the amount of the luminous flux directly emitted into the upper hemisphere. Other factors include the reflective qualities of illuminated surfaces and finally conditions in the atmosphere. Based on knowledge of the percentage of directly emitted luminous flux into the upper hemisphere, depending on the surrounding (size of the agglomeration, national park, observatory, etc.) we can classify obtrusive light into several groups according to the norms EN 12464-2 and EN 12 193. In accordance with the norms they are devided to only 4 environmental zones from E1 (for example observatories – dark) to E4 (for example commercial zones – light). If there is a project of outdoor lighting system it is possible to calculate the amount (or percentage) and simply classify this potential source of obtrusive light according to norms to the environmental zone. By these calculations can be also evaluated if the lighting system is a significant contributor to the amount of obtrusive light or not. This article tries to describe problems in larger areas where different zones can exist side by side. Environmental zones should not pass more than one degree (for example E1 to E2 only) at once. The aim of this paper is to establish methodologies for the classifications into the environmental zones. Specific examples of classification are related to 420 kV outdoor distribution stations, which are located in selected areas of the Czech Republic.

1 Introduction

The aim of the article is an example of the classification of distribution stations to environmental zones listed for example in the publication CIE 126 – 1997 and EN 12464-2. Classification of selected areas to the environmental zones is carried out according to the type of residential areas, distances from natural parks and distances from major observatories. In large outdoor light sources the classification to environmental zones limits direct radiation to the upper hemisphere. In the above mentioned references there are listed maximal values of direct radiation from outdoor lighting systems into the upper hemisphere. Obtrusive light is divided into four environmental zones. Table 1 shows besides the maximal acceptable values of the luminous flux emitted directly into the upper hemisphere (URL) and illuminance on objects (dominantly vertical) and the maximum luminous intensity of the used luminaries. The last two columns of the table contain the maximal values of luminance on the facades of buildings and on traffic signs.

In larger surveyed areas may appear different zones together. If so, environmental zones should not pass for more than one degree. The boundaries between zones should not also be sharp but gradual. Table 2 gives recommendations for minimal spacing between environmental zones. But it should be noted that the definition of the reference point is not fixed. It means that especially for large areas (e.g. national parks) it is not clear whether the reference point is (center of the area or its periphery). Some experts even believe that the distances between the zones listed in Table 2 should be doubled at least.

At present time neither designers nor the officials of construction authorities classify the environmental zones, because it is a relatively new issue in the Czech Republic. There is no norm which would regulate the classification. For these reasons it is not quite clear in what environmental zone the area is located. The following chapter suggests the methodology for classification of areas

into environmental zones. This suggestion is based on the example of classifying of outdoor high voltage distribution station 420 kV.

Table 1: Characteristic of environmental zones in terms of obtrusive light [2]

Environmental zone	Light on properties		Luminaire intensity		Upward light	Luminance	
	E_v (lx)		I (cd)		ULR (%)	L_b (cd·m^{-2})	L_s (cd·m^{-2})
	Pre-curfew [a]	Post-curfew	Pre-curfew	Post-curfew		Building facade	Signs
E1	2	0	2500	0	0	0	50
E2	5	1	7500	500	5	5	400
E3	10	2	10000	1000	15	10	800
E4	25	5	25000	2500	25	25	1 000

[a] In case no curfew regulations are available, the higher values shall not be exceeded and the lower values should be taken as preferable limits.

Where:

- E1 represents intrinsically dark areas, such as national parks or protected sites;
- E2 represents low district brightness areas, such as industrial or residential rural areas;
- E3 represents medium district brightness areas, such as industrial or residential suburbs;
- E4 represents high district brightness areas, such as town centers and commercial areas.

Table 2: Minimal distance between the reference point and the border zone [1]

Environmental zone	Minimal distance between the borders of neighboring zones according to classification (km)		
	E1 – E2	E2 – E3	E3 – E4
E1	1	10	100
E2		1	10
E3			1
E4	No limitation		

2 Proposal for classification of outdoor distribution stations 420 kV in Kletné

The above mentioned area has been chosen as an example for fundamental reasons. Distribution stations are usually built far from other sources of obtrusive light. It is possible to measure them while excluding effects of other light sources and because we usually have their light-technical calculations available we can model direct and total luminous flux reflected by the distribution station into the upper hemisphere. Arrangement itself will be used by architects of outdoor light systems. They have to respect the restrictions of directly reflected luminous flux into the upper hemisphere.

In accordance with recommendations mentioned in literature sources [1, 2] it is possible to base determination of environmental zones on distances from areas where requirements on environmental zones have been determined in respect to their functions. This mainly concerns observatories, protected landscape areas, industrial, commercial and residential areas too.

- On the basis of the distance from astronomical and other observatories and protected landscape areas (zone E1)
- On the basis of the distance from residential areas and industrial and commercial areas (zone E2-E4)

Determination of an environmental zone, where a distribution station is situated depends on distances from the above mentioned areas, where their classification into environmental zones is obvious from their specification.

In order to classify outdoor distribution stations on the basis of the above information, following boundary conditions have been set:

Table 3: Boundary conditions characteristic for particular zones

zone E1 ▪ national parks plus 1 km from its borders ▪ protected landscape areas including 1 km environs ▪ important observatories (Ondřejov, Kleť) including 1 km environs	**zone E2** ▪ at least 10 km from the borders of zone E1 ▪ intravilans of villages and its surroundings 1 km ▪ observatories of lesser importance including 1 km environs
zone E3 ▪ extravilans of cities with their surroundings 1 km	**zone E4** ▪ city centers – a zone is at least 1 km in diameter

Picture No 1 shows a map of geographical lay-out of nearest critical areas affected by the classification of distribution station Kletné into environmental zones.

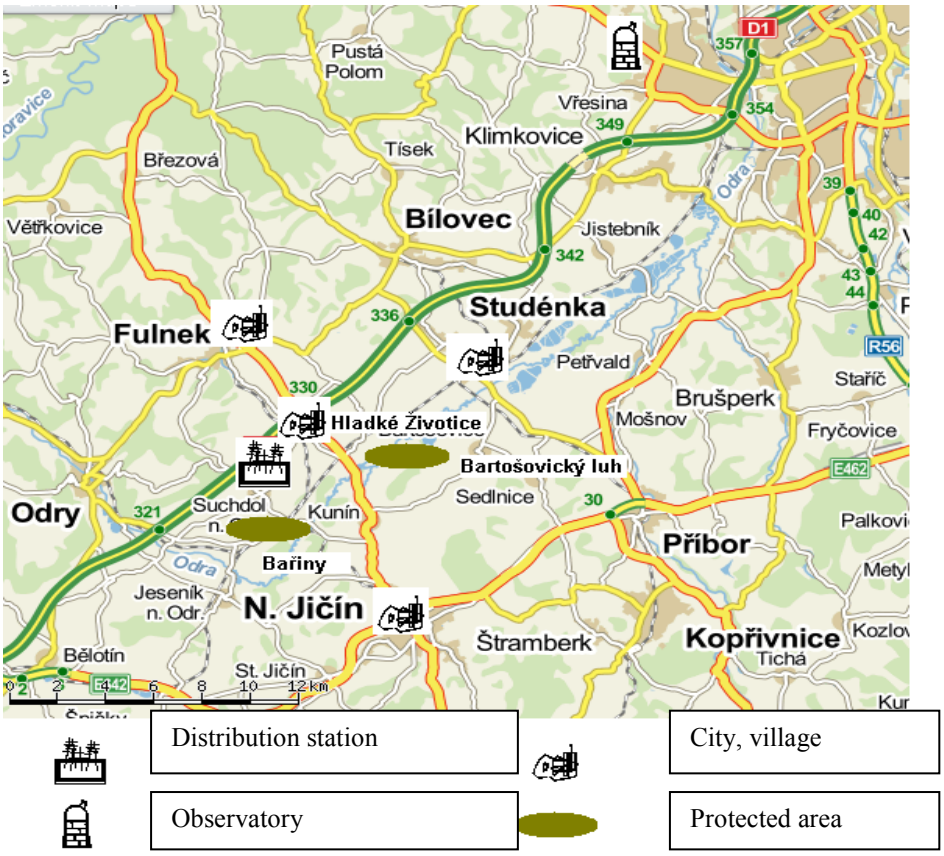


Figure 1: Map of places of importance near the distribution station [3].

In the distribution station vicinity there are several national parks, astronomical observatories, villages and towns.

Table 4: Distribution station and distances from reference points

Observatories	Ostrava Valašské Meziříčí Vsetín	24km 24km 37km
National parks	PR Bařiny PR Bartošovický luh	5,2 km 5,9 km
Villages	obec Hladké Životice obec Kletné	1,3 km 2,2 km
Towns	Nový jičín Příbor Studénka Ostrava	9,8 km 15,5 km 10,9 km 29,8 km

Picture No 2 shows maps of the distribution station with its environs marked. The distribution station is positioned at the outskirts of a village of Hladké Životice with population of 959 inhabitants.

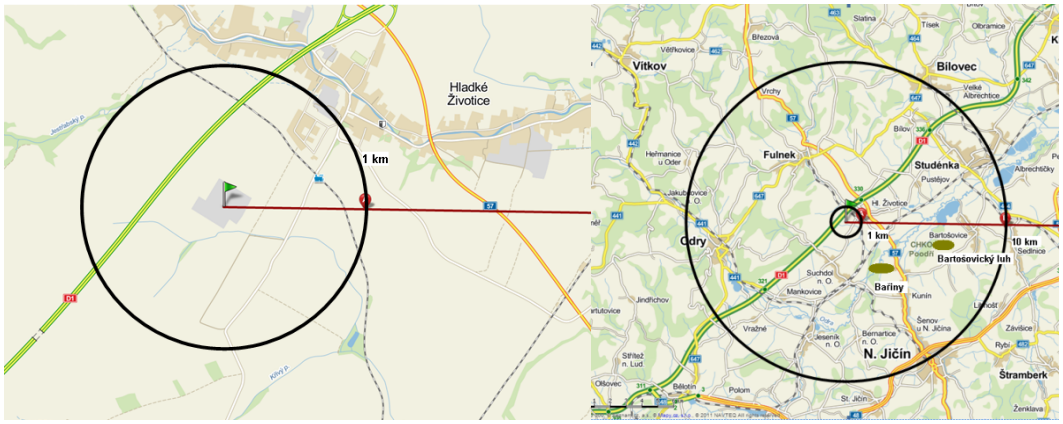


Figure 2: The immediate surroundings distribution stations [3].

The classification of a zone of a distribution station is based on:

- Immediate surroundings of the power station on the left and surroundings of the distribution station with 10 km area marked on the right
- The distance from the nearest village of Hladké Životice. This exceeds 1 km (see picture No 2). Which means that on it can be classified as zone E3-E1 the basis of distance.
- The distance from the nearest nature preserve Bařiny. This is up to 10 km from the zone determined by the nature preserve (see picture No 2). Which means it can be classified as environmental zones E2 – E1
- The distance from the nearest town of Nový Jičín (see picture No 1). If we classify the centre of Nový Jičín as environmental zone E4, in regard to its illuminated historical centre, then we cannot classify the distribution station as only environmental zone E1.
- The distance from the nearest observatory of lesser importance in Ostrava does not influence the classification of environmental zone of the distribution station.

Based on the above partial classifications we can classify the 420 kV distribution station in Kletné as E2 with direct illumination of the upper hemisphere allowance of 5% of the overall illuminated current produced by lightning systems of the distribution station.

3 Modeling of illuminating characteristics of the distribution station into the upper hemisphere

The light-technological proposal of the distribution station TR Kletné contains several individual illuminating systems. Among the main ones comes service lightning of the distribution station, lightning of the transformers, lightning of road network and the guard lights. The used lights with their parameters are shown in Table 5. The total luminous flux produced by halogenid and high-pressure sodium lamps which all lights used in the proposal are fitted with is 2 127 502 lm. The direct luminous flux illuminated into the upper hemisphere has been calculated with DIALUX program by illuminating characteristics and the tilt of the lights.

The calculated figure of 95 738 lm equals 4,5 % of the overall illuminated luminous flux. When we compare this figure to the requirements mentioned in the previous chapter we find out that the technical proposal meets the requirements of an environmental zone E2.

Table 5: Calculation of direct flux into the upper half-space [4].

The curves of luminosity of used luminaries	Amount of luminaries (pc)	Luminous flux of luminaire (lm)	Total luminous flux (lm)	Direct luminous flux to upper hemisphere (lm)	Total ULR (%)
	12	7207	2 127 502	95 738	**4,5**
	100	4101			
	64	14807			
	28	22728			
	14	3349			

Luminous flux emitted directly into the upper hemisphere does not describe real light flux emission into the upper hemisphere, though. Given there is no direct methodology nowadays regarding measurement of the overall emitted light flux into the upper hemisphere we present here a procedure of how to obtain not only total luminous flux into the upper hemisphere, but also a radiating characteristic of the whole distribution station with the help of programmes designed for projecting illuminating systems. Such a model can be used by astronauts, or environmentalists when establishing new protected areas, or building new observatories.

A network of calculating points placed in the upper hemisphere had been set up for modeling of illuminating characteristics of the distribution station into the upper hemisphere with the DIALUX programme.

The midpoint of this hemisphere is situated at the level with centers of the lights which are above

the centre of the distribution station At the points situated on the surface of the hemisphere of 750 m diameter illuminance were calculated in the inwards direction. (see picture No 3). The diameter of 750 m is not fivefold of the maximum size of the distribution station (250 m) which means we cannot consider it as a point source. This issue is caused by the limitations of programming devices used. However, if we examine the distribution of illumination in the distribution station itself, we can conclude that the maximum luminous flux takes place only on about 150 m diameter, which is a limit when we can consider the distribution station a point source of light.

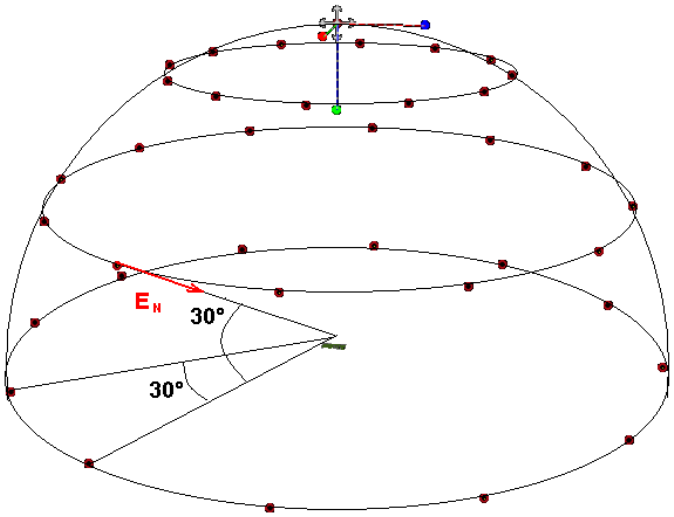


Figure 3: Position of measurement illuminance points [5].

The calculations are made for direct luminous flux emitted into the upper hemisphere (ρ = 0) as well as for different types of reflexive characteristics of the terrain (ρ = 0,15 – 0,8). On the basis of such acquired figures we can model curves of luminosity of the whole distribution station in different situations.

Table 6: Calculated figures illuminances in the upper hemisphere – direct luminous flux ρ = 0 and total luminous flux for ρ = 0,15.

Illuminance (lx)		**Reflectance ϱ = 0**		**Reflectance ϱ = 0,15**			
		Elevation		**Elevation**			
		Horizon 0°	**30°**	**Horizon 0°**	**30°**	**60°**	**Zenith 90°**
Azimuth	**J 180°**	0,08	0,00	0,04	0,08	0,07	0,08
	210°	0,11	0,00	0,04	0,11	0,07	0,08
	240°	0,10	0,00	0,04	0,10	0,07	0,08
	Z 270°	0,06	0,00	0,04	0,06	0,07	0,08
	300°	0,09	0,00	0,04	0,09	0,07	0,08
	330°	0,10	0,00	0,04	0,11	0,07	0,08
	S 0°	0,08	0,00	0,04	0,08	0,07	0,08
	30°	0,09	0,00	0,04	0,09	0,07	0,08
	60°	0,09	0,00	0,04	0,09	0,07	0,08
	V 90°	0,07	0,00	0,04	0,07	0,07	0,08
	120°	0,09	0,00	0,04	0,10	0,07	0,08
	150°	0,11	0,00	0,04	0,11	0,07	0,08

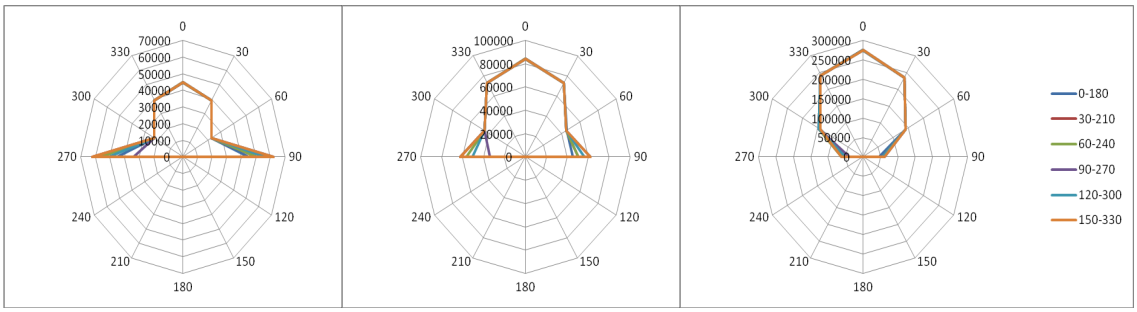


Figure 4: Reflective characteristics of substation – direct and reflected luminous flux of surface reflectivity 0,15 ; 0,3 and 0,8

Changes of the shape of the characteristic are given by rising ratio of reflected part of luminous flux while rising reflectivity of surface (see table 7).

Table 7: Calculation of flux going into the upper half-space from the luminance curves (see Figure 4) by the of bandpass factors

	Reflectance ϱ (-)	Luminous flux Φ (lm)
Direct and indirect luminous flux	0,15	222 305
Direct and indirect luminous flux	0,3	356 150
Direct and indirect luminous flux	0,8	806 145
Direct luminous flux calculate by programme (ULR = 4,5%)	0	95 738

4 Conclusion

This paper shows the possibilities of how to approach classification of large sources of intrusive illumination into environmental zones. Suggested methodology of classifying such luminous sources, considering distances from residential areas, protected landscape areas, observatories and astronomical observatories, was used at the example of distribution station Kletné. In this example we classified it as a zone E2. Because its design and realization were carried out in accordance with this classification we continued in calculating luminous flux into the upper hemisphere. Calculations were made not only for direct flux illuminated into upper hemisphere, but also for summation of direct and reflected luminous flux.

On the grounds of calculations of luminous flux entering the upper hemisphere of distribution station in Kletné we determined that 4,5 % of the total luminous flux of all lights is directly emitted into the upper hemisphere. This means that light system of distribution station TR Kletné complies with the requirements of environmental zone 2.

By modeling of different reflective types of surface we can see the changes in the behavior of reflected flux into the upper hemisphere. These models can be used not only for investigating of factual effects of new lighting systems on their environ, but also for verifying Mathematics- Physical models which describe dispersive characteristics of the sky. With the knowledge of distribution of brightness in the sky, atmospheric properties and emitting characteristics we can verify models of the distribution of obtrusive light. After their verification it will be also possible to ascertain effects of individual sources of obtrusive light on particular studied places only on the grounds of measuring the brightness of the sky and dispersive conditions in the atmosphere.

Acknowledgments

This paper was published with support of the project SP2013/88 – The research of usage of light sources LED and OLED in special applications.

References

[1] Guidelines for Minimizing Sky Glow CIE 126 - 1997, ISBN 3 900 734 83 6

[2] ČSN EN 12464-2 Světlo a osvětlení – Osvětlení pracovních prostorů – Část 2: Venkovní pracovní prostory,

[3] http://www.mapy.cz

[4] http://www.hormen.cz

[5] http://www.dial.de/DIAL/en/dialux-international-download.html

[6] T. Novak, K. Sokansky, P. Zavada (2011): Measurement of obtrusive light in terms of Czech Republic:, Przeglad Elektrotechniczny Volume: 87, Issue: 4, Pages: 32-34.

Index of Authors

Altan M.	9
Aslan B.	9
Aslan Z.	9
Aubé M.	19, 87, 119
Baddiley Ch.	25
Canal-Domingo R.	113
Catalan Light Pollution Official Service	113
Darula S.	51
Dick R.	57
Espey B.	71
Gómez Castaño J.	121
Jimenéz J.	77
Jones A.	83
Kausch W.	83
Kimeswenger S	83
Kundracik F.	133
Lavallée J.-P.	87
Luginbuhl Ch. B.	93
Martín F.	77
McCauley J.	71
Mirzakhalil S. H.	99
Noll S.	83
Novák T.	139
Ozdemir S.	9
Pascual S.	121
Posch T.	105
Puschnig J.	105
Ribas S. J.	113
Roby J.	119
Sánchez de Miguel A.	121
Sokanský K.	139
Solano Lamphar H. A.	133
Szyszka C.	83
Uttenthaler S.	105
Zamorano J.	121
Závada P.	139

Contents

Proceedings 7

M. Altan, B. Aslan, S. Ozdemir, Z. Aslan: Sky brightness measurement and light pollution mapping Case study: Eskisehir city center and surroundings 9

M. Aubé: An online mapping of sky radiance contribution and sensitivity from sky radiance model ILLUMINA 19

C. Baddiley: Modelling sky glow from luminaire designs 25

S. Darula: Windows in buildings: potential source of light pollution 51

R. Dick: Applied scotobiology in luminaire design 57

B. Espey, J. McCauley: Light pollution measurements in Ireland 71

J. Jiménez, F. Martín: Dark sky conservation in Sierra Sur range (Spain): The astronomy as a tool of social revitalization and environmental conservation 77

A. Jones, S. Noll, S. Kimeswenger, W. Kausch, C. Szyszka: An improved scattered moonlight model for the sky background 83

J.-P. Lavallée, M. Aubé: Optimized optical filter for LED lighting 87

C. B. Luginbuhl: How effective are lighting codes? 93

S. H. Mirzakhalil: A new definition of light pollution based on the status of light pollution in Iran 99

T. Posch, J. Puschnig, S. Uttenthaler: Night sky brightness measurements and night sky spectroscopy performed at the Vienna University Observatory 105

S. J. Ribas, R. Canal-Domingo, Catalan Light Pollution Official Service: Measuring light pollution in Montsec: a protected area 113

J. Roby, M. Aubé: Impact of light pollution before and after the creation of the first International Dark Sky Reserve, OMM, Quebec, Canada 119

A. Sánchez de Miguel, J. Zamorano, J. Gómez Castaño, S. Pascual: Evolution of the energy consumed by street lighting in Spain estimated with DMSP-OLS data 121

H. A. Solano Lamphar, F. Kundracik: A microcontroller based system for measurement skyglow levels with the use of DSLR cameras 133

P Závada, T. Novák, K. Sokanský: Environmental zones classification in the Czech Republic 139

Index of Authors 147

Contents 148